

https://dspace.org/

Modulation of growth and stemness in colorectal cancer cells by anticancer agents

Mdluli, Nokubekezela Thembeka

2020
https://hdl.handle.net/10539/31979

Downloaded from a DSpace repository. https://dspace.org/

MODULATION OF GROWTH AND STEMNESS IN COLORECTAL CANCER CELLS BY ANTICANCER AGENTS

Nokubekezela Thembeka Mdluli

A Dissertation submitted to the Faculty of Health Sciences, University of the Witwatersrand, Johannesburg, in fulfilment of the requirements for the degree of Master of Science in Medicine

Johannesburg, 2020

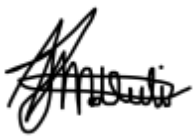
Declaration

SENATE PLAGIARISM POLICY

I Nokubekezela Thembeka Mdluli (Student number: 917036) am a student registered for the degree of Masters of Science in Medicine in the academic year 2020 .

I hereby declare the following:

- I am aware that plagiarism (the use of someone else's work without their permission and/or without acknowledging the original source) is wrong.
- I confirm that the work submitted for assessment for the above degree is my own unaided work except where I have explicitly indicated otherwise.
- I have followed the required conventions in referencing the thoughts and ideas of others.
- I understand that the University of the Witwatersrand may take disciplinary action against me if there is a belief that this is not my own unaided work or that I have failed to acknowledge the source of the ideas or words in my writing.
- I have included as an appendix a report from "Turnitin" (or other approved plagiarism detection) software indicating the level of plagiarism in my research document.

Signature:  Date: 2020/10/11

Presentation arising from this research study

Nokubekezela Thembeka Mdluli, Youns Wani, Amber Khan, Paul Ruff, Clement Penny. MBRT PG Research Day (2019), 28-November. University of Witwatersrand, Johannesburg South Africa. **Modulation of Growth and Stemness in Colorectal Cancer Cells by Anticancer Agents.** Poster presentation.

Abstract

Background: Existing chemotherapeutic drugs are inefficient in addressing the rising incidences of recurrent colorectal cancer (CRC). Cancer stem cells are a tumour subset population underlying CRC recurrence. To combat recurrent CRC, novel therapeutic strategies involving the discovery of novel anticancer drugs targeting cancer stem cells are urgently required. We therefore evaluated anticancer activity of novel series of synthetic tetrazole dithiocarbamate derivatives (TDTCs) in CRC cells and explored their modulatory anticancer effects on CRC stem cell biomarkers. **Methods:** Anticancer activity of ten novel TDTCs were assessed by an initial qualitative screening using Alamar Blue, followed by a quantitative cell death counting using Trypan blue; and the inhibitory concentrations (IC50) were determined in HT29 and DLD1 CRC cells. CRC cells were monitored for their growth response to tested TDTCs using the Muse cell cycle assay and the xCelligence real time cell analyser. The CRC stem cells were studied for their ability to form spheroids in response to the TDTCs using real time microscopy imaging. The effect of the active TDTCs on CRC stem cell markers was evaluated using a proteome profiler assay and real time PCR **Results:** TDTC1, 2, 4 and 5 were found to be the most active compounds (IC50<0.1 to 0.4mg/ml) among the tested TDTCs against CRC cells. Active TDTCs induced cell cycle arrest in different phases in HT29 and DLD1 cells. Active TDTCs targeted exponential and stationary growth phases in treated CRC cells. TDTCs also prevented spheroid formation in HT29 stem cells. Active TDTCs upregulated E-cadherin, and Sox17, and downregulated β-catenin, VEGF1, VEGFR1 and FoxA2 in CRC stem cells. **Conclusion:** Active TDTCs were potent anticancer agents as evident by the present study and warrant further *in vivo* validation.

Acknowledgments

Umuntu ngumuntu ngabantu; A person is a person through other people. For any task to be completed successfully it takes a diligent community to come together and work timeously.

For my Master of Medicine in Science degree to become a reality. God showed me his power and grace paving the way to be guided and supported by wonderful individuals and organizations.

I will love to acknowledge my supervisors, Dr Clement Penny and Dr Amber Khan. They have imparted knowledge and wisdom to me in the field of research. I have acquired lots of skills from my supervisors. Special acknowledgement goes to our collaborator, Dr. MY Wani from the Department of Chemistry at the University of Jeddah Kingdom of Saudi Arabia.

The study would not have been completed if it wasn't for the support of my fellow colleagues. I will love to thank Dr Aijaz Ahmad and Dr Shabir Lone from the Department of Clinical Microbiology & Infectious Diseases in the School of Pathology, University of Witwatersrand. Dr Ekene Emmanuel Nweke from the Department of Surgery. Dr Gavin Owen and his team from the HIV Pathogenesis Research Unit. Dr Rodney Hull, Dr Sheefa Mirza, Dr Aadilah Omar, Vivash Naidoo and Alaouna Mohammed from the Department of Internal Medicine at the Medical Oncology Division. Dr Aurelie Deroubaix and Dr Constance King from the Hepatitis Virus Diversity Research Unit; and Yasir Hoosen from the Department of Pharmacy and Pharmacology. These individuals have assisted me so much from giving advice, to generously allowing me to use their analytical software.

I humbly give thanks to the National Research Foundation and the University of Witwatersrand for funding my two years of the Master's degree.

Lastly a special thanks goes to my caring family- my Father, Mandlenkosi Mosenthal Mdluli, Mother, Nompumelelo Judith Mdluli, my brothers, Hlalunolwazi and Mlekeleli Mdluli and my little sister, Sekuhlelekile Nqobile Mdluli who has been pushing me to do good as a big sister.

"Great works are performed not by strength but by perseverance.'' By Samuel Johnson.

Table of Content

Declaration II
Presentation arising from this research study III
Abstract IV
Acknowledgments V
List of figures XI
List of Tables XIII
Abbreviations XIV
Chapter 1 1
Introduction 1
1.1 Colorectal cancer in South Africa 1
1.1.1 South African colorectal cancer epidemiology 1
1.2 CRC in young individuals 3
1.2.1 CRC is aggressive in young individuals 3
1.2.2 What is CRC and how is it diagnosed? 4
1.2.3 Additional factors included in staging, influence treatment and prognosis 6
1.3. Poorly differentiated tumours are source of aggressive metastatic CRC. 6
1.3.1 Wnt signaling pathway is implicated in the occurrence of poorly differentiated tumours 6
1.3.2 Cancer hallmarks 7
1.3.3 Genome instability 7
1.3.4 Evasion of tumour suppression mechanisms 8
1.3.5 Resisting death and gaining immortality 8
1.3.6 Angiogenesis 9
1.3.7 Stimulation of invasion and metastasis 10
1.4 Colon cancer stem cells 11
1.5 Dysregulation of β-Catenin and downstream effects 12
1.5.1 Beta-catenin and angiogenesis 12
1.5.2 β-Catenin and EMT 13
1.6 Need to discover novel drugs of prognostic value 14
1.6.1 Aggressive CRC and patient relapse 14
1.6.2 Drug resistance, Selectivity, and inefficacy of anti-tumour drugs 14
1.7 Tetrazole-dithiocarbamate derivatives 15

1.7.1 Tetrazole moiety.....15
1.7.2 The dithiocarbamate moiety.....15
1.7.3 Tetrazole dithiocarbamate.....16
1.8 Conventional drugs used in treating colorectal cancer 18
1.8.1 Targeted Therapy 18
1.8.2 VEGF/VEGFR targeted therapy 19
1.8.4 Immunotherapy 19
1.8.5 Chemotherapy in South Africa 20
1.8.6 Use of positive control drugs 20
1.9 Aims 22
1.10 Objectives of the study..... 22
Chapter 2..... 23
Materials and Methods..... 23
The research approach is represented in the flow diagram..... 23
2.1 Cell Lines, cell culture conditions..... 24
2.1.1 Stem cell isolation.....25
2.2 Synthesis of tetrazole based dithiocarbamate derivatives..... 26
2.2.1 TDTC treatment of cells. 26
2.2.2 Controls.....26
2.3 Alamar Blue Screening Assay 27
2.4 Trypan Blue Exclusion Assay..... 28
2.5 Selectivity Assay..... 28
2.6 Real-time cell impedance assay, assessing growth rate of the cells 29
2.7 Cell Cycle Assay..... 30
2.8 Spheroid Formation Assay..... 31
2.9 Analysis of the stem cell biomarker proteome..... 32
2.9.3 Proteome Procedure 33
2.9.3.1 Membrane incubation with protein lysate.....33
2.9.3.2 Primary antibody incubation.....33
2.9.3.3 Streptavidin-HRP incubation 34
2.10 Quantitative Polymerase Chain Reaction (qPCR) (relative quantification)34
2.10.1 RNA Sample Preparation.....34
2.10.2 RNA isolation.....35

2.10.3 Quality Assessment of RNA 35
2.10.5 Primer Preparation 36
2.10.7 Relative real time quantitative PCR (qPCR) 39
Chapter 3 40
Results 41
3.1 Anticancer activity of TDTCs 41
3.2 Active TDTCs induced cell death in CRC cell lines (stage II and stage III)42
3.4 The active TDTCs affects the growth phases of CRC cells 43
3.5 Effect of the active TDTCs on cell cycle in CRC cell lines 46
3.6 The active TDTCs can modulate self-renewal of stem cells 52
3.7 The active TDTC compounds modulated stem cell biomarkers 54
3.8 The active TDTCs regulated gene expression of important factors involved in self-renewal and maintenance of stem cells 65
3.8.1 β-catenin 65
3.8.2 FoxA2 67
3.8.3 VEGF was downregulated in late-stage CRC by the active TDTCs 68
3.8.4 VEGFR1 was downregulated by active TDTCs 70
Chapter 4 72
Discussion 72
4.1 The TDTCs were selectively active 77
4.2 Active TDTCs affected growth phases of CRC cells 79
4.3 Active TDTCs arrested cell cycle in CRC cells 80
4.4 Active TDTCs inhibited spheroid formation in CRC stem cells 81
4.5 Active TDTCs modulated CRC stem cell proteome 82
4.5.1 E-cadherin and Nanog 82
4.5.2 FoxA2 83
4.5.3 SOX17 83
4.5.4 VEGFR2 83
4.5.5 Oct3/4 84
4.5.6 Sox2 84
4.5.7 GATA-4 84
4.5.8 PDX-1 85
4.5.9 Otx2 85

4.5.10 Goosecoid....85
4.5.11 Snail....85
4.5.12 HCG....86
4.5.13 TP63....86
4.5.13 AFP....86
4.6 Active TDTCs modulated gene expression of stem cell biomarkers.... 87
4.6.1 β-catenin....87
4.6.2 FoxA2....87
4.6.3 VEGF-A....87
4.6.4 VEGFR1 was downregulated in late stage of CRC stem cells....88
4.7 Anticancer activity of TDTC might be associated with their chemical structures.... 88
4.8 Future directions.... 89
4.9 Conclusion.... 89
4.10 The relevance of the study.... 90
5. References.... 91
6 Appendices.... 113
6.1 Appendix A: Human Pluripotent Stem Cell Biomarker Proteome Array (R&D) profiling of HT29 and DLD1 cells.... 113
6.2 Appendix B: Human pluripotent stem cell array kit (R&D Systems Biotechne Brand), coordinates.... 116
6.3 Appendix C: Cell cycle assay scatter plots used to gate out doublets.... 117
6.4 Appendix D: TDTC working solutions for Alamar Blue screening.... 119
6.5 Appendix E: TDTC solutions.... 119
6.6 Appendix F: Solutions and Recipes.... 123
6.7 Appendix G: Protein concentrations obtained from the Qubit 2.0 Fluorometer (Life Technologies).... 125
6.8 Appendix H: RNA concentration, quality and purity ratios.... 125
6.9 Appendix I: cDNA concentration, quality and purity ratios.... 126
6.10 Appendix J: qPCR plate set up for the ABI 7500 Real Time PCR Instrument (Thermofisher).... 127
6.11 Appendix K: Amplification Plots.... 130
6.12 Appendix L: Melting curves.... 132
6.13 Appendix M: Troubleshooting unsuccessful Amplification.... 135

6.13.1 Gradient PCR after noticing primer dimer formation non-specificity of VEGFR1, VEGFR2, VEGFR3, E-Cadherin and Sox17. 135
6.13.2 PCR product visualization 136
6.13.3 Sample Loading 137
6.13.4 The gene targets were subjected to troubleshooting using qPCR 138
6.14 Appendix N: Cell count statistical analyses 139
6.15 Appendix O: Cell Cycle Statistics 140
6.16 Appendix P: Proteome Results statistics 142
6.17 Appendix Q: Ethical Clearance 145
6.18 Appendix R: Turnitin Report 146

List of figures

Figure 1: Younger patients show polyps on left side of the descending colon. 4
Figure 2: CRC staging (TNM system). Adapted from Cancer Research UK. 5
Figure 3: Hallmarks of cancer 7
The tetrazole based dithiocarbamate derivative scaffold 17
Figure 4: Schematic of the T1-T10 novel synthetic compounds 17
Figure 5: Positive drug controls 21
Figure 7: Synthesis of tetrazole based dithiocarbamate derivatives 26
Figure 8: Bar graph representing the cell death profile after TDTC treatment in each of HT29, DLD1 and HEK293 cells 42
Figure 9: HT29 cell growth phases are affected by the active TDTC compounds 44
Figure 10: DLD1 cell growth phases are affected by the active TDTC compounds 46
Figure 11: TDTC compounds induced differential cell cycle arrest in HT29 cells ..... 48_Toc50644836
Figure 12: Bar graph representing the DLD1 cell cycle phase following treatment with TDTC for 48hours 49
Figure 13: Cell cycle histograms of HT29 cells following TDTC treatments. a. Control (0.1% DMSO); b. TDTC 1 0.4 mg/ml; c. TDTC 2 0.4 mg/ml; d. TDTC 4 0.3 mg/ml; e. TDCT 5 0.5mg/ml. 50
Figure 14: Cell cycle histograms of DLD1 cells. a. Control (0.1% DMSO); b. TDTC1 0.4 mg/ml; c. TDTC 2 0.4 mg/ml; d. TDTC 4 0.3 mg/ml; e. TDCT 5 0.5mg/ml. 51
Figure 15: The active TDTCs can modulate self-renewal of stem cells 54
Figure 16: Active TDTCs upregulated E-cadherin 57
Figure 17: FoxA2 was profoundly downregulated by the active TDTCs 57
Figure 18: Sox17 protein expression levels in HT29 and DLD1 stem cells 58
Figure 19: VEGFR2 protein expression levels in HT29 and DLD1 stem cells. TDTC 1 and TDTC 4 show potential in reducing angiogenesis 58
Figure 20: Oct3/4 protein expression levels in HT29 and DLD1 stem cells. TDTC 1 modulates Oct3/4 59
Figure 21: Sox2 protein expression levels in HT29 and DLD1 stem cells. TDTC 1 suppresses Sox2 59
Figure 22: GATA-4 protein expression levels in HT29 and DLD1 stem cells. TDTC 4 differentially modulated GATA-4 60
Figure 23: PDX-1 protein expression levels in HT29 and DLD1 stem cells. PDX-1was differentially modulated in the HT29 and DLD1 cell lines 60
Figure 24: Otx2 protein expression levels in HT29 and DLD1 stem cells, Otx2 was modulated by TDTC 4 61
Figure 25: Goosecoid expression was modulated by the active TDTCs. 61
Figure 26: Snail protein expression levels in HT29 and DLD1 stem cells. TDCT 4 differentially modulated Snail 62
Figure 27: HCG protein expression levels in HT29 and DLD1 stem cells. Active TDTCs did not affect HCG protein expression 62
Figure 28: TP63 protein expression levels in HT29 and DLD1 stem cells. TP63 was not modulated by the active TDTCs 63
Figure 29: AFP protein expression levels in HT29 and DLD1 stem cells. AFP was not influenced by the active TDTCs 64

Figure 30: Nanog protein expression levels in HT29 and DLD1 stem cells. Nanog expression was not affected by the active TDTCs....64
Figure 31: β-catenin is highly expressed in late-stage CRC cells....66
Figure 32: Active TDTCs mainly downregulated β-catenin....66
Figure 33: FoxA2 mRNA expression was reduced by active TDTCs....67
Figure 34: FoxA2 was downregulated by the active TDTCs....68
Figure 35: VEGF is highly expressed in the late stage of differentiated CRC cells....69
Figure 36: Active TDTCs downregulated VEGF in DLD1 stem cells....69
Figure 37: VEGF1 mRNA was downregulated by the active TDTCs....70
Figure 38: The active TDTCs downregulated VEGFR1 mRNA....71
Figure 39: Wnt Pathway and its association with CRC....75
Figure 40: TDTCs Mode of Action....76
Figure 41: The active TDTC compounds modulate stemness....115
Figure 42: Cell cycle scatter plot used to gate out doublets for HT29 cells following TDTC treatments. a. Control (0.1% DMSO); b. TDTC 1 0.4 mg/ml; c. TDTC 2 0.4 mg/ml; d. TDTC 4 0.3 mg/ml; e. TDTC 5 0.35 mg/ml.....117
Figure 43: Cell cycle scatter plot used to gate out doublets for DLD1 cells following TDTC treatments. a. Control (0.1% DMSO); b. TDTC 1 0.4 mg/ml; c. TDTC 2 0.4 mg/ml; d. TDTC 4 0.3 mg/ml; e. TDTC 5 0.35 mg/ml....119
Figure 44: qPCR set up....128
Figure 45: qPCR set up plate 4....129
Figure 46: Amplification plot of plate 1....130
Figure 47: Amplification plot of plate 2....130
Figure 48: Amplification plot of plate 3....131
Figure 49: Amplification plot of plate 4....131
Figure 50: Melt Curve of plate 1....132
Figure 51: Melt Curve of plate 1, with non-specific amplification....132
Figure 52: Melt Curve of plate 2....133
Figure 53: Melt Curve of plate 2, with non-specific amplification....133
Figure 54: Melt Curve of plate 3....134
Figure 53: Melt Curve of plate 3, with non-specific amplification....134
Figure 54: Melt Curve of VEGFR3....135
Figure 55: No product formed by 58, 59 and 61°C primer annealing temperatures....137
Figure 56: No clear amplicons were seen at 55, 56 and 57°C....138

List of Tables

Table 1: Summary of the histological diagnosis of CRC in South Africa in 2014 according to gender, age and ethnicity. Adapted from (4) 2
Table 2: Summary of the primers used in the assessment of active TDTC modulation of gene expression of colorectal stem cells. 37
Table 3: Summary of each primer's specific characteristics (IDT) 38
Table 4: The Cycles for qPCR 40
Table 6: Alamar Blue assay, anticancer screening of TDTC compounds against HT29 CRC cell lines. 41
Table 7: Indicates the IC50 of the active TDTC compounds against HT29 (stage II) and DLD1 (stage III). 43
Table 8: Stock solution for Alamar Blue screening. 119
Table 9: Final experimental concentrations of the compounds for Alamar Blue screening. 119
Table 10: Working concentration of active TDTCs selected from Alamar Blue screening were added to increase (Stock concentrations were increased to minimize DMSO percentage). 120
Table 11: Concentrations of active TDTCs used for the Trypan Blue Exclusion assay. 121
Table 12: The amount of the active compounds and positive control drugs used for the experiment. 122
Table 13: Summary solutions and recipes. 123
Table 14: Summary of protein concentrations from samples. 125
Table 15: Summary of RNA concentration and purity ratios 125
Table 16: Summary of cDNA concentration and purity ratios. 126
Table 17: Summary of components and reaction volume for performing standard gradient PCR 135
Table 18: Cycling conditions for PCR. 136
Table 19: Summary of cell count statistical analyses of HEK293, HT29 and DLD1. 139
Table 20: Summary of cell count statistical analyses of HT29 cells. 139
Table 21: Summary of cell count statistical analyses of DLD1 cells. 139
Table 22: Summary of statistical analyses of HEK293 cells 140
Table 23: Summary of cell cycle statistical analyses of G0/G1 phase in HT29 cells. 140
Table 25: Summary of cell cycle statistical analyses of G2/M phase in HT29 cells. 141
Table 26: Summary of cell cycle statistical analyses of G0/G1 phase in DLD1 cells. 141
Table 27: Summary of cell cycle statistical analyses of S phase in DLD1 cells. 141
Table 29: Summary of human stem cell biomarker proteome array statistical analyses of HT29 stem cells. 142
Table 30: Summary of human stem cell biomarker proteome array statistical analyses of DLD1 stem cells. 143

Abbreviations

5- FU	5-Fluorouracil
ADME	Administration, distribution, metabolism
AFP	Alpha-fetoprotein
APC	Adenomatous polyposis coli
Bak	Bcl-2 homologous antagonist/killer
Bax	BCL2 Associated X
Bcl-2	B-cell lymphoma 2
BSA	Bovine serum albumin
cDNA	Complementary Deoxyribonucleic acid
Chemi Reagent	Chemiluminescent reagents
CRC	Colorectal Cancer
CRCLM	CRC liver metastatic
CRC-PAFP	CRC-producing AFP
DAPI	4′,6-diamidino-2-phenylindole
DMEM-F12	Dulbecco's Modified Eagle’s Medium
DMSO	Dimethyl sulfoxide
DNA	Deoxyribonucleic acid
E-cadherin	Epithelial cadherin
EDTA	Ethylenediaminetetraacetic acid
EGF	Epidermal growth factor
EGFR	Epidermal growth factor receptor
EMT	Epithelial Mesenchymal Transitioning
ESC	Embryonic stem cells
FBS	Fetal bovine serum

FDA	Federal Drug Administration
FGF	Fibroblast growth factor
FoxA2	Forkhead box protein A2
FRA-1	Fos-related antigen 1
GATA-4	GATA Binding Protein-4
GSC	Goosecoid
GSK3	Glycogen synthase kinase
HCG	Human chorionic gonadotropin
HKG	Housekeeping gene
HNF1A	Hepatocyte nuclear factor 1 homeobox A
hTERT	human Telomerase Reverse Transcriptase
IC50	Inhibitory concentration
LSD1	Lysine Specific Demethylase 1
MACS separator	Magnetic-activated cell sorting separator
MB	Medullablastoma
miRNA	Micro Ribonucleic acid
MLH1	MutL homolog 1
MMP-7	Matrix metalloproteinase-7
mRNA	Messenger Ribonucleic acid
MS columns	Magnetic separation columns
MSH 2	MutS homolog 2
MSH 6	MutS homolog 6
NCBI	National Centre of Biotechnology
Oct 4	Octamer-binding transcription factor 4
Otx2	Orthodenticle Homeobox 2

PBS	Phosphate Buffered Saline
PCR	Polymerase chain reaction
PDCs	Poorly differentiated clusters
PDX-1/IPF1	Pancreatic and duodenal homeobox 1
Pen-strep	Penicillin Streptomycin
PTEN	Phosphatase and tensin homolog
qPCR	Quantitative Polymerase Chain Reaction
Rb	Retinoblastoma
RNA	Ribonucleic acid
RTCA	Real-Time Cell Analysis
SAHA	Suberanilohydroxamic acid
SEM	Standard Error of the Mean
Smuc	Snail-related in muscle cells
Sox17	SRY-Box Transcription Factor 17
SOX2	(Sex determining region Y)-box 2 specific transcription factors
Streptavidin-HRP	Streptavidin-horseradish peroxidase
TA	Tubular adenomas
TCF/LEF factors	Lymphoid enhancer binding factor/T-cell
TDTC	Tetrazole dithiocarbamate derivatives
TG	Target Gene
TP63/TP73L	Transformation-related protein 63
TRAIL	TNF-related apoptosis-inducing ligand
VEGF	Vascular endothelial growth factor
VEGFR1	Vascular endothelial growth factor

	receptor 1
VEGFR2	Vascular endothelial growth factor
	receptor 2
WHO	World Health Organization
XIAP	X-linked inhibitor of apoptosis protein
α- and γ-catenin	Alpha and gamma-catenin
β-catenin	Beta-catenin

Chapter 1

Introduction

1.1 Colorectal cancer in South Africa

1.1.1 South African colorectal cancer epidemiology

Globally, cancer remains one of the most fatal non-communicable diseases (1). Even after treatment, the most devastating aspect of this cancer is recurrence, which is increasingly observed due to the prevalence of anticancer drug resistance in patients receiving chemotherapy (2).

Cancer of colon and rectum, also known as colorectal cancer (CRC) has a high mortality rate globally. It is ranked among the top three cancers in terms of prevalence and in the top five, with regards to mortality. According to a recent WHO report on cancer surveillance, the global CRC burden is expected to increase by 3.1 million new cases and 1.5 million deaths are expected to occur by the year 2040 (3). In South Africa, it is ranked sixth most common cancer diagnosed in females, with a crude incidence of 5.86/100 000 per year; and fourth in males with a crude incidence of 7.34/100 000 per year. The histological CRC frequency in South Africa is summarised in Table 1 (4). In South Africa, an average of 18% of all CRC cases consist of patients under 50 years of age, of which approximately 7% are younger than 40 years (5).

Table 1: Summary of the histological diagnosis of CRC in South Africa in 2014 according to gender, age and ethnicity. Adapted from (4)

Age Group	Asian Female	Asian Male	Black Female	Black Male	Coloured Female	Coloured Male	White Female	White Male
0-4	0	0	0	0	0	0	0	0
5-9	0	0	0	0	0	1	0	0
10-14	0	0	0	0	0	0	1	0
15-19	0	0	0	1	0	0	0	0
20-24	0	1	8	6	0	1	1	0
25-29	0	2	15	12	1	7	5	6
30-34	0	0	21	25	5	4	11	7
35-39	4	4	23	22	8	3	12	21
40-44	3	8	24	39	10	13	28	30
45-49	3	9	43	48	18	13	48	33
50-54	6	14	75	58	21	22	58	72
55-59	12	23	49	71	21	43	69	111
60-64	11	22	55	71	31	41	95	143
65-69	14	28	41	47	35	42	137	171
70-74	7	11	24	31	31	33	114	174
75-79	15	11	27	21	21	30	112	113
80-84	7	4	13	12	17	19	73	83
85+	1	3	9	7	7	11	54	32
Unknown	3	9	30	6	2	1	2	3
Total	86	149	457	477	228	284	820	999

1.2 CRC in young individuals

1.2.1 CRC is aggressive in young individuals

The incidence of CRC has been increasing in recent decades and is predicted to continue to rise in the coming decades (6). This is attributed to a rise in the incidence of CRC in young adults (<50 years old), which has been named Early-Onset CRC (EOCRC) (7). The occurrence of CRC in young individuals presents as an aggressive metastatic disease. Generally, CRC may be familial (inherit mutated gene/genes) or sporadic (driven by an accumulation of genetic mutations over the time, appearing late in life) (8-10). Demographic patterns show that most cases are present with sporadic CRC. However, in young individuals, familial and sporadic CRC are more aggressive in comparison to older people of >50 years of age (11). CRC in young individuals is diagnosed at more advanced stages (stage II, III and stage IV), often presenting with a high-grade CRC, leading to poor prognosis (12, 13). These bring about challenges in the management of CRC as the cancer might have reached metastasis. The high-grade CRC is reported as consisting of poorly differentiated tumours with vascular invasion (14, 15). This type of histopathology accounts for 10-16% of all CRC, but for young individuals accounts for some 20-64% of cases. This histological pattern is similarly observed in several places in different countries including the United States, England, Japan and West Africa (12, 16). In South Africa, tumours are commonly invasive adenocarcinomas and are often present in the left colon (Fig 1). The polyps however are tubular adenomas (TAs) and are generally low grade dysplasia (5). The common global histological pattern of CRC further highlights CRC as a global burden.

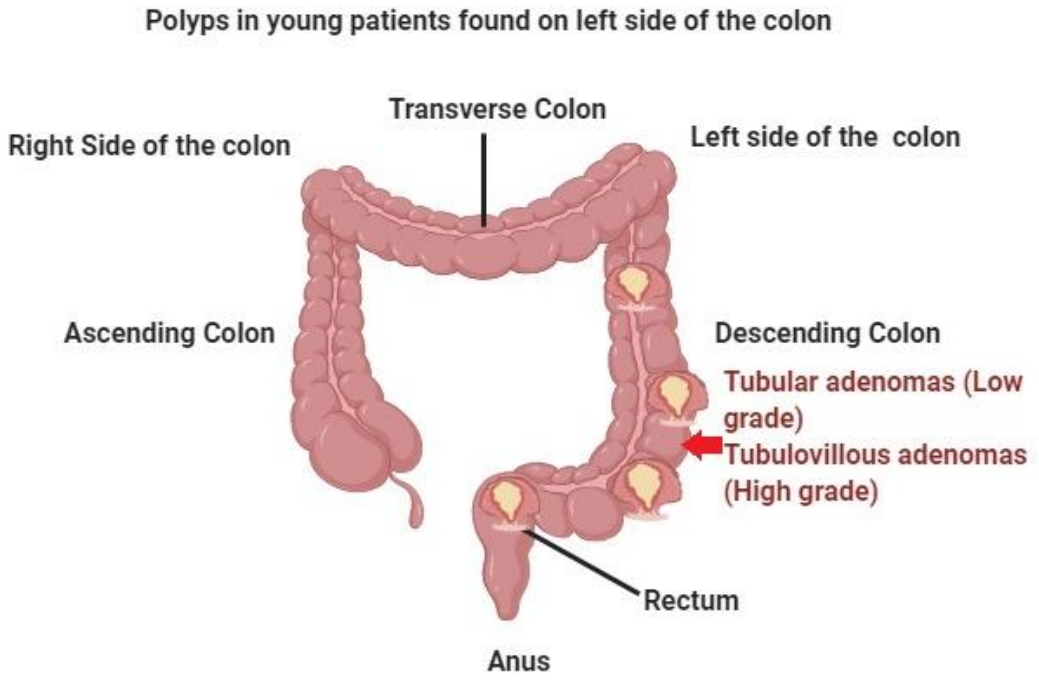


Figure 1: Younger patients show polyps on left side of the descending colon. Arrow indicates the tubular adenomas and tubulovillous adenomas. Adapted from (5).

1.2.2 What is CRC and how is it diagnosed?

CRC is a malignancy that arises from the inner wall of the colon (large intestine). It is characterized by adenomas or polyps, these being a mass of cells that proliferate rapidly, which eventually protrude through the gastro-intestinal tract (17). The polyp penetrates through the gastro-intestinal tract to spread eventually to distant organs (18). CRC is diagnosed through the identification of polyps using various techniques, including colonoscopy (19). The colorectal polyps are classified as adenomatous neoplastic, hyperplastic, hamartomatous or inflammatory (17). The neoplastic polyps are of importance as they have the potential to develop into a malignant tumour (20).

The malignant tumour is staged by physicians to indicate the spread of the colorectal tumour. The staging is critical for assigning the possible treatment for the patient, where the earliest stage for CRC is termed stage 0 and then continues from stage I (1) to stage IV (4), these are known as stage grouping. Each tumour is described in detail, including size of the tumour, tumour growth and breadth of tumour spread (21, 22). The staging provides an indication of patient survival.

The TNM system is commonly used for the staging of cancer. The staging tool is maintained by the American Joint Committee on Cancer (AJCC) and the International Union for Cancer Control

(UICC) (23). The system describes the size of the tumour (**T**). This is how far has the tumour grown into the wall of the colon or rectum. The layers of the colon from the inner to the outer region include the mucosa (inner lining), from which all CRC tumours originate. The mucosa includes the muscular mucosa (thin muscle layer), the submucosa (fibrous tissue beneath muscularis mucosa); the muscularis propria (thick muscle layer); and the subserosa and serosa, the thin outermost layers that cover colon, but not the rectum) (see Fig. 2 below). Cancer spreading to the nearby lymph nodes is denoted by **N** (Fig 2)**.** In the staging process, metastasis is denoted by **M**, this being the spreading of the cancer to distant lymph nodes or distant or organs, for example liver or lungs. There are numbers or letters that follow after T, N, and M that give more details on each of the staging criteria. The higher the number, the more advanced the cancer. Once all mentioned categories are combined, stage grouping is done to assign the overall stage of cancer (21, 24, 25).

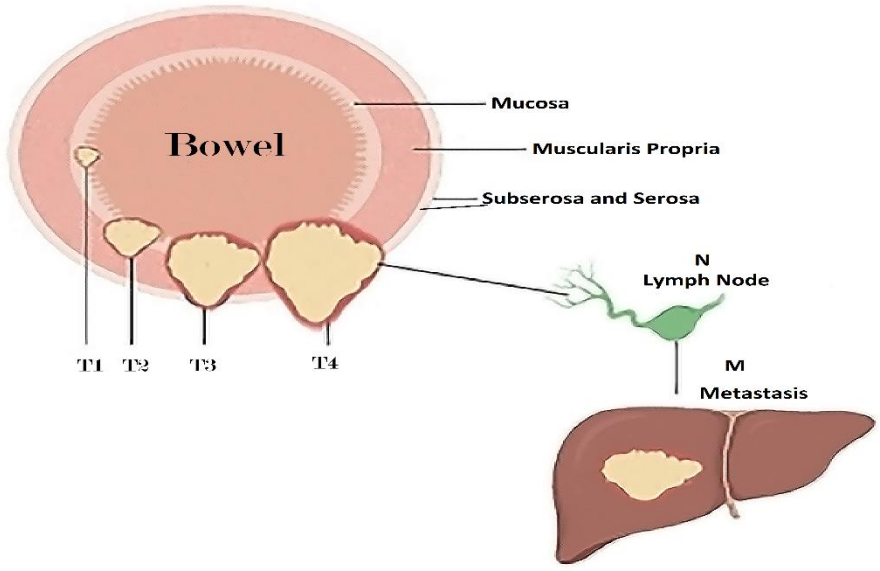


Figure 2: CRC staging (TNM system). Adapted from Cancer Research UK (26). Key: T1 to T4 represents the stage groupings. N is associated with tumour residing in the lymph node. The tumour has metastasized (M), moved into distant organ.

1.2.3 Additional factors included in staging, influence treatment and prognosis

Other factors can be taken into consideration when staging tumours, for example, grading. Grading informs on how well-differentiated the cancer cells are. A number is usually assigned when grading the cancer cells (27). A low-grade means the cancer cells are well-differentiated, while high-grade cancer cells are poorly differentiated (28). High-grade cancers tend to grow rapidly and have a worse prognosis (29). Although the grading of cancer does not affect the cancer staging it may affect prognosis and treatment. High- and low-grade cancers may be treated differently due to the difference in the rate of cancer cell growth (24).

1.3. Poorly differentiated tumours are source of aggressive metastatic CRC.

Poorly differentiated of tumours are reported to contain colon stem cells and progenitor cells that fail to differentiate; and epithelial cells undergoing mesenchymal transitions that lead to increased motility and migration of the cells (30). Such cells drive the aggressive nature of CRC and lead to metastasis. It is reported that poorly differentiated clusters (PDCs) are associated with poor prognosis, especially when there is a large amount of PDCs, irrespective of cancer stage (31).

1.3.1 Wnt signaling pathway is implicated in the occurrence of poorly differentiated tumours

The PDCs are strongly associated with the dysregulation of the Wnt/Beta-catenin signalling pathway leading to overexpression of metalloproteinases and stem cell biomarker dysfunction of E-cadherin a cell-cell adhesion protein (32). As a result, cells are enabled to evade cell cycle checkpoints while proliferating. The dysregulation of normal cellular behaviour is described as hallmarks of cancer (33).

1.3.2 Cancer hallmarks

The "hallmarks of cancer" coined by Weinberg and Hannahan characterise the behavioural characteristics of cancer cells (33, 34) Briefly, cancer cells are able to sustain proliferative signalling, evade growth suppressors, resist cell death, acquire immortality, induce angiogenesis, and stimulate invasion and metastasis (Fig 3). Underlying these altered characteristics is genome instability, which helps drive the genetic diversity of the tumour, promoting the accumulation of multiple hall-marks (34). Each of the hallmarks are described in more detail below.

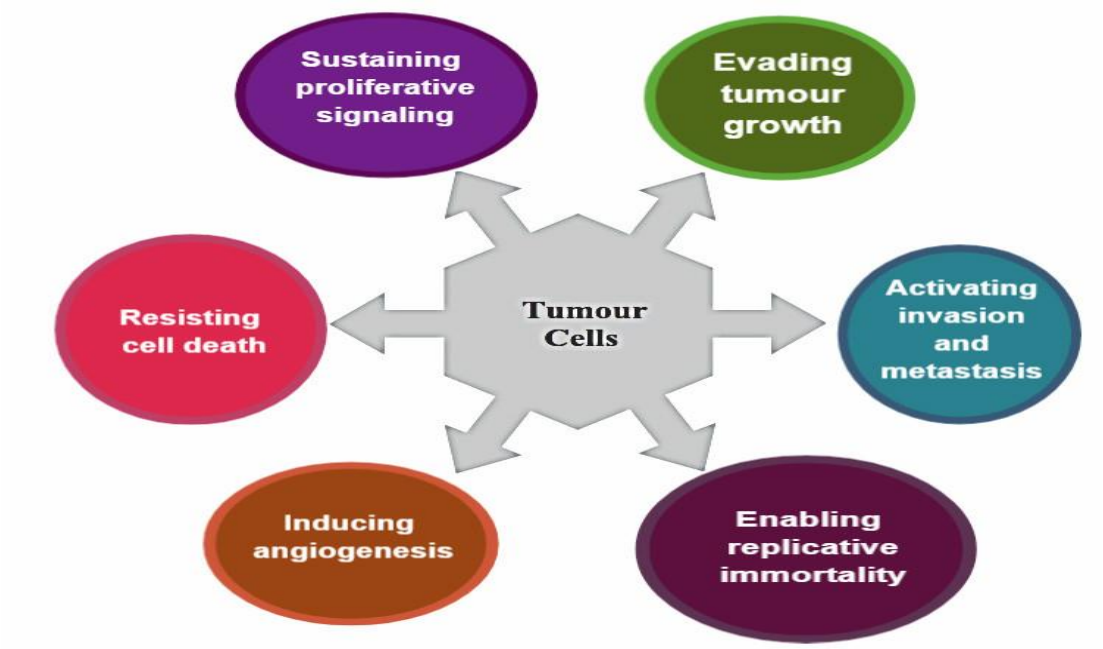


Figure 3: Hallmarks of cancer (Adapted from (33, 34)).

The figure summarises tumour cell behaviour. These characteristic features are referred to as the hallmarks of cancer. Primary hallmarks of cancer include sustaining proliferative signalling, evading growth suppressors, resisting cell death, inducing angiogenesis, enabling replicative immortality, activating invasion and metastasis.

1.3.3 Genome instability

Genome instability is characterized by mutations in proto-oncogenes (β-catenin), DNA repair genes (MLH1, MSH 2 and 6) and tumour suppressor genes (APC, PTEN, and p53) (11, 35). Epigenetics has a secondary role in destabilizing the genome. For instance, in cancer, proto-oncogene promoters are generally hypomethylated, leading to an increase in expression of the onco-proteins. Similarly, tumour suppressor promoters are hypermethylated in most cancers, thus preventing gene transcription; and the tumour continues growth expressing onco-proteins (36). Histone modifications have a similar influence on cancer hallmarks.

The histones are responsible for condensing the DNA (chromatin), protecting its integrity and regulating gene expression. Histones can alter the expression status of the whole stretch of chromatin and can change chromatin into its different forms, that is, heterochromatin and euchromatin (37). Modification of histones occurs covalently on histone tails and can include acetylation, methylation, phosphorylation, ubiquitination, sumoylation and non-coding RNA regulation (38). Modification on histones can lead to formation of a relaxed state of chromatin or euchromatin, where the DNA is accessible to be transcribed. This situation results in some 90% of proto-oncogenes being irregularly transcribed through histone modification. On the other hand, histone modification induced heterochromatin formation leads to chromatin condensation restricting access to transcription factors. Since tumour suppressor genes, occur within heterochromatin they remain untranscribed in cancer (39). mRNA regulation also determines the fate of expression of proto-oncogenes or tumour suppressor genes. Commonly miRNAs are non-coding RNAs and they bind to target mRNA leading to its degradation. Normally miRNAs acts as suppressors of oncogenes and are downregulated (40).

Genome instability of any sort promotes aberrant cell behaviour. wherein proliferative signalling is sustained , involving changes in growth signalling pathways, abnormalities in cell cycle regulation and marked alterations in cellular homeostasis (33, 34).

1.3.4 Evasion of tumour suppression mechanisms

Tumour suppressor genes are essential to regulate cell proliferation and importantly they inhibit the proliferation of the cells containing mutated DNA (41). Tumour suppressors can activate many cell death pathways, like apoptosis, which can eliminate tumour cells (42). Sometimes, the tumour suppressors are silenced either by epigenetic regulation or acquired through mutations rendering by non-active proteins, for example, TP53, Rb (retinoblastoma), APC (Adenomatous Polyposis Coli) and PTEN are inactivated in many types of cancers (18, 43, 44).

1.3.5 Resisting death and gaining immortality

Uncontrolled cell proliferation of cancer cells occurs due to them escaping from cell death mechanisms (apoptosis). Apoptosis or programmed cell death is activated in normal cells with the detection of genomic instability. However in cancer, cells evade apoptosis by down-regulating pro-apoptotic genes, such as, caspases, TRAIL, Bak and Bax (45, 46); and upregulating anti-

apoptotic genes, including, Bcl-2, survivin, and XIAP (47, 48). Resistance to apoptosis hence leads cancer cells to acquire immortality.

Usually, cell proliferation is permitted when there are no DNA mutations. In every successive proliferative cycle, DNA length decreases. In normal cells, this decrease eventually leads to cell death. To a certain extent DNA length is maintained by the telomeres, repeat sequences found at the end of DNA, which to protect chromosomal ends. The telomere shortens with each successive cell division. The telomere lengths are maintained by the enzyme hTERT (human reverse transcriptase) (49, 50). As compared to normal somatic cells, cancer cells have enhanced activity of telomerase, the enzyme which extends the telomeres (51). The expression of telomerase is upregulated through mutations on the promoter of hTERT (52). Cancer cells may also use homologous recombination to sustain their telomere length (53). Continued maintenance of telomere length leads to cell immortalization in cancer cells. Similarly stem cell populations also possess an increased telomerase activity (54). In contrast, normal somatic cells have a specific life span wherein telomere length is not continuously maintained.

1.3.6 Angiogenesis

Angiogenesis is a process involving the proliferation, morphogenesis and migration of endothelial cells from existing vessels into new blood vessels in a time limited manner. This occurs under physiological conditions. Tumour angiogenesis occurs in a time independent manner. It does continue to occur if the tumour promoting angiogenesis is present (55).

In growing cancers, endothelial cells which form blood vessels are energetically active because of the release of growth stimulating factors, for example, VEGF, prostaglandin E1, oestrogen, basic and acidic FGF; and these can stimulate endothelial cell growth and motility, even if the anti-angiogenic factor production is reduced (56, 57). The endothelial cells proliferate and migrate into the perivascular zone, where they form primary sprouts. These primary sprouts mature to form capillary loops that lead to the synthesis of the new basement membrane and blood vessels (58). Tumour cells depend on local neovascularization to supply the tumour with oxygen, crucial nutrients, dispose of metabolic waste, sustain tumour extension and infiltrate to nearby adjacent tissues (59). Neovascularization is characterized by formation of new blood vessels usually in the form of functional microvascular networks, capable of perfusion by red blood cells, that form to serve as primary circulation in response to local poor perfusion especially in tumour cells (60).

Local neovascularization is essential for distant metastasis. Local neovascularization happens when tumour cell migrates away into a hypoxic environment whereby the cells express high levels of VEGF. VEGF initiates neovascularization. As cells receive oxygen from the primary sprouts VEGF expression is decreased (61). Local neovascularization is supported by neighbouring tissue/cells. VEGF is generated and secreted by tumour cells so signalling and , activating the angiogenesis pathway in neighbouring cells (62). In this way, tumour cells thus depend on new blood vessels initiated by surrounding cells (58, 63)

1.3.7 Stimulation of invasion and metastasis

The onset of angiogenesis coexists with an amplified entry of neoplastic cells into the circulation to enable metastasis (64). Epithelial to mesenchymal transition (EMT) is thought to be one of the key initial steps of metastasis. In this process, epithelial cells lose their properties of cell-cell adhesion and undergo trans-differentiation to form motile mesenchymal cells. These cells retain a mixture of epithelial and mesenchymal traits during the transition (65). EMT provides epithelial neoplastic cells with an increase ability of invasiveness together with an ability to degrade extracellular matrix proteins (66). During EMT there is a loss in epithelial biomarkers like E-cadherin (67), with an increase in mesenchymal proteins, such as fibronectin, N-cadherin, and vimentin (68). The process of EMT is regulated by specific EMT-transcription factors, including Twist1, Twist 2, Slug, Zeb 1, Zeb2, Smuc and Snail (69). Another migratory process, amoeboid migration is independent of proteolytic matrix degradation and adhesion to the extracellular matrix, that facilitates invasion. This process requires enhanced cell contractility and is quicker than mesenchymal migration (70). With these events, the tumour cells are able to migrate and invade the surrounding stroma, blood vessels and lymph nodes leading to metastasis (71).

A tumour is physically and genetically a heterogenous mass of cells (72), consisting of epithelial cells, transitioning cells (EMT) and cancer stem cells (73, 74). The intratumour genetic heterogeneity arises from different epigenetic and genetic profiles of these cell subtypes (75). Transitioning cells and cancer stem cells accelerate the progression of cancer (76). Evidence of cancer stem cells or stem cell-like cells was deduced from the investigations of circulating tumour cells (CTCs). In these cells, it was found that binding sites of transcription factors such as Oct4, NANOG, SOX2 which are associated with stemness, were hypomethylated (77). This means that the transcription factors have unrestricted access to their target genes, thus stemness is

maintained. Aggressiveness and poor prognosis associated with stem cells or stem cell-like cells, makes these cells important as drug targets by anticancer agents as they accelerate tumour progression. As cancer stem cells express Oct4, NANOG, SOX2 they may be identified and be functional in diagnosis.

1.4 Colon cancer stem cells

Colon cancer stem cells (derived from adult intestinal stem cells) have a capacity known as 'stemness' to self-renew and form progenitor cells that can differentiate into different cell types. Stemness is regulated by stem cell biomarkers (Oct4, NANOG, SOX2) which are controlled and maintained by the Wnt Pathway (78). CRC stem cells have been implicated in resistance to therapy. There are many other stem cell biomarkers such as alpha-fetoprotein (AFP), GATA-4, PDX-1/IPF1, Otx2, TP63/TP73L, Goosecoid, HCG, Sox17 and FoxA2 involved in mediating anticancer drug resistance and stem cell properties. AFP acts as a stem cell biomarker in liver stem cells (79). This well-recognized liver injury biomarker is also at times found in CRC tumours (80). GATA-4 is known to be involved in cardiogenesis by promoting differentiation of cardioblasts. Absence of GATA-4 halts cardiogenesis and it leads to extensive apoptosis of cardioblasts (81). In CRC, GATA-4 is a tumour suppressor (prevents continuous replication of colon stem cells), and its expression is found reduced in CRC (82). PDX-1/IPF1 controls pancreatic cell proliferation and differentiation. Its overexpression in human pancreatic adenocarcinoma is associated with metastasis (83), while in CRC, it is overexpressed in metastatic tissue (84). Otx2 is overexpressed in medulloblastoma, driving proliferation of medulloblastoma tumour cells by activating cell cycle genes (85). During development Otx2 facilitates differentiation of embryonic stem cells into endoderm and ectoderm (86). TP63/TP73L is predominantly expressed in keratinocyte stem cells promoting the survival of the cells. TP63/TP73L also allows the stem cell to differentiate (87, 88). Goosecoid (Gsc) is a homeobox transcription factor and acts as a facilitator of cell migration as a gastrula organizer. In human breast tumours, GSC is overexpressed and the tumours have very invasive characteristics (89). GSC expression in ovarian tumours induced chemoresistance (90). HCG expressed in adenocarcinomas leads to bowel invasion. HCG-positive tumours are also found susceptible to lymph node, peritoneal or liver metastases (91, 92). CRC-liver metastasis is driven by FOXA2 and HNF1A which are liver-specific transcription factors (93). Most recognised stem cell biomarkers are implicated in cancer proliferation, migration, and metastasis.

1.5 Dysregulation of β-Catenin and downstream effects

β-catenin is a key transcription factor associated with the Wnt signalling pathway, possessing both structural and signalling functions. Structurally, it associates with E-cadherin at the cell membrane, where α and γ-catenin units form cell-adherence junctions and help to maintain cell-cell contact (94). As an integral cell signalling factor, it interacts with various transcription factors, allowing for expression or repression of targeted genes.

The signalling function is facilitated by critical accumulations of β-catenin in the cytoplasm, leading to its translocation to the nucleus. Within the nucleus, β-catenin interacts with TCF/LEF factors facilitating the transcription of its target genes involved in cell proliferation, metastasis, and cell survival (95). The target genes include c-JUN, FRA 1 (transcription factors), cyclin D1, c-MYC, human reverse transcriptase (hTERT), vascular endothelial growth factor (VEGF), matrix metalloproteinase-7 (MMP-7) and Survivin (96-100). These genes regulated by β-catenin-TCF/LEF complex are implicated in progression of CRC and other cancers.

1.5.1 Beta-catenin and angiogenesis

Wnt/β-catenin signalling regulates vessel development in normal and pathological conditions (101). In Wnt/β-catenin-addicted CRC cells, there is a link between β-catenin and vascular endothelial growth factor receptor 1 (VEGFR1). VEGFR1 is a synthetic lethal partner to the Wnt Signalling (102). In an experiment, it was observed that VEGFR tyrosine kinase inhibitors were able to inhibit the growth of Wnt/β-catenin addicted CRC cells, but not in controls having normal Wnt function (103). This supports the link between overexpressed β-catenin and VEGFR1. VEGF binds to both VEGFR1 and VEGFR2, these are the primary receptors participating in angiogenesis. In non-pathological angiogenesis, VEGFR1 has weak tyrosine kinase activity compared to VEGFR2. Fascinatingly, VEGF binds to VEGFR2 with weaker affinity than to VEGFR1, but VEGFR2 has far stronger tyrosine kinase activity (104). VEGFR1 is primarily localized intracellularly in endothelial cells. It has been observed in tumour angiogenesis that VEGFR2 undergoes endocytosis, nuclear translocation, and is subjected to ubiquitination in response to VEGF induced signalling through the JNK/c-Jun pathway. Then VEGF/VEGFR1 signals the Akt/ERK pathway to halt constitutive ubiquitination and induce rapid accumulation of VEGFR1

in endothelial cells (105). In CRC cells VEGFR1 is also strongly expressed and is localized intracellularly (106).

1.5.2 β-Catenin and EMT

The cytoplasmic rise in β-catenin is related to the down-regulation of E-cadherin (107), allowing epithelial cells to gain motility to escape their original niche (108). This leads to epithelial to mesenchymal transitioning (EMT) leading to initiation of metastasis. β-catenin is also involved in the regulation of genes involved in the EMT process. One of the genes that is controlled by β-catenin is the transcription factor TWIST (109). Twist is upregulated during CRC metastasis, and acts in suppressing the transcription of E-cadherin (110). In turn, expression of N-cadherin and fibronectin is induced by the transcription factor TWIST. N-cadherin and fibronectin are inducers of EMT and cellular invasion (111). E-cadherin is also repressed by Snail 1 and 2, whereby these transcriptional factors are modulated by β-catenin. Snail 2 transcription is promoted by β-catenin (112, 113). Once the Wnt signalling is stimulated, upregulation of Snail 1 is induced (114). Inactivation of glycogen synthase kinase 3 (GSK3) also corresponds to the increase of Snail 1. GSK3 phosphorylates Snail 1 and β-catenin to be targeted for degradation (115). β-catenin is therefore crucial in the initiation of EMT in CRC.

1.6 Need to discover novel drugs of prognostic value

1.6.1 Aggressive CRC and patient relapse

Combating aggressive CRC and patient relapse requires urgent attention to improve prognosis. As mentioned above since CRC stem cells and stem-like cells do accelerate tumour progression and they also persist after chemotherapy leading to tumour relapse (116, 117), a broader range of therapeutic options particularly targeted novel drugs therefore need to be identified. In this view, we propose to evaluate the anticancer effects of a novel series of synthetic compounds, the tetrazole dithiocarbamate derivatives against CRC adenocarcinoma stem cells and their biomarkers**.**

1.6.2 Drug resistance, selectivity, and inefficacy of anti-tumour drugs

Drug resistance is mostly promoted by intratumour heterogeneity (72, 73). This leads to the prevention of drug binding, activation of compensatory pathways, gain of the cancer stem cell state and an increase in epithelial mesenchymal transitions (74-76, 118). It can also lead to relapse after remission.

Besides the ineffectiveness of anticancer agents, the chemotherapeutic drugs also fall short in many instances. Their effectiveness is reduced by poor selectivity for tumour cells, inadequate concentrations (lower than required) of the drugs at the target site and occurrence of systemic/localised toxicity in body/organ systems (119).

Therefore, it is important to introduce more drug candidates that will prevent tumour acquired drug resistance and act as effective anticancer agents. The current global aim is to introduce anticancer agents that will be target-specific and less toxic to the human body. The anticancer agents must address the intramural tumour heterogeneity and the existing limitations of drugs.

1.7 Tetrazole-dithiocarbamate derivatives

1.7.1 Tetrazole moiety

The focus of this study is tetrazole and dithiocarbamate compounds which have been reported to have potent anticancer activity (120, 121).Tetrazole is a heterocyclic compound that has four nitrogen atoms in a five-membered ring. They are used as non-classical bioisostere replacing carboxylic acid which has poor administration, distribution, metabolism and excretion (ADME) properties (122). The pharmacophore is highly lipophilic having exceptional interaction with its targets due to strong hydrogen bonding capacity and it is very thermostable (123-126). The tetrazole derivatives have shown a range of biological activities including antifungal, antibacterial, antihypertensive, anti-inflammatory and anticancer properties (127).

The tetrazole derivatives have shown significant interaction with proteins. For instance, 1,5-diaryl substituted tetrazole derivatives inhibited cyclooxygenase-2 binding at the active site of the enzyme, cyclooxygenase has been implicated in many cancers (124). Recently, patented tetrazole derivatives have been reported to inhibit the cytochrome p450 family (128). This inhibition results in elevation of endogenous retinoic acid resulting in a ceasing of cell proliferation. The inhibitory effect on cytochrome p450 family contributes to the treatment of various disorders such as prostate cancer, bowel inflammatory disease, atherosclerosis vascularization, post-menopausal breast cancer and skin disorder (128). Forty-three tetrazole based drugs have been approved by the FDA thus far, making it an important chemical scaffold to be used to synthesize novel compounds (129, 130).

1.7.2 The dithiocarbamate moiety

Another important moiety, dithiocarbamate, is part of the carbamate family with two sulphur atoms instead of oxygen atoms (131). The moiety is a good chelating agent, a biological linker capable of binding to enzymes and contributes to increasing the biological activity of a drug (132, 133). It has also been observed that dithiocarbamate can protect amine groups within the drug (134). The combination of the moiety and other molecular structures has elicited various biological activities such as antifungal properties (131, 135). The potency of the dithiocarbamate moiety being combined with other molecular structures as shown in the conjugation of dithiocarbamate with gold (III) which has shown anticancer potency against cisplatin-resistant cancer cells (136). The

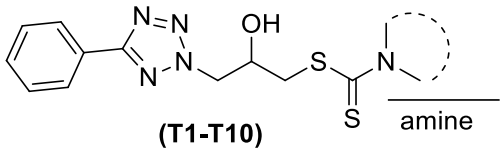
moiety has also shown an inhibitory effect on VEGFR2 and mTOR (mammalian target of rapamycin) serving as a potential angiogenesis inhibitor (137).

1.7.3 Tetrazole dithiocarbamate

Triazole (tetrazole)-dithiocarbamate derivatives, have shown to be potent anticancer agents (138). Zheng et al., (2013) synthesized triazole-dithiocarbamate compounds that specifically inhibited Lysine Specific Demethylase 1 (LSD1) which is overexpressed in many cancers such as breast, colon and gastric cancer (138-140). It was observed that the triazole-dithiocarbamate compounds impeded cell invasion, reduced cell proliferation and reduced tumour mass *in vivo* with no signs of adverse side effects (138). The tetrazole-dithiocarbamate derivatives have thus proved to be effective compounds possessing the potential of combating anticancer drug resistance mechanisms, cancer cell invasion and being tumour selective.

Based on the potential of tetrazole dithiocarbamate acting as anticancer and antiangiogenic scaffold, ten novel tetrazole dithiocarbamate derivatives termed TDTC 1-10 (**fig 4a & b**) were synthesized (by our collaborator Dr. MY Wani at the Department of Chemistry, University of Jeddah, Kingdom of Saudi Arabia) and were proposed as possessing possible anticancer activity against CRC adenocarcinoma cells representing an early (HT29) and late (DLD1) tumour stage, respectively. The identified anticancer TDTC compounds were then screened to target the CRC stem cells of the early and late stage tumour cells. As stem cells are believed to directly influence CRC recurrence and drug resistance, the effect of active TDTCs on the expression of stem cell regulatory markers was assessed.

a



The tetrazole based dithiocarbamate derivative scaffold (141).

b

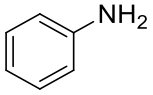
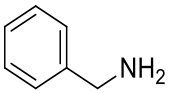
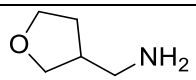
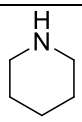
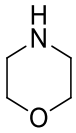
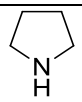
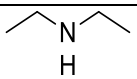
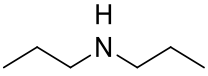
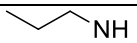
Compound	Amine
T1	
T2	
T3	
T4	
T5	
T6	
T7	
T8	
T9	
T10	

Figure 4: Schematic of the T1-T10 novel synthetic compounds. (141, 142)

4a. The scaffold structure of the benzene ring conjugated to tetrazole based dithiocarbamate moiety is represented above. 4b. The scaffold has amine substituents, which are a unique for each compound (TDTC 1-10) illustrated by the diagram 4b.

1.8 Conventional drugs used in treating colorectal cancer

Individuals diagnosed with early-stage (Stage I-IIC) CRC are treated with surgery to remove the tumour and to drain the lymph nodes according to standard oncologic principles (143). In comparison, patients with advanced tumour stages (Stage III-IVC) and relapse are given conventional chemotherapy or targeted therapy (144). Briefly, the drugs used to treat advanced tumours and relapse are as follows.

1) Fluorouracil (5- FU), can be given intravenously with a second drug known as leucovorin, which boosts 5-FU activity (145). As 5-FU was used in the present study, it is described further below.

2) Capecitabine (oral 5- FU) is a prodrug that once reaching the target site converts into 5-FU (146).

3) Oxaliplatin is a platinum derivative that is active against digestive tract cancers. It causes DNA damage in cancer cells inducing apoptosis (147). Oxaliplatin is given intravenously (146).

4) Irinotecan is a DNA topoisomerase inhibitor, which is given intravenously (148). Irinotecan an analogue of camptothecin, when upon binding to topoisomerase I it causes DNA single-strand breaks, resulting in cell cycle arrest followed by cell death (149).

5) Trifluridine-tipiracil has two components trifluridine and tipiracil and is given orally. This drug is used for patients who are resistant to conventional chemotherapy and can't be treated with the above mentioned drugs (150). Trifluridine-tipiracil is an antimetabolite agent, where trifluridine is a thymidine-based nucleoside analogue. Tipiracil is a thymidine phosphorylase inhibitor. Trifluridine is activated by phosphorylation; and once it has been phosphorylated, the drug intercalates with the DNA leading to the cessation of cell proliferation . Tipiracil enhances the availability of trifluridine in the system (151). These drugs target rapidly growing cancer cells and non-dividing cells are therefore supposed to be less affected by chemotherapy. However, in addition, rapidly dividing somatic cells including hair, lining of the gastrointestinal tract and bone marrow are also affected by these drugs (146).

1.8.1 Targeted Therapy

In more recent years so-called targeted therapies have been developed against cancer cells. These are typically either antibodies or small molecules that inhibit specific proteins implicated in the growth and survival of cancer. These are said to be more specific and depending on their target, have unique side effects (152). Some of these therapeutic agents are described below (see 1.9.6).

1.8.2 VEGF/VEGFR targeted therapy

Currently used targeted therapy in CRC includes Bevacizumab, which binds to VEGF (153). Bevacizumab improves the anti-tumour effect of other chemotherapy drugs. It is given with other drugs such as 5-FU (or capecitabine), irinotecan and oxaliplatin (154). Ramucirumab is a monoclonal antibody that binds to VEGFR2 and also improves the anti-tumour activity of chemotherapy drugs. It is used in combination with an oxaliplatin-containing regimen, or with the irinotecan-based regimen in patients treated with bevacizumab (155, 156). Intravenously administered Aflibercept traps VEGF, preventing it from interacting with its receptors on tumour cells (157). It is taken in combination with the irinotecan-based regimen. It is given to patients, where the tumour has progressed while using an oxaliplatin-containing regimen, with or without bevacizumab (146). Regorafenib is given orally in the form of a pill and blocks VEGF receptors nd other kinases. It is given to patients who show resistance to fluoropyrimidine, irinotecan and oxaliplatin containing regimens and other targeted therapies (158).

1.8.3 EGF/EGFR Targeted Therapy

Cetuximab (Erbitux), is a monoclonal antibody which is effective in targeting uncontrolled growth factor responses. In particular, it binds to the epidermal growth factor receptor (EGFR) preventing binding of epidermal growth factor that normally stimulates cell proliferation (159). It is effective either alone or in combination with other chemotherapeutic drugs. It is more effective in tumours that have mutations in the RAS oncogene. Also it is effective in tumours that possess a specific mutation in the BRAF oncogene, termed V600E (160). Another monoclonal antibody, Panitumumab also targets EGFR, effectively acting on tumours lacking RAS or BRAF (V600E) mutations (146, 161).

1.8.4 Immunotherapy

Immunotherapy is a more recent development in cancer therapy, being used to stimulate a patient's immune system to attack and kill cancer cells (162). Nivolumab (Opdivo) and pembrolizumab (Keytruda) are both monoclonal antibodies which are inhibitors of immune checkpoints. These are effective in patients having a tumour that has mismatch repair deficiency (163).

1.8.5 Chemotherapy in South Africa

Both early and advanced CRC in South Africa is treated with Capecitabine alone or in combination with other chemotherapeutic agents. The Capecitabine is administered orally which is preferred over intravenous 5-FU/Leucovorin due to practicality reasons. Another well used drug is Oxaliplatin which is used alone or in combination with fluoropyrimidine. The second line regimen irinotecan is also used in certain cases of CRC (164).

1.8.6 Use of positive control drugs

In the present study, 5-FU a conventional treatment for CRC was used as a positive control drug. 5-FU exerts its anticancer activity through inhibiting thymidylate synthase (TS) resulting in incorporation of thymine pyrimidines into DNA and RNA thus inhibiting DNA and RNA synthesis (165). Also, Vorinostat (SAHA) a histone deacetylase inhibitor was utilised as it is known to target cancer stem cells by altering the epigenome (166) (**fig 5**). SAHA was originally approved by the Federal Drug Administration (FDA) to treat cutaneous T-cell lymphomas, a heterogeneous group of non-Hodgkin's lymphomas (164). This is a cancer of the immune system whereby the monoclonal T-cells penetrate the skin (167). SAHA is being investigated in other cancers, such as breast, pancreatic, head and neck cancer(168-170), and preliminary results have shown the ability of SAHA to target cancer stem cells (171).

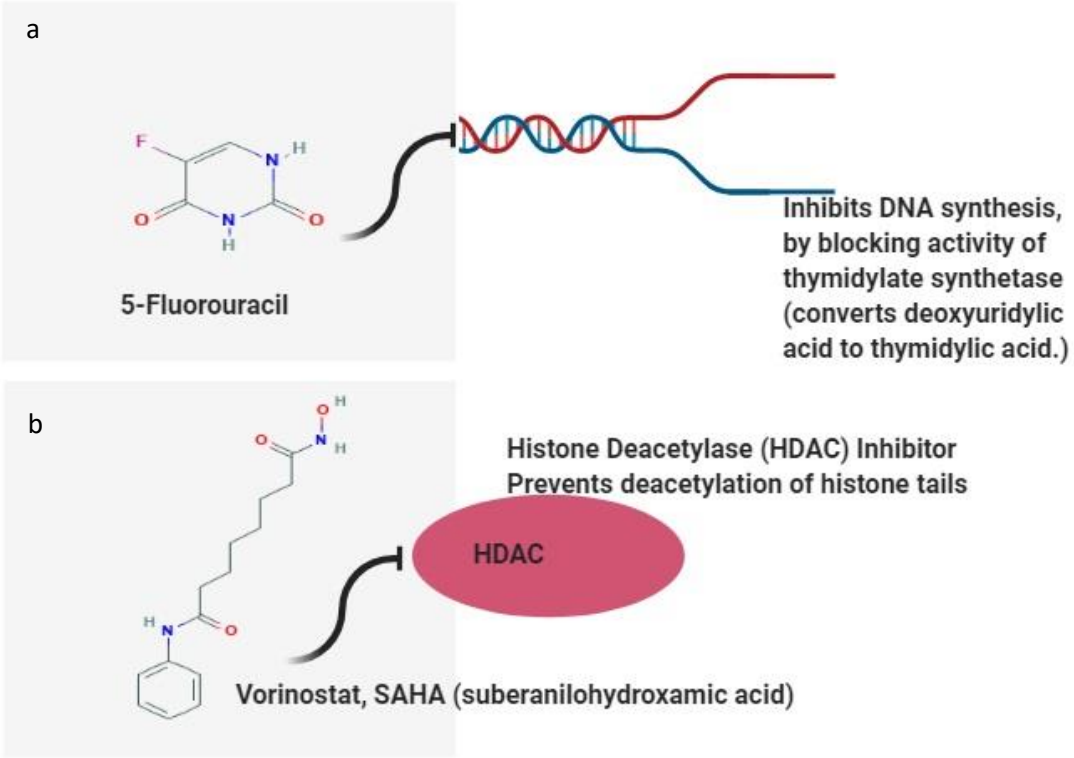


Figure 5: Positive drug controls, adapted from (172, 173).

a.5-Fluorouracil is an anticancer agent commonly used to treat colorectal cancer. It inhibits DNA synthesis, through blocking the activity of thymidylate synthetase which normally acts to convert deoxyuridylic acid to thymidylic acid. b. Vorinostat also known as Subernilohydroxamic acid (SAHA) is a Histone Deacetylase (HDAC) Inhibitor, it prevents deacetylation of histone tails.

1.9 Aims

This study aims to investigate the possible anticancer activity of novel synthetic tetrazole-dithiocarbamate derivatives and to evaluate their ability to target CRC stem cells.

1.10 Objectives of the study

The objectives of the present study include the following:

1. To study the anticancer activity of TDTC 1-10 by determining inhibitory concentrations (IC50) against a CRC stage II cell line (HT29) and CRC stage III cell line (DLD1), to identify the active anticancer compound(s).
2. To identify if the compounds are selectively toxic to cancer cells only. For this objective, non-cancerous cells (HEK293 (Human embryonic kidney cells) were exposed to the active TDTC compounds and were used to study their off-target inhibitory effects (at their respective IC50s).
3. To study the effect of active TDTCs on the growth phases of the stage II (HT29) and stage III (DLD1) CRC cells. A real-time cell impedance assay was performed using a real-time RTCA cell analyser in the CRC cells in the absence/presence of TDTCs.
4. To investigate if the active TDTC compounds can arrest the cell cycle in HT29 and DLD1 cells, respectively.
5. To evaluate the effect of active TDTCs on stemness of CRC stem cells by studying spheroid formation ability of HT29 stem cells (isolated CD133+ fraction) in the presence/absence of active TDTCs.
6. To assess the effect of active anticancer compound(s) on the stemness of isolated stem cell (CD133+) fractions of HT29 and DLD1cells by evaluating the stem cell biomarker proteome response to the active compound in treated stem cells using a dedicated human pluripotent stem cell array kit.
7. To confirm the gene expression of selected proteins modulated by active TDTCs using relative quantitative real-time PCR.

Chapter 2

Materials and Methods

The research approach is represented in the flow diagram below (**fig 6**).

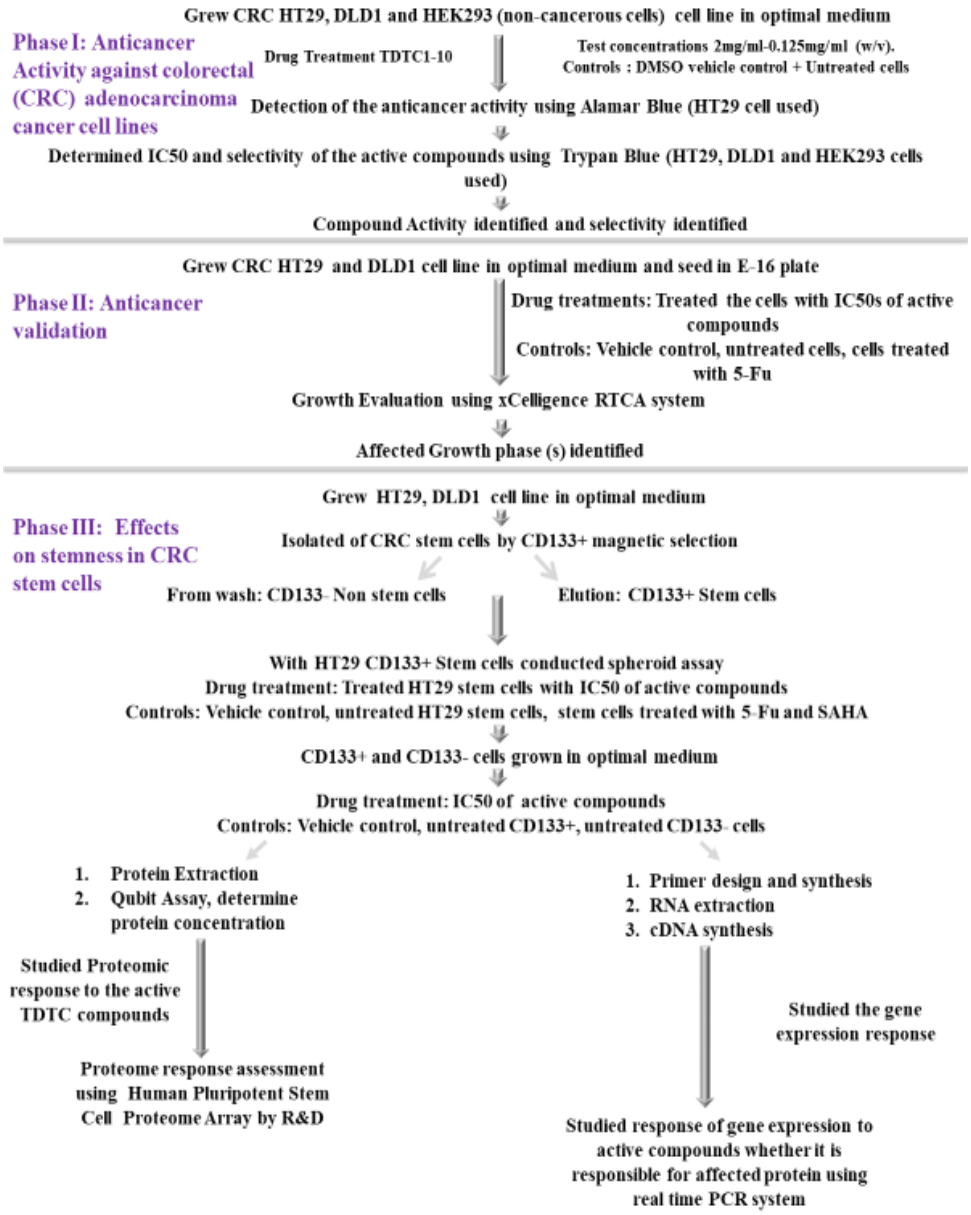


Figure 6: Flow diagram representing the experimental procedures performed. In a self-illustrative workflow explained above, the anticancer activity of novel tetrazole based dithiocarbamate derivatives were assessed first by screening with Alamar blue to identify the active compounds and then by quantifying cell death induced by the active

compounds using Trypan Blue staining. The selectivity of the active compounds was assessed by treating non-cancerous cells (HEK293) with the active compounds. The anticancer activity of the compounds was further evaluated using the xCelligence real time cell analyser to monitor cell growth. Colon cancer stem cells (CD133+) were isolated from the HT29 and DLD1 colon cancer cell lines using magnetic cell separation. After this, the ability of the stem cells to form spheroids was assessed in the presence/absence of the active TDTCs. A proteome profiler array was used to determine the response of stem cell associated factors to TDTC treatment; and finally, mRNA expression of selected genes was quantified using Real time PCR.

2.1 Cell Lines, cell culture conditions

The colorectal adenocarcinoma cell lines HT29 ATCC® HTB38 ™ (stage II), DLD1 ATCC® CCL-221 ™ and HEK 293 ATCC® CRL-1573™ (Human embryonic kidney cells) were all maintained and grown in Dulbecco's Modified Eagle's Medium-Hams F12 (DMEM-F12) (1:1) (Gibco®, USA), supplemented with 10% v/v Foetal Bovine Serum (FBS) (Gibco®, USA) and 1000 u/ml v/v penicillin-streptomycin. Cultures were incubated at 37°C in 95% humidity with 5% atmospheric carbon dioxide (CO_2).

During sub-culturing, the previous medium was discarded, and the cells were washed with 1-2 ml of phosphate buffered saline (PBS) (Gibco) two-three times. Then 1-2 ml trypsin was added to the cells, and incubated for 3 minutes at 37°C. After this incubation, the trypsin was inactivated with DMEM-F12 supplemented with 10% FBS. The cells were collected into a 15 ml falcon tube and centrifuged for 3 minutes at 300 x g to pellet the cells. The supernatant was aspirated and fresh DMEM-F12 supplemented with 10% v/v FBS and 1000 u/ml penicillin-streptomycin was added to the cells. Then the cells were aliquoted into flasks with 5 ml of fresh DMEM-F12 supplemented with 10% FBS and 1000 u/ml v/v penicillin-streptomycin. The flasks were labelled with the passage number, cell type, and date and incubated at 37°C in 95% humidity with 5% atmospheric CO_2.

2.1.1 Stem cell isolation

HT29 and DLD1 stem cells were isolated from the heterogeneous cell mixture. Isolation of the stem cells was based on the differential cell surface expression of CD133 between the general cancer cell population and stem cells. The stem cells were isolated using Hematopoietic Human Tissue Kit (Miltenyi Biotec), using CD133 MicroBeads. These beads recognise and bind specifically to the CD133 epitope on the cancer stem cells, thus isolating stem cells from the entire cancer cell population It should be noted that only the cancer stem cells expressed cell surface CD133.

Anti-CD133 labelled magnetic microbeads captured the stem cells of the HT29 and DLD1 cells, respectively. Stem cell isolation buffer containing PBS, pH 7.2, 0.5% (v/v) bovine serum albumin (BSA) (Sigma-Aldrich) and 2 mM of EDTA (Sigma-Aldrich) was prepared. The buffer was kept at 4 °C allowing for optimum functioning. The unseparated cell population was cultured to 90% confluency and then harvested using trypsin. The cells were trypsinized and washed as described above and centrifuged for 3 minutes at 300 x g to pellet the cells. The supernatant was discarded, and 5 ml of PBS was used to wash the cells. The washed cell suspension was centrifuged for 10 minutes at 300 x g. The resulting pellet was subjected to 300 µl of stem cell isolation buffer, 100 µl of the FcR Blocking Reagent was added together with 100 µl of CD133 MicroBeads. The solution was mixed well and incubated for 30 minutes in the refrigerator.

After the incubation, magnetic separation was performed with MS columns. MACS separator was placed on the magnetic field, followed by the insertion of the column. The column was rinsed with 500 µl of stem cell isolation buffer. After this, 500 µl of the microbeads solution was passed through the column. The column was further washed 3 times with 500 µl of isolation buffer to elute the unlabelled cells. The column was then removed from the magnetic field and 1 ml of the stem cell isolation buffer was pipetted into the column. Immediately the magnetically labelled cells (stem cells) were flushed into a sterile collection tube by pushing the plunger.

The isolated CD133 positive (CD133+) stem cells were grown and maintained with PluriSTEM Human ES/iPS Cell Medium (Merck). The CD133 negative (CD133-) population was grown and maintained in DMEM: Hams F-12 medium supplemented with 5% (v/v) FBS and antibiotics. The cells were cultured in an incubator with 5% CO_2, 95% humidity at 37°C.

For all of the reported assays, the cells were grown and maintained under the above conditions.

2.2 Synthesis of tetrazole based dithiocarbamate derivatives

The tetrazole based dithiocarbamate derivatives (TDTC) used in the present study were a kind donation from Dr W. Younis at the University of Jeddah, Kingdom of Saudi Arabia, who originally synthesized these compounds (141) . For information purposes, the synthesis of the derivatives is briefly described below.

The TDTC derivatives **(T1-T10)** were obtained from 5-phenyl-2H-tetrazole (**fig 7**, [**2])** through an intermediate 2-(oxiran-2-ylmethyl)-5-phenyl-2H-tetrazole (**fig 7**, [**3])** by treating the former with epichlorohydrin at 120°C for 8h (142) . The reaction of [**3]** with different amines in 1:1 molar ratio in presence of CS_2 and H_2O at room temperature for 8h, resulted in the formation of the respective target derivatives TDTC 1-TDTC 10 **(fig 4)**. The structures of each of these derivatives were established by elemental analyses, including FTIR, ^{1}NMR, ^{13}CNMR and ESI-MS spectra (141, 142).

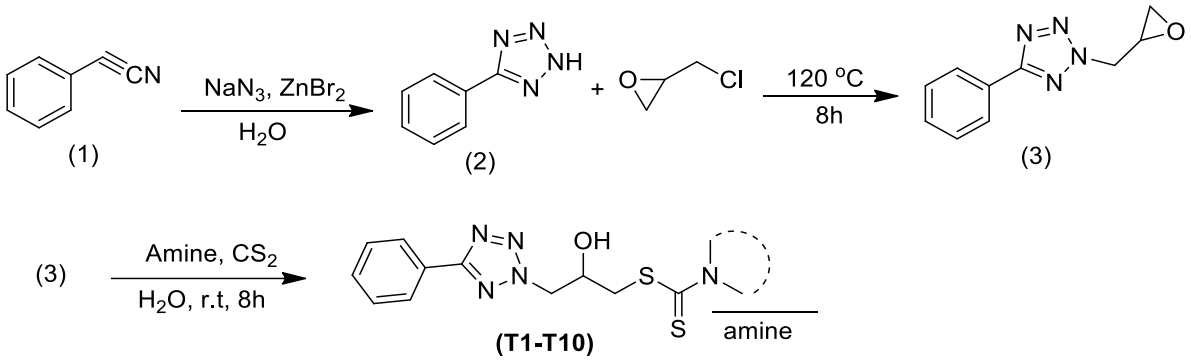


Figure 7: Synthesis of tetrazole based dithiocarbamate derivatives (141)

2.2.1 TDTC treatment of cells.

For use in *in vitro* cell culture analyses, stock solutions of the TDTC were solubilized in dimethyl sulfoxide (DMSO) (Sigma Aldrich, Germany) and stored at -20°C. These stock solutions were further diluted to the required concentrations in culture medium.

2.2.2 Controls

The control experiments consisted of either untreated cells and/or vehicle controls, where an equivalent volume of DMSO used in diluting the TDTC compounds was added to the culture

medium. In downstream studies such as real-time cell impedance 5-FU was used as a drug positive control. In sphere assay 5-FU was used and SAHA was used as drug positive control that targets colon cancer stem cells.

2.3 Alamar Blue Screening Assay

The Alamar Blue screening assay is high throughput drug screening tool used to monitor cell metabolism. Alamar Blue is a non-toxic resazurin dye that is metabolized by living cells to form the product resorufin that gives a magenta colour in culture media. When cells are exposed to test compounds, this dye is included to discriminate compounds that may have anticancer activity, through inducing cell death. The colour change induced by test compounds may be assessed both qualitatively, or quantitatively as Alamar Blue emits fluorescence. The fluorescence was measured with the 96 well plate spectrophotometer at 570 nm with 600 nm as a reference wavelength. With active anticancer compounds, the dye remains blue as the affected cells are metabolically inactive.

The cells were cultured to reach 60-70% confluency in 96 well culture plates (White Head Scientific). At this point, the cells were washed with sterile Phosphate Buffered Saline (PBS) (Gibco) and serum starved for 10 hours. Next, cells were treated with concentrations ranging from 0.01-0.4 mg/ml of each of the 10 TDTC compounds for 48 hours. Controls included untreated cells and vehicle control (0.2-0.5% v/v of DMSO). After 40 hours of treatment, HT29 cells were stained with a solution of 2.5 mM Alamar Blue. Metabolically active cells reduced Alamar Blue (resazurin) producing a magenta colour; while with non-responsive cells, Alamar Blue remained unchanged in colour. In the case of effective test compounds, it was expected for the Alamar Blue to remain unreduced. While the approach was to screen HT29 cells with the test compounds, to identify the active TDTCs, subsequently DLD1 cells representing stage III of colorectal cancer were treated with these selected active compounds.

2.4 Trypan Blue Exclusion Assay

Where treated cells were identified by the Alamar Blue assay to be metabolically inactive, these cultures were further subjected to the Trypan Blue dye exclusion assay. This was done to assess the percentage of cell death caused by the TDTC compounds and to determine the inhibitory concentration at which 50% of the cells were non-viable (IC50%). The IC50 concentration was obtained by exposing the cells to different concentrations of the compounds. Cell death percentages were obtained using automated cell counting. The concentration at which 50% cells were dead and 50% cells were living was considered as the IC50 concentration. Readings were done in duplicate.

Both HT29 and DLD1 cells were used in this assay. The cells were seeded into 6 well plates (2-5 10^4 cells/well) and cultured until reaching 60-70% confluency and were then serum starved overnight to synchronise the cells in G0 of the cell cycle. After this, they were treated for 48 hours with the active compounds diluted in culture medium containing serum. Following TDTC treatment, the cells were rinsed in PBS, harvested with trypsin and further washed with PBS before staining with 0.2% (v/v) Trypan Blue. Stained cells were mixed by pipetting and immediately loaded into a haemocytometer slide and read in a Countess II FL automated cell counter (Life Technologies, Germany). These readings were performed in duplicate and with two biological repeats. The cell viability percentage was retrieved from the cell count. The percentage of dead cells were expressed as mean ± Standard Error of the Mean (SEM).

2.5 Selectivity Assay

A selectivity assay was performed to identify whether the active compounds were selectively toxic to cancer cells only. Here, HEK293 cells (Human embryonic kidney cells) were used as the non-cancerous cell model that were exposed to the respective IC50 of each active compound for 48 hours. As described above, Trypan Blue was used to assess the toxicity of the active compounds against HEK293 cells.

The HEK293 cells were seeded into 6 well plates (2-5 x10^4 cells/well) and treated with each active concentration after reaching 60-70% confluency and being serum starved overnight. After drug treatment for 48 hours, the cells were rinsed in PBS, harvested with trypsin digestion and further washed with PBS before staining with 0.2% (v/v) Trypan Blue. As described above the stained

cells were subjected to the Countess II FL cell counter to obtain the cell viability and the percentage of dead cells [mean ± Standard Error of the Mean (SEM)].

2.6 Real-time cell impedance assay, assessing growth rate of the cells

The xCelligence Real Time Cell Impedance instrument (ACEA Biosciences Inc) is able to non-invasively monitor cell status, including factors such as number, shape or size and cell adhesion. The cells are seeded on high density gold electrode array plates. The cell adheres and grow on the gold electrode plates influencing the electrical impedance across the array. This electrical impedance is recorded and measured by xCelligence software as the Cell Index. The more rapid the cell growth the greater the value of the cell index. It is possible to monitor cell shape, size and cell adhesion by this instrument in real time (174). In this study, it was used specifically to assess the growth rate of the cells by plotting a growth curve in real time. Before cell preparation, the experimental schedule was programmed into the RTCA control unit. Such information included the layout of the experiment, incorporating the number and types of cells seeded, and the treatment and control wells. Each experiment was performed in duplicate.

The non-stem cell population ($CD133^-$ cells) of the HT29 and DLD1 CRC cell lines were isolated during the magnetic cell isolation process as explained above in section 2.1.1. The cells were maintained in DMEM-F12 medium (Gibco) supplemented with 5% FBS (Sigma-Aldrich) and penicillin-streptomycin antibiotics (Thermofisher). These were cultured to 100% confluency and then were harvested. A cell count was performed using 0.4% Trypan blue staining, for seeding into the wells of the RTCA plates. For HT29 cells, 1.345×10^7cells/ml were harvested, and 50 000 cells were seeded per well in the xCelligence 16 E-plate (ACEA Bioscience Inc). For DLD1 cells, $8,25 \times 10^6$ cells/ml were harvested, and 40 000 cells were seeded per well. The seeded cells were maintained with 200 µl of DMEM-F12 medium supplemented with 5% FBS and penicillin-streptomycin antibiotics. Before seeding the cells, for calibration purposes 100 µl of the culture medium was added to E-plates and a blank reading was performed for 1 minute. Once the cells were seeded, they were allowed to settle for 30 minutes and were then cultured for 24-25 hours before TDTC treatment. With treatment, old culture medium was replaced with fresh medium containing the relevant IC50 concentration/s of the DMSO solubilized TDTC compounds.

The IC50 concentrations of the drugs used were: -

TDTC 1= 0.4 mg/ml; TDTC 2= 0.4 mg/ml; TDTC 4= 0.3 mg/ml; TDTC 5= 0.35 mg/ml. The treatments lasted for 100-120 hours.

2.7 Cell Cycle Assay

The cell cycle assay was conducted using the MUSE™ Cell Cycle Kit (Merck Millipore, Germany), which contains the DNA intercalating dye propidium iodide (PI) and RNAse to distinguish cell cycle stages and increase specificity. The HT29 and DLD1 cells were seeded in 6 well culture plates (2-5x10^4 cells/well) grown to 60-70% confluency and were serum starved overnight. Next, the cells were exposed to the IC50 of the active TDTC compounds. The treatment was done for 48 hours; and it included both untreated cells and vehicle control (DMSO), respectively.

After 48 hours the cells were washed and harvested with trypsin. The cells were then transferred to a 12 x 75- mm polystyrene tube and centrifuged at 300 x g for 5 minutes at room temperature. The supernatant was discarded, and cells were further washed with 1 ml PBS and centrifuged again at 300 x g for 5 minutes. The supernatant was discarded without disturbing the cell pellet, leaving 50 µl of PBS. Next, the cells were resuspended in the residual PBS and then 1 ml of 70% chilled ethanol prepared with cold deionized water (stored at -20°C prior to using) was added in a dropwise fashion, whilst vortexing. The tube and the chilled 70% ethanol were always kept in ice. The ethanol-fixed cells were immediately stored in -80°C for future use.

For Muse cell cycle analysis, ethanol-fixed cells were thawed and 200 µl of the cells were transferred to new 12 x 75-mm polystyrene test tube, centrifuged at 300 x g for 5 minutes and the supernatant was discarded. The cell pellet was resuspended with 1ml of PBS and centrifuged at 300 x g for 5 minutes. The supernatant was aspirated off and the cells were resuspended with 200 µl of MUSE™ Cell Cycle Reagent and incubated at room temperature for 30 minutes in the dark. For cell cycle analysis, 50 µl of the stained cell suspension was diluted with 150 µl of PBS in 1.5 ml microcentrifuge tubes and then analysed using the flow cell. Doublet discrimination was performed by excluding cells that were not sorted as single form. The cells that did not form part of definite cluster were excluded, being considered as cells below baseline. HT29 cells that were included had a cell size index ranging from 2-4, with an increasing DNA content index ranging

from 4-10 throughout the treatment. Similarly, DLD1 cells that were included for analysis had a cell size index ranging from 2-4, but with an increasing DNA content index ranging from 2-9.

2.8 Spheroid Formation Assay

A 1.5 % solution of agar (BioRad) was prepared in sterile water in a Schott bottle and then placed in an autoclave for a cycle of 30 minutes to melt and sterilize it for cell culture use. Once cooled, the agarose was stored at 4°C. When the cells were ready for harvesting, the agar was warmed in a microwave at medium heat for 2 minutes. Once liquefied, 1.5 ml of agar was pipetted into each well of a 6 well plate. The gel was left to set for 20 minutes at room temperature in the laminar flow.

Following this, the CD133+ HT29 CRC stem cells grown to confluency of 80-90% were harvested. The CD133+ HT29 stem cells were isolated from the HT29 CRC population as explained in section 2.1.1

HT29 CRC stem cells were maintained as adherent cultures in 25 cm^3 flasks in PluriSTEM™ culture medium (Merck) supplemented with pen-strep antibiotics. Accutase (Biowest) was used to harvest the stem cells. Accutase is preferred over trypsin for stem cell harvesting, as it specifically dissociates non-adherent cells growing in clusters. The cell count was done using 0.4% Trypan Blue, and the cells were mixed thoroughly by pipetting to ensure that there was a single cell suspension, to obtain accurate readings. A final volume of 3ml was prepared containing a cell suspension of 30 000 cells, in PluriSTEM™ stem cell medium supplemented with pen-strep antibiotics. Included in this solution was either an active TDTC compound or a positive drug control (5-FU and SAHA)(refer to the test compound and positive drug formulation appendix F, table 12). The 3 ml solution was pipetted into each of the wells. The cells were placed in the incubator and cultured for 7 days (168 hours). Each day the cells were monitored for sphere formation. In order to replenish evaporated medium on day 4 of culture, 1.5 ml of fresh medium was added with half the concentration of the active compounds, to each culture well. Digital images were captured at different time points using the Floid™ Cell Imaging System (Thermofisher).

2.9 Analysis of the stem cell biomarker proteome

The cancer stem cell biomarker proteome was analysed using the "Proteome Profiler Human Pluripotent Stem Cell Antibody Array Kit" (R & D Systems, Biotechne). This is a membrane-based antibody array that simultaneously detects 15 recognised stem cell biomarkers. The included stem cell biomarkers were Oct4/3, Nanog, Sox2, E-cadherin, Sox17, AFP, Snail, VEGFR2, HCG, GATA-4, Goosecoid, Otx2, FoxA2, PDX-1 and TP63.

This analysis required the preparation of cell lysates that were incubated with a nitrocellulose membrane spotted with 15 different antibodies printed in duplicate, to detect the stem cell markers. All required buffers, biotinylated detection antibodies, streptavidin-HRP, and chemiluminescent reagents were included with this kit to enable the detection of stem cell markers from cell lysates. The preparation of the cell lysates is described below.

2.9.2 Proteome sample preparation

The HT29 and DLD1 stem cells were grown under the above-mentioned conditions. The stem cells were treated with the active compounds TDTC 1 (0.4 mg/ml), TDTC 2 (0.4 mg/ml), TDTC 4 (0.3 mg/ml) and TDTC 5 (0.35 mg/ml), DMSO (vehicle control), respectively, at a confluency of 60-70%. The treatment duration was for 48 hours. Before cell treatment, the cells were synchronized by serum starvation overnight: the PluriStem medium was removed, the stem cells were rinsed in serum-free DMEM-F12 and were maintained with DMEM-12 medium containing only antibiotics. The study also included the untreated CD133- population of the HT29 and DLD1 cells, respectively.

After the 48 hours of treatment, the cells were rinsed in PBS and harvested by mechanical scraping. After adding 2 ml of fresh PBS into the flask, using a sterile cell scraper, the cells were dislodged from the culture surface into solution. The PBS cell solution was transferred into a 15 ml Falcon tube and centrifuged at 300 x g for 3 minutes, to pellet the cells. After this the supernatant was aspirated off, and the cells were further washed in 2 ml of PBS by centrifugation; and the PBS was aspirated off. The cell pellet was solubilized in Lysis Buffer 16 (R & D) that contained a protease inhibitor cocktail. The solution was mixed by pipetting and then the cell lysate was rocked gently at 4 °C for 30 minutes. After this, the solution was transferred to microcentrifuge tubes and centrifuged at 14 000 x g for 5 minutes at room temperature. The supernatants were aliquoted into clean test tubes and stored at -70°C for further use.

To normalize protein concentrations, protein concentration was determined using the Qubit Protein Assay (Thermofisher), as compared to Qubit Protein Standards. The protein standards and protein samples were mixed with Qubit working solution in clear PCR tubes (The Qubit working solution was made up of Qubit Protein Reagent and Qubit Protein Buffer using a dilution of 1:200). Ten microliters of protein standard were mixed with 190 µl of the working solution. To measure the protein samples, 2 µl of the protein was mixed with 198 µl of the working solution. The mixture was incubated for 15 minutes at room temperature. After 15 minutes the standards and samples were read in the Qubit 2.0 Fluorometer (Thermofisher).

2.9.3 Proteome Procedure

2.9.3.1 Membrane incubation with protein lysate

Once concentrations obtained from Qubit were normalized with reference to the lowest protein concentration, protein profiling was carried out. The maximum protein volume that was required for incubation with the membrane was 167 µl; and where there was a deficit in volume, this was supplemented with Lysis Buffer 16. To the 167 µl of protein volume, 833 µl of Array Buffer 1 was added to each sample. Before normalization, the membranes were blocked with Array Buffer 1 at room temperature in a multi-well dish for an hour on an orbital shaker. All procedures were performed whilst membranes were on the shaker. After an hour's incubation, Array Buffer 1 was aspirated off, and the 1 ml solution of protein sample was added into each well and incubated overnight at 4°C.

2.9.3.2 Primary antibody incubation

Following overnight incubation with protein lysates, the membranes were washed 3 times for 10 minutes with Washing Buffer prepared according to manufacturer's protocol. The primary biotinylated antibody cocktail was reconstituted with deionized water, then further diluted with Array Buffer 2/3 (a mixture of Array Buffer 2 and Array Buffer 3). When the washing was done, 1 ml of primary antibody solution was added to the membrane and incubated for two hours at room temperature.

Note: Note that following each incubation in the detection procedure was followed by washes. During washing, the membranes were placed in separate containers whilst the multi-well dish was cleaned with deionized water. After the wash, the excess wash buffer was drained off from the

membranes. After this the membranes were always placed into the multi-well dish with liquid already present in the dish.

2.9.3.3 Streptavidin-HRP incubation

After washing off unbound primary antibody, the next step in the procedure was to incubate the membrane with Streptavidin-HRP The streptavidin conjugated to horseradish-peroxidase was diluted with Array Buffer 2/3 according to the dilution factor supplied on the vial which is 1:2 . Once the washes were completed, membranes were immersed in 1 ml of Streptavidin-HRP solution and incubated for 30 minutes at room temperature.

Whilst the membranes were being washed Chemi Reagent 1 (hydrogen peroxide solution) and 2 (luminol solution) were prepared by mixing equal amounts of the two solutions; and this mixture was protected from light. When the washing was completed, 500 µl of Chemi Reagent Mix was pipetted onto the membranes and incubated for one minute. After this, the excess reagent was removed through a capillary effect and the membranes were then carefully wrapped with plastic wrap. It was important to ensure that the Chemi Reagent Mix was evenly spread and that there were no air bubbles trapped between the membrane and the plastic wrap. The membranes were exposed for 10 minutes in the ChemiDoc™ XRS + System (BioRad). The membranes were analysed using H image software, to give the spot intensity.

2.10 Quantitative Polymerase Chain Reaction (qPCR) (relative quantification)

Relative real time reverse transcription quantitative PCR was used to assess messenger RNA levels of selected genes following treatment with the active TDTCs. The sample preparation for RT-PCR is described below.

2.10.1 RNA Sample Preparation

As described previously, the HT29 and DLD1 CRC stem cells were maintained in PluriStem™ medium (Merck) to a growth confluency of 60-70%. After reaching this growth phase, fresh culture medium was supplemented with the IC50 concentrations of the active TDTCs and cells were cultured for a further 48 hours.

After 48 hours, the culture medium was aspirated off and the cells were washed once in sterile PBS. After adding 2 ml of fresh PBS into the flask, using a sterile cell scraper, the cells were mechanically dislodged from the culture surface into solution. The PBS cell solution was transferred into a 15 ml Falcon tube and centrifuged at 300 x g for 3 minutes, to pellet the cells. After this the supernatant was aspirated off, and the cells were further washed in 2 ml of PBS by centrifugation; and the PBS was aspirated off. Then, in preparation for RNA extraction, 600 µl of RTL lysis buffer (Qiagen) was added to the pellet and the cells were gently mixed until the solution was homogenous. Once completely lysed, the samples were stored at -80°C until RNA isolation was performed.

2.10.2 RNA isolation

RNA extraction was performed using the RNeasy RNA extraction kit (Qiagen), according to the manufacturer's instructions. Briefly, the samples were thawed on ice. Then 700 µl of 70% ethanol was added to the samples. Next, this solution was transferred into an RNeasy Mini spin column, placed in a 2 ml collection tube. The spin columns were centrifuged for 15 seconds (s) at 8080 x g, this being done twice. After each centrifugation, the flow-through was discarded. Subsequently, 700 µl of buffer RW1 (wash buffer) was added to the spin column and this centrifuged for 15s; followed by adding 500 µl of RPE buffer to the spin column and centrifuging for 15s. Following this, 500 µl of RPE was added to the column for centrifugation for 2 minutes. Prolonged centrifugation ensures that no residual ethanol is left as this may have a negative effect on a downstream application, such as qPCR. The RNeasy spin column was placed into a new labelled 1.5 ml tube. Thirty microliters of RNase-free water were added directly to the spin column membrane. This was centrifuged for 1 minute to produce an eluate of purified RNA. Since RNA is susceptible to enzymatic degradation, the tube was placed immediately in ice. The RNA was then stored at -80°C for further processing.

2.10.3 Quality Assessment of RNA

The RNA was thawed on ice for evaluation using the Nanodrop Spectrophotometer; to quantify the RNA, to assess sample purity (A260/280 ratio) and quality (A260/230 ratio). Before reading the concentration of the RNA, the Nanodrop pedestal was cleaned with RNase-free water and blanked with the RNase-free water. An amount of 2 µl of each RNA sample was placed on the instrument's pedestal for spectrophotometric measurement. A260/A280 ratio assesses the purity of the RNA, checking for DNA/Protein contamination. The A260/A230 ratio, assesses for the residual ethanol or salt contamination.

The Nanodrop gave RNA concentrations ranging from 93,47-355,89 ng/µl. The RNA was pure as the A260/A280 ratio was ~ 2 and above. The RNA had a little trace of residual ethanol or salt contamination as the A260/A230 ratios ranged between 1,42 (shows trace of residual ethanol or salt contamination) to 2,07 (free of residual ethanol or salt contamination). Please see Appendix H the table of RNA concentrations together with values obtained for the ratios.

2.10.4 Complementary DNA (cDNA) synthesis.

The RNA concentration was normalized with reference to the lowest concentration. For cDNA synthesis 747,76 ng of RNA was used. Those samples with high RNA concentrations were diluted with nuclease-free water to achieve 747,76 ng of RNA in a thin wall PCR reaction tube, as 8 µl was the final volume for the RNA template. The 8 µl was supplemented with 1 µl of 10X dsDNase Buffer and 1 µl of dsDNase (Thermo Scientific). All reagents were stored on ice. After gently mixing, the mixture was briefly centrifuged using a Combi-spin mini-fuge (BOECO) for 30 s. The tubes were then incubated for 2 minutes at 37°C in an MJ Mini preheated thermocycler (Bio-Rad). After this, the RNA template solution was chilled in an ice block and briefly spun for 30 s and placed in the ice block again. In the same tubes, more components were added including, 4 µl of 5X Reaction Mix, 4 µl of nuclease-free water and 2 µl of Maxima Enzyme Mix (Thermo Scientific). The components were gently mixed and centrifuged in the Combi-spin for 30 s. Then, incubated in thermomixer (MJ Mini preheated thermocycler (Bio-Rad) for 10 mins at 25 °C followed by 15 mins at 50°C and the reaction was terminated by heating the solutions at 85°C for 5 mins. The cDNA was stored at -20°C for qPCR. cDNA quality and concentration were assessed using again the Nanodrop Spectrophotometer. Pure cDNA was obtained the A260/A280 ratio were > then 1,6 and A260/A230 ratio was > 1,5, the samples were free of contamination. The cDNA concentrations ranged from 1166,82-22367,10 ng/µl. Please see Appendix I for each sample's concentration and ratios. The cDNA was diluted with a 1:180 dilution with nuclease-free water and further normalized with reference to the lowest concentration, <4667,28 ng of cDNA was used for qPCR.

2.10.5 Primer Preparation

Primers were designed using the Primer-Blast from National Centre for Biotechnology Information (NCBI). *Homo-sapiens* transcripts/mRNA were specifically used retrieved from GeneBank, NCBI. Amplicon products were less than 235 nucleotides, an acceptable product size for real-time PCR

(175) . The length of the primers ranged from 19-22 nucleotides. The melting temperatures of the primers were 60±0.7°C; and the GC content was approximately 45-60%. The self-complementarity score was <4 and self3' complementarity was <1. This is important to prevent the dimerization of primers. Low complementary scores indicate less chances of primer dimerization. The Gene Bank accession numbers for each gene used for the primer design are summarized in Table 2.

Table 2: Summary of the primers used in the assessment of active TDTC modulation of gene expression of colorectal stem cells.

Gene Name of the Primer	Gene Bank Accession Number	Sequence	Gene Identity	Optimal Annealing Temperature (°C)
RPL0-Forward (F)	NM_001002.4 NM_053275.3	CAATGTTGCCAGTGTCTGTCTG	Housekeeping gene (HKG)	60
RPL0-Reverse (R)		TTGACCTTTTCAGCAAGTGGGA	HKG	60
E-cadherin-F	Z13009.1	AGCCCTTTCTGATCCCAGGT	Target Gene (TG)	54
E-cadherin-R		CGTACCGCTGATTGGCTGA	TG	54
Beta Catenin-F	NM_001904.4	TGCTAGGGTGGTGAGTGTTTG	TG	60
Beta Catenin-R		GGTCCACGGTTCCCATTTAGT	TG	60
Fox A2-F	NM_153675.3	GGCGAGTTAAAGTATGCTGGGA	TG	60
Fox A2-R		CATGTTGCTCACGGAGGAGT	TG	60
Sox17-F	NM_022454.4	GGACCGCACGGAATTTGAAC	TG	54
Sox17-R		GGACACCACCGAGGAAATGG	TG	54
VEGFA-F	NM_001025366.3 NM_001171623.1	TCACCAAGGCCAGCACATAG	TG	60
VEGFA-R		CACCAACGTACACGCTCCA	TG	60
VEGFR1-F	NM_002019.4	GGTCTTTGCCTGAAATGGTGAG	TG	60
VEGFR1-R		TGGTTTGCTTGAGCTGTGTTC	TG	60 and 54 (HT29 cells)
VEGFR2-F	NM_002253.3	CTCTGTGGGTTTGCCTAGTGT	TG	54
VEGFR2-R		AAGCCAGTCCAAGTCCCTCT	TG	54
VEGFR3-F	NM_182925.5	CCATGACCCCAACGACCTAC	TG	Not established (Gene not amplified)
VEGFR3-R		CTCCGACAGCTCCCCATACT	TG	Not established (Gene not amplified)

2.10.6 Solubilization of Primers

The primers were synthesized by Integrated DNA Technologies (IDT) (Whitehead Scientific). The lyophilized primers contained in sterile tubes were first centrifuged in a mini-fuge for 30 s; and then nuclease-free water was added (Table 3) to solubilize them. Using nuclease free water, the primers were prepared as a 10 x nanomole stock solution, according to the data sheet. From this stock, 20 µl of each primer solution was aliquoted into a sterile tube for qPCR. The primers were stored at -20°C for subsequent use. Nine genes were used for the gene expression study.

Table 3: Summary of each primer's specific characteristics (IDT)

Primer	Molecular Weight (g/mol)	Moles (nmol)	Nuclease-free Water added (µl) (nmol x 10)	Melting Temperature (°C)
VEGFA-F	6.080	40	400	57.4
VEGFA-R	5.686	30.7	307	57.7
RPLO-F	6.732	45.5	455	56.4
RPLO-R	6.765	37.7	377	56.9
VEGFR3-F	5.957	37	370	57.7
VEGFR3-R	5.957	39.7	397	58.5
VEGFR2-F	6.450	45.3	453	57
VEGFR2-R	6.022	39.4	394	58.2
VEGFR1-F	6.821	35.9	359	56.3
VEGFR1-R	6.465	33.4	334	56.2
β-catenin-F	6.529	36.5	365	57.2
β-catenin-R	6.388	40.1	401	57.1
FoxA2-F	6.879	48.1	481	57
FoxA2-R	6.173	38.1	381	57.3
Sox17-F	6.151	37.9	379	57
Sox17-R	6.185	36.8	368	58.2
E-Cadherin-F	6.044	43.2	432	58.4

E-Cadherin-R	5.819	39.3	393	57.6

2.10.7 Relative real time quantitative PCR (qPCR)

Following on from the results obtained in the proteome analysis, eight significantly downregulated and upregulated proteins were selected for mRNA expression analysis using relative quantitative real time PCR. Log2 (fold change) values >2 for upregulated genes and > -0.1 for downregulated genes were considered as values that indicated the effectiveness of the test compounds on the stem cell biomarker gene expression. This was done using SYBR green assays. SYBR Green dye binds to double-stranded DNA especially at the minor grooves of the double-stranded DNA. The fluorescence intensity of the dye increases as it binds to newly synthesized double-stranded DNA in the polymerase chain reaction. Thus the quantified fluorescence intensity correlates to the amount of DNA amplified (176).

Four MicroAmp^{TM} Optical 96-well Reaction Plates (Thermofisher) were run in triplicate using the Applied Biosystems 7500 real-time PCR system. Each well contained 5 µl of SYBR green master mix, 0,5 µl of forward and reverse primer, 4 µl of cDNA. The cDNA as mentioned above was further diluted.

Normalization calculations were done, with the lowest concentration being used as a reference. Samples with high cDNA were further diluted with nuclease-free water to a total volume of 4 µl. The mixing of components was all performed in the MicroAmp^{TM} Optical 96-well Reaction Plates (Thermofisher) on an ice block. After adding all components to the plates, these were briefly centrifuged at 1500 rpm for 1 min to ensure proper mixing of the solution and to remove air bubbles. The reaction cycle is described in Table 4 below. After the PCR amplification, a melt curve analysis was run for each gene. The majority of the primers produced a specific amplification with single amplitude curves being observed, indicating a lack of primer dimer formation (Appendix L).

Table 4: The Cycles for qPCR			
Cycling conditions	Duration	Temperature °C	Reason
Step 1	5 minutes	95	Hold stage and Activate the polymerase
Step 2 (40 cycles)	15 seconds	95	Denaturing Double-Stranded cDNA
	15 seconds	60 and 54	Primer annealing
	10 seconds	72	Elongation
Melt cycle conditions	10 seconds	95	Initial Dissociation of Double-Stranded DNA (amplicon)
	10 seconds	0.2 increment each from 60-95	Final Dissociation of Double-Stranded DNA (amplicon)

Chapter 3

Results

3.1 Anticancer activity of TDTCs

Out of the ten TDTC compounds tested, four of these showed anticancer activity against HT29 CRC cells as indicated by Alamar Blue screening. Alamar Blue remained unreduced in cells exposed to each of TDTC 1, 2, 4 and 5. The anticancer activity of the TDTC compounds was seen at concentrations of 0.22-0.4 mg/ml. TDTC 1 and TDTC 2 were actively inhibiting the CRC cells at 0.4 mg/ml, TDTC 4 was active at 0.22 mg/ml and TDTC 5 was inhibitory at 0.35 mg/ml. Alamar Blue was reduced in cells treated with DMSO (vehicle control), indicating that DMSO had no toxic effects on cell metabolism and thus did not contribute to the effects of the active TDTC compounds (Table 6).

Table 6: Alamar Blue assay, anticancer screening of TDTC compounds against HT29 CRC cell lines.

TDTC compounds	**Concentration (mg/ml) HT29 CRC cell line**			
TDTC 1	0.4	0.2	0.1	0.05
Active[a]	Yes	No	No	No
TDTC 2	0.4	0.2	0.1	0.05
Active[a]	Yes	No	No	No
TDTC 3	0.4	0.2	0.1	0.05
Active[a]	No	No	No	No
TDTC 4	0.22	0.11	0.055	0.0275
Active[a]	Yes	No	No	No
TDTC 5	0.34	0.17	0.085	0.0425
Active[a]	Yes	No	No	No
TDTC 6	0.16	0.08	0.04	0.02
Active[a]	No	No	No	No
TDTC 7	0.6	0.3	0.015	0.0075
Active[a]	No	No	No	No
TDTC 8	0.14	0.07	0.035	0.0175
Active[a]	No	No	No	No
TDTC 9	0.34	0.17	0.085	0.0425
Active[a]	No	No	No	No
TDTC 10	0.14	0.07	0.035	0.0175
Active[a]	No	No	No	No

[a] For active compounds Alamar Blue remained blue (not reduced) indicating that cells are metabolically inactive. ≥ 40% of the cells should be metabolically inactive if Alamar Blue is not reduced.

3.2 Active TDTCs induced cell death in CRC cell lines (stage II and stage III)

TDTC compounds (TDTC 1, 2, 4 and 5) were selected for further anticancer evaluation using the Trypan Blue dye exclusion assay. HT29 (stage II) and DLD1 (Stage III) cells were treated with the compounds for 48 hours (**fig 8**). With HT29 cells, at 0.3 mg/ml TDTC 1, 2, and 5 induced approximately 64.74±2.90% to 52.62±1.80% cell death. Whilst in DLD1 cells 56.36±10.97% to21.70±0.94% cell death was observed. At 0.2 mg/ml in HT29 cells 25.56±3.32% to 16.72±3.89% cell death was induced by TDTC 1, 2, 4 and 5; whilst in DLD1 cells, at 0.2 mg/ml 63.41±3.31% to 9.18±0.69% cell death was induced. For 0.1 mg/ml, 31.53±0.26% to11,99±1.21% cell death was induced in HT29 cells by TDTC 1, 2, 4 and 5. In DLD1 cells 68.94±4.89% to 8.28±0.2% cell death was induced. TDTC 4 at 0.22 mg/ml induced 66.13±3.11% in HT29 cells; and in DLD1 cells 53.75±2.00% cell death was induced. The active TDTC compounds were less effective in HEK293 cells (Human Embryonic Kidney cells), having a cell death percentage ranging from 8.82±1.75% to 1.85±1.61%. Overall, the TDTC 1, 2 and 5 compounds were more effective at low concentration against the DLD1 cell line.

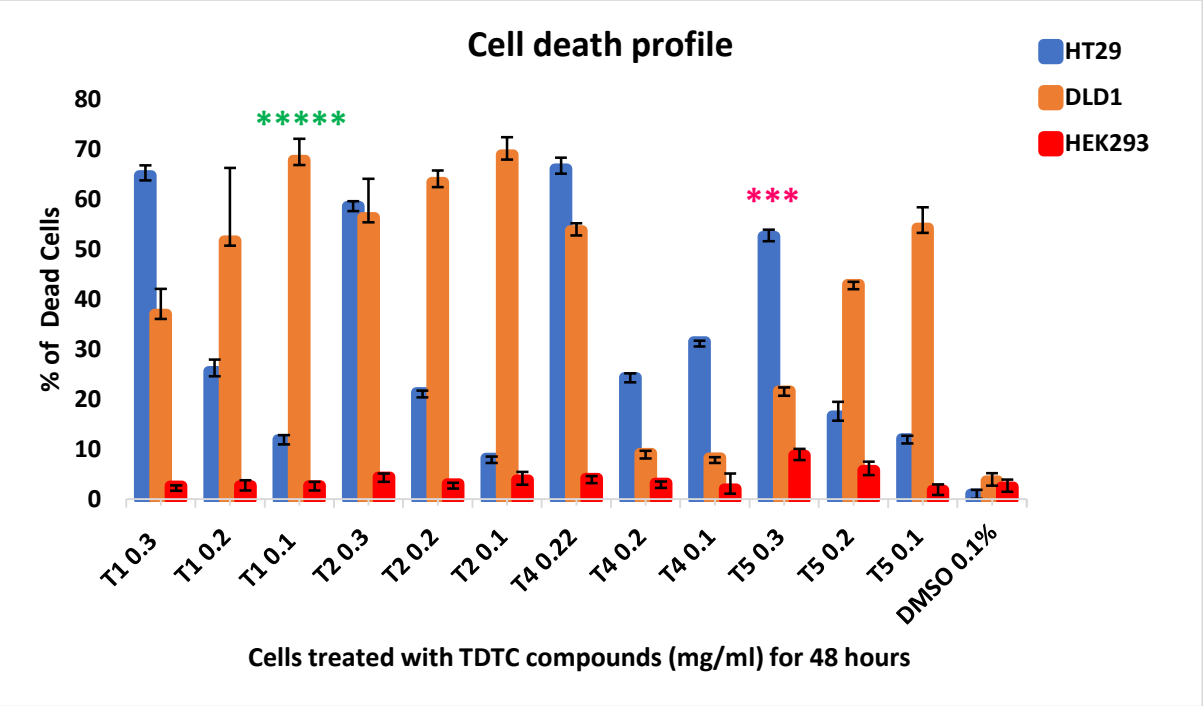


Figure 8: Bar graph representing the cell death profile after TDTC treatment in each of HT29, DLD1 and HEK293 cells.

The **c**ell death profile was evaluated with the Trypan Blue dye exclusion assay. Anticancer activity is represented in terms of mean ± SEM of the cell death percentage (y-axis) induced by the TDTC 1, 2, 4 and 5 (x-axis) in HT29, DLD1 and HEK293 cells. The TDTC compounds induced cell death ranging from 66%-68% for HT29 cells. In 69%-68% cell death was induced by the compounds in DLD1 cells. In HEK293 (normal non-cancerous cells), only 9%-2% cell death was observed at respective IC50s of the tested TDTCs. 0.1% DMSO represents the vehicle control where the cells were treated for 48 hours. The values were significant at p-value of ≥ 0,0001 (***) and for p value of <0,000001 (*****) for the relationship between the three cell lines. Comparing between HT29 and HEK 293 cells; and between DLD1 and HEK 293 cells. The concentration effects of TDTCs on cell death is represented in appendix N, table 20. Data was analysed using a t-test for independent samples using STATISTICA software.

As high concentration of the active TDTCs caused 50% cell death (Table 7). Whilst low concentration of the active TDTC (**fig 8**) rendered a higher percentage of cell death. The IC50 of the HT29 was higher than that of the DLD1 for TDTC 1 and 4, while TDTC 5 had the same IC50 concentration for both cell lines. The IC50 of HT29 was 0.4 mg/ml for TDTC 1 and 2, 0.3 mg/ml for TDTC 4 and 0.35 mg/ml for TDTC 5. In DLD1 the IC50 were 0.3 mg/ml for TDTC 1, < 0.1 mg/ml of TDTC 2, 0.25 mg/ml for TDTC 4 and 0.35 mg/ml for TDTC 5.

Table 7: Indicates the IC50 of the active TDTC compounds against HT29 (stage II) and DLD1 (stage III).

	IC50 concentration	
TDTC compounds	**HT29**	**DLD1**
TDTC 1	0.4 mg/ml	0.3 mg/ml
TDTC 2	0.4 mg/ml	<0.1 mg/ml
TDTC 4	0.3-0.22 mg/ml	0.25-0.22 mg/ml
TDTC 5	0.35-0.3 mg/ml	0.35 & 0.2 mg/ml

3.4 The active TDTCs affects the growth phases of CRC cells

The real time cell impedance (xCelligence) assay was used to assess the growth of the CRC cells exposed to the respective IC50 of the active test compounds and conventional CRC drug 5-fluoruracil (5-Fu) for 100-120 hours. For each treatment, the cell index which correlates to the ability of the cells to adhere to the culture surface and proliferate, was calculated using the xCelligence analysis software.

As shown in the HT29 growth curve (**fig 9**), some of the active TDTCs may have similar mode of action to 5-FU. The conventional drug allowed the cells to grow exponentially to reach a steep

peak (cell index 1.5) at 48 hrs, followed by a drop in cell growth after 48 hrs. The cells exposed to 5-Fu reached a negative cell index of -0,2.

TDTC 1 (0.4 mg/ml), there was no steep growth and a slight decline in cell index was observed from a cell index of 1.2 to 0.4 at 116 hrs. At 0.2 mg/ml TDTC 1, showed a much better inhibitory effect on cell growth compared to when the concentration of TDTC 1 is higher (0.4 mg/ml) TDTC 1 (0.2 mg/ml) had a decline of cell index from 1.3 to 0.1. TDTC 2 (0.4 mg/ml), prevented the cells from growing exponentially, accelerated decline of cell growth was observed from cell index of 1 at 44 hrs to 0.3 at 116 hrs. TDTC 4 (0.3 mg/ml) showed no significant inhibitory effect on the CRC cells as the growth pattern of the cells were similar to untreated cells.. The growth pattern observed with cells exposed to TDTC 5 at 0.35 mg/ml was like cells exposed to 5-Fu. The cells exposed to TDTC 5 had a pronounced growth indicated by cell index of 1.8, which was followed by decline in cell growth to a cell index of 0.75 at 116 hrs.

The conventional drug 5-Fu may show greater cell growth inhibition, but the active TDTCs appear to be inhibiting the exponential phase. 5-Fu inhibits growth at the beginning of stationary phase. TDTC 1 is effective around the late stationary phase, it is also shown that a lower concentration of the compound is more active. TDTC 2 reduces the exponential growth phase, this is advantageous. TDTC 4, has shown no impact on the growth phases, as its pattern is like the untreated HT29 cells. Effects of TDTC 5 was similar to 5-FU but was less potent in reducing cell growth.

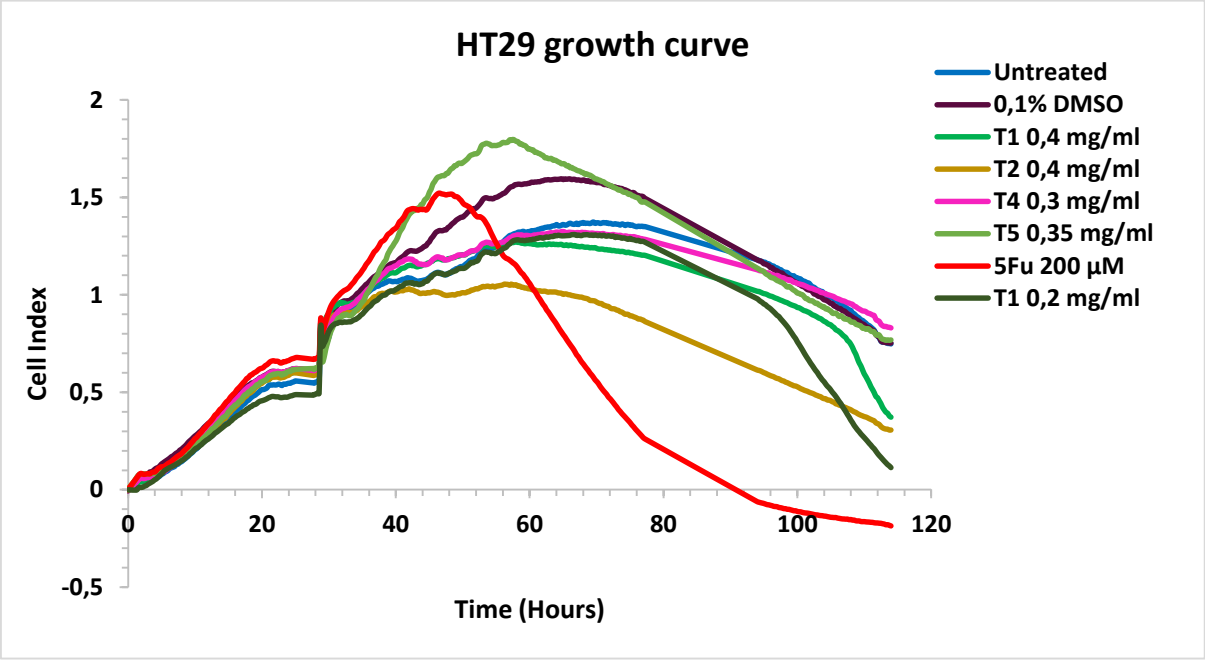


Figure 9: HT29 cell growth phases are affected by the active TDTC compounds.

A cell index vs time plot shows the growth of the HT29 cells exposed to active TDTC compounds. The ability of the cells to attach and grow is reflected as the cell index. A decrease in cell index indicates less cell attachment to the substrate indicating loss of cell viability. TDTC 1 (T1 0.4 mg/ml green) and 0.2 mg/ml TDTC 1 (dark green) were effective around late stationary phase of cell growth. TDTC 2 (T2 0.4 mg/ml orange) reduced exponential growth phase of the cells (cell index of 1 reduced to 0.3). TDTC 4 (T4 0.3 mg/ml pink) was similar to untreated cells which had high cell index of 1.3 and low index of 0.8 at 116 hrs. TDTC 5 (T5 0.35 mg/ml light green) had similar growth suppressive trend as 5-Fu having steepest cell index 1.8 at exponential phase and a drop of cell index to 0.75. 5-FU (5Fu-200 µl red) showed greater potency in terms of reducing the cell index. It had steep growth, but the cell index dropped to -0.2. 5- Fu was most effective at the early stationary phase.

In late stage CRC cell line DLD1 (stage III) (**fig 10**), the compounds and conventional drug (5-FU) affected the cells growth differently. DLD1 cells grew rapidly reaching a maximum cell index of 6.6 at 24 hrs, whilst HT29 cells reached maximum cell index of 0.7 at 28 hrs. 5-Fu (200 µM) was potent in inhibiting cell growth of DLD1 cells from maximum cell index of 8.6 to 0.2. TDTC 1 (0.4 mg/ml) reduced the cell growth of DLD1 cells from 9.8 cell index to 3.2. TDTC 1 (0.2 mg/ml) had same effect on the cells as TDTC 1 (0.4 mg/ml). TDTC 2 (0.4 mg/ml) reduced cell index from 8.8 to 3.2. TDTC 4 (0.3 mg/ml) had a maximum cell index of 10.2, the compound reduced the index to 6.8. Untreated DLD1 and cells exposed to 0.1% DMSO (vehicle control) had similar cell index and growth pattern. Untreated DLD1 cells and vehicle controls grew reaching a maximum cell index of 9 and 9.4, respectively. In the span of 100 hours the growth of the untreated DLD1 and vehicle control dropped to cell index of 6.4 and 6.2, respectively. TDTC 4 and TDTC 5 had similar growth pattern as that of the untreated DLD1 and vehicle control.

In DLD1 cells, 5-FU reduced cell growth at late exponential phase. TDTC 1 was most effective at late stationary phase. TDTC 2 reduced cell growth at late exponential phase. TDTC 4 and TDTC 5 had no effect on the cell growth phases when compared to untreated and vehicle controls.

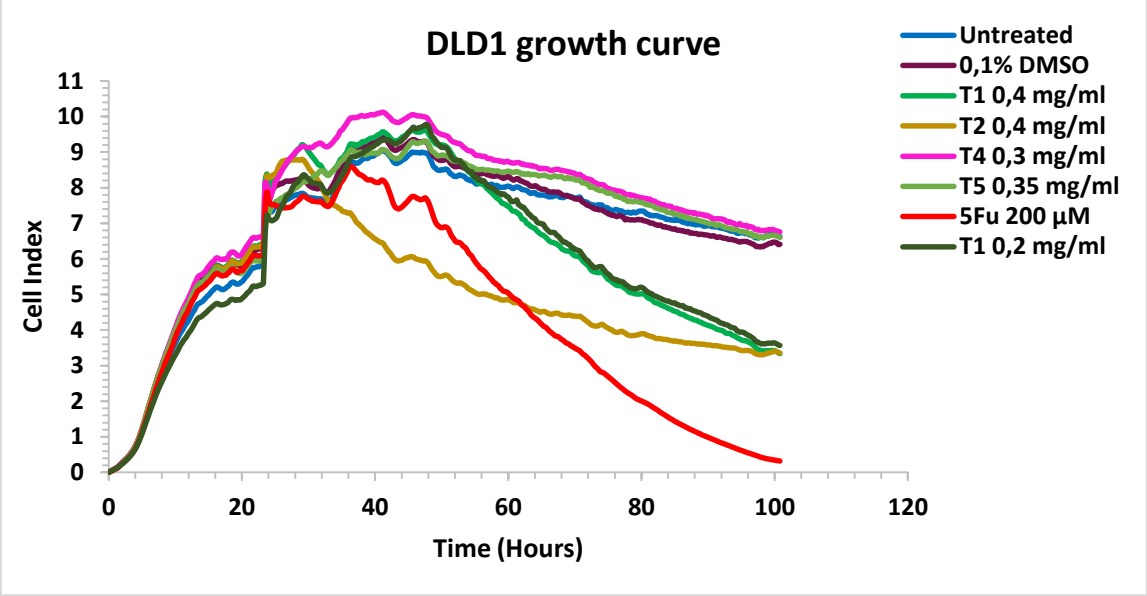


Figure 10: DLD1 cell growth phases are affected by the active TDTC compounds.

A cell index vs time plot shows the growth of the DLD1 cells exposed to active TDTC compounds. The ability of the cells to attach and grow is reflected in terms of the cell index. A decrease in cell index indicated detachment of the cells from substrate as a result of cell death. TDTC1 (T1 0.4 mg/ml green) was effective around late stationary phase of cell growth. Same was with T1 0.2 mg/ml (dark green), both concentrations had a maximum cell index of 9.2 and cell index reduced to 3.2. TDTC 2 (T2 0.4 mg/ml orange) reduced cell growth at late exponential phase reducing cell index from 8.8 to 3.2. TDTC 4 (T4 0.3 mg/ml pink) and TDTC 5 (T5 0.35 mg/ml light green) had similar cell growth pattern as untreated DLD1 and vehicle control (0,1% DMSO). The maximum cell indexes of TDTC 4,5 and untreated DLD1 cells and vehicle control ranged from 10.2-9. Cell indexes were reduced to 6.8-6.2. 5-Fu (5Fu-200 µl red) showed greater potency in terms of reducing the cell index. It was effective at late exponential phase; it reduced the cell index from 8.2 to 0.2.

3.5 Effect of the active TDTCs on cell cycle in CRC cell lines

An analysis of the cell cycle was conducted on HT29 (stage II) and DLD1 (stage III) CRC cell lines to confirm the effectiveness of the compounds, cell cycle arrest being an important property for anticancer agents. The compounds arrested cell cycle in a differential manner in HT29 cells. In comparison in DLD1 cells, the compounds induced a uniform pattern of cell cycle arrest.

In HT29 cells, TDTC 1 at 0.4 mg/ml had minimal cell cycle arrest at G2/M phase. With TDTC 2 (0.4 mg/ml) treatment a G0/G1 phase cell cycle arrest was observed. TDTC 4 (0.3 mg.ml) arrested cells at S phase and TDTC 5 arrested cells at G0/G1 phase (**fig 11 & 13**).

For HT29 cells, TDTC 2, 4 and 5 the cell cycle arrest was significant.

In the DLD1 cell line, all of the TDTCs treatments (1,2,4 and 5) arrested cells in the S phase (**fig 12 & 14**).

When comparing the vehicle control (0.1% DMSO) with the test compounds, the difference observed for HT29 cells treated with TDTC 1 (0.4 mg/ml) was a 3.75% ± 3.18% and 4.5% ± 3.68% increase in gated cells for diploid nucleus and aneuploid cells respectively. There was 7.05% ± 4.88% increase in double diploid gated cells. In DLD1, diploid cells were decreased by 20.40% ± 3.68%, aneuploid and double diploid gated cells increased by 18.45% ± 8,70% and 8.65% ± 2.48% respectively in the presence of TDTC 1.

With HT29 cells exposed to TDTC 2 (0.4 mg/ml) there was a 41.05% ± 17.61% and 4.50% ± 3.68% increase in diploid and aneuploid gated cells respectively, whilst there was a 31.15% ± 7.57% decrease in double diploid gated cells. DLD 1 diploid cells decreased by 26.1 ± 3.25%, aneuploid and double diploid cells increased by 22.35% ± 2.76% and 3.8% ± 0.28% respectively.

HT29 cells, exposed to TDTC 4 (0.3 mg/ml) had an increase of 10.40% ± 5.66% diploid cells, 32.80% ± 5.66% increase in aneuploid gated cells and 31% ± 5.94% decrease in double diploid gated cells. Whilst in DLD1, diploid population decreased by 22.60% ±5.94% and aneuploid and double diploid population increased by 12.45% ± 4.60% and 9% ± 2.69% individually.

The HT29 cells, exposed to TDTC 5 (0.35 mg/ml) had a 27.85% ± 10.39% and 16.5% ± 2.40% increase in gated cells for diploid and aneuploid population respectively. Decrease of 32.35% ± 4.31% gated cells were observed for double diploid population. In DLD1 cells diploid population and aneuploid population increased by 11.25% ± 5.59% and 11.1% ± 8.77% respectively, while double diploid decreased by 6.7 ± 74.95%.

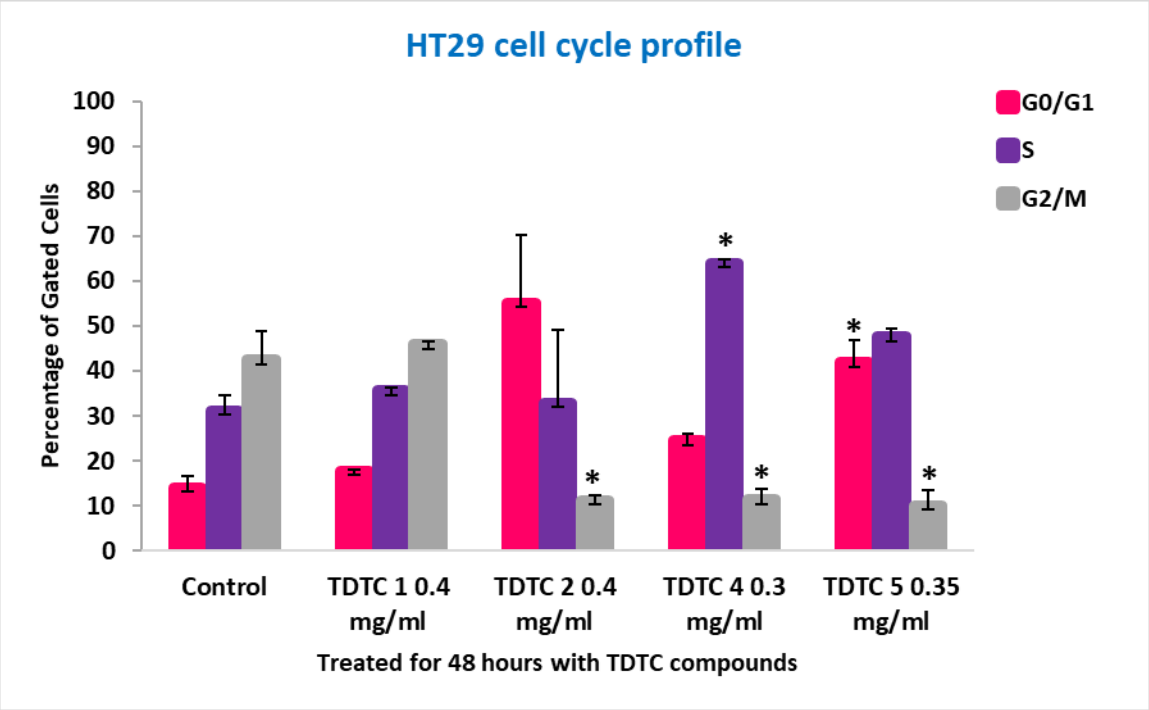


Figure 11: TDTC compounds induced differential cell cycle arrest in HT29 cells.

With reference to the control (0.1% DMSO), HT29 cells that were treated with TDTC 1 (0.4 mg/ml), showed no significant increase/decrease in the percentage of gated cells. With cells exposed TDTC 2 (0.4 mg/ml), there was an increased percentage of gated cells in G0/G1, when compared to the vehicle control; and a significant decrease in cells gated in G2/M phase ($p < 0.05$*). There was an increase in gated cell G0/G1 phase compared to control and decrease in G2/M phase cell. Significant of the G2/M phase was illustrated by (*, $p < 0.05$). TDTC 4 (0.3 mg/ml), S phase cell cycle arrest was observed ($p=0.01$ (*)) and a significant ($p=0.04$ (*)) decrease in G2/M gated cells. For TDTC 5 (0.35 mg/ml), compound induced significant G0/G1 cell cycle arrest and significant decrease in G2/M gated cells. The increase in gated cells with reference to the control indicates the phase at which cell cycle arrest occurred. T-test for independent samples was conducted for statistics using STATISTICA software. P-value <0.05 considered to be significant and n=2 for each treatment. The graph plot is of Mean ± SEM.

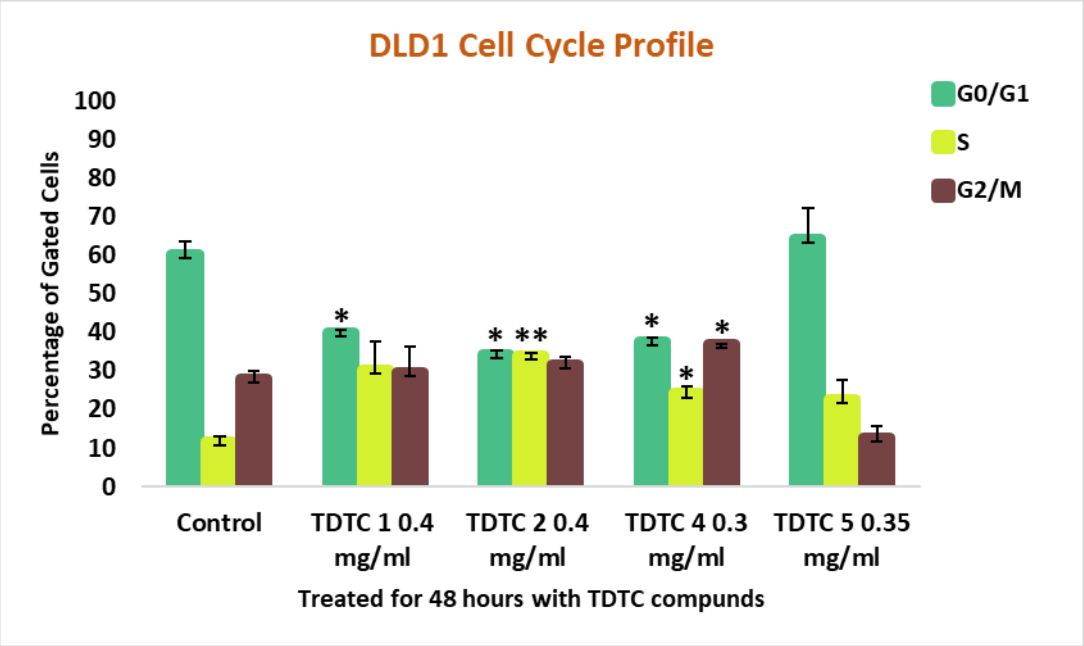


Figure 12: Bar graph representing the DLD1 cell cycle phase following treatment with TDTC for 48hours. TDTC compounds induced a uniform cell cycle arrest in DLD1 cells

With reference to the control cells (0.1% DMSO), TDTC 1 (0.4 mg/ml), TDTC 2 (0.4 mg/ml), TDTC 4 (0.3 mg/ml) and TDTC 5 (0.35 mg/ml) had an increase of gated cells in the S phase. A minimal increase was observed for TDTC 5. TDTC 1 had a pronounced (*, $p < 0.05$) decrease of G0/G1 gated cells. TDTC2 treatment resulted in a significant decrease in G0/G1 gated cells, but with a significant (**, $p \geq 0.001$) increase in S phase cells. For TDTC 4, there was a significant decrease in G0/G1 gated cells, increase in S phase and G2/M cells. The increase in gated cells with reference to the control indicates the phase at which cell cycle arrest occurred. A t-test for independent samples was conducted using STATISTICA software. P-value <0.05 considered to be significant and n=2 for each treatment. Plots is of Mean ± SEM.

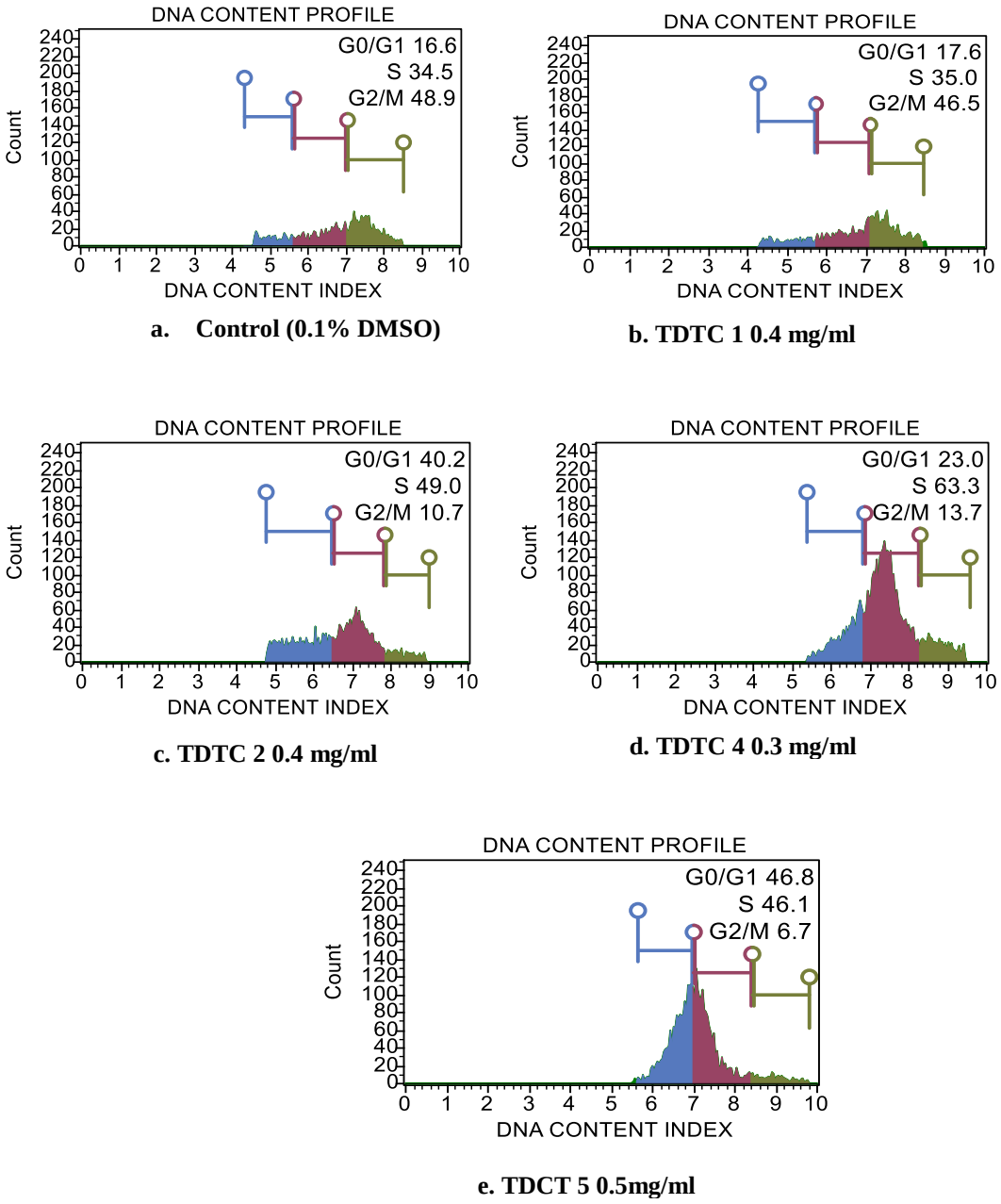
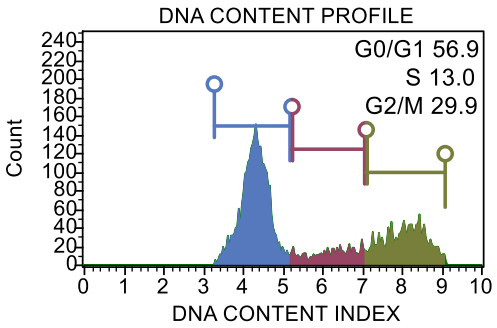
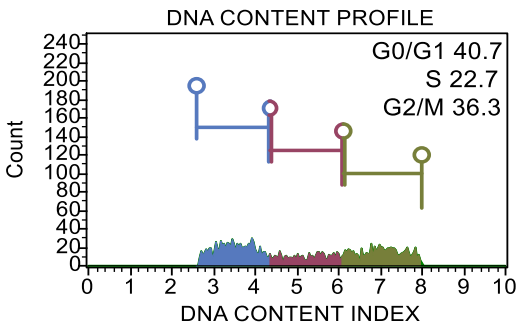


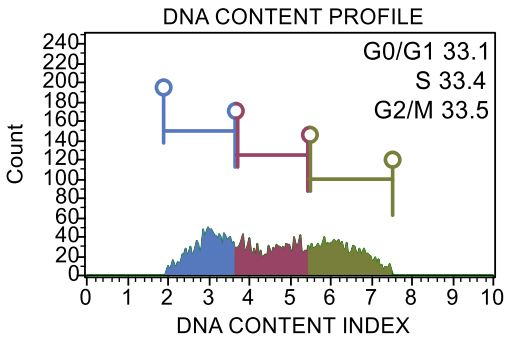
Figure 13: Cell cycle histograms of HT29 cells following TDTC treatments. a. Control (0.1% DMSO); b. TDTC 1 0.4 mg/ml; c. TDTC 2 0.4 mg/ml; d. TDTC 4 0.3 mg/ml; e. TDCT 5 0.5mg/ml. (b) TDTC 1 had a similar profile of gated cells in comparison to the control (a). (c) With TDTC 2 an increase in G0/G1 gated cells was observed. (d) There was an increase in cells in S-phase with TDTC 4. In HT29 cells treated with TDTC 5 there was an increase in percentage of gated cells in G0/G1 and S phase, with a larger percentage of cells being in G0/G1.



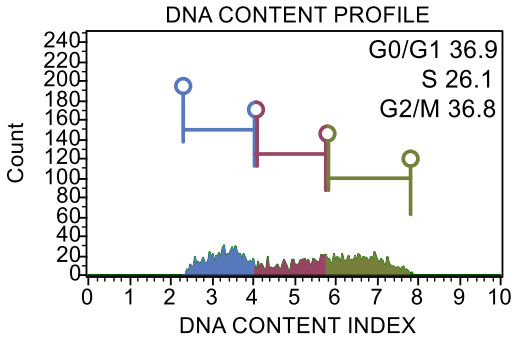
a. Control (0.1% DMSO)



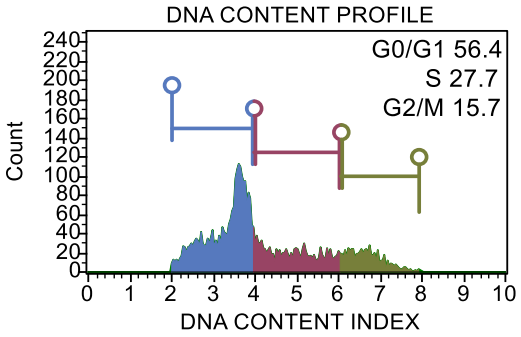
b. TDTC 1 0.4



c. TDTC 2 0.4 mg/ml



d. TDTC 4 0.3 mg/ml



e. TDTC 5 0.35mg/ml

Figure 14: Cell cycle histograms of DLD1 cells. a. Control (0.1% DMSO); b. TDTC1 0.4 mg/ml; c. TDTC 2 0.4 mg/ml; d. TDTC4 0.3 mg/ml; e. TDCT 5 0.5mg/ml. TDTC 1 (b), TDTC 2 (c), TDTC 4 (d), and TDCT 5 (e) treated cells in comparison to control (0.1% DMSO) had increase of gated cells in the S phase. In the control, approximately 56%, 13% and 30%of the cells were in G0/G1, S and G2/M phase respectively. In comparison to the control TDTC 1 had an increased percentage of gated cells in S phase which was 23%. TDTC 2, 4 and 5 had an increased percentage of gated cells in S phase, 33%, 26% and 28% respectively. All the compounds induced S phase cell cycle arrest.

3.6 The active TDTCs can modulate self-renewal of stem cells

A spheroid formation assay was performed to assess if the active TDTCs can prevent formation of stem cell spheroids in HT29 CRC stem cells. The formation of spheroids by cancer stem represents a morphological measure of stemness, whereby stem cells are able to self-renew and prevent penetration of compounds to the inner cells of the spheroid, promoting persistent tumour progression (177).

The HT29 stem cells were grown under ultra-low attachment conditions in agar coated wells and treated with either the active TDTCs, 0,1% DMSO, 5-Fluorouracil or Suberoylanilide Hydroxamic Acid (SAHA) for 168 hours. HT29 stem cells grew in ultra-low attachment conditions, being able to rapidly form spheroids (178).

It was observed that the active compounds are potent in preventing spheroid formation. The active compounds prevented stem cell aggregation (colony formation) and cells appeared to remain in single cell form. The vehicle control and untreated cells were healthy, lacking any irregularities in cell morphology (cells size was normal) and as expected formation of spheroids was observed. Notably, the active TDTCs showed greater potency in halting spheroids than SAHA. With regards to the conducted assay, SAHA did compromise the health of HT29 stem cells, although the stem cells appeared to shrink compared to untreated, 0.1% DMSO and 5-Fu at 168 hours, they nevertheless still did aggregate with each other (**fig 15 a, b & g**). The conventional drug used to treat CRC was not effective in preventing HT29 stem cells from forming spheroids (**fig 15 g**). TDTC 1 and 2 was more effective as it prevented spheroid formation from 48 hours of culture (**fig 15 c & d**).

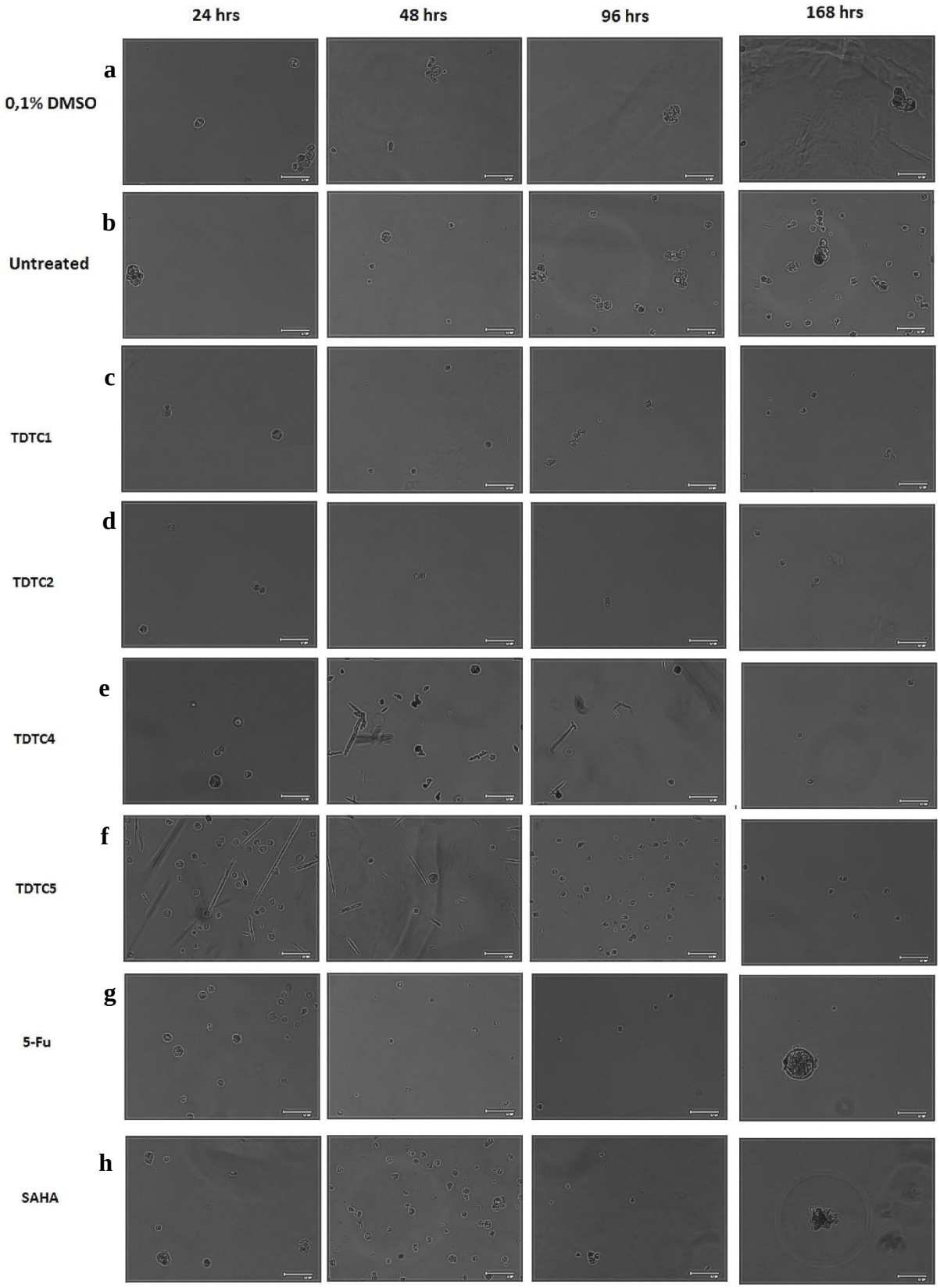

24 hrs
48 hrs
96 hrs
168 hrs
a
0,1% DMSO
b
Untreated
c
TDTC1
d
TDTC2
e
TDTC4
f
TDTC5
g
5-Fu
h
SAHA

Figure 15: The active TDTCs can modulate self-renewal of stem cells. a, b, c, d, e, f and h.

Vehicle control (0.1% DMSO) and untreated HT29 CRC stem cells from 24 hours to 168 hours formed spheroids (**a** and **b** respectively). TDTC 1 (0.4 mg/ml) reduced spheroid formation from 24 hours till 168 hours (**c**). The cells did not aggregate and remained as single cells. TDTC 2 (0.4 mg/ml) had same effect as TDTC 1 (**d**). TDTC 4 (0.3 mg/ml) and TDTC 5 (0.35 mg/ml) similarly prevented spheroid formation effect was seen later around 96 hours (**e** and **f** respectively). Spheroid formation occurred in the presence of 5-Fluorouracil (5-Fu, 200 µM) see 5-FU-168 hrs (**g**). Also, Suberoylanilide Hydroxamic Acid (SAHA 0.5 mg/ml) failed to impede spheroid formation; and these formed even though the stem cells had decreased in size when compared to vehicle control and untreated cells (**h**). Digital images were captured at different time points using the Floid^{TM} Cell Imaging System. Scale bar= 100 µm.

3.7 The active TDTC compounds modulated stem cell biomarkers

A human pluripotent stem cell proteome array was used to assess the effect of the TDTC compounds on stem cells. The proteome array contained 15 stem cell biomarkers, including E-cadherin, VEGFR2, HCG, Nanog, Alpha-fetoprotein (AFP), Snail, Oct3/4, Goosecoid, Sox17, Sox2, TP63, GATA-4, FoxA2, PDX-1, and Otx2. DLD1 cells were exposed to TDTC 1, 2, 4 and 5, whilst HT29 were only exposed to TDTC 1, 2 and 4 (this was done due to a limited number of membranes). The compounds selected for the HT29 cells were chosen according to cell cycle results and included TDTC 1, 2 and 4 as these all induced cell cycle arrest. TDTC5 was omitted because it had the same cell cycle arrest profile as TDTC 1. The reason for treating DLD1 cells with all the TDTC compounds was based on the Trypan Blue dye exclusion assay, as these were more effective on the DLD1 cells. The cells were exposed to respective IC50 concentrations of the compounds for 48 hours.

The active TDTC compounds showed a significant ability to modulate the stemness of the CRC stem cells. The expression profile of the stem cell biomarkers was deduced from the pixel intensity obtained from the exposed membrane image of protein expression. This pixel intensity represents the protein expression of the stem cell biomarkers after TDTC treatment of the DLD1 and HT29 stem cells. The significance of the compound's modulation capability was compared to vehicle control (CD133+ cells exposed to DMSO), using Student's t-test. The significance of a compound's modulation was based on a p value < 0.05. Each of the biomarkers is briefly described below.

E-cadherin an epithelial marker, whereby its downregulation promotes stemness was upregulated by TDTC 1, 2 and 4 in HT29 stem cells. In DLD1 stem cells, the expression of E-cadherin was similar to the vehicle control, except for TDTC 5 which downregulated E-cadherin (**fig 16**).

FoxA2 a factor that is essential in the development of digestive system, was significantly modulated by the active compounds. The active compounds downregulated FoxA2 in both HT29 and DLD1 stem cells (**fig 17**).

Sox17 a tumour suppressor was upregulated by TDTC 1 and 2 in DLD1 stem cells. In HT29 TDTC 4 upregulated the tumour suppressor (**fig 18**).

VEGFR2 a tyrosine kinase receptor that participates in normal and pathological angiogenesis was downregulated by TDTC 1 in HT29 stem cells. TDTC 4 downregulated VEGFR2 in DLD1 stem cells but upregulated the receptor expression in HT29 stem cells (**fig 19**).

Oct3/4 an important transcription factor that is involved in regulation of stem cells functioning was downregulated by TDTC 1 in HT29 stem cells. Whilst TDTC 4 elevated the expression of Oct3/4. While the rest of the TDTCs had no effect on the expression of the protein (**fig 20**).

Another transcription factor that interacts with Oct3/4 to maintain stemness of cancer stem cells Sox2 was downregulated by TDTC 1 in HT29 stem cells. While TDTC 2 had no effect on HT29 and DLD1 stem cells. TDTC 4 and 5 upregulated Sox 2 in HT29 stem cells and DLD stem cells respectively (**fig 21**).

GATA-4 is a tumour suppressor was successfully upregulated by TDTC 4 in HT29 stem cells but downregulated the protein in DLD1 stem cells. The rest of the TDTCs did not affect the expression of GATA-4 (**fig 22**).

PDX-1 is a transcription factor that regulates insulin expression in the beta cells of the pancreas. The protein was upregulated by TDTC 1 and 2 in HT29 stem cells. TDTC 4 and 5 downregulated the protein in DLD1 stem cells (**fig 23**).

Otx2 is known to promote self-renewal and growth of cancer stem cells in medullablastoma. The protein was upregulated by TDTC 4. TDTC 1, 2, 4 and 5 had no effect on the expression of Otx2 in DLD 1 stem cells (**fig 24**).

Goosecoid (GSC) is a transcription factor that facilitates cell migration in embryonic development. GSC was downregulated by TDTC 1 in HT29 stem cells. TDTC 2 and 4 upregulated the protein in HT29 stem cells. In DLD1 stem the compounds had no effect on the expression of the protein (**fig 25**).

Snail is a transcription factor that regulates epithelial to mesenchymal transitioning in cancer cells prior to metastasis. Differential modulation of Snail by TDTC 4 was observed. TDTC 4 downregulated the protein in HT29 stem and upregulated the protein in DLD1 stem cells. TDTC 1, 2 and 5 had no effect on the expression of Snail in DLD1 and HT29 stem cells (**fig 26**).

HCG is well known for facilitating embryo implantation during pregnancy. The active TDTCs had no impact on the expression of HCG protein in both HT29 and DLD1 stem cells (**fig 27**).

TP63 is a tumour suppressor that can activate p53 response genes. There was no change in protein expression after the HT29 and DLD1 stem cells were exposed to the active TDTCs. The expression of TP63 was similar to the vehicle control (**fig 28**).

AFP is a marker of hepatocellular and embryonic carcinoma. The protein expression was not altered by the compounds (**fig 29**).

Nanog like Oct3/4 and Sox2 is an essential transcription factor required for the maintenance of stem cell activity. Nanog expression was not altered by the compounds (**fig 30**)

A uniform trend of modulation (up/down-regulation) of stem cell biomarkers (E-cadherin, Sox17, FoxA2) was observed in response to active TDTCs in both the HT29 and DLD1 CRC stem cells. A low expression of the stem cell biomarkers was observed in CD133- cells of both HT29 and DLD1; and high expression was seen in the CRC stem cells (Appendix A). The effects of the active compounds on the stem cell biomarkers will be mapped in detail in the discussion.

E-cadherin is an epithelial marker, its downregulation promotes stemness, its expression in HT29 and DLD1 stem cells is represented below (fig 16).

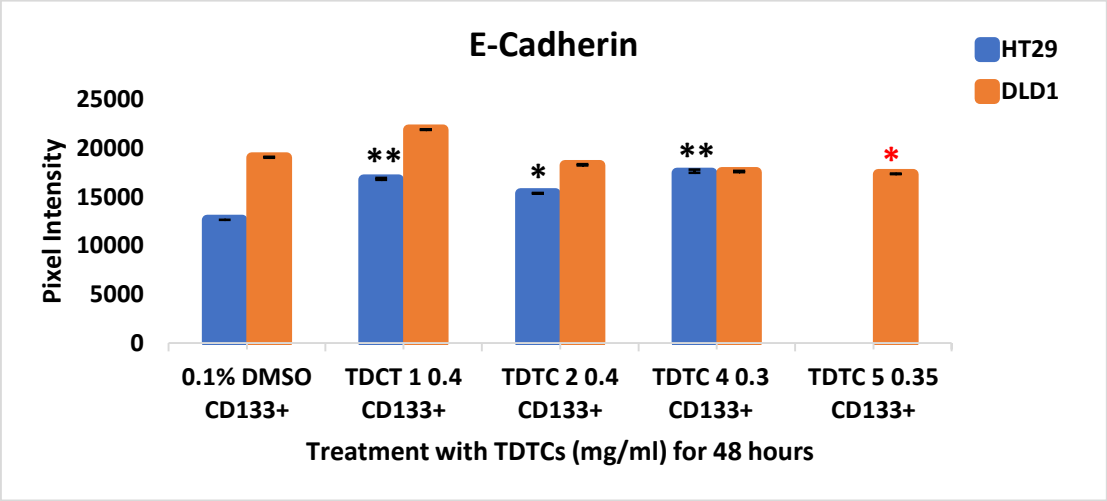


Figure 16: Active TDTCs upregulated E-cadherin. The t-test for independent samples was conducted using STATISTICA 13 software. P-value <0.05 considered to be significant and n=2 for each treatment. The stem cells were treated with TDTCs for 48 hours. E-cadherin was upregulated by most of the active TDTCs compared to vehicle control (0.1% DMSO). It was significantly upregulated by TDTC 1 (**), TDTC 2 (*) and TDTC 4 (**) in HT29 CRC stem cells. In DLD1 CRC stem cells, the expression of E-cadherin was similar to the vehicle control; except TDTC 5 (*) downregulated E-cadherin, * p< 0.05 and **, p≥0.001. The graph plot of protein expression is Mean ± SEM, n=2.

FoxA2 is important in the development of digestive system and its upregulation promotes CRC, its expression is represented below (fig 17).

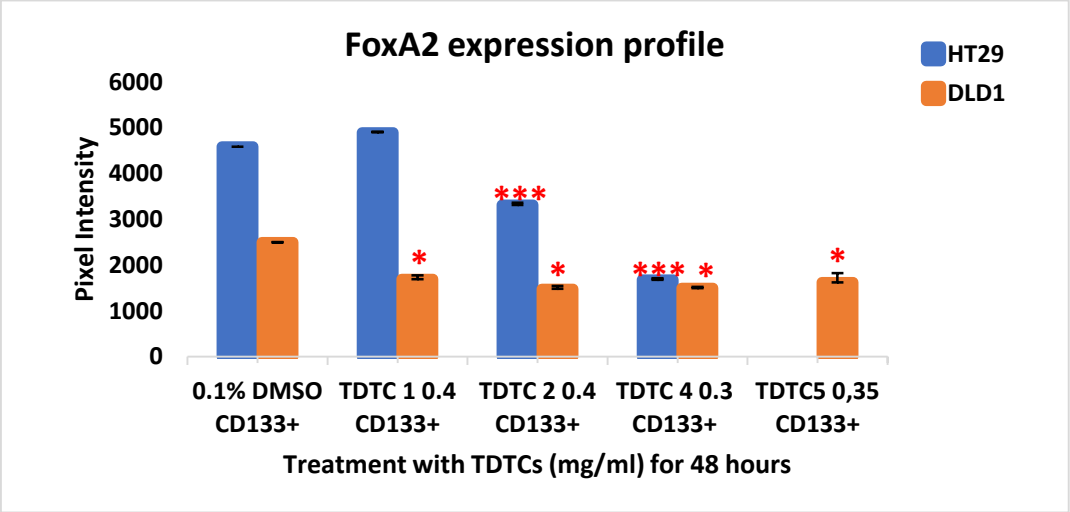


Figure 17: FoxA2 was profoundly downregulated by the active TDTCs.

TDTC 1 (* p < 0.05 (DLD1)), TDTC 2 (*** p≥0.0001(HT29), * p <0.05 (DLD1)), TDTC 4 (*** p≥0.0001 (HT29),* p<0.05 (DLD1)) and TDTC 5 (* p<0.05) significantly downregulated FoxA2 compared to the vehicle control (0.1% DMSO). The stem cells were exposed to TDTCs for 48 hours. T-test for independent samples was conducted using STATISTICA 13 software. P-value <0.05 was considered to be significant. The graph plot of protein expression is Mean ± SEM, n=2.

The expression levels of Sox17 a tumour suppressor is depicted in the plot below (fig. 18)

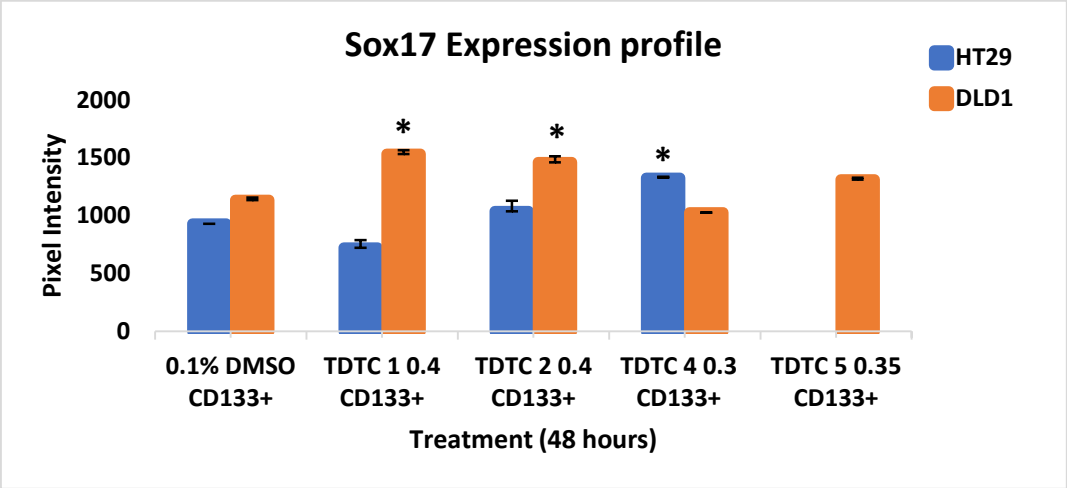


Figure 18: Sox17 protein expression levels in HT29 and DLD1 stem cells.

Sox17 was upregulated by the active TDTCs. Sox17 a tumour suppressor was significantly upregulated by TDTC 1 (DLD1), TDTC 2 (DLD1) and TDTC 4 (HT29) (* $p < 0.05$), in comparison to the vehicle control. CRC stem cells were exposed to active TDTCs for 48 hours. The t-test for independent samples was conducted using STATISTICA 13 software. P-value <0.05 considered to be significant. The graph plot of protein expression is Mean ± SEM, n=2.

VEGR2 is a receptor functional in the angiogenic pathway, its activity being required for vascularization (fig 19).

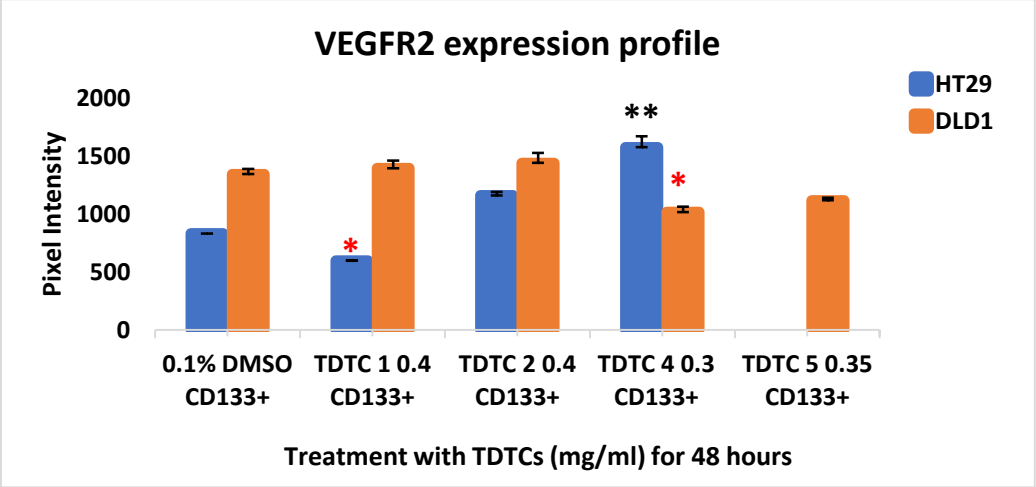


Figure 19: VEGFR2 protein expression levels in HT29 and DLD1 stem cells. TDTC 1 and TDTC 4 show potential in reducing angiogenesis.

TDTC 1 downregulated VEGFR2 (* $p<0.05$) in HT29 stem cells, and TDTC 4 downregulated VEGFR2 in DLD1 stem cells (* $p<0.05$). Interestingly TDTC 4 upregulated VEGFR2 (** $p \geq 0.001$) in HT29 stem cells, in comparison to the vehicle control (0.1% DMSO). The stem cells were exposed to TDTCs for 48 hours. The t-test for independent samples was conducted using STATISTICA 13 software. P-value <0.05 considered to be significant. The graph plot protein expression is Mean ± SEM, n=2.

Oct3/4 is an essential transcription factor required for the maintenance of stem cell functionality (fig 20).

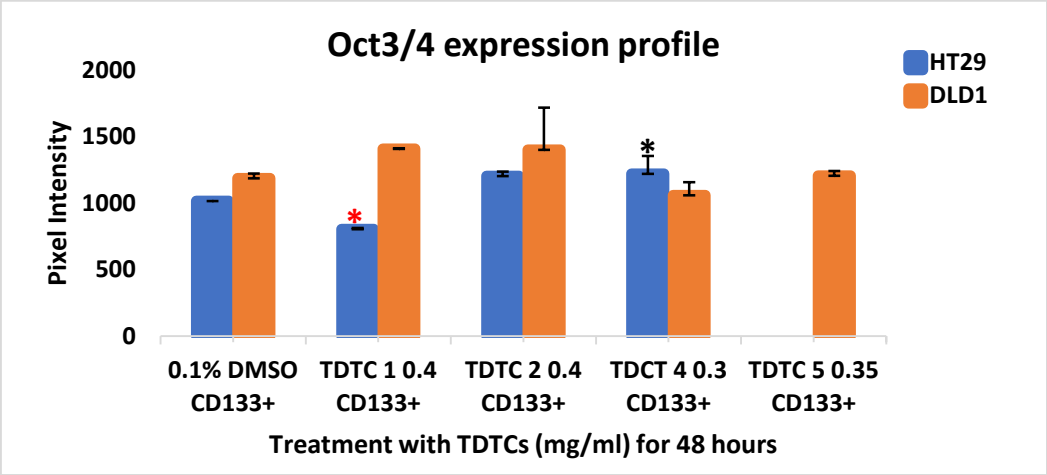


Figure 20: Oct3/4protein expression levels in HT29 and DLD1 stem cells. TDTC 1 modulates Oct3/4.

TDCT 1 downregulates (* $p<0.05$) Oct3/4 in HT29 stem cells whilst other TDCTs had no effect. TDTC 4 acted to upregulate Oct3/4 (* $p<0.05$). The stem cells were exposed to TDTCs for 48 hours. The t-test for independent samples was conducted using STATISTICA 13 software. P-value <0.05 considered to be significant. The graph plot of protein expression is Mean ± SEM, n=2.

Sox2 is a transcription factor that is responsible for stemness of cancer stem cells (fig 21).

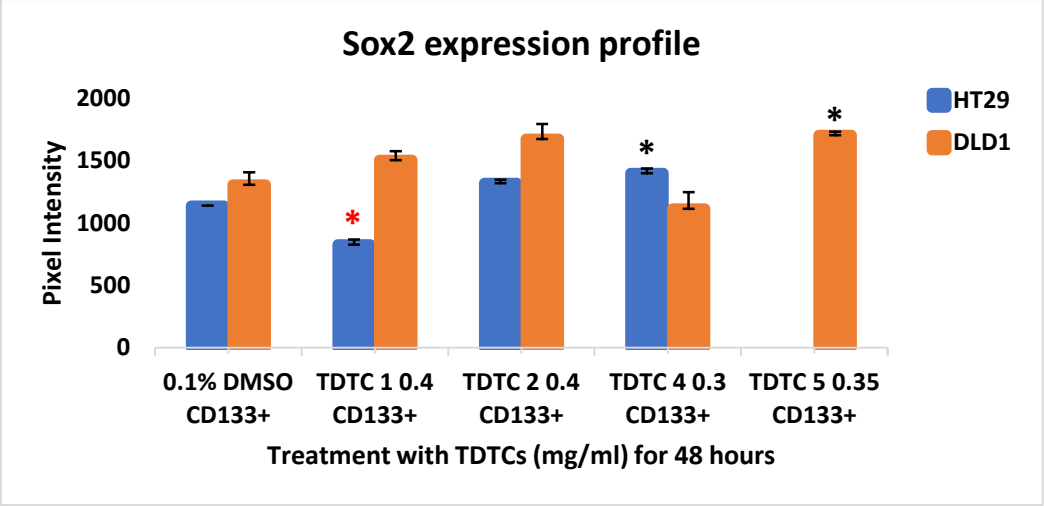


Figure 21: Sox2 protein expression levels in HT29 and DLD1 stem cells. TDTC 1 suppresses Sox2.

TDTC 1 downregulates (* $p<0.05$) Sox2 in HT29 stem cells while other TDTCs have no effect on Sox2 especially TDTC 2 in comparison to the vehicle control (0.1% DMSO). TDTC 4 (HT29 stem cells) and TDTC 5 (DLD1 stem cells) upregulated Sox2 (* $p<0.05$). The stem cells were exposed to TDTCs for 48 hours. The t-test for independent samples was conducted using STATISTICA 13 software. P-value <0.05 considered to be significant. The graph plot of protein expression is Mean ± SEM, n=2.

GATA4 functions as tumour suppressor, regulating anticancer genes (fig 22).

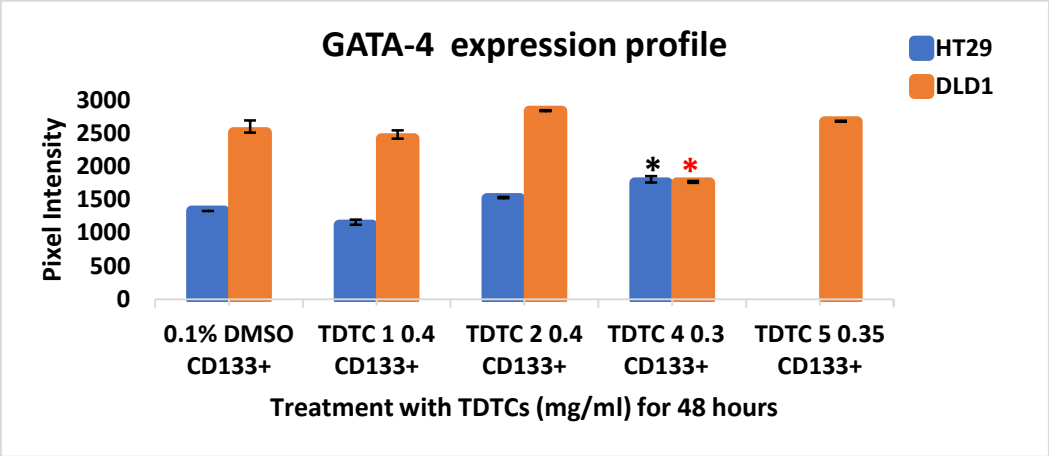


Figure 22: GATA-4 protein expression levels in HT29 and DLD1 stem cells. TDTC 4 differentially modulated GATA-4.

TDCT 4 upregulated (* $p<0.05$) GATA-4 in HT29 cells and downregulated (* $p<0.05$) GATA-4 in DLD1 stem cells when compared to the vehicle control (0.1% DMSO). TDTC 1 and TDTC 2 had no effect, GATA-4 expression was similar to the vehicle control. The stem cells were exposed to TDTCs for 48 hours. The t-test for independent samples was conducted using STATISTICA 13 software. P-value <0.05 considered to be significant. The graph plot protein of expression is Mean ± SEM, n=2.

PDX-1 is a transcription factor that regulates expression of insulin in beta-cells of the pancreas (fig 23).

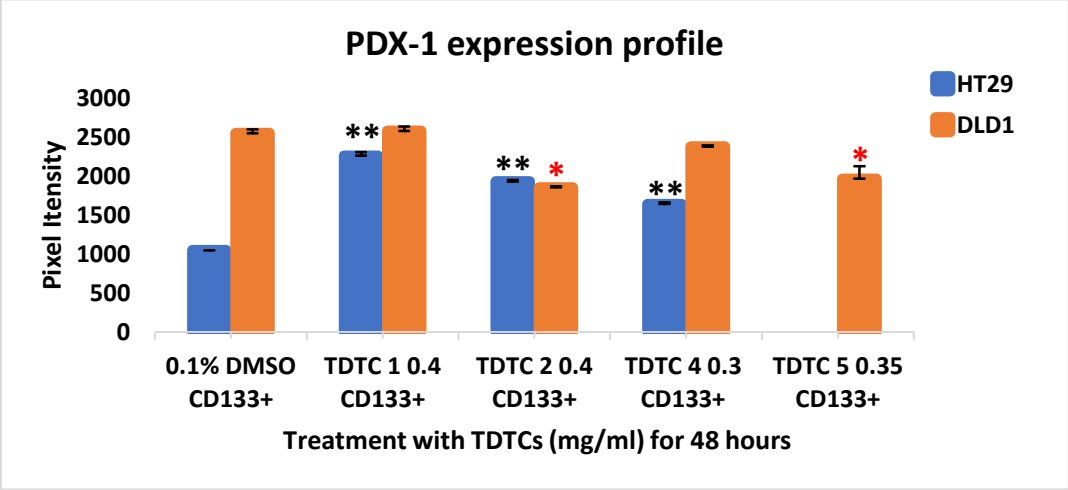


Figure 23: PDX-1 protein expression levels in HT29 and DLD1 stem cells. PDX-1was differentially modulated in the HT29 and DLD1 cell lines.

PDX-1 was upregulated in HT29 by TDTCs 1, 2 and 4 (** $p\geq0.001$), in comparison to the vehicle control (0,1% DMSO). TDTC 4 and TDTC 5 downregulated (* $p< 0.05$) PDX-1 in DLD1 stem cells. The stem cells were exposed

to TDTCs for 48 hours. The t-test for independent samples was conducted using STATISTICA 13 software. P-value <0.05 considered to be significant. The graph plot of protein expression is Mean ± SEM, n=2.

Otx2 promotes self-renewal and growth of cancer stem cells in medulloblastoma (fig 24)

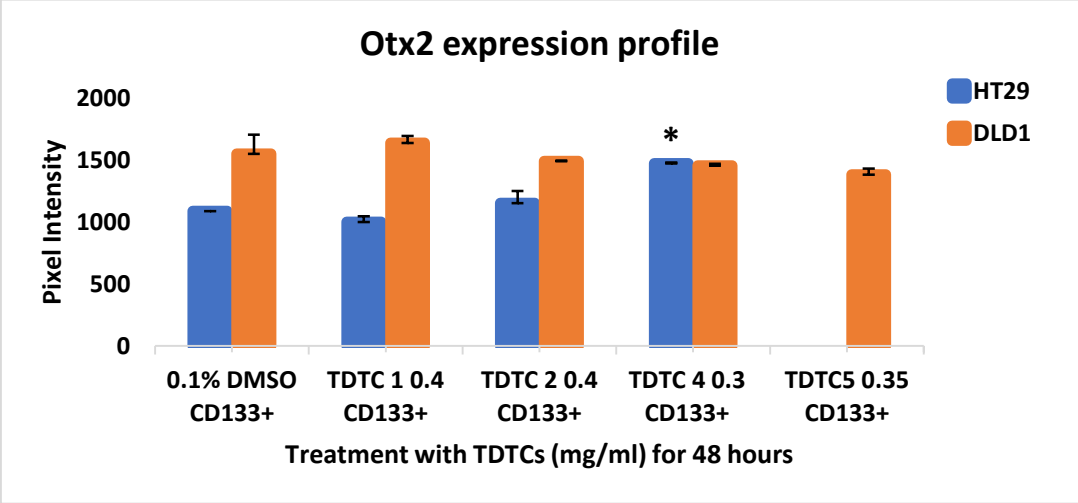


Figure 24: Otx2 protein expression levels in HT29 and DLD1 stem cells, Otx2 was modulated by TDTC 4.

In comparison to the vehicle control (0.1% DMSO), TDCT 4 upregulated (* p<0.05) Otx2 in HT29 stem cells. No effect of the TDTCs 1, 2, 4 and 5 is seen in DLD1 stem cells. The stem cells were exposed to TDTCs for 48 hours. The t-test for independent samples was conducted using STATISTICA 13 software. P-value <0.05 considered to be significant. The graph plot of protein expression is Mean ± SEM, n=2.

Goosecoid is a primary transcription factor that facilitates cell migration in embryonic development (fig 25)

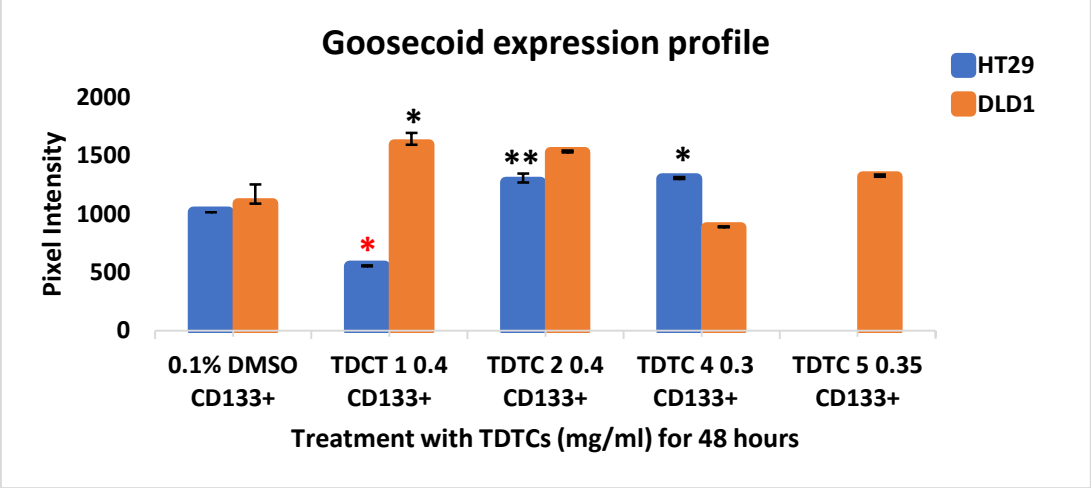


Figure 25: Goosecoid expression was modulated by the active TDTCs.

Goosecoid was downregulated by TDTC 1 (* p< 0.05) in HT29 stem cells but was upregulated (* p<0.05) in DLD1 stem cells with reference to the vehicle control (0.1% DMSO). TDCT 2 (** p≥0.001) and TDCT 4 (* p<0.05) upregulated the protein in HT29 stem cells. The stem cells were exposed to TDTCs for 48 hours. The t-test for

independent samples was conducted using STATISTICA 13 software. P-value <0.05 considered to be significant. The graph of plot protein expression is Mean ± SEM, n=2.

Snail is a transcription factor required for epithelial to mesenchymal transitions (EMT) when cancer cells become motile prior to metastasis (fig 26).

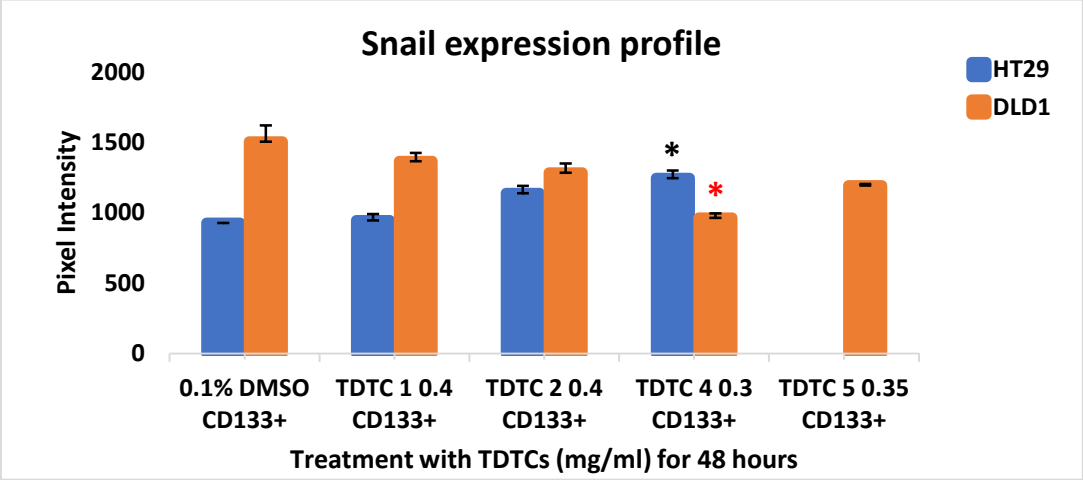


Figure 26: Snail protein expression levels in HT29 and DLD1 stem cells. TDCT 4 differentially modulated Snail.

In comparison with the vehicle control (0.1% DMSO) TDCT 4 downregulated (* p<0.05) Snail in DLD1 stem cells; and upregulated (* p < 0.05) it in HT29 stem cells. TDTC 1, 2 and 5 had no effect on either HT29 or DLD1 stem cells, compared to vehicle control (0.1% DMSO). The stem cells were exposed to TDTCs for 48 hours. The t-test for independent samples was conducted using STATISTICA 13 software. P-value <0.05 considered to be significant. The graph plot of protein expression is Mean ± SEM, n=2.

HCG is secreted by syncytiotrophoblast and it facilitates embryo implantation (fig 27).

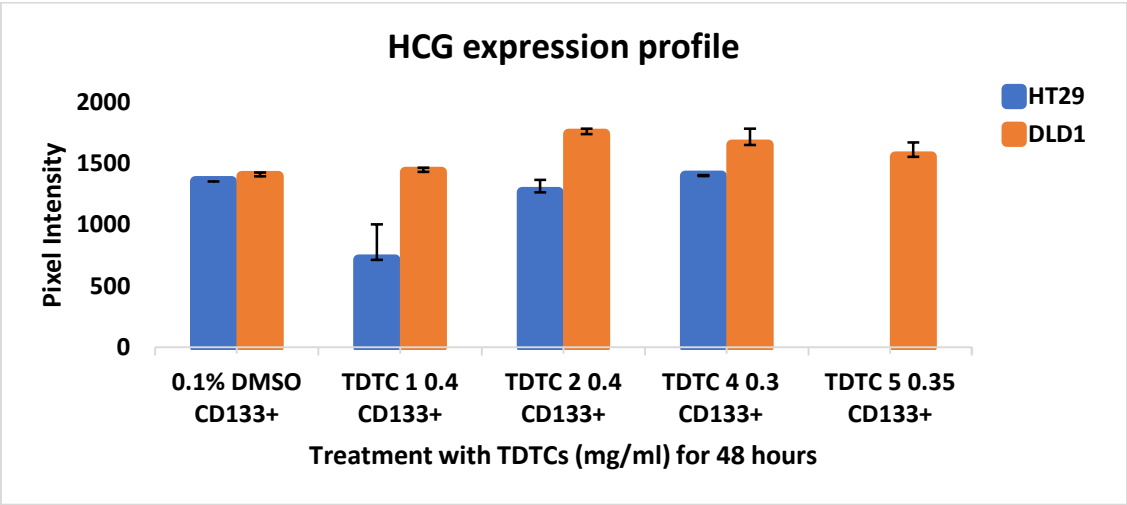


Figure 27: HCG protein expression levels in HT29 and DLD1 stem cells. Active TDTCs did not affect HCG protein expression.

TDCTs 1, 2, 4 and 5 had no effect on HCG protein expression in the HT29 and DLD1 stem cells, relative to the vehicle control (0.1% DMSO). The stem cells were exposed to TDTCs for 48 hours. The t-test for independent samples was conducted using STATISTICA 13 software. P-value <0.05 considered to be significant. The graph plot of protein expression is Mean ± SEM, n=2.

TP63 is a tumour suppressor that can activate p53 response genes, resulting in cell cycle arrest and apoptosis.

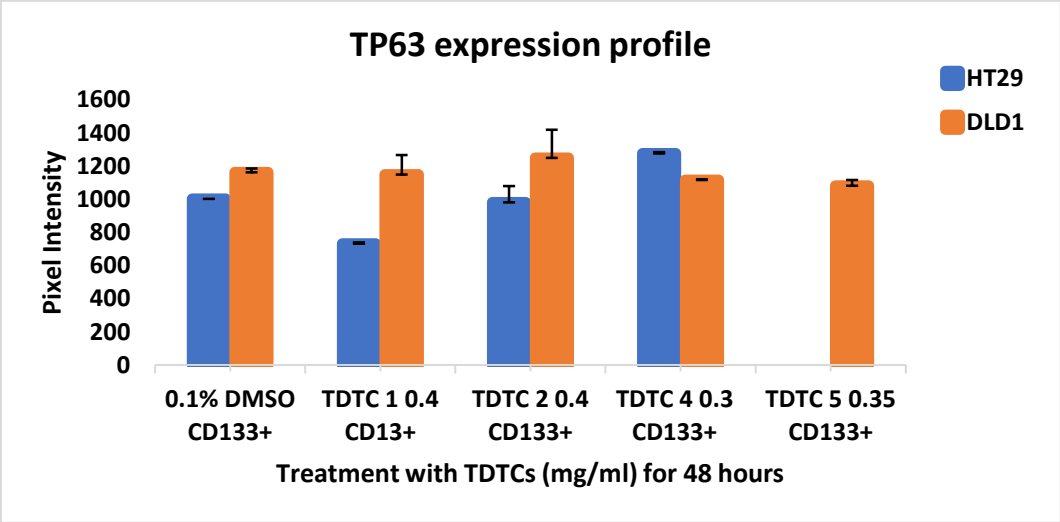


Figure 28: TP63 protein expression levels in HT29 and DLD1 stem cells. TP63 was not modulated by the active TDTCs.

No significant changes to the expression of TP63 were observed after HT29 and DLD1 stem cells were treated with either TDCT 1, 2, 4 or 5, with relation to the vehicle control (0.1% DMSO). The stem cells were exposed to TDTCs for 48 hours. The t-test for independent samples was conducted using STATISTICA 13 software. P-value <0.05 considered to be significant. The graph plot of protein expression is Mean ± SEM, n=2.

AFP is a marker of hepatocellular and embryonic carcinoma (fig 29)

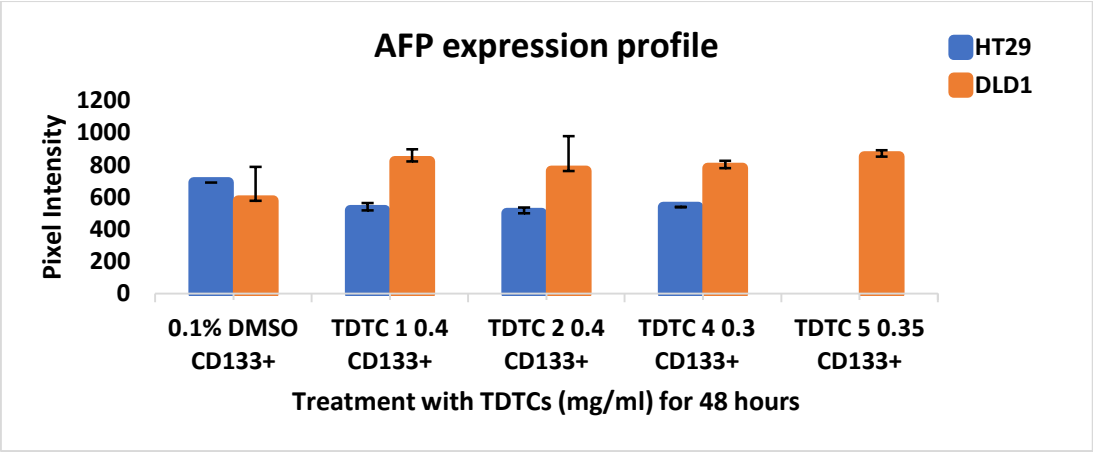


Figure 29: AFP protein expression levels in HT29 and DLD1 stem cells. AFP was not influenced by the active TDTCs.

TDTC 1, 2, 4 and 5 did not affect AFP on the HT29 and DLD1 stem cells, its expression being similar to the vehicle controls (0.1% DMSO). The stem cells were exposed to TDTCs for 48 hours. The t-test for independent samples was conducted using STATISTICA 13 software. P-value <0.05 considered to be significant. The graph plot of protein expression is Mean ± SEM, n=2.

Nanog like Oct3/4 and Sox2 is an essential transcription factor required for the maintenance of stem cell activity (fig 30).

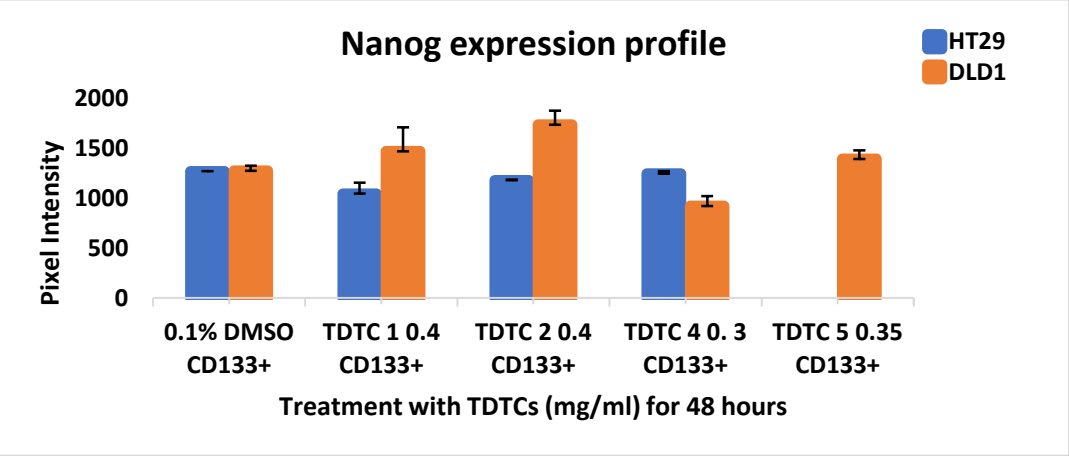


Figure 30: Nanog protein expression levels in HT29 and DLD1 stem cells. Nanog expression was not affected by the active TDTCs.

TDTC 1, 2, 4 and 5 did not modulate Nanog in both HT29 and DLD1 stem cells. The expression of Nanog protein was similar to the vehicle control (0.1% DMSO). The stem cells were exposed to TDTCs for 48 hours. The t-test for independent samples was conducted using STATISTICA 13 software. P-value <0.05 considered to be significant. The graph plot of protein expression is Mean ± SEM, n=2.

3.8 The active TDTCs regulated gene expression of important factors involved in self-renewal and maintenance of stem cells

The stem cell biomarkers that were uniformly modulated in the HT29 and DLD1 CRC stem cells were further subjected to gene expression analysis as to understand whether the active TDTCs were modulating the biomarker at protein expression level or also affecting the biomarker's gene expression. As a central stemness regulator, β-catenin was also included in the panel of genes that were studied presently. The CRC stem cells were exposed to respective IC50s of the active TDTCs for 48 hours. RNA was extracted and reverse transcribed to complementary DNA (cDNA) and was amplified and quantified using SYBR green as reporter in a quantitative real time PCR (qPCR).

3.8.1 β-catenin

β-catenin was observed to be highly expressed in late-stage CRC cells (differentiated cells [CD133-], **fig 31**). With the CRC stem cells, although β-catenin was expressed, this was not as high, as compared to differentiated cells (**fig 31**). Some of the active TDTCs further decreased the expression of β-catenin in the CRC stem cells. TDTC 1 (0.4 mg/ml) downregulated the mRNA production in both HT29 and DLD1 stem cells. Having a log2(fold change) of -0.12 for HT29 stem cells and -0.3 for DLD1 stem cells. TDTC 2 (0,4 mg/ml) slightly downregulated gene expression in HT29 stem cells, log2(fold change) was -0.1. Whilst in DLD1 stem cells, β-catenin was upregulated by the TDTC 2 compounds, log2(fold change) was 0.14. TDTC 4 (0.3 mg/ml) downregulated expression in HT29 stem cells, log2(fold change) was -0.3. DLD1 stem cells had upregulation of gene expression by 0.02. TDTC 5 (0.35 mg/ml) downregulated mRNA expression of both HT29 (log2(fold change) = -0,18) and DLD1 stem cells (log2(fold change) = -0.04) (**fig 32**).

Beta-catenin is a transcriptional activator that regulates stemness of CRC stem cells (fig 31 & 32).

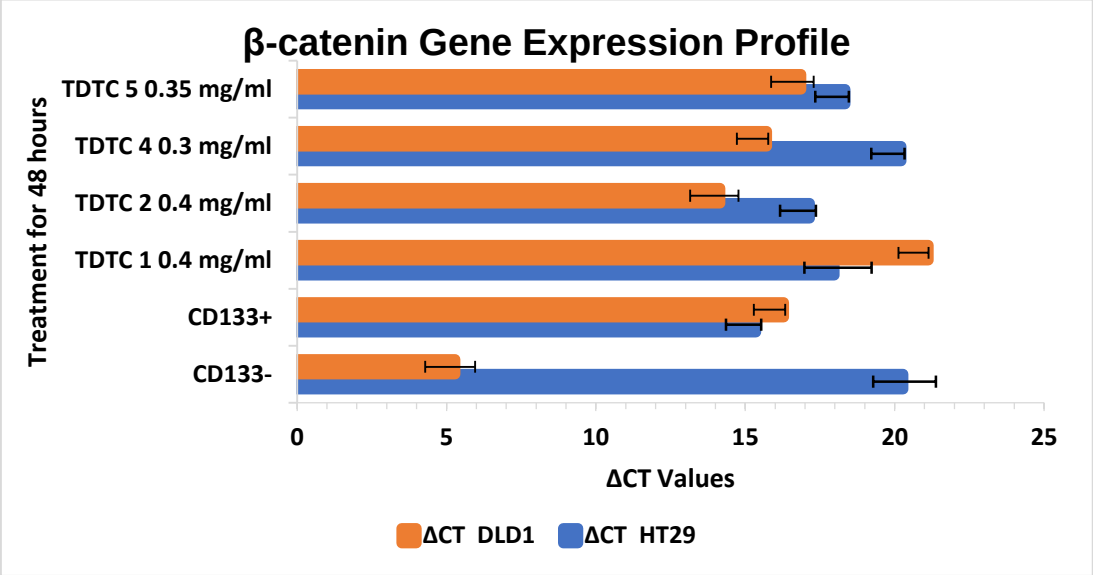


Figure 31: β-catenin is highly expressed in late-stage CRC cells.

Differentiated DLD1 cells had high expression of β-catenin compared to HT29 cells (ΔCT = 5.29 for DLD1 and 20.28 for HT29). CRC stem cells had lower expression of β-catenin compared to differentiated cells as the ΔCT values were much higher (ΔCT=15.36 for HT29 and 16.29 for DLD1 stem cells). HT29 and DLD1 stem exposed to TDTC 1 (0.4 mg/ml) had higher ΔCT values compared to untreated stem cells (CD133+). TDTC2 (0.4 mg/ml) rendered ΔCT value of 17.16 in HT29 stem cells, whilst in DLD1 stem cells a value of 14.20 was observed. TDTC 4 ΔCT value for HT29 stem cells was 20.22 and DLD1 is 15.8. TDTC 5 ΔCT value was 18.3 for HT29 stem cells, while in DLD1 ΔCT value is 16.87. The cells were exposed to the treatment for 48 hours. The graph was plotted with Stds (standard deviations). Higher ΔCT value indicates lower gene expression; and low-value indicates high gene expression. ΔCT= CT value of test compound- CT value of housekeeping gene.

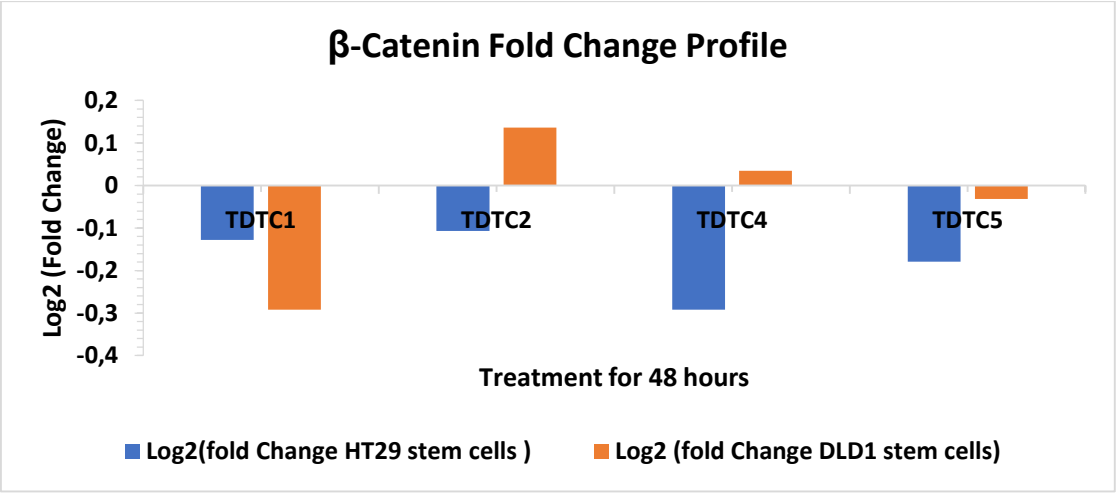


Figure 32: Active TDTCs mainly downregulated β-catenin.

β-catenin expression was downregulated by the TDTC 1 in HT29 and DLD1 stem cells with log2(fold change) -0.12 and -0.3 respectively. HT29 stem cells exposed to TDTC 2 and TDTC 4 had reduced expression of β-catenin (log2(fold change) = -0.12 and -0.3 respectively), whilst in DLD1, β-catenin expression was slightly upregulated (log2(fold change) = 0,14 and 0.03 respectively). TDTC 5 also downregulated β-catenin expression in HT29 and DLD1 (log2(fold

change = -0.18 for HT29 and -0.03 respectively). The CRC stem cells were exposed to the compounds for 48 hours. The treatments were compared to vehicle control treated stem cells.

3.8.2 FoxA2

FoxA2 gene expression was more pronounced in late-stage DLD CRC cells, then in early stage HT29 cells (**fig 33**). DLD1 CD133- cells had higher expression of FoxA2 then HT29 CD133- cells (ΔCT = 6.32 for DLD1 CD133- and 13.42 for HT29 CD133- respectively) (**fig 33**). The active TDTC compounds reduced the gene and protein expression of FoxA2 in both HT29 and DLD1 stem cells (**fig 33 & 17**). TDTC 1 downregulated the gene expression in HT29 stem cells by log2(fold change) of -0.34 and in DLD1 by -0.3. TDTC 2 downregulated FoxA2 by log2(fold change) of -0.35 and -0.3 in HT29 and DLD1 stem cells respectively. FoxA2 was downregulated by log2(fold change) of -0.31 and -0.26 in HT29 and DLD1 stem cells exposed to TDTC 4 respectively. HT29 and DLD1 stem cells exposed to TDTC 5 had a log2(fold change) of -0.38 and -0.21 respectively, FoxA2 was downregulated (**fig 34**).

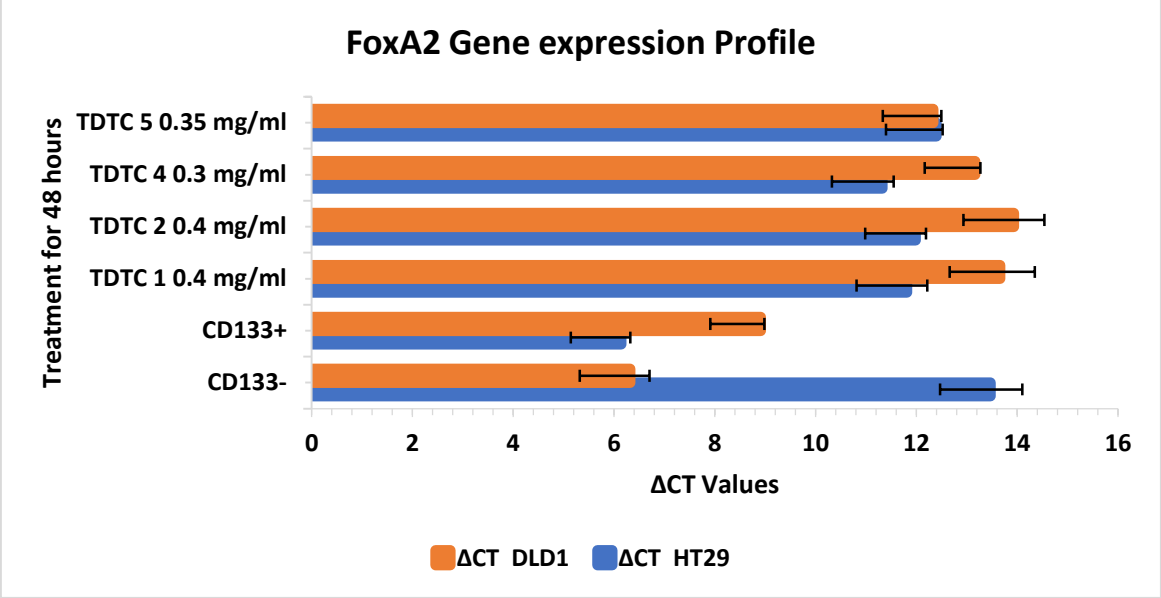


Figure 33: FoxA2 mRNA expression was reduced by active TDTCs.

FoxA2 mRNA expression was reduced in HT29 and DLD1 CRC stem cells when compared to CD133-. DLD1 CD133- cells had a high expression (ΔCT=6.32) of FoxA2 mRNA, whilst HT29 CD133- had less mRNA (ΔCT=13.47). Untreated CD133+ cells had more FoxA2 expression (ΔCT ranged from 6.41-8.91). The TDTC compounds reduced the mRNA expression (ΔCT ranged from 11.32-13,93). The higher the ΔCT value lesser the mRNA expression. The cells were exposed to TDTC 1 (0.4 mg/ml), TDTC2 (0.4 mg/ml), TDTC 4 (0.3 mg/ml) and TDTC 5 (0.35 mg/ml). The treatment was for 48 hours. ΔCT= CT value of test compound- CT value of housekeeping gene.

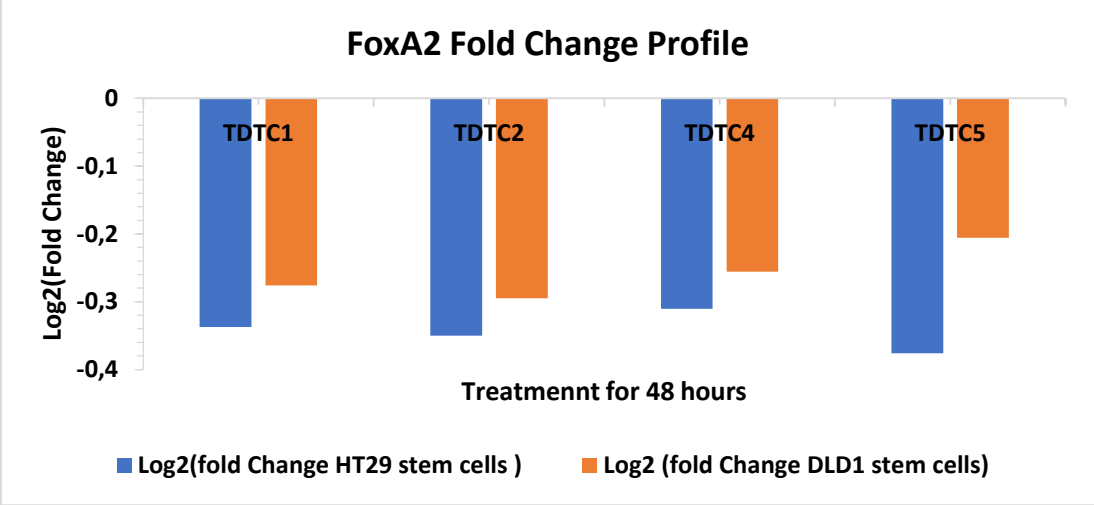


Figure 34: FoxA2 was downregulated by the active TDTCs.

FoxA2 was downregulated by all the active TDTC compounds. TDTC1 induced downregulation of FoxA2 depicted by log2(fold change) of was -0,34 and -0,3 for HT29 and DLD1 stem cells respectively. TDTC 2 downregulated FoxA2 in HT29 and DLD1 with a log2(fold change) of -0.35 and -0.3 respectively. HT29 and DLD1 stem cells exposed to TDTC 4 reduced FoxA2 gene expression this was depicted by log2 (fold change) of -0.31 and -0.26 in HT29 and DLD1 stem cells. TDTC 5 downregulated FoxA2 mRNA in HT29 and DLD1 stem cells (log2 (fold change) = -0.38 for HT29 stem cells and -0.21 for DLD1 stem cells). The treatments were compared to vehicle control treated stem cells.

3.8.3 VEGF was downregulated in late-stage CRC by the active TDTCs

Differentiated CRC cells at early stage (HT29 CD133-) showed less expression of VEGF mRNA, whilst in late stage (DLD1 CD133-) the VEGF expression is high. Untreated CRC stem cells have similar VEGF expression as early stage CRC cells (HT29 CD133-) (**fig 35**). All active TDTCs managed to downregulate expression of VEGF in DLD1 stem cells. TDTC1,2,4 and 5 downregulated VEGF in DLD1 stem cells by log2(fold) of -0.21, -0.03, -0.012 and -0.22 respectively. In HT29 stem cells TDTC 1 and 5 downregulated VEGF (log2(fold change) = -0.10 and -0.46 respectively). TDTC 2 and TDTC 4 upregulated VEGF mRNA expression in HT29 stem cells (log2(fold change) = -0.08 and 0.06 respectively) (**fig 36**).

VEGF is a growth factor that promotes angiogenesis (fig 35 & 36).

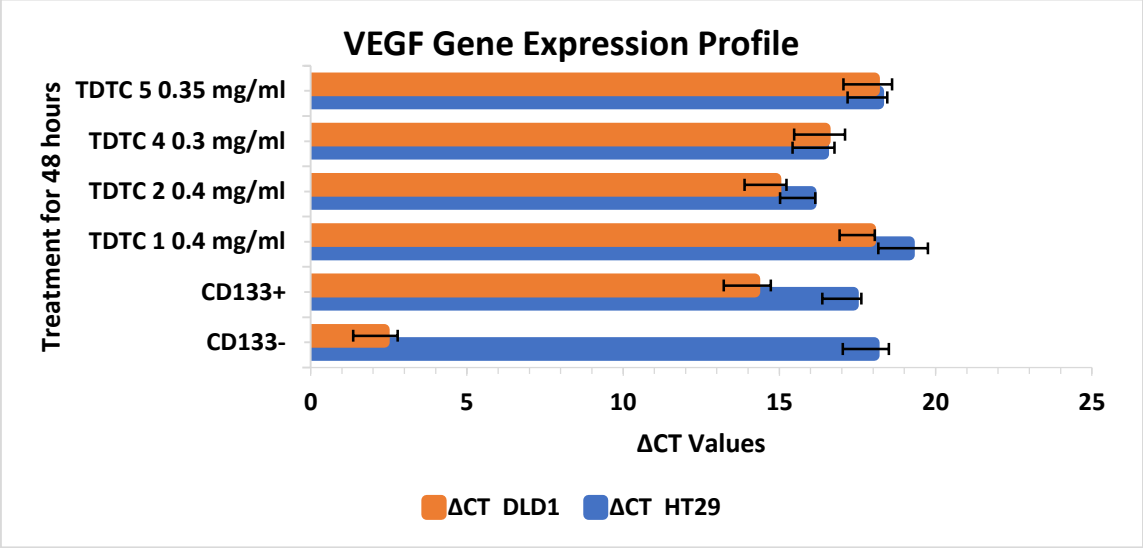


Figure 35: VEGF is highly expressed in the late stage of differentiated CRC cells.

VEGF was highly expressed in DLD1 CD133- cells (ΔCT value = 2.36), low expression was seen in HT29 CD133- cells (ΔCT value =18.04). DLD1 and HT29 stem cells (CD133+) (ΔCT value = 14.22 and 17.37 respectively) had low expression of VEGF as compared to DLD1 CD133- cells. TDTC 1 had a ΔCT value 19.17 for HT29 stem cells and 17.93 for DLD1 stem cells. TDTC 2 had a ΔCT value of 16.02 for HT29 stem cells and 14.89 for DLD stem cells. ΔCT value of 16.43 for HT29 stem cells and 16.48 for DLD1 stem cells was observed when the cells were exposed to TDTC 4. TDTC 5, HT29 stem cells had a ΔCT value of 18.19 and DLD1 stem cells were 18.05. The greater the ΔCT value the lesser is the mRNA expressed. The treatment was for 48 hours. ΔCT= CT value of test compound - CT value of housekeeping gene.

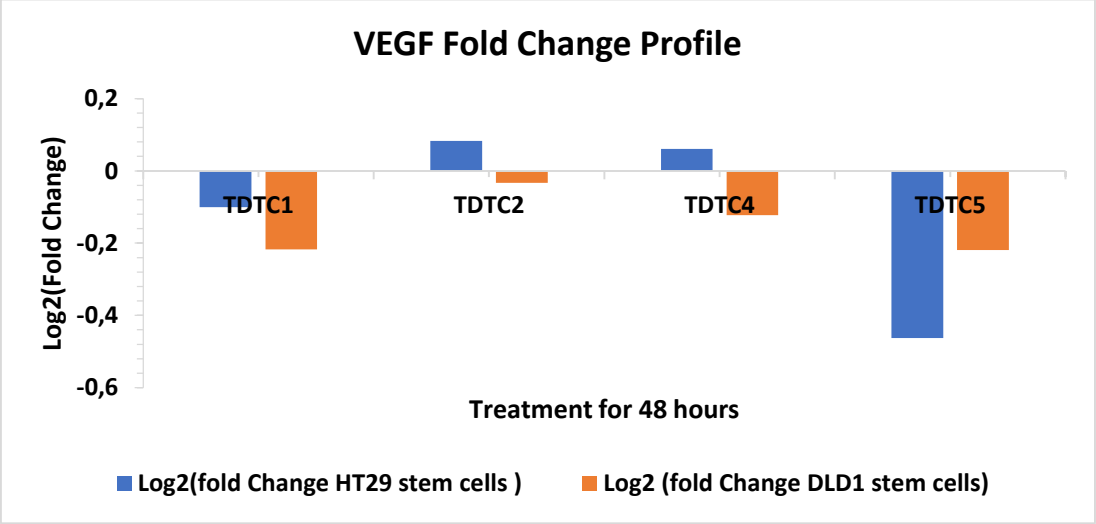


Figure 36: Active TDTCs downregulated VEGF in DLD1 stem cells.

TDTC 1 downregulated VEGF mRNA in HT29 and DLD1 indicated by log2 (fold change) of -0.10 and -0.22 respectively., TDTC 2 downregulated VEGF mRNA by log2(fold change) of -0.03 in DLD1 stem cells VEGF mRNA in HT29 stem cells was slightly upregulated (log2 (fold change = 0.08)).TDTC 4 downregulated VEGF mRNA by log2 (fold change) of -0.12 in DLD1 stem cells. HT29 stem cells exposed to TDTC 4 had slightly upregulated VEGF mRNA (log2 (fold change) of 0.06). TDTC 5 downregulated VEGF mRNA in HT29 and DLD1 stem cells (log2 (fold change) = -0.46 and -0.22 respectively). The treatments were compared to vehicle control treated stem cells.

3.8.4 VEGFR1 was downregulated by active TDTCs

VEGFR1 mRNA was similarly and abundantly expressed in both the differentiated and DLD1 stem cells. The active TDTCs downregulated VEGFR1 (**fig 37**). The log2(fold change) in gene expression, as compared to untreated cells was -0.09, -0.4, -0.48 and -0.58 for TDTC 1, TDTC 2, TDTC 4 and TDTC 5 respectively (**fig 38**).

VEGFR1 is a receptor that initiates angiogenesis, it interacts with VEGF under pathological condition (fig 37 & 38)

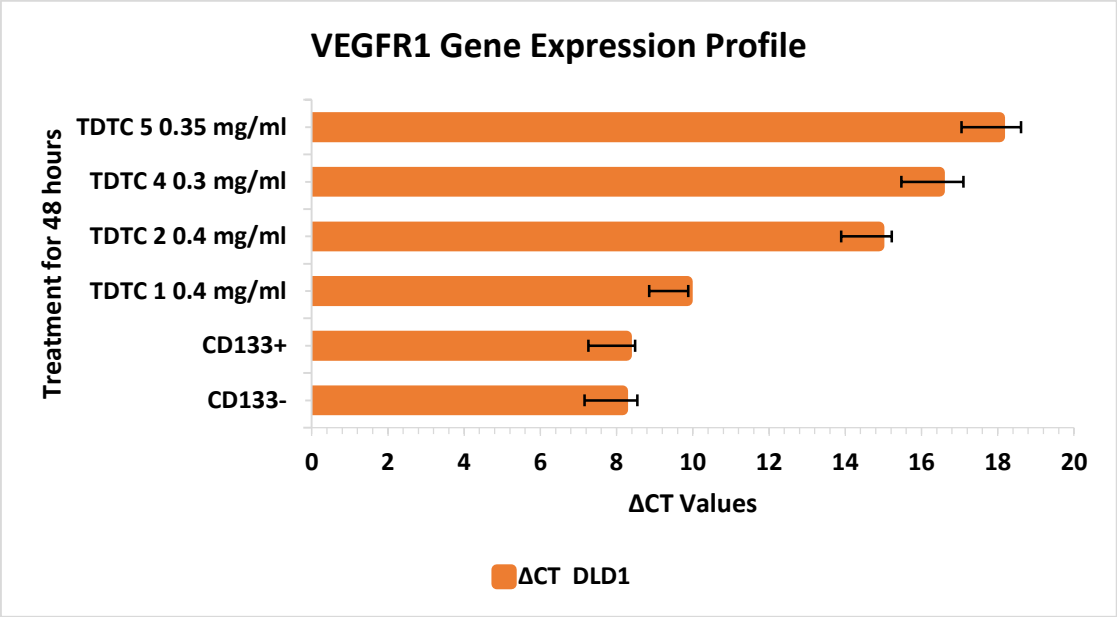


Figure 37: VEGF1 mRNA was downregulated by the active TDTCs.

DLD1 CD133- and DLD1 stem cells had similar expression of VEGFR1 (ΔCT value =8.16 for DLD1 CD133- and 8.26 for DLD1 stem cells. TDCT 1 (0.4 mg/ml) reduced VEGFR1 mRNA expression ΔCT value = 9.86 in DLD1 stem cells TDTC 2 also reduce VEGFR1 gene expression ΔCT value was 14.89. TDTC 4 and TDTC 5 reduced mRNA of VEGFR1 indicated by ΔCT value of 16.48 and 18.05, respectively. The treatment was for 48 hours. ΔCT= CT value of test compound - CT value of housekeeping gene.

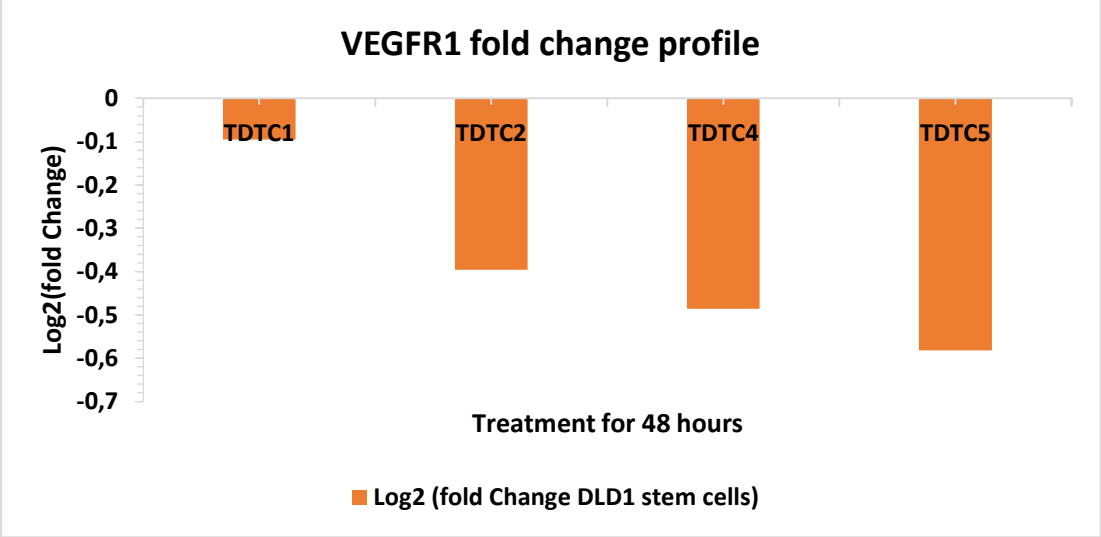


Figure 38: The active TDTCs downregulated VEGFR1 mRNA.

The relative gene expression log2(fold change) was -0.09, -0.4, -0.48 and -0.58 for TDTC 1, TDTC 2, TDTC 4 and TDTC 5 respectively. The DLD1 stem cells were exposed to the active TDTC compounds for 48 hours). The treatments were compared to vehicle control treated stem cells.

Proteins modulated by the compounds were further studied at their transcriptional level, to confirm whether the protein expression matched mRNA expression. In this pursuit, genes such as Sox17, E-cadherin, VEGFR-3, VEGFR-2 in HT29 and DLD1 stem cells; and VEGFR-1 in HT29 stem cells were not amplified. Due to time constraints, it was not possible to complete this aspect of the work and will be done at a future time point. Troubleshooting was done by performing gradient PCR and qPCR was performed again. The genes were amplified through primer annealing temperature of 54°C instead of 60°C (Table 8). Due to time constraints, the amplification of the genes was not done.

Chapter 4

Discussion

CRC is reported as being an aggressive and recurrent disease in younger South African individuals (<40 years of age). CRC recurrence is caused by intrinsic (primary resistance) or acquired resistance (adaptive resistance) to conventional chemotherapy which results in patient relapse (179). The resistance in most cases is steady or heritable resulting in increased drug tolerance even if chemotherapy is reintroduced after a while (180). The resistance persists because of tumour heterogeneity. The tumour consists of differentiated cells, stem cells and stem-like cells (epithelial cells transitioning into mesenchymal cells). The observed inefficacy of the chemotherapy is influenced by CRC stem cells and stem-like cells (181). The CRC stem cells, and stem-like cells possess self-renewal properties and the ability to differentiate into heterogenous lineages of cancer cells, in response to chemotherapy. Also, as CRC stem cells may be quiescent, conventional chemotherapy cannot target these cells (182). The referenced properties are responsible for the inefficacy of the conventional chemotherapy (183).

In addition, chemotherapies are toxic and not specific to the tumour. Therefore novel anticancer compounds and new therapies are required to combat drug resistance, drug toxicity and drug inefficacy In considering this, novel tetrazole dithiocarbamate derivatives were tested for their anticancer activity CRC adenocarcinoma cells representing earlier (HT29 stage II) and later (DLD1 stage III) tumour stages. In addition, anticancer mechanisms of the active derivative compounds were tested in cancer stem cells.

In the present study 10 TDTCs were screened using Alamar Blue to identify active anticancer candidates. Alamar Blue gives an indication of which compounds induced cell death. The cells treated with the compounds were stained with the non-toxic Alamar Blue dye and incubated approximately for 4 hours. After incubation, where the dye retains its blue colour remaining unreduced, this indicates cell death has been induced by the compounds. When the dye changes colour to pink/magenta this means the cells are alive and can reduce the dye to change colour. Out of the ten 10 TDTCs, 4 TDTCs were potentially shown to possess anticancer activity, these being TDTC 1, 2 4 and 5. These active TDTCs were further subjected to the Trypan Blue dye exclusion assay to further validate their anticancer activity by assessing cell viability and to further identify the IC50 concentration for each compound. The DMSO vehicle controls notably had no effect on cell viability. Interestingly, the TDTCs had no effect on the non-cancerous Human Embryonic

Kidney cell line, HEK293, when treated with the equivalent IC50 values as applied to the colon cancer cell lines. It thus seemed that at the experimentally deduced IC50 values, the TDTCs were selectively active only against the CRC cells. Overall, cell death induced by the TDTCs was much greater in DLD1 (stage III) cells compared to HT29 (stage II). In HT29 cells, TDTC 1 had strongest effect in inducing cell death followed by TDTC 4 and TDTC 2. TDTC 5 had the weakest effect in inducing cell death in HT29 cells. With DLD1 cells TDTC 2 was the strongest, followed by TDTC 2, TDTC 5 and least effective was TDTC 5.

Having noted the effects on cell viability and on cell proliferation using cell impedance assays, a cell cycle analysis was performed on both the HT29 and DLD1 CRC cells. The compounds effectively reduced the growth rate of the CRC cells. Also, cell cycle arrest was induced by the compounds. In DLD1 cells, a uniform cell cycle arrest occurred at S phase being induced by all the compounds. In comparison in HT29 cells a different cell cycle response was seen, where G0/G1, S, G2/M cell cycle arrest was observed.

The study also assessed the effects of the TDTCs on CD133 positive stem cells isolated from each CRC cell line. An important indicator of putative stem cells is their ability to form spheroids, these being 3-dimensional aggregates of cells in culture. This capability was tested in the HT29 stem cells (CD133+) which did indeed form spheroids confirming their "stemness". Notably here, spheroid formation was inhibited by TDTC treatment. Following this, the response of the HT29 stem cells to TDTC treatment was evaluated using both protein and gene expression approaches.

As depicted in the diagram, a colon cancer tumour may be composed of CRC stem cells (CD133+) possessing the ability to self-renew and undergo multilineage differentiation, together with non-stem cells (CD133-), that are able to proliferate and differentiate. As the stem cells are resistant to chemotherapies, they persist after treatment and may cause patient relapse (179).

The tumour population is maintained and regulated by many different signalling pathways. The CD133+ and CD133- proliferation is regulated by important growth and development proteins such as β-catenin (78). A key pathway in intestinal development and stem cell regulation is the Wnt pathway in CRC (see **fig 39**). In CRC the Wnt associated transcription factor β-catenin may be constitutively expressed, leading to excessive cell proliferation (95) Factors maintaining stem cells and their self-renewal properties including FoxA2, VEGF, VEGFR 1, VEGFR 2, Sox2, Nanog, Oct3/4, Goosecoid, Snail, PDX-1, Otx2, HCG, GATA-4, AFP together with β-catenin are upregulated in CRC. E-cadherin a marker of differentiation has been found downregulated in

cancer cells. Tumour suppressor genes such as Sox17, GATA-4 and TP63 are downregulated during tumour progression (104, 184-188).

In the present study, TDTC treatment downregulated mRNA expression of β-catenin, FoxA2, VEGF, VEGFR 1 and VEGFR 2 in HT29 and DLD1 stem cells. Reduced expression of β-catenin implies that the Wnt signalling is inactivated. The Wnt pathway is involved in proliferation through expression of β-catenin. Reduction expression of the β-catenin retards cell proliferation, which is important in halting tumour progression. As VEGF is an important growth factor required for angiogenesis, the formation of blood vessels required to supply nutrients to tumours (189), the downregulation of this pathway by TDTC is of importance.

Proteins that were significantly upregulated included Sox17, a tumour suppressor gene; and E-cadherin an epithelial cell adhesion protein normally expressed in differentiated cells (110, 190). It would thus seem that TDTCs acted to reduce stem cell "markers" in the cancer stem cells and increased biomarkers associated with cell differentiation.

Aside from affecting the angiogenic pathway, the TDTCs potentially impeded the Wnt signalling pathway in reducing B-catenin expression. As mentioned above the Wnt Pathway is important for regulating s colonic stem cell growth, preventing differentiation of cells, promoting angiogenesis and EMT through expression of β-catenin as it accumulates in the nucleus (191). When dysregulated, the Wnt pathway contributes to excessive stem cell proliferation and tumorigenesis.

In conclusion, the TDTCs have the potential to prevent colon cancer stem cell growth, angiogenesis and EMT acting to promote cell differentiation. These findings are of particular interest, since to date no successful therapies have been developed to target the Wnt pathway. From this analysis a possible mode of action of the TDTCs was mapped and is presented below in Fig 40.

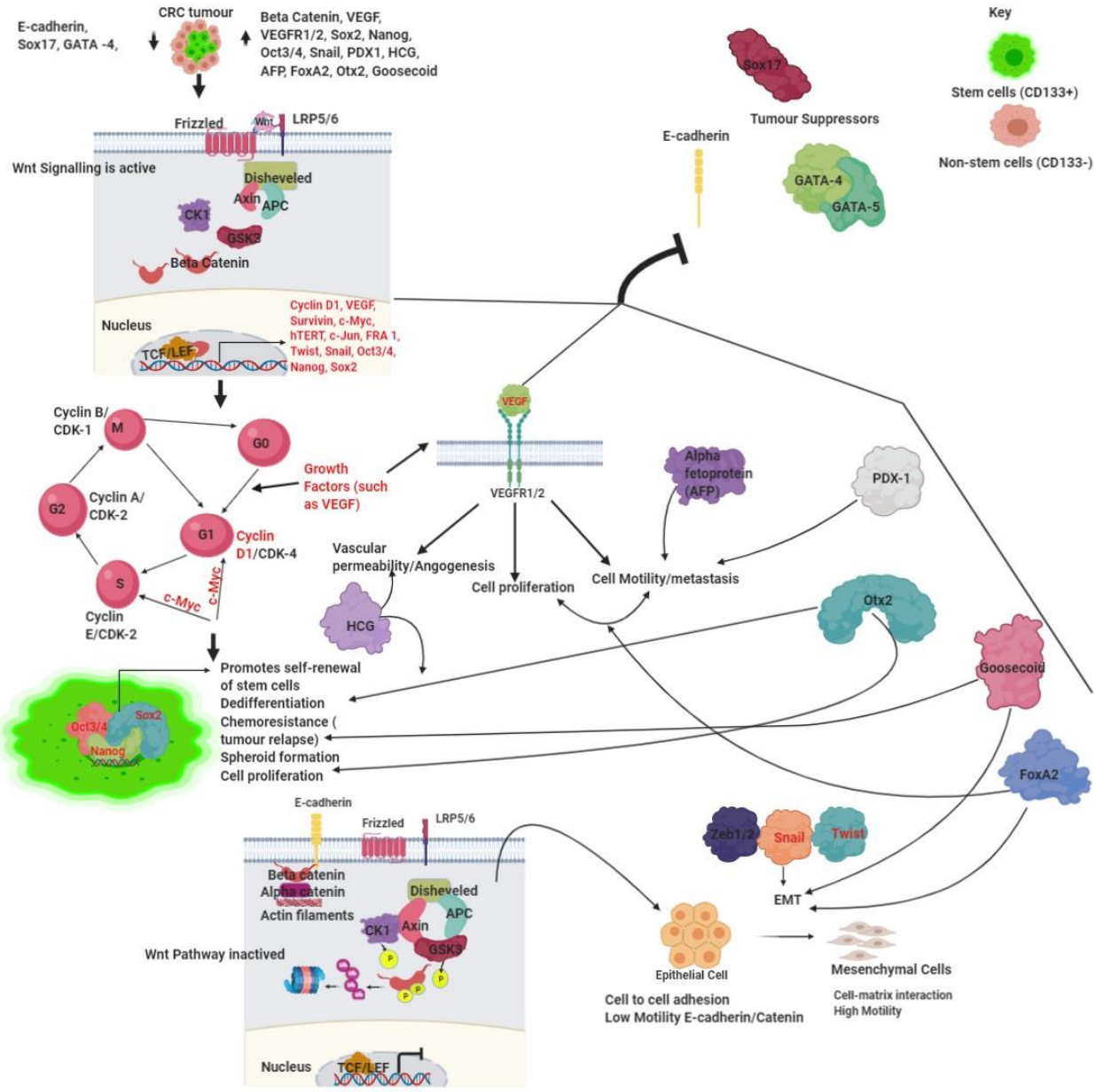


Figure 39: Wnt Pathway and its association with CRC adapted from (191) The Wnt Pathway is essential in intestinal development, it is active through the transcription factor, β-catenin. In absence of Wnt signal β-catenin in the cytosol is phosphorylated by the destruction complex (Axin, APC, GSK3 and CK1) and is marked for ubiquitination end up in proteasome for degradation. In the absence of the Wnt signal β-catenin also interacts with E-cadherin to with alpha catenin and actin filament. In this state differentiation of colon epithelial cells and reduced stem cell growth occurs. Angiogenesis and EMT promoted by β-catenin are inhibited. In the presence of the Wnt signal β-catenin phosphorylation by the destruction complex is ceased, E-cadherin is ablated. This results in accumulation of β-catenin in the nucleus, it interacts with co-transcription factor TCF. The interaction results in transcription of several

genes such as c-Jun, Fra 1, surviving, Oct3/4, Sox2, Nanog, Cyclin D, VEGF, c-Myc, hTERT, Twist and metalloproteinase 7. The activation of these genes results in proliferation of stem cells, angiogenesis and EMT are promoted especially in CRC. PDX-1, AFP, Goosecoid Otx2 and FoxA2 also regulated EMT, angiogenesis, proliferation of stem cells. Differentiation is inhibited. During activation of oncogenes tumour suppressors such GATA-4/GATA-5, Sox17, are E-cadherin are repressed.

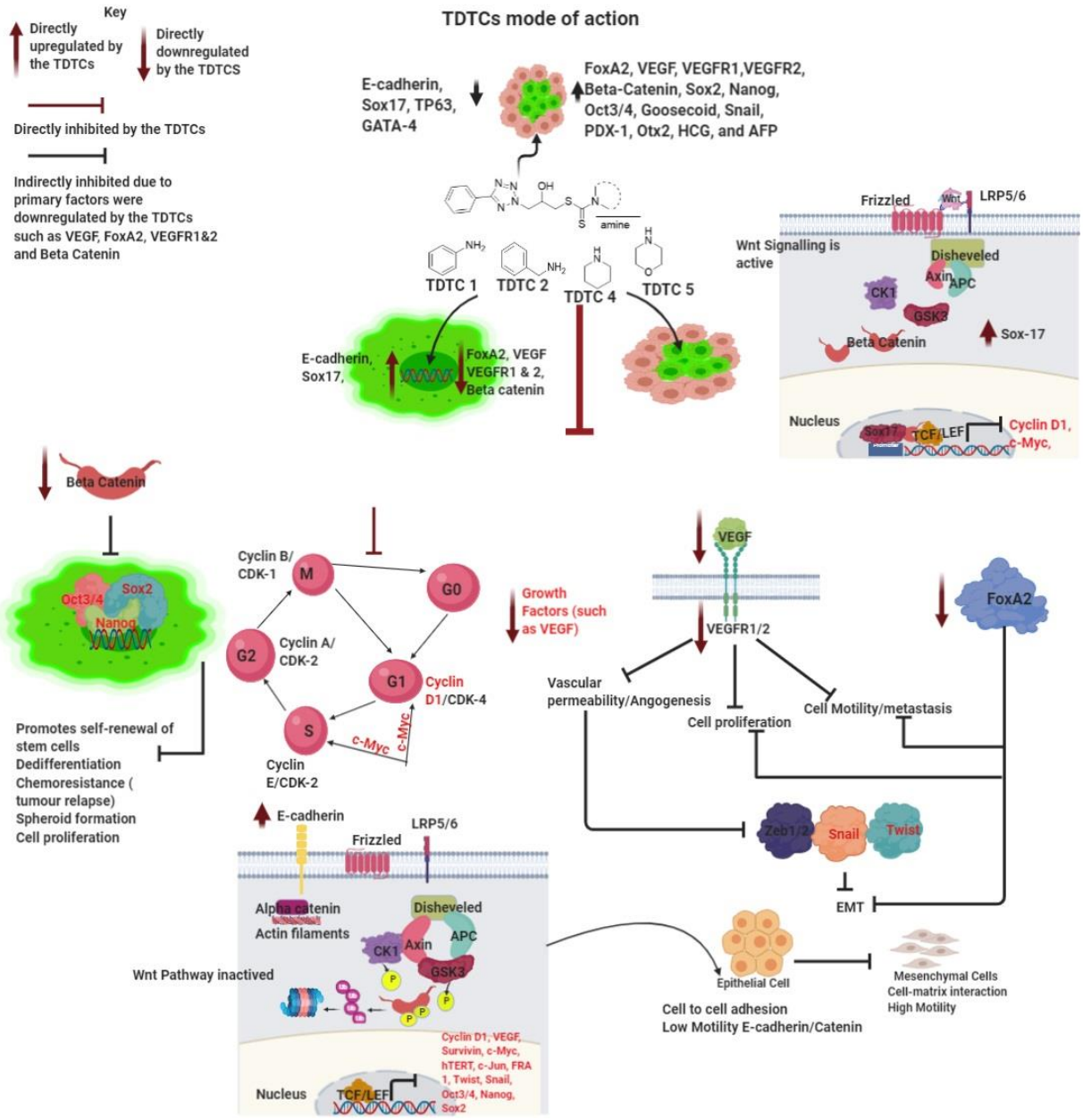


Figure 40: TDTCs Mode of Action

A tumour is heterogeneous containing cells in varying states of differentiation. A small subpopulation of cells are tumour stem cells (CD133+ cell population can form spheroids) while the majority of cells are non-stem cells (CD133-

population). An indicator of putative stem cell is their ability to form spheroids, these being 3-dimensional aggregates of cells in culture. During tumour progression certain factors are upregulated and downregulated. Factors that are upregulated they maintain cell profileration and stem cell growth. These upregulated factors are FoxA2, VEGF, VEGFR1, VEGFR2, β-catenin, Sox2, Nanog, Oct3/4, Otx2, PDX-1, HCG, AFP and Snail, Goosecoid. Downregulated factors are tumour suppressor such as Sox17, GATA-4 and TP63. Epithelial marker E-cadhein is also downregulate. CD133+ and mixed cell population were exposed to TDTC 1, 2, 4 and 5. Cell viability assays were performed, cell cycle assay, spheriod assays followed by protein and gene analyses on CD133+ cells. The finding from the experiments aided in mapping the TDTCs mode of action, the compounds inhibited cell proliferation (CD133+ and CD133- cells), spheriod formation (CD133+) and cell cycle in the mixed population. With protein and gene analysis, it was observed that E-cadherin and Sox17 were upregulated. FoxA2, VEGF, VEGFR1, VEGFR2 and β-catenin were downregulated. The compounds do have the capability to interact with the DNA. The compounds subsituents have been reported that they interact with DNA. Evidence for this is that genes such FoxA2, β-catenin, VEGF and VEGFR1 were downregulated.

4.1 The TDTCs were selectively active

CRC adenocarcinoma cells (HT29 and DLD1) were exposed to the TDTC compounds for 48 hours and were stained using Alamar Blue for an initial colorimetric screening to identify active TDTCs. Trypan Blue exclusion assay was then performed to quantify the cell death induced by the active TDTCs in CRC cells and non-cancerous cells (HEK293). The compounds have shown to have anticancer activity in CRC cell lines. The Trypan blue results further showed that higher concentrations of TDTC 1, 2, 4 and 5 caused less cell death in DLD1 cells than at lower concentrations. It is possible here that the compounds at lower concentrations effectively disrupted an essential pathway that the cells depend on for survival. An analogous example is Taxol which at a low concentration was reported to disrupt the normal cellular microtubule cytoskeleton and resulted in G2/M phase cell cycle arrest in association with inactivated Raf-1, which is essential in blocking cells from entering G2/M phase (192). Activated Raf-1 was however observed at raised concentrations of Taxol. Similarly the low concentrations of active TDTCs may be disrupting an essential cellular pathway in the CRC cells, leading to cell death. This would require further investigation with regards to cell cycle arrest and the initiation of cell death pathways.

Table 6 summarizes the IC50 of the active TDTCs compounds, where the HT29 and DLD1 cells were exposed to the TDTCs. The compounds were highly effective in DLD1 cells as the IC50s were much lower indicating that the compounds are more effective in targeting late stage CRC cells than early stage CRC cells. The compounds This means that the active compounds do have

the potential in reducing metastasis as they were more effective in late stage CRC cell line. In terms of the cell death induced by the compounds, compound **4** was more effective in HT29 cells, followed by compound **1**, compound **2** showed moderate anticancer activity and compound **5** had weak anticancer activity. In DLD1 cells, compound **2** had much greater anticancer efficacy, followed by compound **1**, compound **5** had moderate anticancer activity and the least active compound was compound **4**. The anticancer activity was analysed through quantifying the cell death of the cells.

The active TDTCs showed selective anticancer activity, as they did not induce significant cell death in the non-cancerous human embryonic kidney cells (HEK 293). The selectivity may be due to the presence of different functional groups attached to common tetrazole dithiocarbamate scaffold as moieties or substituents. Compounds **1** and **2** have benzene rings conjugated to tetrazole and dithiocarbamate, where compound **1** benzene ring has a primary amine (aniline)as a substituent. The Compound **2** benzene ring contains a methylamine as substituent. Compound **4** moiety conjugated to the tetrazole and dithiocarbamate is a piperidine. Compound 5, the least selective compound, contains a morpholine moiety conjugated to the tetrazole and dithiocarbamate. The substituents together with the scaffolds (tetrazole and dithiocarbamate) are well known for specific interactions with cancer cells. In this regard, particular chemical moieties have been reported to interact specifically with deficiently repaired DNA of cancer cells, allowing for the formation of DNA adducts. Included here among others are aniline mustards with selectivity towards a leukaemia derived cell line (193, 194); the methylamine substituent fits within the category of alkylating agents, which have shown cancer cell selectivity (195); piperidine derivatives which intercalated with tumour cell DNA were reported to have a higher cytotoxicity in renal cancer cells, prostate cancer cells and breast cancer cells compared to non-cancerous cells (196); and the morpholine substituent has been found to interact with phosphoinositide 3-kinase (PI3K) in melanoma cancer cells. Thus it is feasible to map precisely which substituents of the active TDTCs are essential for their selective anti-cancer properties.

4.2 Active TDTCs affected growth phases of CRC cells

Growth phases are used to predict the growth rate of the cells. There are four different phases, lag phase, exponential phase, stationary or plateau phase and decline or death phase (199). We treated CRC cells, HT29 (50 000 cells) and DLD1 (40 000 cells) with respective IC50s of test compounds and 5-Fu. The growth was recorded in real time in 16 well plate by real time cell analyser (xCelligence) for 100-120 hours.

The active TDTCs compounds had a greater growth inhibitory profile than the conventional drug 5-FU, even though 5-FU was much more potent in inducing cell death in CRC cells. The 5-FU killing effect was noted in the stationary phase in HT29 cells, whilst in DLD1 cells, it was occurred during the late exponential growth phase. At the late exponential and stationary phases, the cell's mitotic index decreases. (200), this being the rate at which the cells divide to form daughter cells. Cells became quiescent as the mitotic index decreases in late exponential and stationary phase. Quiescent cells are not found to be susceptible to anti-cancer drug 5-FU. 5-FU targets rapidly proliferating cells with increased mitotic index. The observation of 5-FU inhibiting cell growth at late exponential and stationary phase is disadvantageous. The observed inhibitory of 5-FU at late exponential and stationary phase shows how acquired resistance occurs. Acquired resistance to chemotherapeutic agents is alarming in clinical settings. Drug resistance is acquired when some of the cells stop proliferating (become quiescent) and remain at G0/G1 phase of the cell cycle. As the drug decreases in surrounding, these quiescent cells start proliferating again to form a new tumour (201, 202).

Compound **1** induced cell death at late stationary phase in HT29 cells and DLD1 cells. It is also effective at lower concentration. In late exponential and stationary phases, there is a large proportion of cells that are quiescent. Quiescent cells are not easily targeted by compounds especially if the compounds are targeting rapidly proliferating cells. The active TDTCs have the capability to target quiescent cells as the compounds prevented spheroid formation of isolated HT29 stem cells (CD133+).

Compound **2** was effective at hindering cell growth at initial exponential phase in HT29 cells whilst in DLD1 cells the compound induced cell death at the late exponential phase. It has been assumed that cells growing at exponential phase have constant cell-cell interactions (203). Compound **2**

ability to inhibit cell growth at initial exponential phase, shows the compound 2 influences cell-cell interactions. Cell-cell interactions are responsible for promoting the tumour cell growth (203).

Compound **4** did not induce any death phase on both HT29 and DLD1 cells. Compound **5** induced a decline in cell growth at stationary phase, but the induced cell death was not as great as compared to compound **1**, **2** and 5-Fu. However, there was no cell death observed in DLD1 cells. Even though low capacity in inhibiting growth was observed for compound **4** and **5**, they did prevent spheroid formation in the HT29 stem cells (CD133+).

4.3 Active TDTCs arrested cell cycle in CRC cells

It is important when evaluating anticancer effects of compounds that cell-cycle functioning is assessed, since tumour cells dysregulate their cell-cycle, resulting in continuous proliferation. The cell cycle assay was conducted using the MUSE™ Cell Cycle Kit. HT29 and DLD1 cells were exposed to the compounds with respective IC50s for 48 hours. The compounds induced cell cycle arrest in HT29 and DLD 1 CRC cell lines. Differential cell cycle arrest was observed in HT29 and in DLD1 the compounds induced uniform cell cycle arrest. In HT29 cells, active compounds induced cell cycle arrest at G2/M phase (Compound **1**), G0/G1 (Compound **2** and **5**) and S phase (Compound **4**). All compounds arrested cell cycle at S phase in DLD 1 cells.

G0/G1 cell cycle arrest was facilitated by active compound **2** and **5** in HT29 cells. A significant reduction in the percentage of gated cells was observed in G2/M phase in HT29 cells exposed to compound **2** and **5,** where G0/G1 cell cycle arrest was observed. G0 phase in the cell-cycle is characterized by quiescent cells, the cells are not dividing to form daughter cells but are metabolically active. G1 phase of the cell cycle is a preparatory phase before proliferation. Growth factors are produced, and proliferating signals are activated preparing the cells for proliferation. At late G1 phase, cells do not require growth factors (this is the restriction point), its progression into S phase solely depends on cell size and DNA integrity (204). If the cell cycle is arrested at G0/G1 phase, initiation of proliferation is prevented.

Compound **4** induced cell cycle arrest at S phase in HT29 cells. Whilst in DLD1 cells, all compounds induced S phase cell cycle arrest. S phase cell cycle arrest is a result of modulation of cell cycle genes or proteins involved in S phase progression. S phase cell cycle arrest can occur

due to DNA damage, malfunction or downregulation of proteins involved in DNA replication such as DNA topoisomerase (205, 206).

Compound **1** induced G2/M cell cycle arrest in HT29 cells. After synthesis of the DNA, DNA is further scanned for incomplete DNA replication that could result in improper DNA ligation. The DNA repair occurs in G2 phase (207). After DNA repair, cells proceed to M phase where the sister chromatids and daughter cells separate (208). The G2/M cell cycle arrest surely prevents the completion of mitosis. The cell cycle arrest induced in this study by the compounds could indicate an interaction with the DNA.

While compounds **4** and **5** induced cell death as observed in the Trypan Blue exclusion assay and cell cycle arrest, their growth inhibitory effect was not deduced from the real time cell growth analyses. The growth phases that are deduced from real time cell growth analysis are associated with cell cycle phases (201). In this regard it is expected that a compound arresting the cell cycle should also have inhibited cell growth as measured by real time cell analysis. Further investigation must be conducted using slightly increased concentration (s) as to link how compounds **4** and **5** induced cell death and cell cycle arrest and their inhibitory effect on CRC cell growth.

4.4 Active TDTCs inhibited spheroid formation in CRC stem cells

Spheroid assays are important as these mimic *in vivo* tumour growth, providing a 3D representation of cell growth (209); and notably, cancer stem cells form spheroids (184). Cells growing as spheroids have two zones, an outer and an inner zone. The outer zone contains rapidly proliferating tumour cells, while the inner zone contains cells that are quiescent and are hypoxic (177). Conventional drugs cannot penetrate through to the inner zone. However, even if they do, they lack the ability to target the quiescent cells (210). For instance, 5-FU only affects rapidly proliferating cancer cells and would therefore only affect the outer zone of dividing cells and not the inner quiescent zone.

With the spheroid formation assay, HT29 stem cells (30 000 cells) were exposed to the IC50 of the test compounds, 5-FU and SAHA (Vorinostat) for 168hours. HT29 stem cells were selected over DLD1 cells, as they readily formed spheroids in *in vitro* culture conditions. All compounds at their respective IC50s prevented formation of spheroids in HT29 stem cells. In comparison, SAHA and 5-FU did not prevent spheroid formation even after 168 hours. The effects of the tetrazole

compounds on inhibiting this fundamental property of stem cells to form spheroids indicates that they target CRC stem cells and block their ability to self-renew.

4.5 Active TDTCs modulated CRC stem cell proteome

The effectiveness of the compounds at targeting CRC stem cells was further investigated at a protein expression level by quantifying key stem cell biomarkers following treatment of HT29 and DLD1 CRC stem cells; and here, biomarkers that are essential in maintaining stem cells and tumour progression were differentially expressed. In particular, there were changes in the protein levels of E-cadherin, Sox17 and FoxA2 in both HT29 and DLD1 stem cells. Notably, E-cadherin and Sox17 were upregulated in HT29 stem cells, while FoxA2 was downregulated after treatment.

4.5.1 E-cadherin and Nanog

E-cadherin is implicated in the initiation of EMT. The loss of E-cadherin in epithelial cells, converts epithelial cells into mesenchymal cells. This is when the epithelial cells gain stem-like properties, whereby they express stem cell biomarkers. The transitioned cells are termed stem-like cells (211). The stem-like cells have upregulated stem cell biomarkers such as Nanog, Oct4, SOX2 and EpCAM. Various small molecules have upregulated E-cadherin expression in CRC, leading to the reversal of EMT, reduction in cell proliferation and over-coming drug resistance (212). In the present study, the synthesized compounds upregulated E-cadherin. In terms of stem-like cells, the compounds might affect EMT, which is implicated in metastasis and drug resistance. Compounds **1** and **4** were more effective in upregulating E-cadherin in HT29 stem cells, while Nanog expression was unaffected.

With regards to CRC stem cells, upregulation of E-cadherin may lead to continuous proliferation. In embryonic stem cells (ESC), E-cadherin can regulate transcription of Nanog through phosphorylation of STAT3 in ESC (213, 214). It has been found that CRC primary tumours have two distinct populations of cancer stem cells, one population with upregulated E-cadherin and the other lacking E-cadherin. The cells that expressed E-cadherin, were highly proliferative, while cells without E-cadherin were quiescent. Moreover cells which expressed E-cadherin also expressed Nanog at high levels (215). Nanog is a pluripotent transcription factor, that impedes the differentiation of stem cells allowing them to continuously proliferate symmetrically. Compound

5 downregulated E-Cadherin in DLD1 stem cells, implying that it may inhibit proliferation of DLD1 stem cells. The compounds neither upregulated nor downregulated Nanog expression in the proteome profiler array assay.

4.5.2 FoxA2

FoxA2 is essential in the development of the intestines. FOXA2 seems to regulate many genes in diverse pathways contributing to intestinal function, including tube development, regulation of cell morphogenesis and solute transport (216); and it is upregulated in CRC tissues. Its upregulation is correlated with lymphatic metastasis. FoxA2 promotes proliferation, migration, invasion and is also involved in EMT (217). The oncogenicity of FoxA2 is cell type-specific, being able to act as a tumour suppressor in gastric cancer (218). The reduction of FoxA2 in CRC cells has been reported to result in apoptosis and upregulation of E-cadherin (217). With regards to FoxA2 expression and its role in CRC stem cells, this is not well documented. It was previously observed that in patient-derived CRC liver metastatic stem cells (CRCLM) there was a high expression of FoxA2. Triple combination treatment (curcumin, 5-Fu, and oxaliplatin), significantly reduced FoxA2 expression in CRCLM stem cells (219). In the present study, all of the compounds significantly downregulated FoxA2 in both HT29 and DLD1 cells. Compounds **2** and **4** were the most effective in reducing FoxA2 expression in HT29 stem cells.

4.5.3 SOX17

Sox17 is transcription factor that regulates differentiation in pluripotent cells (220). SOX17 has been shown to possess tumour suppressor capabilities in CRC. It has been observed that SOX17 inhibited cell proliferation, stemness and EMT regulated by β-catenin/TCF activity. This resulted in inhibition of invasion and metastasis. Similarly, in cervical cancer SOX17 halted proliferation (186). A microRNA, miR-371-5p was reported to be associated with SOX17 anticancer activity (190). In the present study, compounds **1** and **2** upregulated Sox17 in DLD1 stem cells, while compound **4** upregulated Sox17 in HT29 stem cells.

4.5.4 VEGFR2

The VEGF receptors, VEGFR1 VEGFR2 and VEGFR3 all play a role in angiogenesis. Compound **1** reduced expression of VEGFR2 in DLD1 stem cells and compound **4** reduced VEGFR 2 expression in HT29 stem cells. VEGFR2 in poorly differentiated CRC cells has been found to

promote differentiation of the undifferentiated CRC cells into endothelial cells. The CRC endothelial cells from primitive vascular plexus-like structures, which form matured capillaries. The ablation of VEGFR2 in these stem like-cells inhibits the formation of vascular structures (221). VEGFR2 also has a role in CRC-associated inflammation. VEGFR 2 promotes tumour progression and prevents senescence during acute inflammation (222). Self-renewal of cancer stem cells is also regulated by VEGFR2/STAT3-mediated upregulation of Myc and Sox2, as VEGF interacts with VEGFR2. This has been reported in breast and lung cancer stem cells (223). Compound **1** and compound **4** may act as VEGFR2 inhibitors, especially in stem-like cells. Also, the compounds may reduce inflammation promoted by VEGFR2 in CRC.

4.5.5 Oct3/4

Oct3/4 is essential in maintaining the stem cell state, being implicated in the self-renewal of CRC stem cells and stem-like cells (224). Compound **1** significantly downregulated Oct3/4 in HT29 stem cells, whilst compound **4** upregulated Oct3/4 in HT29 stem cells. Compound **1** has a direct effect on CRC stem cells as it downregulated an essential CSC marker (225).

4.5.6 Sox2

In CRC, SOX2 has a role in EMT, tumour migration and invasion. The expression of Sox2 has been correlated with distant metastases in right-sided colon cancer (226). Overexpression of Sox2 is coupled with quiescence of CRC stem cells (227). Sox2 was significantly downregulated by compound **1** in HT29 stem cells, but compound **4** upregulated Sox2 in HT29 stem cells and compound **5** downregulated Sox2 in DLD1 stem cells. The downregulation of Sox2 may limit metastasis, preventing tumour relapse; and CRC stem cells could potentially be treated with other drugs.

4.5.7 GATA-4

The promoters of GATA-4 and GATA-5 are hypermethylated in primary CRC tissues. GATA -4 has tumour suppressor role, it regulates anticancer genes (228). GATA-4 expression was unaltered by compounds **1, 2** and **5**. Compound **4** upregulated GATA-4 in HT29 stem cells and downregulated the protein in DLD1 stem cells. GATA4/5 proteins inhibit proliferation, colony formation, migration, invasion and anchorage-independent growth in CRC cells.

4.5.8 PDX-1

PDX-1 is a transcription factor, that regulates the expression of insulin in β-cells of the pancreas. PDX-1 has been classified as an oncogene in pancreatic cancer. Its knock-down improved survival and halted tumour growth in xenograft mouse models (83, 185). PDX-1 has been found in CRC cells, especially in metastatic cells (84). Compounds **1, 2** and **4** upregulated PDX-1 in HT29 stem cells equally and was downregulated by Compounds **4** and **5** in DLD1 stem cells. It is suggested here that these compounds may combat metastasis associated with PDX-1 expression.

4.5.9 Otx2

Otx2 is a well-known medulloblastoma (MB) oncogene. Otx2 promotes self-renewal and growth of MB, preventing differentiation by inhibiting the expression of axon guidance genes (229). Little is known about Otx2 role in CRC. In this study both DLD1 and HT29 stem cells expressed Otx2, which was upregulated by compound **4** in HT29 stem cells.

4.5.10 Goosecoid

Goosecoid (GSC) is primarily a transcription factor that participates in cell migration in embryonic development (230). GSC has been implicated in chemoresistance. Its high expression in ovarian and breast cancer has been associated with metastasis. GSC overexpression confers both cancers to be resistant to chemotherapy (90). In CRC, GSC functions as an EMT-inducing transcription factor (231). HT29 stem cells exposed to compound **2** and **4** had upregulated GSC expression, while compound **1** downregulated GSC in HT29 stem cells, but upregulated GSC in DLD1 stem cells.

4.5.11 Snail

Snail is implicated in EMT through repressing E-cadherin associated with cell membranes. Its overexpression results in stem-like cells in CRC and causes metastasis (187). It is also expressed in CRC stem cells (232). Compound **4** downregulated Snail in DLD1 stem cells and upregulated Snail in HT29 stem cells. The other active compounds did not have any effect on Snail expression.

4.5.12 HCG

Human chorionic gonadotropin (HCG) facilitates embryo implantation and is secreted by the syncytiotrophoblast. Non-trophoblastic solid tumours express β-HCG, this includes renal carcinoma, hepatocarcinoma, and bladder carcinoma. In CRC, the β-HCG expression is shown to correlate with poor prognosis of CRC patients (92). The cells that express HCG become embryonic cells, it's further implicated in angiogenesis and invasion (233). HCG expression in DLD1 and HT29 stem cells was not modulated by the compounds, enabling them to be considered as anticancer agents that can target EMT and cancer stem cells.

4.5.13 TP63

The TP63/p63 gene encodes 6 different isoforms TAp63α, TAp63β, TAp63γ, ΔNp63α, ΔNp63β, and ΔNp63γ**.** In CRC, high expression of p63 was associated with increased survival. TAp63 acts as a tumour suppressor, whilst ΔNp63 is an oncogene. High levels of TAp63 are responsible for activating p53 response genes, resulting in cell cycle arrest and apoptosis (234). All of the tested compounds failed to modulate the TP63 protein. It would be essential to discriminate the different isoforms whilst exposing the stem cells to the compounds. As mentioned, different isoforms have different roles in CRC and other cancers. In squamous cancer, TP63 promotes tumour progression (235).

4.5.13 AFP

Elevated levels of AFP are associated with hepatocellular carcinoma or embryonic cell carcinoma. Lung, kidney, gastrointestinal tract and ovary cancer also have high levels of AFP. CRC-producing AFP (CRC-PAFP) is extremely rare. Poor prognosis is associated with CRC producing AFP, because lymph node or liver metastases occurred during the time of diagnosis (188, 236). The compounds did not have any effect on AFP.

4.6 Active TDTCs modulated gene expression of stem cell biomarkers

4.6.1 β-catenin

It has been suggested that β-catenin regulates the expression of most stem cell biomarkers directly or indirectly. β-catenin is also important in intestinal development (237). Thus, we investigated here if β-catenin gene expression was modulated by the test compounds. It was observed that two compounds, 1 and 5, downregulated β-catenin gene expression in DLD1 stem cells. In comparison, all four compounds downregulated β-catenin gene expression in the HT29 stem cells. Only compounds **2** and **4** upregulated β-catenin mRNA in DLD1 stem cells. The range at which the mRNA was downregulated by the compounds was -0,04 to -0,3 (log2(fold change)). Log2(fold change) of -0,1 and below and 2 and above has been considered significant in our study. It was observed that late-stage CRC cells expressed much higher levels of β-catenin compared to CRC stem cells. This hints at the involvement of β-catenin in EMT (32). The reduction of β-catenin mRNA in HT29 stem cells by all compounds and DLD1 stem cells by compounds **1** and **5** suggests a role in halting the maintenance and proliferation of CRC stem cells (238).

4.6.2 FoxA2

In association with a downregulation in mRNA expression, protein levels of FoxA2 were decreased. Moreover, FoxA2 mRNA levels were reduced in both HT29 and DLD1 CRC stem cells, by all of the compounds. With regards to decreased protein levels, the effects were similar for all, except for compound **1** in HT29 stem cells. Compound **1** downregulated FoxA2 mRNA, whilst the protein lacked any significant downregulation. As FoxA2 is dysregulated in cancer, this may be an important regulatory effect by these compounds.

4.6.3 VEGF-A

VEGF is a growth factor that is actively involved in angiogenesis (189). VEGF mRNA was downregulated in DLD1 stem cells by all the active compounds. In HT29 stem cells compound **1** and **5** particularly downregulated VEGF mRNA levels. The active compounds have the potential to regulate angiogenesis. The compounds downregulation of VEGF-A gene expression can be reflected through how miR-1 downregulates VEGF-A expression. MiR-1 targets VEGF-A in CRC cells. The downregulation of VEGF-A in CRC leads to a reduction in cell proliferation and invasion. VEGF-A also activates the MAPK and PI3K/AKT pathways. These pathways are

implicated in cancer progression. MiR-1 may affect the MAPK and PI3K/AKT pathway through downregulating VEGF-A (239). Furthermore, the downregulation of VEGF-A mRNA controls the production of intracellular VEGF-A in CRC. Intracellular VEGF-A has been implicated in ECM invasion and migration

4.6.4 VEGFR1 was downregulated in late stage of CRC stem cells

When VEGFA encounters VEGR1 this results in pathological angiogenesis (240). VEGF-A/VEGF-B-VEGFR-1 activation has led to the promotion of ERK-1/2 and JNK MAPK downstream signalling pathways, which has resulted in cell migration, invasion, and colony formation. Cell migration is regulated by the VEGF-A/VEGFR1 pathway through modulation of FAK activity (241). VEGFR-1 is expressed by immune cells that are present in the tumour niche, the cells contribute to angiogenesis and cancer progression. VEGFR1 mRNA was downregulated by the compounds in DLD1 stem cells. Compound **5** had much greater effect on the downregulation of VEGFR1 with log2(fold change) of -0,58 followed by compound **4**, compound **2** and compound **1**.

4.7 Anticancer activity of TDTC might be associated with their chemical structures

The compounds ability to interact with DNA lies in their substituent and ability of their moieties to interact with DNA. Compound **1** has an aniline substituent that has been implicated in interacting with the DNA via hydrogen bonding (242). A methylamine substituent found in compound **2,** is associated with chromatin restructuring and causes DNA cleavage. The methylamine substituent has been reported to trigger anticancer activity through DNA cleavage resulting in programmed cell death (243). Compound **4** has a piperidine moiety, which is known for intercalating with the DNA (196). Compound **5** has a morpholine moiety, which interacts with DNA through groove binding, electrostatic interactions and intercalation. The results from the present study indicate that the test compounds do interact with DNA/RNA.

4.8 Future directions

It would be important to perform confocal microscopy to validate the results obtained from the human pluripotent stem cell biomarker proteome array. This will give a visual representation of the stem cell biomarkers at a subcellular level.

4.9 Conclusion

Potent anticancer activity was demonstrated by the active TDTC compounds. The compounds targeted both differentiated CRC and CRC stem cells. The non-cancerous HEK293 cells were not affected by these compounds, making the TDTCs selectively active only against cancer cells.

The synthesised TDTCs were classified as weak, moderate and active anticancer agents. The compounds were able to arrest different phases of the cell cycle in CRC cells, thus modulating their growth during the in exponential phase of growth.

Active TDTCs also prevented the spheroid formation in CRC stem cells. The compounds modulated important stem cell biomarker proteins involved in regulating and maintaining stemness. The compounds might target EMT, as many important factors involved in EMT were modulated by the compounds such E-cadherin. Compound **5** has a potential of halting CRC stem cell proliferation through downregulating E-cadherin in DLD1 stem cells. High expression of E-cadherin in CRC stem cells is correlated with excessive proliferation of stem cells. The compounds might also be speculated to inhibit metastasis, as they downregulate FoxA2 expression at gene and protein level. Pathological angiogenesis in CRC might also be alleviated by the compounds in a unique manner, as the compounds downregulated VEGFR-1 and VEGF-A mRNA.

The screening of different stem cell biomarkers proteins has showed potential drug resistance that may occur, as the compound **2** and **4** upregulated Goosecoid which is implicated in chemoresistance. The functional group substituents/moieties present on compounds indicate that the compound does interact with DNA/RNA. Indeed, the compounds did downregulate mRNA of β-catenin, FoxA2, VEGF-A and VEGFR1. The compounds can be used to treat early and late stage of CRC.

4.10 The relevance of the study

The study assessed the activity of TDTCs against the early and late stages of CRC. The compounds will provide useful scaffolds upon which to design and test more refined anti-cancer compounds that may be beneficial to the healthcare community. The present compounds were very selective, and with further development may exclusively kill cancer cells. This study has the potential to be preclinically translated; animal studies would need to be carried out to confirm the the anti-tumour activities of the compounds and pharmacokinetic studies would need to be performed. Detailed mapping of the compounds using *in-silico* modelling would assist with understanding their modes of action.

The study as shown that the compounds can target CRC stem cells and could potentially prevent patient relapse due to stem cell persistence. The compounds may also be able to reduce/inhibit metastasis and pathological angiogenesis as factors involved in these processes were downregulated. Finally, in conclusion, it would seem that these compounds may be beneficial to cancer therapy as they will address the current situation with conventional therapy wherein stem cells remain unaffected.

5. References

1. Chakraborty S, Rahman T. The difficulties in cancer treatment. ecancermedicalscience. 2012;6:ed16.
2. Alfarouk KO, Stock C-M, Taylor S, Walsh M, Muddathir AK, Verduzco D, et al. Resistance to cancer chemotherapy: failure in drug response from ADME to P-gp. Cancer Cell International. 2015;15:71-.
3. Cancer Tomorrow [Internet]. International Agency for Research and Cancer, Globocan 2018. 2018 [cited 5/3/2020]. Available from: http://gco.iarc.fr/tomorrow/graphic-isotype?type=1&population=900&mode=population&sex=0&cancer=39&age_group=value&apc_male=0&apc_female=0.
4. Cancer in South Africa [Internet]. 2014 [cited 2018/08/24]. Available from: http://www.nicd.ac.za/centres/national-cancer-registry/.
5. McCabe M, Perner Y, Magobo R, Mirza S, Penny C. Descriptive epidemiological study of South African colorectal cancer patients at a Johannesburg Hospital Academic institution. Journal of Gastroenterology and Hepatology Open. 2019.
6. Zhang L, Cao F, Zhang G, Shi L, Chen S, Zhang Z, et al. Trends in and Predictions of Colorectal Cancer Incidence and Mortality in China From 1990 to 2025. Frontiers in Oncology. 2019;9(98).
7. Mauri G, Sartore-Bianchi A, Russo A-G, Marsoni S, Bardelli A, Siena S. Early-onset colorectal cancer in young individuals. Molecular Oncology. 2019;13(2):109-31.
8. Rustgi AK. Familial pancreatic cancer: genetic advances. Genes & development. 2014;28(1):1-7.
9. Hardiman KM. Update on sporadic colorectal Cancer genetics. Clinics in colon and rectal surgery. 2018;31(03):147-52.
10. Schubert SA, Morreau H, de Miranda NF, van Wezel T. The missing heritability of familial colorectal cancer. Mutagenesis. 2019.
11. Ahnen DJ, Wade SW, Jones WF, Sifri R, Mendoza Silveiras J, Greenamyer J, et al. The Increasing Incidence of Young-Onset Colorectal Cancer: A Call to Action. Mayo Clinic Proceedings. 2014;89(2):216-24.

12. Davis DM, Marcet JE, Frattini JC, Prather AD, Mateka JJ, Nfonsam VN. Is it time to lower the recommended screening age for colorectal cancer? Journal of the American College of Surgeons. 2011;213(3):352-61.
13. Campos FG. Colorectal cancer in young adults: A difficult challenge. World journal of gastroenterology. 2017;23(28):5041.
14. Jung SH, Kim SH, Kim JH. Prognostic Impact of Microsatellite Instability in Colorectal Cancer Presenting With Mucinous, Signet-Ring, and Poorly Differentiated Cells. Annals of coloproctology. 2016;32(2):58-65.
15. Cronje L, Paterson AC, Becker PJ. Colorectal cancer in South Africa: a heritable cause suspected in many young black patients. South African medical journal = Suid-Afrikaanse tydskrif vir geneeskunde. 2009;99(2):103-6.
16. Murphy CC, Singal AG, Baron JA, Sandler RS. Decrease in Incidence of Young-Onset Colorectal Cancer Before Recent Increase. Gastroenterology. 2018;155(6):1716-9.e4.
17. Shussman N, Wexner SD. Colorectal polyps and polyposis syndromes. Gastroenterology report. 2014;2(1):1-15.
18. Hyer W, Tavares M, Thomson M. Polyps and other tumors of the gastrointestinal tract. Textbook of Pediatric Gastroenterology, Hepatology and Nutrition: Springer; 2016. p. 587-605.
19. Saini MK, Juneja M, Mittal A. Colorectal Cancer Detection from Colonoscopy Videos: A Comprehensive Survey of Computer-Aided Diagnosis Techniques. 2018.
20. Chen P-J, Lin M-C, Lai M-J, Lin J-C, Lu HH-S, Tseng VS. Accurate classification of diminutive colorectal polyps using computer-aided analysis. Gastroenterology. 2018;154(3):568-75.
21. Edge SB, Edge SB. AJCC Cancer Staging Manual 8th Ed: Springer; 2017.
22. Colorectal Cancer Stages [Internet]. 2018 [cited 10/11/19]. Available from: https://www.cancer.org/about-us/online-help/contact-us.html.
23. Compton CC, Greene FL. The staging of colorectal cancer: 2004 and beyond. CA: A cancer journal for clinicians. 2004;54(6):295-308.
24. How is the stage determined? [Internet]. 2018 [cited 10/11/19]. Available from: https://www.cancer.org/cancer/colon-rectal-cancer/detection-diagnosis-staging/staged.html.

25. Weiser MR. AJCC 8th edition: colorectal cancer. Annals of surgical oncology. 2018;25(6):1454-5.
26. Bowel Cancer [Internet]. Cancer Research UK. 2018 [cited 2/2/20]. Available from: https://www.cancerresearchuk.org/about-cancer/bowel-cancer.
27. Konishi T, Shimada Y, Lee LH, Cavalcanti MS, Hsu M, Smith JJ, et al. Poorly Differentiated Clusters Predict Colon Cancer Recurrence: An In-Depth Comparative Analysis of Invasive-Front Prognostic Markers. The American journal of surgical pathology. 2018;42(6):705-14.
28. Saitoh T, Takamura A, Watanabe G. Endoscopic and clinicopathological features of intramucosal, histologically mixed-type, low-grade, well-differentiated gastric tubular adenocarcinoma with the potential for late-onset lymph node metastasis. BioMed Central gastroenterology. 2018;18(1):189.
29. Suzuki M, Nakatani Y, Ito H, Narimatsu H, Yamada K, Yoshioka E, et al. Pulmonary adenocarcinoma with high-grade fetal adenocarcinoma component has a poor prognosis, comparable to that of micropapillary adenocarcinoma. Modern Pathology. 2018;31(9):1404-17.
30. Kevans D, Wang LM, Sheahan K, Hyland J, O'Donoghue D, Mulcahy H, et al. Epithelial-mesenchymal transition (EMT) protein expression in a cohort of stage II colorectal cancer patients with characterized tumor budding and mismatch repair protein status. International journal of surgical pathology. 2011;19(6):751-60.
31. Bonetti LR, Barresi V, Bettelli S, Domati F, Palmiere C. Poorly differentiated clusters (PDC) in colorectal cancer: what is and ought to be known. Diagnostic pathology. 2016;11(1):31.
32. Basu S, Cheriyamundath S, Ben-Ze'ev A. Cell-cell adhesion: linking Wnt/β-catenin signaling with partial EMT and stemness traits in tumorigenesis. F1000Research. 2018;7:F1000 Faculty Rev-488.
33. Weinberg R, Hanahan D. The hallmarks of cancer. Cell. 2000;100(1):57-70.
34. Hanahan D, Weinberg RA. Hallmarks of cancer: the next generation. Cell. 2011;144(5):646-74.
35. Grazioso TP, Brandt M, Djouder N. Diet, Microbiota and Colorectal Cancer. iScience. 2019.

36. McMahon KW, Karunasena E, Ahuja N. The Roles of DNA Methylation in the Stages of Cancer. Cancer journal (Sudbury, Mass). 2017;23(5):257-61.
37. Shimamoto Y, Tamura S, Masumoto H, Maeshima K. Nucleosome–nucleosome interactions via histone tails and linker DNA regulate nuclear rigidity. Molecular biology of the cell. 2017;28(11):1580-9.
38. Qin J, Wen B, Liang Y, Yu W, Li H. Histone Modifications and their Role in Colorectal Cancer. Pathology & Oncology Research. 2019:1-11.
39. O'Hagan HM. Chromatin modifications during repair of environmental exposure-induced DNA damage: A potential mechanism for stable epigenetic alterations. Environmental and molecular mutagenesis. 2014;55(3):278-91.
40. Khabar KS. Hallmarks of cancer and AU-rich elements. Wiley Interdisciplinary Reviews: RNA. 2017;8(1):e1368.
41. Wang L-H, Wu C-F, Rajasekaran N, Shin YK. Loss of tumor suppressor gene function in human cancer: an overview. Cellular Physiology and Biochemistry. 2018;51(6):2647-93.
42. Wong RSY. Apoptosis in cancer: from pathogenesis to treatment. Journal of Experimental Clinlical Cancer Research. 2011;30(1):87-.
43. Chen C-Y, Chen J, He L, Stiles BL. PTEN: Tumor Suppressor and Metabolic Regulator. Frontiers in Endocrinology. 2018;9(338).
44. Tian X, Doerig K, Park R, Can Ran Qin A, Hwang C, Neary A, et al. Evolution of telomere maintenance and tumour suppressor mechanisms across mammals. Philosophical Transactions of the Royal Society B: Biological Sciences. 2018;373(1741):20160443.
45. Pinhu L, Qin Y, Xiong B, You Y, Li J, Sooranna SR. Overexpression of Fas and FasL is associated with infectious complications and severity of experimental severe acute pancreatitis by promoting apoptosis of lymphocytes. Inflammation. 2014;37(4):1202-12.
46. Bhola PD, Letai A. Mitochondria—judges and executioners of cell death sentences. Molecular cell. 2016;61(5):695-704.
47. Silke J, Meier P. Inhibitor of apoptosis (IAP) proteins–modulators of cell death and inflammation. Cold Spring Harbor perspectives in biology. 2013;5(2):a008730.
48. Chen L, Zeng Y, Zhou S-F. Role of Apoptosis in Cancer Resistance to Chemotherapy. Current Understanding of Apoptosis: Programmed Cell Death. 2018:125.

49. Kim NW, Piatyszek MA, Prowse KR, Harley CB, West MD, Ho PdL, et al. Specific association of human telomerase activity with immortal cells and cancer. Science. 1994;266(5193):2011-5.
50. Shay JW. Role of telomeres and telomerase in aging and cancer. Cancer discovery. 2016;6(6):584-93.
51. Akincilar SC, Unal B, Tergaonkar V. Reactivation of telomerase in cancer. Cellular and Molecular Life Sciences. 2016;73(8):1659-70.
52. Spiegl-Kreinecker S, Lötsch D, Neumayer K, Kastler L, Gojo J, Pirker C, et al. TERT promoter mutations are associated with poor prognosis and cell immortalization in meningioma. Neuro-oncology. 2018;20(12):1584-93.
53. Tacconi EM, Tarsounas M. How homologous recombination maintains telomere integrity. Chromosoma. 2015;124(2):119-30.
54. Simonatto M, Latella L, Puri PL. DNA damage and cellular differentiation: more questions than responses. Journal of cellular physiology. 2007;213(3):642-8.
55. Bielenberg DR, Zetter BR. The Contribution of Angiogenesis to the Process of Metastasis. Cancer Journal. 2015;21(4):267-73.
56. Mousa S, Davis P. Anti-angiogenesis Strategies in Cancer Therapies: Academic Press; 2016.
57. Pavlakovic H, Havers W, Schweigerer L. Multiple angiogenesis stimulators in a single malignancy: implications for anti-angiogenic tumour therapy. Angiogenesis. 2001;4(4):259-62.
58. Rajabi M, Mousa SA. The role of angiogenesis in cancer treatment. Biomedicines. 2017;5(2):34.
59. Winkler F. Hostile takeover: how tumours hijack pre-existing vascular environments to thrive. The Journal of pathology. 2017;242(3):267-72.
60. Skalak TC, Price RJ. The role of mechanical stresses in microvascular remodeling. Microcirculation. 1996;3(2):143-65.
61. Xu H, Zhang Y, Peña MM, Pirisi L, Creek KE. Six1 promotes colorectal cancer growth and metastasis by stimulating angiogenesis and recruiting tumor-associated macrophages. Carcinogenesis. 2017;38(3):281-92.
62. Katayama Y, Uchino J, Chihara Y, Tamiya N, Kaneko Y, Yamada T, et al. Tumor Neovascularization and Developments in Therapeutics. Cancers. 2019;11(3):316.

63. Nishida N, Yano H, Nishida T, Kamura T, Kojiro M. Angiogenesis in cancer. Vascular Health Risk Management. 2006;2(3):213-9.
64. de Herreros AG, Baulida J. Cooperation, amplification, and feed-back in epithelial–mesenchymal transition. Biochimica et Biophysica Acta (BBA)-Reviews on Cancer. 2012;1825(2):223-8.
65. Saitoh M. Involvement of partial EMT in cancer progression. The Journal of Biochemistry. 2018;164(4):257-64.
66. Smith BN, Bhowmick NA. Role of EMT in metastasis and therapy resistance. Journal of clinical medicine. 2016;5(2):17.
67. Lo HC, Zhang XH-F. EMT in metastasis: finding the right balance. Developmental cell. 2018;45(6):663-5.
68. Suarez-Carmona M, Lesage J, Cataldo D, Gilles C. EMT and inflammation: inseparable actors of cancer progression. Molecular oncology. 2017;11(7):805-23.
69. Garg M. Epithelial-mesenchymal transition - activating transcription factors - multifunctional regulators in cancer. World Journal of stem cells. 2013;5(4):188-95.
70. Talkenberger K, Cavalcanti-Adam EA, Voss-Böhme A, Deutsch A. Amoeboid-mesenchymal migration plasticity promotes invasion only in complex heterogeneous microenvironments. Scientific reports. 2017;7(1):9237-.
71. Gerashchenko TS, Novikov NM, Krakhmal NV, Zolotaryova SY, Zavyalova MV, Cherdyntseva NV, et al. Markers of Cancer Cell Invasion: Are They Good Enough? Journal of clinical medicine. 2019;8(8):1092.
72. Easwaran H, Tsai H-C, Baylin SB. Cancer epigenetics: tumor heterogeneity, plasticity of stem-like states, and drug resistance. Molecular cell. 2014;54(5):716-27.
73. Gerlinger M, Rowan AJ, Horswell S, Math M, Larkin J, Endesfelder D, et al. Intratumor heterogeneity and branched evolution revealed by multiregion sequencing. The New England journal of medicine. 2012;366(10):883-92.
74. Rich JN. Cancer stem cells: understanding tumor hierarchy and heterogeneity. Medicine. 2016;95(1S):S2-S7.
75. Rybinski B, Yun K. Addressing intra-tumoral heterogeneity and therapy resistance. Oncotarget. 2016;7(44):72322-42.

76. Boesch M, Spizzo G, Seeber A. Concise Review: Aggressive Colorectal Cancer: Role of Epithelial Cell Adhesion Molecule in Cancer Stem Cells and Epithelial-to-Mesenchymal Transition. Stem cells translational medicine. 2018;7(6):495-501.
77. Yu M. Metastasis stemming from circulating tumor cell clusters. Trends in cell biology. 2019;29(4):275-6.
78. Aponte PM, Caicedo A. Stemness in Cancer: Stem Cells, Cancer Stem Cells, and Their Microenvironment. Stem cells international. 2017;2017:5619472.
79. Zhu M, Li W, Lu Y, Dong X, Chen Y, Lin B, et al. Alpha fetoprotein antagonizes apoptosis induced by paclitaxel in hepatoma cells in vitro. Scientific Reports. 2016;6(1):26472.
80. Sell S. Alpha-fetoprotein, stem cells and cancer: how study of the production of alpha-fetoprotein during chemical hepatocarcinogenesis led to reaffirmation of the stem cell theory of cancer. Tumour Biology. 2008;29(3):161-80.
81. Grepin C, Nemer G, Nemer M. Enhanced cardiogenesis in embryonic stem cells overexpressing the GATA-4 transcription factor. Development. 1997;124(12):2387.
82. Hellebrekers DM, Lentjes MH, van den Bosch SM, Melotte V, Wouters KA, Daenen KL, et al. GATA4 and GATA5 are potential tumor suppressors and biomarkers in colorectal cancer. Clinical Cancer Research. 2009;15(12):3990-7.
83. Yu J, Liu S-H, Sanchez R, Nemunaitis J, Rozengurt E, Brunicardi FC. PDX1 associated therapy in translational medicine. Annals of Translational Medicine. 2016;4(11):214-.
84. Ballian N, Liu S-H, Brunicardi F-C. Transcription factor PDX-1 in human colorectal adenocarcinoma: a potential tumor marker? World Journal of gastroenterology. 2008;14(38):5823-6.
85. Bunt J, Hasselt NE, Zwijnenburg DA, Hamdi M, Koster J, Versteeg R, et al. OTX2 directly activates cell cycle genes and inhibits differentiation in medulloblastoma cells. International journal of cancer. 2012;131(2):E21-E32.
86. Tsankov AM, Gu H, Akopian V, Ziller MJ, Donaghey J, Amit I, et al. Transcription factor binding dynamics during human ES cell differentiation. Nature. 2015;518(7539):344-9.
87. Pellegrini G, Dellambra E, Golisano O, Martinelli E, Fantozzi I, Bondanza S, et al. p63 identifies keratinocyte stem cells. Proceedings of the National Academy of Sciences. 2001;98(6):3156.

88. Truong AB, Kretz M, Ridky TW, Kimmel R, Khavari PA. p63 regulates proliferation and differentiation of developmentally mature keratinocytes. Genes & development. 2006;20(22):3185-97.
89. Hartwell KA, Muir B, Reinhardt F, Carpenter AE, Sgroi DC, Weinberg RA. The Spemann organizer gene, Goosecoid, promotes tumor metastasis. Proceedings of the National Academy of Sciences. 2006;103(50):18969.
90. Kang K-W, Lee M-J, Song J, Jeong J-Y, Kim Y-K, Lee C, et al. Overexpression of goosecoid homeobox is associated with chemoresistance and poor prognosis in ovarian carcinoma. Oncology reports. 2014;32(1):189-98.
91. Yamaguchi A, Ishida T, Nishimura G, Kumaki T, Katoh M, Kosaka T, et al. Human chorionic gonadotropin in colorectal cancer and its relationship to prognosis. British journal of cancer. 1989;60(3):382-4.
92. Li J, Yin M, Song W, Cui F, Wang W, Wang S, et al. B subunit of human chorionic gonadotropin promotes tumor invasion and predicts poor prognosis of early-stage colorectal cancer. Cellular Physiology and Biochemistry. 2018;45(1):237-49.
93. Teng S, Li YE, Yang M, Qi R, Huang Y, Wang Q, et al. Tissue-specific transcription reprogramming promotes liver metastasis of colorectal cancer. Cell Research. 2020;30(1):34-49.
94. Hartsock A, Nelson WJ. Adherens and tight junctions: Structure, function and connections to the actin cytoskeleton. Biochimica et Biophysica Acta (BBA) - Biomembranes. 2008;1778(3):660-9.
95. Archbold HC, Yang YX, Chen L, Cadigan KM. How do they do Wnt they do?: regulation of transcription by the Wnt/beta-catenin pathway. Acta Physiologica (Oxf). 2012;204(1):74-109.
96. Mann B, Gelos M, Siedow A, Hanski M, Gratchev A, Ilyas M, et al. Target genes of β-catenin–T cell-factor/lymphoid-enhancer-factor signaling in human colorectal carcinomas. Proceedings of the National Academy of Sciences. 1999;96(4):1603-8.
97. Tetsu O, McCormick F. β-Catenin regulates expression of cyclin D1 in colon carcinoma cells. Nature. 1999;398(6726):422.
98. Novak A, Dedhar S. Signaling through β-catenin and Lef/Tcf. Cellular and Molecular Life Sciences. 1999;56(5-6):523-37.

99. Hoffmeyer K, Raggioli A, Rudloff S, Anton R, Hierholzer A, Del Valle I, et al. Wnt/beta-catenin signaling regulates telomerase in stem cells and cancer cells. Science. 2012;336(6088):1549-54.
100. Lustig B, Behrens J. The Wnt signaling pathway and its role in tumor development. Journal of cancer research and clinical oncology. 2003;129(4):199-221.
101. Olsen JJ, Pohl SÖ-G, Deshmukh A, Visweswaran M, Ward NC, Arfuso F, et al. The Role of Wnt Signalling in Angiogenesis. Clinical Biochemist Reviews. 2017;38(3):131-42.
102. Naik S, Dothager RS, Marasa J, Lewis CL, Piwnica-Worms D. RNA Interference Screen Identifies VEGFR1 as Potentially Synthetic Lethal to Aberrant Wnt/β-catenin Activation in Colon Cancer. Clinical cancer research: an official journal of the American Association for Cancer Research. 2009;15(24):7529.
103. Zeitlin BD, Ellis LM, Nör JE. Inhibition of Vascular Endothelial Growth Factor Receptor-1/Wnt/{beta}-catenin Crosstalk Leads to Tumor Cell Death. Clinical cancer research : an official journal of the American Association for Cancer Research. 2009;15(24):7453-5.
104. Roskoski R, Jr. Vascular endothelial growth factor (VEGF) signaling in tumor progression. Critical Reviews in Oncology/Hematology. 2007;62(3):179-213.
105. Mittar S, Ulyatt C, Howell GJ, Bruns AF, Zachary I, Walker JH, et al. VEGFR1 receptor tyrosine kinase localization to the Golgi apparatus is calcium-dependent. Experimental Cell Research. 2009;315(5):877-89.
106. Bhattacharya R, Ye X-C, Wang R, Ling X, McManus M, Fan F, et al. Intracrine VEGF signaling mediates the activity of prosurvival pathways in human colorectal cancer cells. Cancer research. 2016;76(10):3014-24.
107. Hilbig D, Dietrich N, Wandel E, Gonsior S, Sittig D, Hamann J, et al. The interaction of CD97/ADGRE5 with β-catenin in adherens junctions is lost during colorectal carcinogenesis. Frontiers in oncology. 2018;8:182.
108. Zilhão R, Neves H. Tumor Niche Disruption and Metastasis: The Role of Epithelial-Mesenchymal Transition (EMT). Molecular and Cell Biology of Cancer: Springer; 2019. p. 159-89.
109. Valenta T, Hausmann G, Basler K. The many faces and functions of β-catenin. The EMBO journal. 2012;31(12):2714-36.

110. Loh C-Y, Chai JY, Tang TF, Wong WF, Sethi G, Shanmugam MK, et al. The E-Cadherin and N-Cadherin Switch in Epithelial-to-Mesenchymal Transition: Signaling, Therapeutic Implications, and Challenges. Cells. 2019;8(10):1118.
111. Yang Z, Zhang X, Gang H, Li X, Li Z, Wang T, et al. Up-regulation of gastric cancer cell invasion by Twist is accompanied by N-cadherin and fibronectin expression. Biochemical and biophysical research communications. 2007;358(3):925-30.
112. Conacci-Sorrell M, Simcha I, Ben-Yedidia T, Blechman J, Savagner P, Ben-Ze'ev A. Autoregulation of E-cadherin expression by cadherin-cadherin interactions: the roles of beta-catenin signaling, Slug, and MAPK. The Journal of cell biology. 2003;163(4):847-57.
113. Medici D, Hay ED, Olsen BR. Snail and Slug promote epithelial-mesenchymal transition through β-catenin–T-cell factor-4-dependent expression of transforming growth factor-β3. Molecular biology of the cell. 2008;19(11):4875-87.
114. Tsoumas D, Nikou S, Giannopoulou E, Tsaniras SC, Sirinian C, Maroulis I, et al. Ilk expression in colorectal cancer is associated with emt, cancer stem cell markers and chemoresistance. Cancer Genomics-Proteomics. 2018;15(2):127-41.
115. Zhou BP, Deng J, Xia W, Xu J, Li YM, Gunduz M, et al. Dual regulation of Snail by GSK-3beta-mediated phosphorylation in control of epithelial-mesenchymal transition. Nature Cell Biology. 2004;6(10):931-40.
116. Munro MJ, Wickremesekera SK, Peng L, Tan ST, Itinteang T. Cancer stem cells in colorectal cancer: a review. Journal of clinical pathology. 2018;71(2):110-6.
117. Merlos-Suárez A, Barriga Francisco M, Jung P, Iglesias M, Céspedes María V, Rossell D, et al. The Intestinal Stem Cell Signature Identifies Colorectal Cancer Stem Cells and Predicts Disease Relapse. Cell Stem Cell. 2011;8(5):511-24.
118. Bastos LGdR, de Marcondes PG, de-Freitas-Junior JCM, Leve F, Mencalha AL, de Souza WF, et al. Progeny From Irradiated Colorectal Cancer Cells Acquire an EMT-Like Phenotype and Activate Wnt/β-Catenin Pathway. Journal of cellular biochemistry. 2014;115(12):2175-87.
119. Geng F, Wang Z, Yin H, Yu J, Cao B. Molecular Targeted Drugs and Treatment of Colorectal Cancer: Recent Progress and Future Perspectives. Cancer biotherapy & radiopharmaceuticals. 2017;32(5):149-60.
120. Popova EA, Protas AV, Trifonov RE. Tetrazole Derivatives as Promising Anticancer Agents. Anti-cancer agents in medicinal chemistry. 2018;17(14):1856-68.

121. Buac D, Schmitt S, Ventro G, Kona FR, Dou QP. Dithiocarbamate-based coordination compounds as potent proteasome inhibitors in human cancer cells. Mini Reviews in Medicinal Chemistry. 2012;12(12):1193-201.
122. Herr RJ. 5-Substituted-1H-tetrazoles as carboxylic acid isosteres: medicinal chemistry and synthetic methods. Bioorganic & medicinal chemistry. 2002;10(11):3379-93.
123. Lesnikovich A, Levchik S, Balabanovich A, Ivashkevich O, Gaponik P. The thermal decomposition of tetrazoles. Thermochimica acta. 1992;200:427-41.
124. Al-Hourani BJ, Sharma SK, Mane JY, Tuszynski J, Baracos V, Kniess T, et al. Synthesis and evaluation of 1, 5-diaryl-substituted tetrazoles as novel selective cyclooxygenase-2 (COX-2) inhibitors. Bioorganic & medicinal chemistry letters. 2011;21(6):1823-6.
125. Allen FH, Groom CR, Liebeschuetz JW, Bardwell DA, Olsson TSG, Wood PA. The Hydrogen Bond Environments of 1H-Tetrazole and Tetrazolate Rings: The Structural Basis for Tetrazole–Carboxylic Acid Bioisosterism. Journal of Chemical Information and Modeling. 2012;52(3):857-66.
126. Ballatore C, Huryn DM, Smith AB. Carboxylic Acid (Bio)Isosteres in Drug Design. ChemMedChem. 2013;8(3):385-95.
127. Wei C-X, Bian M, Gong G-H. Tetrazolium Compounds: Synthesis and Applications in Medicine. Molecules. 2015;20(4):5528.
128. Eriksson L, Sirsjö A, Strid Å. Tetrazole derivatives as cytochrome p450 inhibitors. Google Patents; 2019.
129. Neochoritis CG, Zhao T, Domling A. Tetrazoles via Multicomponent Reactions. Chemical Reviews. 2019.
130. Wishart DS, Knox C, Guo AC, Shrivastava S, Hassanali M, Stothard P, et al. DrugBank: a comprehensive resource for in silico drug discovery and exploration. Nucleic Acids Research. 2006;34(Database issue):D668-72.
131. Adeyemi JO, Onwudiwe DC. Organotin(IV) Dithiocarbamate Complexes: Chemistry and Biological Activity. Molecules (Basel, Switzerland). 2018;23(10):2571.
132. Onwudiwe DC, Ajibade PA. Thermal studies of Zn(II), Cd(II) and Hg(II) complexes of some N-alkyl-N-phenyl-dithiocarbamates. International Journal fo Molecular Sciences. 2012;13(8):9502-13.
133. Chaturvedi D. Perspectives on the synthesis of organic carbamates. Tetrahedron. 2012;1(68):15-45.

134. Chaturvedi D. Recent developments on the carbamation of amines. Current Organic Chemistry. 2011;15(10):1593-624.
135. Xue J, Luo Z, Li P, Ding Y, Cui Y, Wu Q. A residue-free green synergistic antifungal nanotechnology for pesticide thiram by ZnO nanoparticles. Scientific reports. 2014;4:5408-13.
136. Altaf M, Monim-ul-Mehboob M, Kawde A-N, Corona G, Larcher R, Ogasawara M, et al. New bipyridine gold(III) dithiocarbamate-containing complexes exerted a potent anticancer activity against cisplatin-resistant cancer cells independent of p53 status. Oncotarget. 2017;8(1):490-505.
137. Mostafa AS, Selim KB. Synthesis and anticancer activity of new dihydropyrimidinone derivatives. European Journal of Medicinal Chemistry. 2018;156:304-15.
138. Zheng Y-C, Duan Y-C, Ma J-L, Xu R-M, Zi X, Lv W-L, et al. Triazole–dithiocarbamate based selective lysine specific demethylase 1 (LSD1) inactivators inhibit gastric cancer cell growth, invasion, and migration. Journal of medicinal chemistry. 2013;56(21):8543-60.
139. Magerl C, Ellinger J, Braunschweig T, Kremmer E, Koch LK, Höller T, et al. H3K4 dimethylation in hepatocellular carcinoma is rare compared with other hepatobiliary and gastrointestinal carcinomas and correlates with expression of the methylase Ash2 and the demethylase LSD1. Human Pathology. 2010;41(2):181-9.
140. Lim S, Janzer A, Becker A, Zimmer A, Schule R, Buettner R, et al. Lysine-specific demethylase 1 (LSD1) is highly expressed in ER-negative breast cancers and a biomarker predicting aggressive biology. Carcinogenesis. 2010;31(3):512-20.
141. Wani MY, Silva MR, Krishnakumar B, Kumar S, Al-Bogami AS, Aqlan FM, et al. Catalytic Synthesis of 5-Substituted Tetrazoles: Unexpected Reactions and Products. Journal of Heterocyclic Chemistry. 2019;56(5):1613-21.
142. Wani MY, Ahmad A, Aqlan FM, Al-Bogami AS. Azole based acetohydrazide derivatives of cinnamaldehyde target and kill Candida albicans by causing cellular apoptosis. American Chemical Society Medicinal Chemistry Letters. 2020.
143. Costas-Chavarri A, Nandakumar G, Temin S, Lopes G, Cervantes A, Cruz Correa M, et al. Treatment of Patients With Early-Stage Colorectal Cancer: ASCO Resource-Stratified Guideline. Journal of Global Oncology. 2019;5:1-19.
144. Deschoolmeester V, Kerr D, Pauwels P, Vermorken JB. Cell Based Therapy: Modified Cancer Cells. Immunotherapy for Gastrointestinal Cancer: Springer; 2017. p. 23-46.

145. Wang S, Wang L, Zhou Z, Deng Q, Li L, Zhang M, et al. Leucovorin enhances the anti-cancer effect of bortezomib in colorectal cancer cells. Scientific reports. 2017;7(1):1-10.
146. Patient education: Colorectal cancer treatment; metastatic cancer (Beyond the Basics) [Internet]. Post TW, ed. UpToDate. 2020 [cited 5/2/20]. Available from: https://www.uptodate.com/contents/colorectal-cancer-treatment-metastatic-cancer-beyond-the-basics.
147. Alcindor T, Beauger N. Oxaliplatin: a review in the era of molecularly targeted therapy. Current oncology. 2011;18(1):18.
148. Chabot GG. Clinical pharmacokinetics of irinotecan. Clinical pharmacokinetics. 1997;33(4):245-59.
149. Fujita K-i, Kubota Y, Ishida H, Sasaki Y. Irinotecan, a key chemotherapeutic drug for metastatic colorectal cancer. World Journal of Gastroenterology. 2015;21(43):12234-48.
150. Burness CB, Duggan ST. Trifluridine/tipiracil: a review in metastatic colorectal cancer. Drugs. 2016;76(14):1393-402.
151. Kang C, Dhillon S, Deeks ED. Trifluridine/Tipiracil: A Review in Metastatic Gastric Cancer. Drugs. 2019;79(14):1583-90.
152. Van der Jeught K, Xu H-C, Li Y-J, Lu X-B, Ji G. Drug resistance and new therapies in colorectal cancer. World journal of gastroenterology. 2018;24(34):3834-48.
153. Wang Y, Fei D, Vanderlaan M, Song A. Biological activity of bevacizumab, a humanized anti-VEGF antibody in vitro. Angiogenesis. 2004;7(4):335-45.
154. Kang BW, Kim TW, Lee J-L, Ryu M-H, Chang HM, Yu CS, et al. Bevacizumab plus FOLFIRI or FOLFOX as third-line or later treatment in patients with metastatic colorectal cancer after failure of 5-fluorouracil, irinotecan, and oxaliplatin: a retrospective analysis. Medical Oncology. 2009;26(1):32-7.
155. Gambardella V, Tarazona N, Cejalvo JM, Roselló S, Cervantes A. Clinical pharmacokinetics and pharmacodynamics of ramucirumab in the treatment of colorectal cancer. Expert opinion on drug metabolism & toxicology. 2016;12(4):449-56.
156. Benson AB, Venook AP, Cederquist L, Chan E, Chen Y-J, Cooper HS, et al. Colon cancer, version 1.2017, NCCN clinical practice guidelines in oncology. Journal of the National Comprehensive Cancer Network. 2017;15(3):370-98.

157. MacDonald DA, Martin J, Muthusamy KK, Luo J-K, Pyles E, Rafique A, et al. Aflibercept exhibits VEGF binding stoichiometry distinct from bevacizumab and does not support formation of immune-like complexes. Angiogenesis. 2016;19(3):389-406.
158. Lin C-Y, Lin T-H, Chen C-C, Chen M-C, Chen C-P. Combination chemotherapy with Regorafenib in metastatic colorectal cancer treatment: A single center, retrospective study. PloS one. 2018;13(1):e0190497-e.
159. Wee P, Wang Z. Epidermal Growth Factor Receptor Cell Proliferation Signaling Pathways. Cancers. 2017;9(5):52.
160. Van Cutsem E, Kohne CH, Lang I, Folprecht G, Nowacki MP, Cascinu S, et al. Cetuximab plus irinotecan, fluorouracil, and leucovorin as first-line treatment for metastatic colorectal cancer: updated analysis of overall survival according to tumor KRAS and BRAF mutation status. Journal of clinical oncology : official journal of the American Society of Clinical Oncology. 2011;29(15):2011-9.
161. García-Foncillas J, Sunakawa Y, Aderka D, Wainberg Z, Ronga P, Witzler P, et al. Distinguishing Features of Cetuximab and Panitumumab in Colorectal Cancer and Other Solid Tumors. Frontiers in Oncology. 2019;9:849.
162. Papaioannou NE, Beniata OV, Vitsos P, Tsitsilonis O, Samara P. Harnessing the immune system to improve cancer therapy. Annals of Translational Medicine. 2016;4(14):261-.
163. Keating M, Giscombe L, Tannous T, Hartshorn K. Prolonged Treatment Response to Pembrolizumab in a Patient with Pretreated Metastatic Colon Cancer and Lynch Syndrome. Case reports in oncological medicine. 2019;2019.
164. Herbst C-l, Miot JK, Moch SL, Ruff P. Access to colorectal cancer (CRC) chemotherapy and the associated costs in a South African public healthcare patient cohort. Journal of Cancer Policy. 2018;15:18-24.
165. Longley DB, Harkin DP, Johnston PG. 5-Fluorouracil: mechanisms of action and clinical strategies. Nature Reviews Cancer. 2003;3(5):330-8.
166. Lee J, R SH. Cancer Epigenetics: Mechanisms and Crosstalk of a HDAC Inhibitor, Vorinostat. Chemotherapy (Los Angel). 2013;2(111):14934.
167. Bagherani N, Smoller BR. An overview of cutaneous T cell lymphomas. F1000Research. 2016;5.

168. Damaskos C, Valsami S, Kontos M, Spartalis E, Kalampokas T, Kalampokas E, et al. Histone deacetylase inhibitors: an attractive therapeutic strategy against breast cancer. Anticancer research. 2017;37(1):35-46.
169. Park SJ, Kim SM, Moon JH, Kim JH, Shin JS, Hong SW, et al. SAHA, an HDAC inhibitor, overcomes erlotinib resistance in human pancreatic cancer cells by modulating E-cadherin. Tumour Biology. 2016;37(4):4323-30.
170. Kumar B, Yadav A, Lang JC, Teknos TN, Kumar P. Suberoylanilide hydroxamic acid (SAHA) reverses chemoresistance in head and neck cancer cells by targeting cancer stem cells via the downregulation of nanog. Genes Cancer. 2015;6(3-4):169-81.
171. Roca MS, Di Gennaro E, Budillon A. Implication for Cancer Stem Cells in Solid Cancer Chemo-Resistance: Promising Therapeutic Strategies Based on the Use of HDAC Inhibitors. Journal of clinical medicine. 2019;8(7):912.
172. 5-Fluorouracil [Internet]. 2005 [cited Mar. 17, 2020]. Available from: https://pubchem.ncbi.nlm.nih.gov/compound/5-Fluorouracil.
173. Vorinostat [Internet]. PubChem Database. 2005 [cited Mar. 17, 2020]. Available from: https://pubchem.ncbi.nlm.nih.gov/compound/Vorinostat.
174. Kho D, MacDonald C, Johnson R, Unsworth CP, O'Carroll SJ, du Mez E, et al. Application of xCELLigence RTCA Biosensor Technology for Revealing the Profile and Window of Drug Responsiveness in Real Time. Biosensors (Basel). 2015;5(2):199-222.
175. Thornton B, Basu C. Real-time PCR (qPCR) primer design using free online software. Biochemistry and Molecular Biology Education. 2011;39(2):145-54.
176. Dragan A, Pavlovic R, McGivney J, Casas-Finet J, Bishop E, Strouse R, et al. SYBR Green I: fluorescence properties and interaction with DNA. Journal of fluorescence. 2012;22(4):1189-99.
177. De La Rosa JR, Wubetu J, Tirelli N, Tirella A. Colorectal tumor 3D in vitro models: advantages of biofabrication for the recapitulation of early stages of tumour development. Biomedical Physics & Engineering Express. 2018;4(4):045010.
178. Botchkina GI, Zuniga ES, Das M, Wang Y, Wang H, Zhu S, et al. New-generation taxoid SB-T-1214 inhibits stem cell-related gene expression in 3D cancer spheroids induced by purified colon tumor-initiating cells. Molecular cancer. 2010;9(1):192.

179. Kuczynski EA, Sargent DJ, Grothey A, Kerbel RS. Drug rechallenge and treatment beyond progression--implications for drug resistance. Natures Reviews in Clinical Oncology. 2013;10(10):571-87.
180. Bell CC, Gilan O. Principles and mechanisms of non-genetic resistance in cancer. British Journal of Cancer. 2019:1-8.
181. Ahmed M, Jinks N, Babaei-Jadidi R, Kashfi H, Castellanos-Uribe M, May ST, et al. Repurposing Antibacterial AM404 as a Potential Anticancer Drug for Targeting Colorectal Cancer Stem-Like Cells. Cancers. 2020;12(1):106.
182. Phi LTH, Sari IN, Yang Y-G, Lee S-H, Jun N, Kim KS, et al. Cancer stem cells (CSCs) in drug resistance and their therapeutic implications in cancer treatment. Stem cells international. 2018;2018.
183. Dotse E, Bian Y. Isolation of colorectal cancer stem-like cells. Cytotechnology. 2016;68(4):609-19.
184. Zhu ZW, Chen L, Liu JX, Huang JW, Wu G, Zheng YF, et al. A novel three-dimensional tumorsphere culture system for the efficient and low-cost enrichment of cancer stem cells with natural polymers. Experimental and therapeutic medicine. 2018;15(1):85-92.
185. Liu S-H, Rao DD, Nemunaitis J, Senzer N, Zhou G, Dawson D, et al. PDX-1 is a therapeutic target for pancreatic cancer, insulinoma and islet neoplasia using a novel RNA interference platform. PloS one. 2012;7(8).
186. Li L, Yang W-T, Zheng P-S, Liu X-F. SOX17 restrains proliferation and tumor formation by down-regulating activity of the Wnt/β-catenin signaling pathway via trans-suppressing β-catenin in cervical cancer. Cell death & disease. 2018;9(7):1-16.
187. Fan F, Samuel S, Evans KW, Lu J, Xia L, Zhou Y, et al. Overexpression of Snail induces epithelial–mesenchymal transition and a cancer stem cell–like phenotype in human colorectal cancer cells. Cancer medicine. 2012;1(1):5-16.
188. Feng Y, Li Y, Dai W, Mo S, Li Q, Cai S. Clinicopathologic Features and Prognostic Factors in Alpha-Fetoprotein-Producing Colorectal Cancer: Analysis of 78 Cases. Cellular Physiology and Biochemistry. 2018;51(5):2052-64.
189. Ahluwalia A, Jones MK, Matysiak-Budnik T, Tarnawski AS. VEGF and colon cancer growth beyond angiogenesis: does VEGF directly mediate colon cancer growth via a non-angiogenic mechanism? Current Pharmaceutical Design. 2014;20(7):1041-4.

190. Li Y, Lv Z, He G, Wang J, Zhang X, Lu G, et al. The SOX17/miR-371-5p/SOX2 axis inhibits EMT, stem cell properties and metastasis in colorectal cancer. Oncotarget. 2015;6(11):9099-112.
191. Basu S, Haase G, Ben-Ze'ev A. Wnt signaling in cancer stem cells and colon cancer metastasis. F1000Research. 2016;5.
192. Torres K, Horwitz SB. Mechanisms of Taxol-induced cell death are concentration dependent. Cancer research. 1998;58(16):3620-6.
193. O'Connor CJ, Denny WA, Fan J-Y, Gamage RSKA. DNA-directed aniline mustards based on 9-aminoacridine: Interaction with DNA. Chemico-Biological Interactions. 1992;85(1):1-14.
194. Jo J, Kim SH, Kim H, Jeong M, Kwak JH, Taek Han Y, et al. Discovery and SAR studies of novel 2-anilinopyrimidine-based selective inhibitors against triple-negative breast cancer cell line MDA-MB-468. Bioorganic & medicinal chemistry letters. 2019;29(1):62-5.
195. Vardanyan R, Hruby V. Synthesis of best-seller drugs: Academic press; 2016.
196. Das S, da Silva CJ, Silva MdM, Dantas MDdA, de Fátima Â, Ruiz ALTG, et al. Highly functionalized piperidines: Free radical scavenging, anticancer activity, DNA interaction and correlation with biological activity. Journal of advanced research. 2018;9:51-61.
197. Fiorot RG, Westphal R, Lemos BC, Romagna RA, Gonçalves PR, Fernandes M, et al. Synthesis, Molecular Modelling and Anticancer Activities of New Molecular Hybrids Containing 1, 4-Naphthoquinone, 7-Chloroquinoline, 1, 3, 5-Triazine and Morpholine Cores as PI3K and AMPK Inhibitors in the Metastatic Melanoma Cells. Journal of the Brazilian Chemical Society. 2019;30(9):1860-73.
198. Kıpçak F, Tok TT, Duyar H, Seferoğlu Z, Gökoğlu E. Synthesis of new morpholine containing 3-amido-9-ethylcarbazole derivative and studies on its biophysical interactions with calf thymus DNA/HSA. Journal of Biomolecular Structure and Dynamics. 2020:1-11.
199. Zhang M, Das C, Vasquez H, Aguilera D, Zage PE, Gopalakrishnan V, et al. Predicting tumor cell repopulation after response: mathematical modeling of cancer cell growth. Anticancer research. 2006;26(4B):2933-6.
200. Watanabe I, Okada S. Stationary phase of cultured mammalian cells (L5178Y). The Journal of cell biology. 1967;35(2):285-94.

201. Pearl Mizrahi S, Gefen O, Simon I, Balaban NQ. Persistence to anti-cancer treatments in the stationary to proliferating transition. Cell cycle (Georgetown, Tex). 2016;15(24):3442-53.
202. Bernard S, Bernard BČ, Lévi F, Herzel H. Tumor growth rate determines the timing of optimal chronomodulated treatment schedules. PLoS computational biology. 2010;6(3).
203. West J, Newton PK. Cellular interactions constrain tumor growth. Proceedings of the National Academy of Sciences. 2019;116(6):1918.
204. Pardee AB. G1 events and regulation of cell proliferation. Science. 1989;246(4930):603-8.
205. Anwar A, Uddin N, Siddiqui BS, Siddiqui RA, Begum S, Choudhary MI. A natural flavonoid lawsonaringenin induces cell cycle arrest and apoptosis in HT-29 colorectal cancer cells by targeting multiple signalling pathways. Molecular Biology Reports. 2018;45(5):1339-48.
206. Huang Y-F, Zhu D-J, Chen X-W, Chen Q-K, Luo Z-T, Liu C-C, et al. Curcumin enhances the effects of irinotecan on colorectal cancer cells through the generation of reactive oxygen species and activation of the endoplasmic reticulum stress pathway. Oncotarget. 2017;8(25):40264-75.
207. Bartek J, Lukas C, Lukas J. Checking on DNA damage in S phase. Nature reviews Molecular cell biology. 2004;5(10):792-804.
208. DiPaola RS. To arrest or not to G2-M Cell-cycle arrest: commentary re: AK Tyagi et al., Silibinin strongly synergizes human prostate carcinoma DU145 cells to doxorubicin-induced growth inhibition, G2-M arrest, and apoptosis. Clin. Cancer Res., 8: 3512–3519, 2002. Clinical cancer research. 2002;8(11):3311-4.
209. Szade K, Zukowska M, Szade A, Collet G, Kloska D, Kieda C, et al. Spheroid-plug model as a tool to study tumor development, angiogenesis, and heterogeneity in vivo. Tumour Biology. 2016;37(2):2481-96.
210. Gambara G, Gaebler M, Keilholz U, Regenbrecht CRA, Silvestri A. From Chemotherapy to Combined Targeted Therapeutics: In Vitro and in Vivo Models to Decipher Intra-tumor Heterogeneity. Frontiers in Pharmacology. 2018;9:77-.
211. Gawlik-Rzemieniewska N, Bednarek I. The role of NANOG transcriptional factor in the development of malignant phenotype of cancer cells. Cancer Biology & Therapy. 2016;17(1):1-10.

212. Song Y, Ye M, Zhou J, Wang Z, Zhu X. Targeting E-cadherin expression with small molecules for digestive cancer treatment. American Journal of Translational Research. 2019;11(7):3932-44.
213. Yao C, Su L, Shan J, Zhu C, Liu L, Liu C, et al. IGF/STAT3/NANOG/Slug signaling axis simultaneously controls epithelial-mesenchymal transition and stemness maintenance in colorectal cancer. Stem cells. 2016;34(4):820-31.
214. Chen X, Xu H, Yuan P, Fang F, Huss M, Vega VB, et al. Integration of external signaling pathways with the core transcriptional network in embryonic stem cells. Cell. 2008;133(6):1106-17.
215. Tamura S, Isobe T, Ariyama H, Nakano M, Kikushige Y, Takaishi S, et al. E-cadherin regulates proliferation of colorectal cancer stem cells through NANOG. Oncology reports. 2018;40(2):693-703.
216. Gosalia N, Yang R, Kerschner JL, Harris A. FOXA2 regulates a network of genes involved in critical functions of human intestinal epithelial cells. Physiological Genomics. 2015;47(7):290-7.
217. Wang B, Liu G, Ding L, Zhao J, Lu Y. FOXA2 promotes the proliferation, migration and invasion, and epithelial mesenchymal transition in colon cancer. Experimental Therapeutic Medicine. 2018;16(1):133-40.
218. Li C, Lu S, Shi Y. MicroRNA-187 promotes growth and metastasis of gastric cancer by inhibiting FOXA2. Oncology reports. 2017;37(3):1747-55.
219. James MI, Iwuji C, Irving G, Karmokar A, Higgins JA, Griffin-Teal N, et al. Curcumin inhibits cancer stem cell phenotypes in ex vivo models of colorectal liver metastases, and is clinically safe and tolerable in combination with FOLFOX chemotherapy. Cancer Letters. 2015;364(2):135-41.
220. Niakan KK, Ji H, Maehr R, Vokes SA, Rodolfa KT, Sherwood RI, et al. Sox17 promotes differentiation in mouse embryonic stem cells by directly regulating extraembryonic gene expression and indirectly antagonizing self-renewal. Genes & development. 2010;24(3):312-26.
221. Liu Z, Qi L, Li Y, Zhao X, Sun B. VEGFR2 regulates endothelial differentiation of colon cancer cells. BMC Cancer. 2017;17(1):593-.

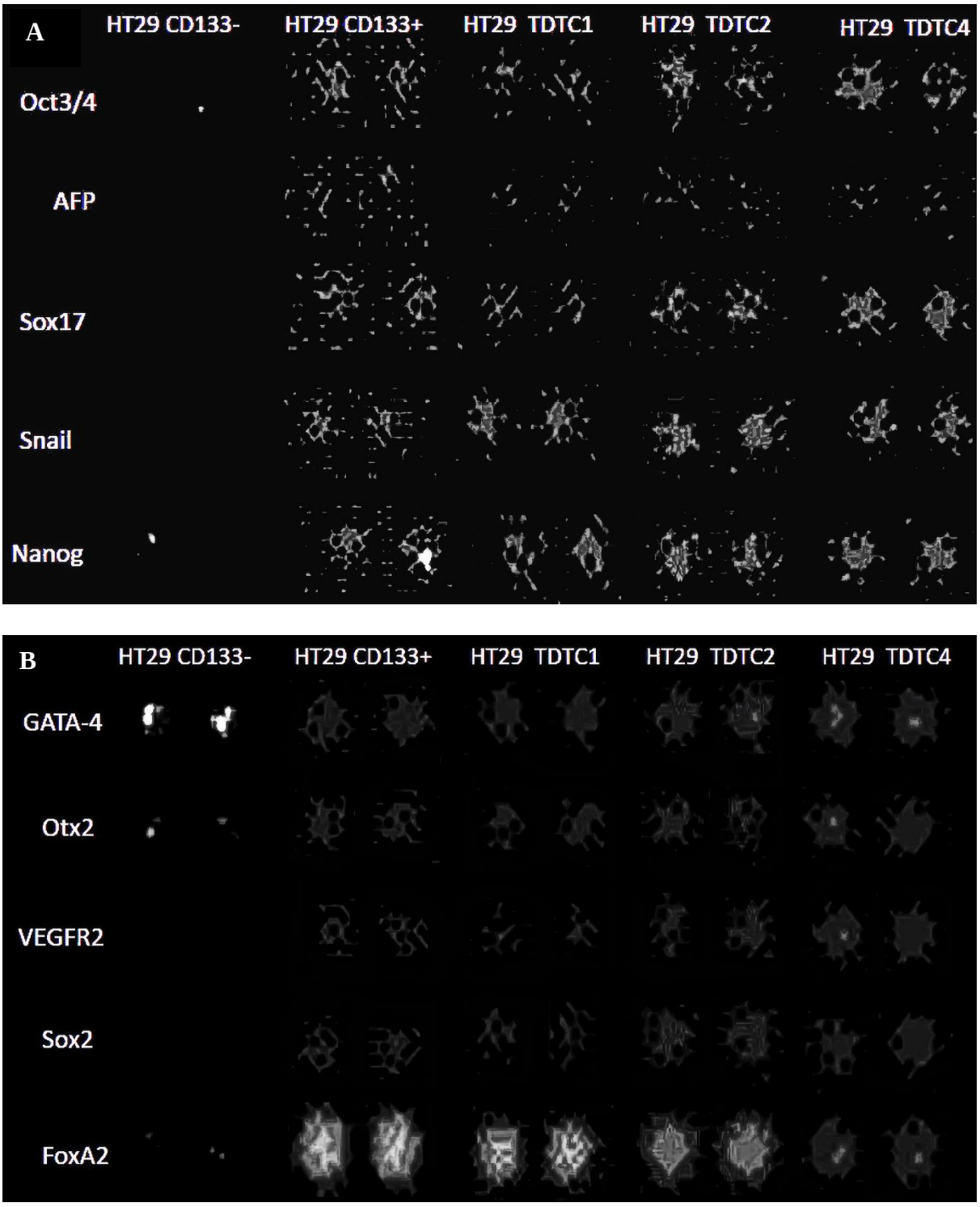
222. Foersch S, Sperka T, Lindner C, Taut A, Rudolph KL, Breier G, et al. VEGFR2 signaling prevents colorectal cancer cell senescence to promote tumorigenesis in mice with colitis. Gastroenterology. 2015;149(1):177-89. e10.
223. Zhao D, Pan C, Sun J, Gilbert C, Drews-Elger K, Azzam D, et al. VEGF drives cancer-initiating stem cells through VEGFR-2/Stat3 signaling to upregulate Myc and Sox2. Oncogene. 2015;34(24):3107-19.
224. Matsuoka J, Yashiro M, Sakurai K, Kubo N, Tanaka H, Muguruma K, et al. Role of the stemness factors sox2, oct3/4, and nanog in gastric carcinoma. Journal of Surgical Research. 2012;174(1):130-5.
225. Szaryńska M, Olejniczak A, Kobiela J, Spychalski P, Kmieć Z. Therapeutic strategies against cancer stem cells in human colorectal cancer. Oncology letters. 2017;14(6):7653-68.
226. Lundberg IV, Edin S, Eklöf V, Öberg Å, Palmqvist R, Wikberg ML. SOX2 expression is associated with a cancer stem cell state and down-regulation of CDX2 in colorectal cancer. BMC Cancer. 2016;16(1):471.
227. Takeda K, Mizushima T, Yokoyama Y, Hirose H, Wu X, Qian Y, et al. Sox2 is associated with cancer stem-like properties in colorectal cancer. Scientific reports. 2018;8(1):1-9.
228. Hellebrekers DM, Lentjes MH, Van Den Bosch SM, Melotte V, Wouters KA, Daenen KL, et al. GATA4 and GATA5 are potential tumor suppressors and biomarkers in colorectal cancer. Clinical cancer research. 2009;15(12):3990-7.
229. Stromecki M, Tatari N, Morrison LC, Kaur R, Zagozewski J, Palidwor G, et al. Characterization of a novel OTX 2-driven stem cell program in Group 3 and Group 4 medulloblastoma. Molecular oncology. 2018;12(4):495-513.
230. Xue T-C, Ge N-L, Zhang L, Cui J-F, Chen R-X, You Y, et al. Goosecoid promotes the metastasis of hepatocellular carcinoma by modulating the epithelial-mesenchymal transition. PloS one. 2014;9(10):e109695-e.
231. Zlobec I, Lugli A. Epithelial mesenchymal transition and tumor budding in aggressive colorectal cancer: tumor budding as oncotarget. Oncotarget. 2010;1(7):651-61.
232. Farhana L, Antaki F, Anees MR, Nangia-Makker P, Judd S, Hadden T, et al. Role of cancer stem cells in racial disparity in colorectal cancer. Cancer Medicine. 2016;5(6):1268-78.

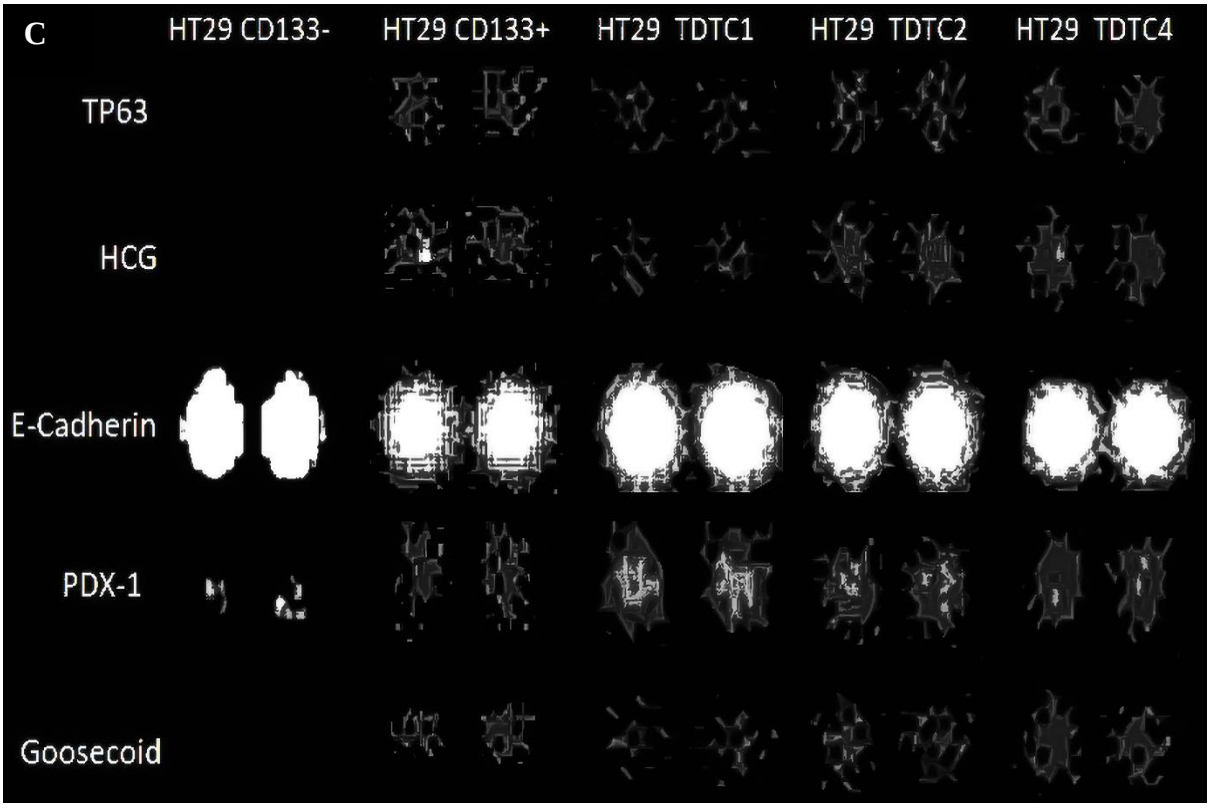
233. Talwar G, Gupta JC, Vyas HK, Puruswani S, Kabeer R. Immunotherapy of advanced stage, invariably drug-resistant cancers expressing ectopically hCG. 100 Years of Human Chorionic Gonadotropin: Elsevier; 2020. p. 293-300.
234. Guo H-Q, Huang G-L, Liu O-F, Liu Y-Y, Yao Z-H, Yao S-N, et al. p63 Expression is a prognostic factor in colorectal cancer. The International journal of biological markers. 2012;27(3):212-8.
235. Jiang Y, Jiang Y-Y, Xie J-J, Mayakonda A, Hazawa M, Chen L, et al. Co-activation of super-enhancer-driven CCAT1 by TP63 and SOX2 promotes squamous cancer progression. Nature communications. 2018;9(1):1-13.
236. Naz Z, Usman S, Saleem K, Ahmed S, Bashir H, Bilal M, et al. Alpha-fetoprotein: A fabulous biomarker in hepatocellular, gastric and rectal cancer diagnosis. 2018.
237. Jacobsen A, Heijmans N, Verkaar F, Smit MJ, Heringa J, van Amerongen R, et al. Construction and Experimental Validation of a Petri Net Model of Wnt/beta-Catenin Signaling. PLoS One. 2016;11(5):e0155743.
238. Basu S, Haase G, Ben-Ze'ev A. Wnt signaling in cancer stem cells and colon cancer metastasis. F1000Research. 2016;5:F1000 Faculty Rev-699.
239. Zhu D, Sun Y, Zhang D, Dong M, Jiang G, Zhang X, et al. miR-1 inhibits the progression of colon cancer by regulating the expression of vascular endothelial growth factor. Oncology reports. 2018;40(2):589-98.
240. D'Haene N, Koopmansch C, Van Eycke Y-R, Hulet F, Allard J, Bouri S, et al. The Prognostic Value of the Combination of Low VEGFR-1 and High VEGFR-2 Expression in Endothelial Cells of Colorectal Cancer. International Journal of Molecular Sciences. 2018;19(11):3536.
241. Ceci C, Atzori MG, Lacal PM, Graziani G. Role of VEGFs/VEGFR-1 Signaling and its Inhibition in Modulating Tumor Invasion: Experimental Evidence in Different Metastatic Cancer Models. International Journal of Molecular Sciences. 2020;21(4):1388.
242. Ali S, Badshah A, Ataf AA, Lal B, Khan KM. Synthesis of 3-ferrocenylaniline: DNA interaction, antibacterial, and antifungal activity. Medicinal Chemistry Research. 2013;22(7):3154-9.
243. Kumar N, Kumar R, Nemaysh V, Lal N, Luthra PM. Bis ((1, 4-dimethyl-9 H-carbazol-3-yl) methyl) amine-mediated anticancer effect triggered by sequence-specific cleavage of

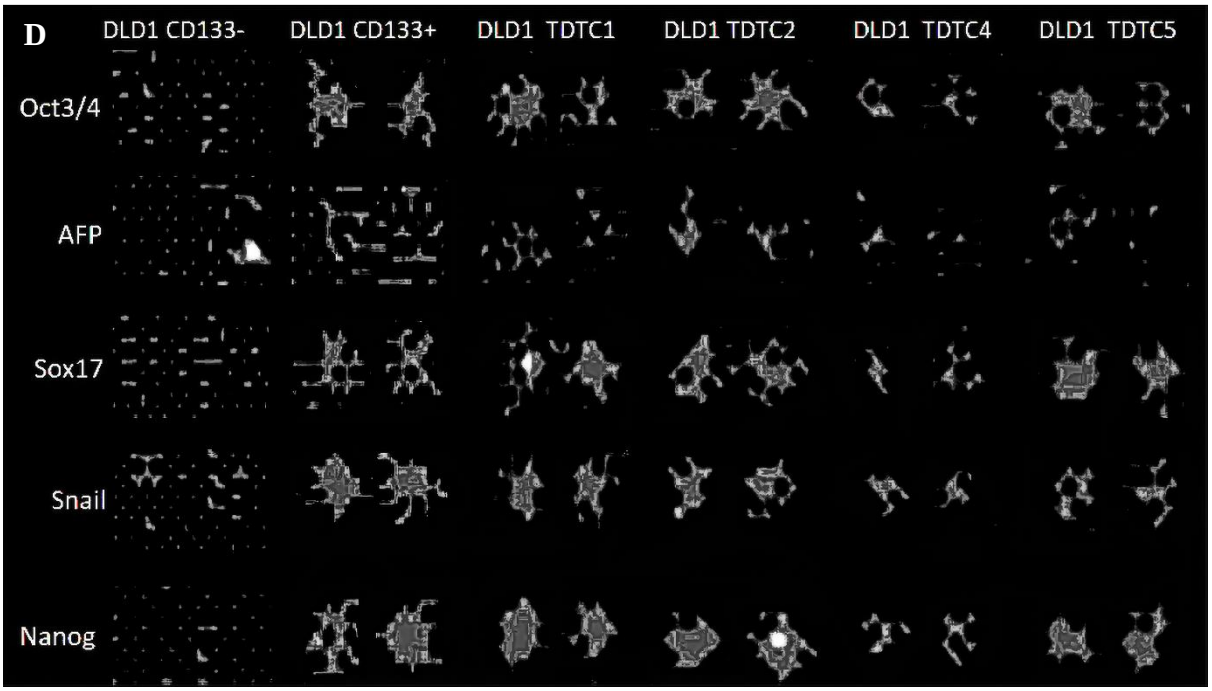
DNA leading to programmed cell death in the human U87 cell line. Royal Society of Chemistryadvances. 2016;6(72):67925-40.

6 Appendices

6.1 Appendix A: Human Pluripotent Stem Cell Biomarker Proteome Array (R&D) profiling of HT29 and DLD1 cells.




C
HT29 CD133-
HT29 CD133+
HT29 TDTC1
HT29 TDTC2
HT29 TDTC4
TP63
HCG
E-Cadherin
PDX-1
Goosecoid


D
DLD1 CD133-
DLD1 CD133+
DLD1 TDTC1
DLD1 TDTC2
DLD1 TDTC4
DLD1 TDTC5
Oct3/4
AFP
Sox17
Snail
Nanog

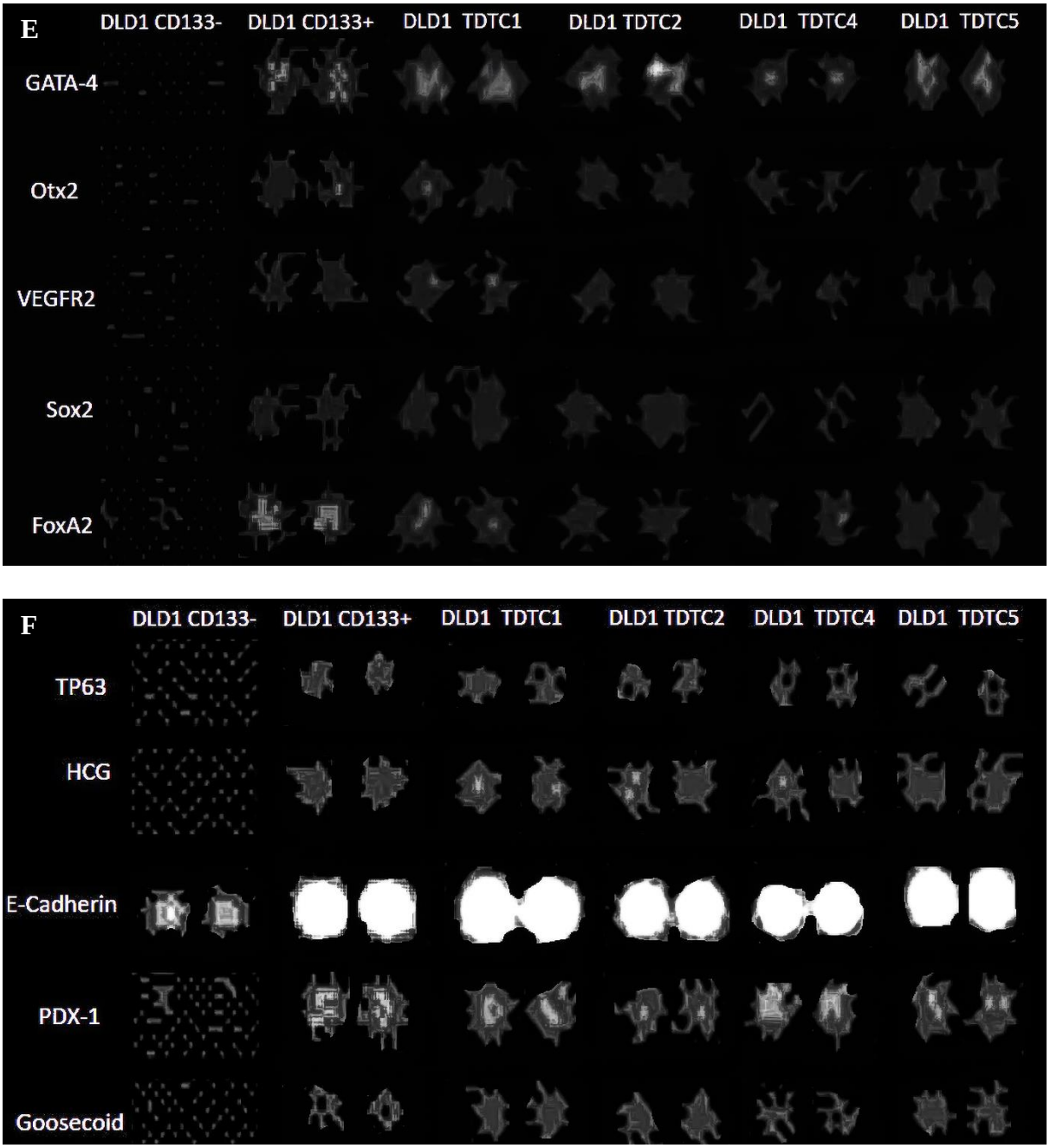
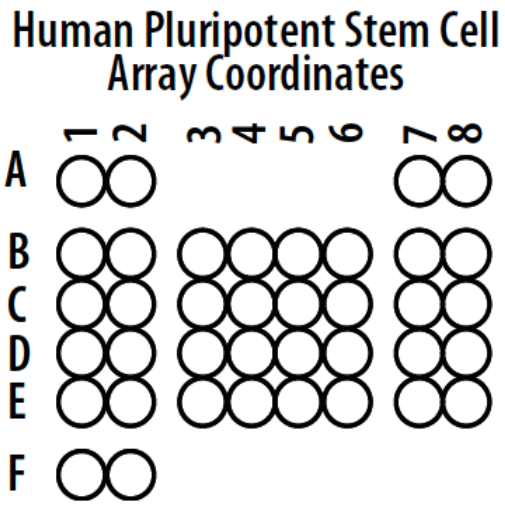


Figure 41: The active TDTC compounds modulate stemness.

The DLD1 and HT29 CRC stem cells were treated with the active TDTCs for 48 hours. Then total proteome was extracted and subjected to Human Pluripotent Stem Cell Biomarker Proteome Array (R&D) profiling. These are the images of the spots found in the membranes of the proteome profiler. The spots represent the 15 human stem cell biomarkers which are E-cadherin, FoxA2, Sox17, Sox2, Goosecoid, HCG, Oct3/4, Nanog, PDX-1, AFP, TP63, GATA-4, Otx2, VEGFR2 and Snail in the following images A, B, C, D, E and F. Most of the active TDTCs compounds modulated E-cadherin in both HT29 and DLD1 stem cells by increasing the expression of the protein (C& F). FoxA2 was downregulated in both HT29 (TDTC 2 and TDTC 4) and DLD1 stem cells by all active TDTCs (B&E). Sox17 was upregulated by TDTC 4 in HT29 stem cells, TDTC 2 and TDTC 4 (A&D). The stemness biomarkers are truly

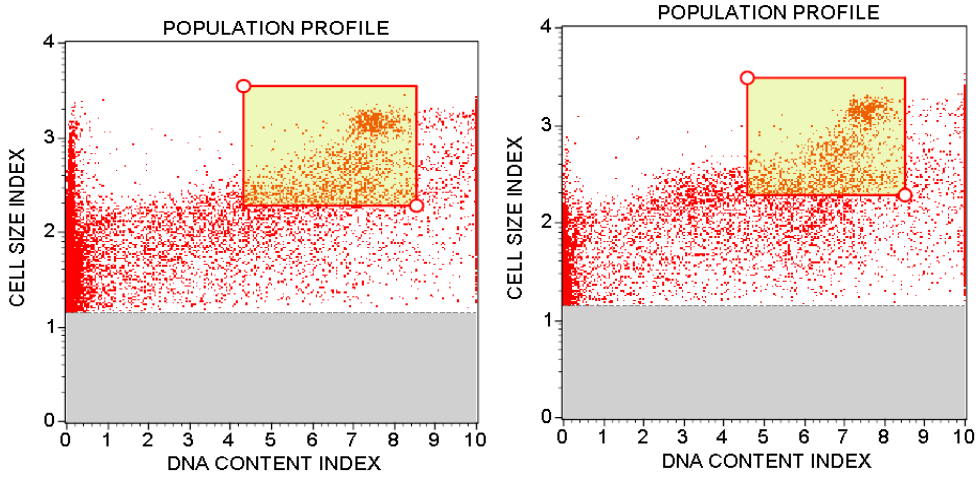
stem cell biomarkers as little to no expression is observed in non-stem cells (CD133-). VEGFR2 was downregulated by TDTC 1 in HT29 cells and TDCT 4 in DLD1 cells (B&E).

6.2 Appendix B: Human pluripotent stem cell array kit (R&D Systems Biotechne Brand), coordinates



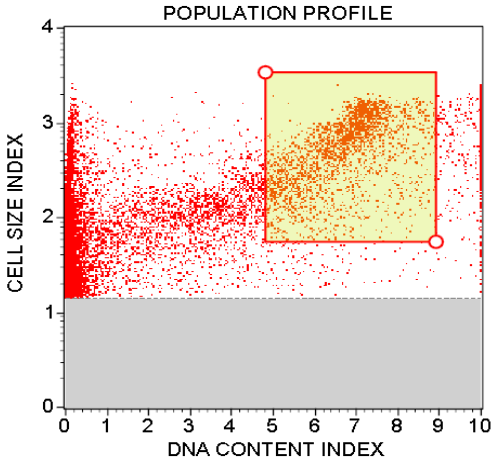
Coordinate	Target/Control
A1, A2	Reference Spots
A7, A8	Reference Spots
B1, B2	Oct-3/4
B3, B4	Nanog
B5, B6	SOX2
B7, B8	E-Cadherin
C1, C2	α-Fetoprotein (AFP)
C3, C4	GATA-4
C5, C6	HNF-3β/FoxA2
C7, C8	PDX-1/IPF1
D1, D2	SOX17
D3, D4	Otx2
D5, D6	TP63/TP73L
D7, D8	Goosecoid (GSC)
E1, E2	Snail
E3, E4	VEGF R2/KDR/Flk-1
E5, E6	HCG
E7, E8	Negative Control (PBS)
F1, F2	Reference Spots

6.3 Appendix C: Cell cycle assay scatter plots used to gate out doublets

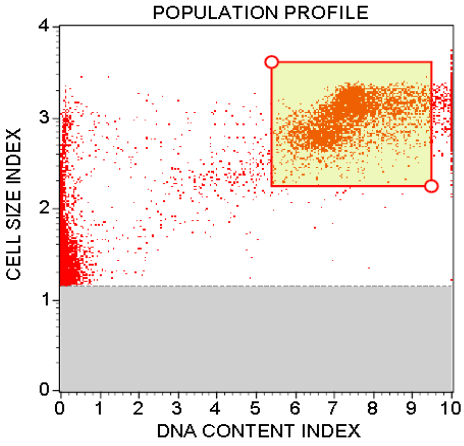


a. Control (0.1% DMSO)

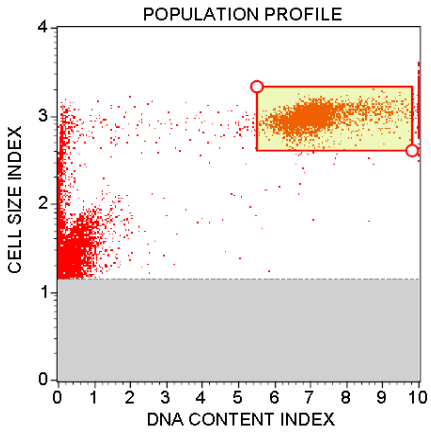
b. TDTC 1 0.4 mg/ml



c. TDTC 2 0.4 mg/ml



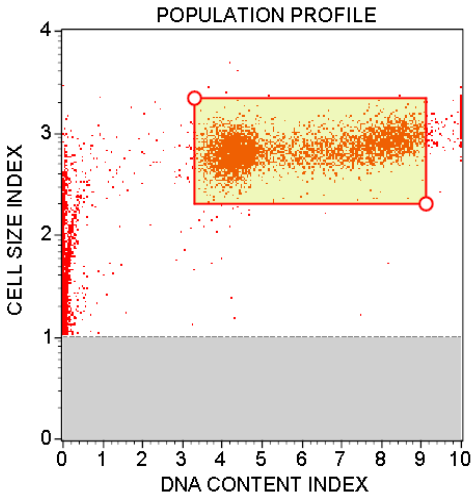
d. TDTC 4 0.3 mg/ml



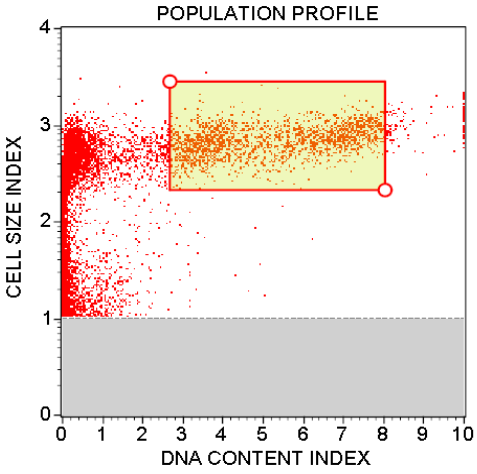
e. TDTC 5 0.35 mg/ml

Figure 42: Cell cycle scatter plot used to gate out doublets for HT29 cells following TDTC treatments. a. Control (0.1% DMSO); b. TDTC 1 0.4 mg/ml; c. TDTC 2 0.4 mg/ml; d. TDTC 4 0.3 mg/ml; e. TDTC 5 0.35

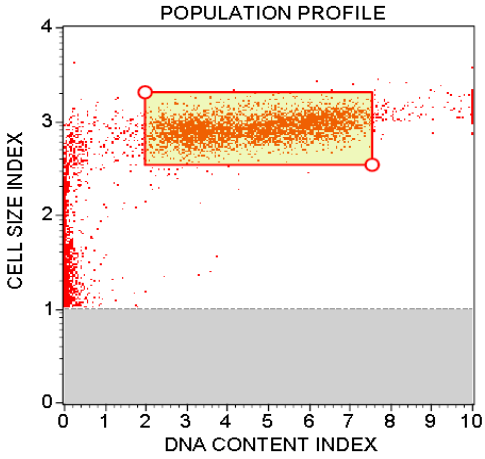
mg/ml. HT29 cells with cell size index ranging from 2-4 and with increasing DNA content index 4-10 throughout the treatments. This was performed to exclude doublets.



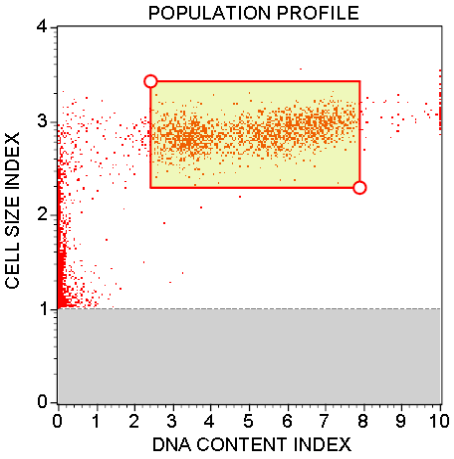
a. Control (0.1% DMSO)



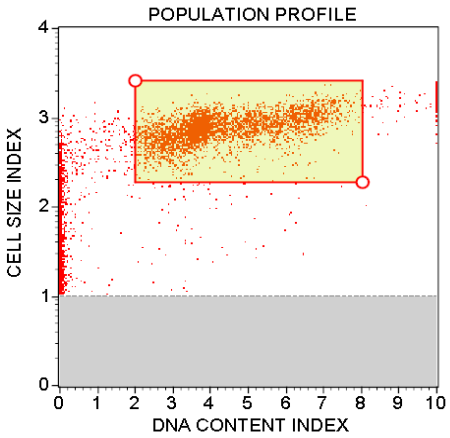
b. TDTC 1 0.4 mg/ml



c. TDTC 2 0.3 mg/ml



d. TDTC 4 0.3 mg/ml



e. TDTC 5 0.35 mg/ml

Figure 43: Cell cycle scatter plot used to gate out doublets for DLD1 cells following TDTC treatments. a. Control (0.1% DMSO); b. TDTC 1 0.4 mg/ml; c. TDTC 2 0.4 mg/ml; d. TDTC 4 0.3 mg/ml; e. TDTC 5 0.35 mg/ml. DLD1 cells with cell size index ranging from 2-4 and with increasing DNA content index 2-9 throughout the treatments. This was performed to exclude doublets.

6.4 Appendix D: TDTC working solutions for Alamar Blue screening

Table 8: Stock solution for Alamar Blue screening.

Compound Name	Amount of the Compound (mg)	Amount of DMSO (ml) (Diluent)	Stock Concentration (mg/ml) (w/v)
TDTC 1	10	0.5	20
TDTC 2	10	0.5	20
TDTC 3	10	0.5l	20
TDTC 4	10	0.9	11
TDTC 5	10	0.6	17
TDTC 6	10	1.2	8
TDTC 7	3	1	3
TDTC 8	10	1.5	7
TDTC 9	10	0.6	17
TDTC 10	10	1.5	7

6.5 Appendix E: TDTC solutions

Table 9: Final experimental concentrations of the compounds for Alamar Blue screening.

Equation used for calculations: $C_1V_1=C_2V_2$

C_1= Compound Stock concentration

V_1=Initial volume of Stock concentration

C_2=Final Concentration of working concentration

V_2=Final Volume of working concentration

Compound Name	Amount of Compound (v/v) (µl) (V_1)	Amount Of Complete Medium (µl) (v/v) (V_2=600 µl)	Compound Concentration (mg/ml) (C_2) (v/v)
TDTC 1	12	588	0.4
	6	594	0.2
	3	597	0.1
	1.5	598.5	0.05
TDTC 2	12	588	0.4
	6	594	0.2
	3	597	0.1
	1.5	598.5	0.05
TDTC 3	12	588	0.4
	6	594	0.2

	3	597	0.1
	1.5	598.5	0.05
TDTC 4	12	588	0.22
	6	594	0.11
	3	597	0.055
	1.5	598.5	0.0275
TDTC 5	12	588	0.34
	6	594	0.17
	3	597	0.085
	1.5	598.5	0.0425
TDTC 6	12	588	0.16
	6	594	0.08
	3	597	0.04
	1.5	598.5	0.02
TDTC 7	12	588	0.6
	6	594	0.03
	3	597	0.015
	1.5	598.5	0.0075
TDTC 8	12	588	0.14
	6	594	0.07
	3	597	0.035
	1.5	598.5	0.0175
TDTC 9	12	588	0.34
	6	594	0.17
	3	597	0.085
	1.5	598.5	0.0425
TDTC 10	12	588	0.14
	6	594	0.07
	3	597	0.035
	1.5	598.5	0.0175

Table 10: Working concentration of active TDTCs selected from Alamar Blue screening were added to increase (Stock concentrations were increased to minimize DMSO percentage).

Name of the compound	**Amount of the compound added (mg)**	**Volume of DMSO added (ml)**	**Final Stock concentration (mg/ml) (w/v) (C_1)**
TDTC1	17	0.2	85
TDTC2	16	0.2	84.5
TDTC4	33.4	0.5	66.8
TDTC5	16.7	83.5	83.5

Table 11: Concentrations of active TDTCs used for the Trypan Blue Exclusion assay.

Equation used for calculations: $C_1V_1=C_2V_2$

C_1= Compound Stock concentration

V_1=Initial volume of Stock concentration

C_2=Final Concentration of working concentration

V_2=Final Volume of working concentration

Compound Name	**Amount of the compound (v/v) (ul) (V_1)**	**Amount of the medium (v/v) (µl) (V_2=2000 µl)**	**Final Concentration (v/v) (mg/ml) (C_2)**	**DMSO percentage (%) (v/v)**
TDTC 1	9.4	1990.6	0.4	0.
	7	1993	0.3	0.3
	5	1995	0.2	0.25
	2	1998	0.1	0.1
TDTC 2	9.5	1990.5	0.4	0.5
	7	1993	0.3	0.35
	5	1995	0.2	0.25
	2	1998	0.1	0.1
TDTC 4	6	1994	0.22	0.3
	5.7	1994.3	0.2	0.29
	9	1991	0.3	0.45
TDTC 5	8	1992	0.35	0.4
	7	1993	0.3	0.35
	5	1995	0.2	0.25
	2	1998	0.1	0.1

Table 12: The amount of the active compounds and positive control drugs used for the experiment.

Equation used for calculations: $C_1V_1=C_2V_2$

C_1= Compound Stock concentration

V_1=Initial volume of Stock concentration

C_2=Final Concentration of working concentration

V_2=Final Volume of working concentration

Final Volume for treatment	**Compound Name**	**Amount of compound (v/v) µl (V_1)**	**Amount of Medium (v/v) µl**	**Compound concentrations (v/v) mg/ml (C_2)**
V_2=5 ml (RNA and proteome treatment)	TDTC 1	23.53	4976.47	0.4
	TDTC 2	23.67	4976.33	0.4
	TDTC 4	21.52	4978.48	0.3
	TDTC 5	20.96	4979.04	0.35
V_2=2 ml (Cell cycle Assay)	TDTC 1	9.4	1990.6	0.4
	TDTC 2	9.5	1990.5	0.4
	TDTC 4	9	1991	0.3
	TDTC 5	8	1992	0.35
	5-Fu	1.3	1998.7	200 µM
	SAHA	11.5	1988.5	10
V_2=0.2 ml (Xcelligience)	TDTC 1	1	199	0.4
	TDTC 2	1	199	0.4
	TDTC 4	0.9	199.1	0.3
	TDTC 5	0.9	199.1	0.35
	TDTC 1	0.5	199.5	0.2
	5-Fu	0.14	199.86	200 µM
V_2=3 ml (Sphere Assay)	TDTC1	14	2986	0.4
	TDTC 2	14	2986	0.4
	TDTC 4	13	2987	0.3
	TDTC 5	13	2987	0.35

	5-Fu	2	2998	200 µM
	SAHA	15	2985	0.05

6.6 Appendix F: Solutions and Recipes

Table 13: Summary solutions and recipes.

Solution	Components	Concentration/Volume	Manufactures
Complete Medium (DMEMF-12 supplemented with 10% FBS and 1000 u/ml pen-strep antibiotics.)	DMEMF-12	45 ml	Gibco
	FBS	10% v/v (5 ml)	Sigma-Aldrich
	1000 u/ml pen-strep antibiotics	150 ml	Gibco
Serum Free Medium (DMEMF-12 supplemented with 1000u/ml pen-strep antibiotics)	DMEMF-12	45 ml	Gibco
	1000 u/ml pen-strep antibiotics	150 ml	Gibco
Cryopreservation Medium (FBS supplemented with 10% DMSO)	FBS	9 ml	Gibco
	DMSO	10% v/v (1 ml)	Sigma-Aldrich
PBS	PBS tablets	2 tablets w/v	Gibco
	Distilled Water	1 L	
Alamar Blue Working Solution 5mg/ml	Alamar Blue powder	75 mg Alamar blue	Sigma-Aldrich
	PBS	15 ml	Gibco
Alamar Blue Experimental solution (50X)	Alamar Blue Solution	0.1 ml	
	PBS	4.9 ml	
0.1 M Ethylenediaminetra-Acetic acid (EDTA)	EDTA	1.5 g	Sigma-Aldrich
	Distilled H2O to pH8.0	50 ml	
	Sodium Hydroxide (NaOH)	10 µl	SAARCHEM
Stem cell isolation buffer	0.1 M EDTA	1 ml	
	PBS	49 ml	
	Bovine Serum Albumin	0.25 g	Lonza

3% Formaldehyde	Formaldehyde	2.8 ml	Polysciences Inc
70% Ethanol	100% Ethanol	70 ml	VWR Prolab Chemicals
	Distill Water	30 ml	
	PBS	32.2 ml	
0.5% BSA/PBS	Bovine Serum Albumin	2.5 g	Santa Cruz Biotechnology
	PBS	500 ml	
0.25% Triton X	Triton X	35 µl	Lonza
	0.5% BSA/PBS	14 ml	
1:200 Mouse β-catenin Primary Antibody	β-catenin Primary Antibody	6 µl	Invitrogen
	0.5% BSA/PBS	1194 µl	
1:100 Rabbit VEGF Antibody	VEGF Primary Antibody	12 µl	Abcam
	0.5% BSA/PBS	1188 µl	
1:300 Goat anti-mouse secondary antibody conjugated to 488 Alexa Fluro®	Secondary Antibody	4 µl	Invitrogen
	0.5% BSA/PBS	1196 µl	
1:300 VEGF, chicken anti-rabbit secondary antibody conjugated to 488 Alexa Fluro®	Secondary Antibody	4 µl	Invitrogen
	0.5% BSA/PBS	1196 µl	
1:1000 4’,6-diamidino-2-phenylindole (DAPI)	DAPI	1 µl	Invitrogen
	PBS	1199 µl	
50X TAE Buffer	Tris-base	242 g	Sigma-Aldrich
	Acetate (100% Acetic acid)	57.1 ml	BOH Chemicals
	0.5 M Sodium EDTA	100 ml	Sigma-Aldrich
	Distilled H_2O	842.9 ml	
1X TAE Buffer	50X TAE Buffer	20 ml	Sigma-Aldrich
	Distilled H_2O	980 ml	

Stem Cell Medium	PluriSTEM™ medium	50 ml	Merck
	1000 u/ml pen-strep antibiotics	50 µl	
Stem cell Cryopreservation Medium	PluriSTEM™ medium	9 ml	
	DMSO	1 ml	

6.7 Appendix G: Protein concentrations obtained from the Qubit 2.0 Fluorometer (Life Technologies)

Table 14: Summary of protein concentrations from samples.

Name	Date	Assay Concentration (µg/ml)	Stock Concentration (µg/ml)	Assay Type	Sample Volume (µl)	Dilution
DLD1 CD+	2019/08/3	26	2600	Protein	2	100
DLD1 CD-	2019/08/3	23.9	2390	Protein	2	100
DLD1 TDTC1	2019/08/3	26	2600	Protein	2	100
DLD1 TDTC2	2019/08/3	21.5	2150	Protein	2	100
DLD1 TDTC4	2019/08/3	24.5	2450	Protein	2	100
DLD1 TDTC5	2019/08/3	22.6	2260	Protein	2	100
HT29 CD+	2019/08/20	21.4	2140	Protein	2	100
HT29 TDTC1	2019/08/20	24	2400	Protein	2	100
HT29 TDTC2	2019/08/20	26	2600	Protein	2	100
HT29 TDTC4	2019/08/20	22.1	2210	Protein	2	100

Note: For DLD1 samples 359.05 µg was used; and 357.38 µg was used for HT29 samples. All samples were normalized according to these amounts of the protein.

6.8 Appendix H: RNA concentration, quality and purity ratios

Table 15: Summary of RNA concentration and purity ratios

Sample Name	Date	Concentration (ng/µl)	A260	A280	A260/A280 (Nucleic acid distinguisher ratio)	A260/A230 (Purity ratio)
HT29 CD-	2019/11/26	202.53	5.063	2.481	2.04	1.21
HT29 CD+	2019/11/26	189.51	4.738	2.357	2.01	1.93
HT29 TDTC1	2019/11/26	355.89	8.897	4.380	2.03	1.95
HT29 TDTC2	2019/11/26	139.75	3.494	1.730	2.02	1.50
HT29 TDTC4	2019/11/26	116.55	2.914	1.449	2.01	1.72

HT29 TDTC5	2019/11/26	209.19	5.230	2.576	2.03	1.86
DLD1 CD-	2019/11/26	93.47	2.337	1.193	1.96	1.66
DLD1 CD+	2019/11/26	203.58	5.090	2.535	2.01	1.99
DLD1 TDTC1	2019/11/26	276.13	6.903	3.419	2.02	1.46
DLD1 TDTC2	2019/11/26	142.85	3.571	1.762	2.03	2.07
DLD1 TDTC4	2019/11/26	162.75	4.069	2.017	2.02	1.91
DLD1 TDTC5	2019/11/26	232.06	5.081	2.856	2.03	1.87

Note 747.76 ng of RNA was used to synthesize cDNA for all samples.
A260/280, ratio of <1,6≤1.8 is the accepted value for pure DNA and ≥2 is accepted value for pure RNA
A260/230, ratio ranging from 1.5 to 2 and greater indicates nucleic acid are free of residual ethanol or salt contamination and ratio <1.5 the nucleic acid as trace of residual ethanol or salt contamination.

6.9 Appendix I: cDNA concentration, quality and purity ratios

Table 16: Summary of cDNA concentration and purity ratios.

Sample Name	**Date**	**Concentration (ng/µl)**	**A260**	**A280**	**A260/A280 (Nucleic Acid distinguisher ratio**	**A260/A230 (Purity ratio)**
HT29 CD-	2019/11/26	1166.82	23.336	14.087	1.66	2.09
HT29 CD+	2019/11/26	1488.52	29.770	18.081	1.65	2.10
HT29 TDTC1	2019/11/26	2028.80	40.576	24.984	1.62	2.19
HT29 TDTC2	2019/11/26	2126.05	42.521	25.801	1.65	2.12
HT29 TDTC4	2019/11/26	2147.11	42.942	26.051	1.65	2.18
HT29 TDTC5	2019/11/26	1982.16	39.643	24.146	1.64	2.11
DLD1 CD-	2019/11/26	2367.10	47.342	28.916	1.64	2.17
DLD1 CD+	2019/11/26	2224.56	44.491	27.109	1.64	2.18
DLD1 TDTC1	2019/11/26	2045.96	40.919	24.938	1.64	2.10
DLD1 TDTC2	2019/11/26	1981.48	39.630	24.014	1.65	2.16
DLD1 TDTC4	2019/11/26	2098.43	41.969	25.482	1.65	2.16
DLD1 TDTC5	2019/11/26	232.06	40.001	24.299	1.65	2.09

Note <4667,28 ng of RNA was used to synthesize cDNA for all samples.
Note 747.76 ng of RNA was used to synthesize cDNA for all samples.
A260/280, ratio of <1,6≤1.8 is the accepted value for pure DNA and ≥2 is accepted value for pure RNA
A260/230, ratio ranging from 1.5 to 2 and greater indicates nucleic acid are free of residual ethanol or salt contamination and ratio <1.5 the nucleic acid as trace of residual ethanol or salt contamination.

6.10 Appendix J: qPCR plate set up for the ABI 7500 Real Time PCR Instrument (Thermofisher)

Each of the 8 genes were analysed: RPLO in row (A); E-cadherin (B); β-catenin (C); FoxA2 (D); Sox17 (E); VEGFA (F); VEGFR1 (G); and VEGFR2 (H). The samples were run in triplicates. Four MicroAmp^{TM} Optical 96-well Reaction Plate (Thermofisher) were used. The first 3 plates were set up to have 4 samples each. The first plate had HT29 CD- (differentiated cells), HT29 CD+ (stem cells), DLD1 CD- and DLD1 CD+. Second plate had HT29 stem cells treated with active TDTC 1, 2, 4 and 5 compounds. The third plate had DLD1 stem cells treated with active compounds 1, 2 4 and 5. The fourth plate was set up to have 12 samples. HT29 CD-, HT29 CD+, DLD1 CD-, DLD1 CD+, HT29 stem cells treated with TDTC1, 2, 4, and 5 compounds and DLD1 stem cells treated with the same compounds. No template control was also included. In this plate VEGFR3 gene was analysed.



Figure 44: qPCR set up

The MicroAmp™ Optical 96-well Reaction Plate (Thermofisher) was set up to have 4 samples, HT29 CD- (differentiated cells), HT29 CD+ (stem cells), DLD1 CD- and DLD1 CD+. Each of the 8 genes were analysed: RPLO in row (A); E-cadherin (B); β-catenin (C); FoxA2 (D); Sox17 (E); VEGFA (F); VEGFR1 (G); and VEGFR2 (H). The samples were analysed in triplicates.

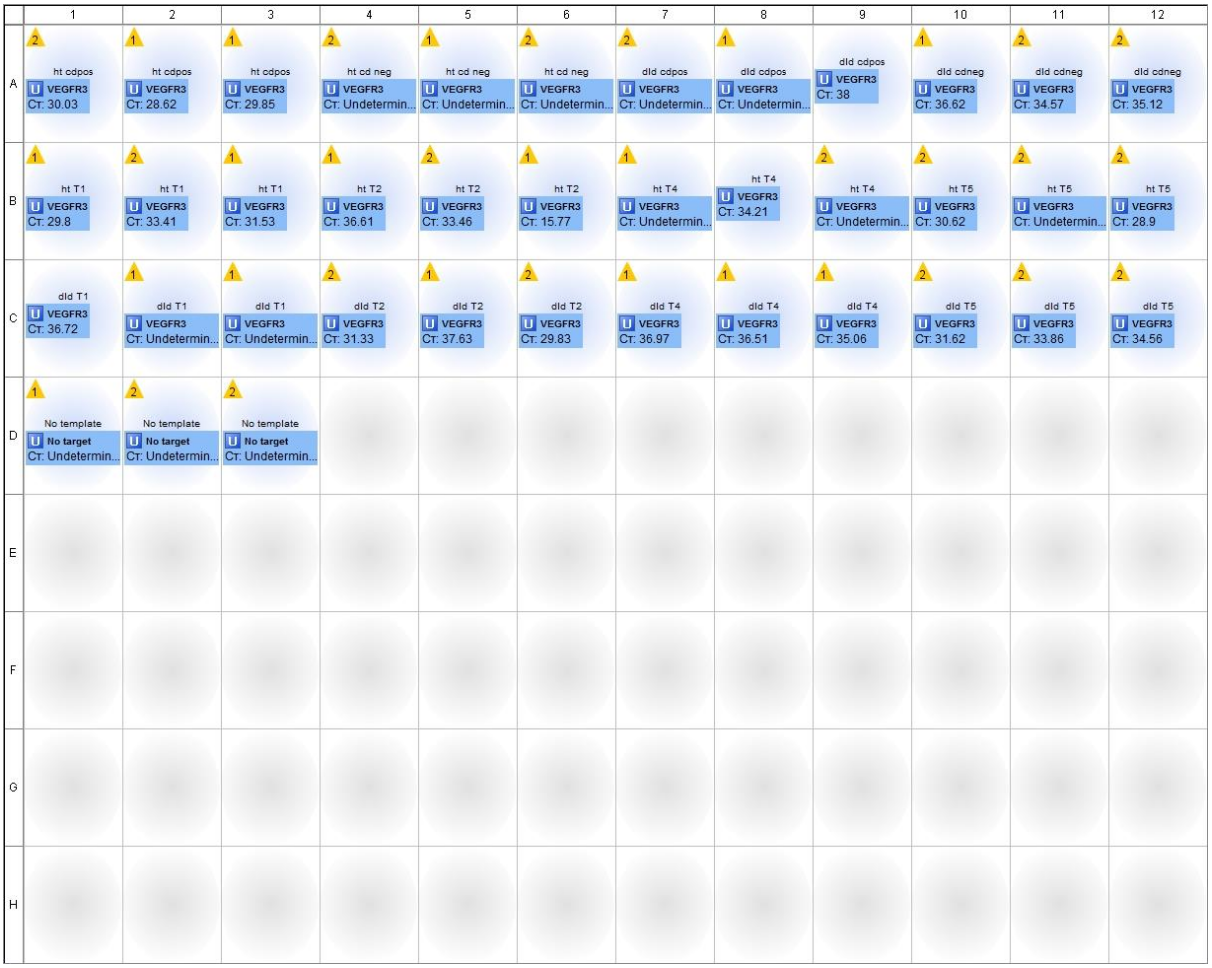


Figure 45: qPCR set up plate 4

The MicroAmpTM Optical 96-well Reaction Plate (Thermofisher) was set up to have 12 samples. HT29 CD-, HT29 CD+, DLD1 CD-, DLD1 CD+, HT29 stem cells treated with TDTC1, 2, 4, and 5 compounds and DLD1 stem cells treated with the same compounds. No template control was also included. VEGFR3 gene was analysed in this set up. The samples were analysed in triplicates.

6.11 Appendix K: Amplification Plots

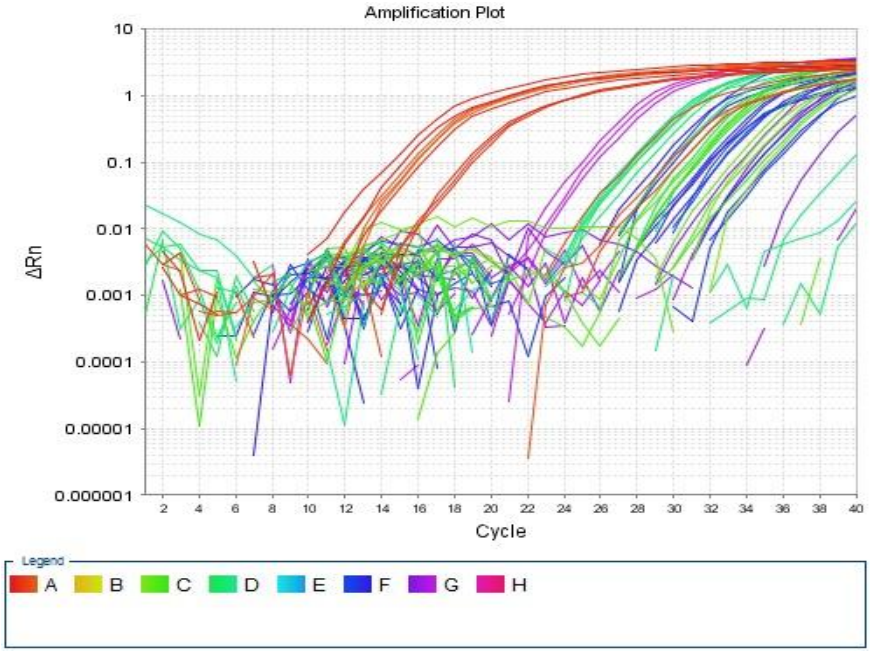


Figure 46: Amplification plot of plate 1

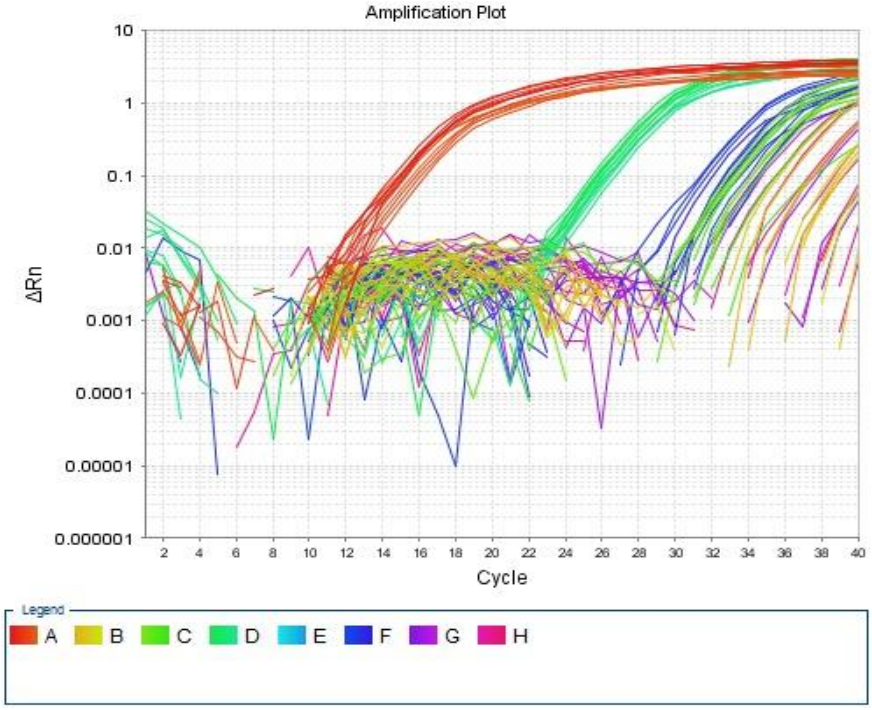


Figure 47: Amplification plot of plate 2

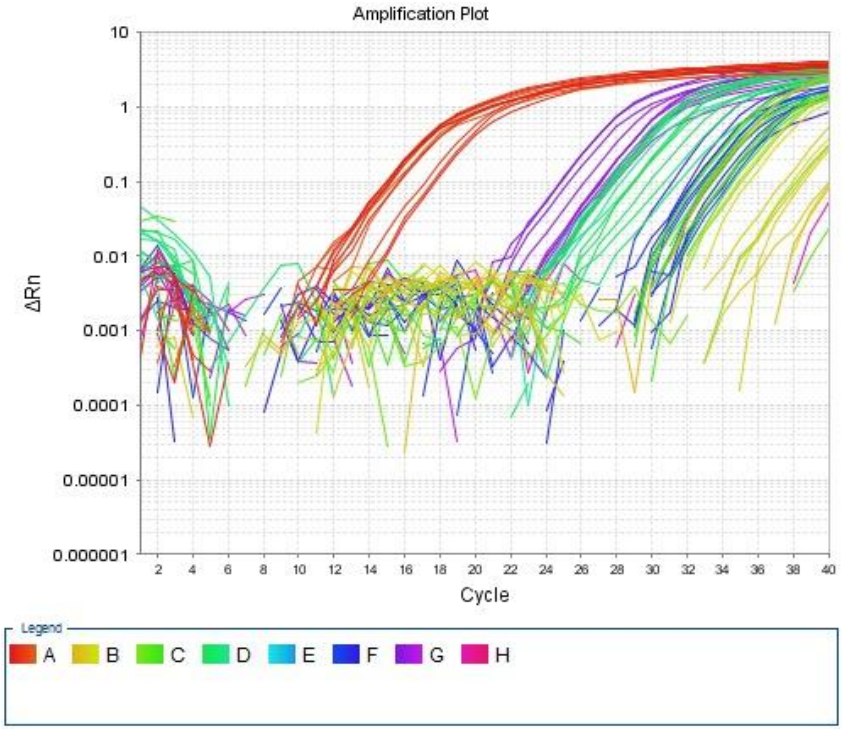


Figure 48: Amplification plot of plate 3

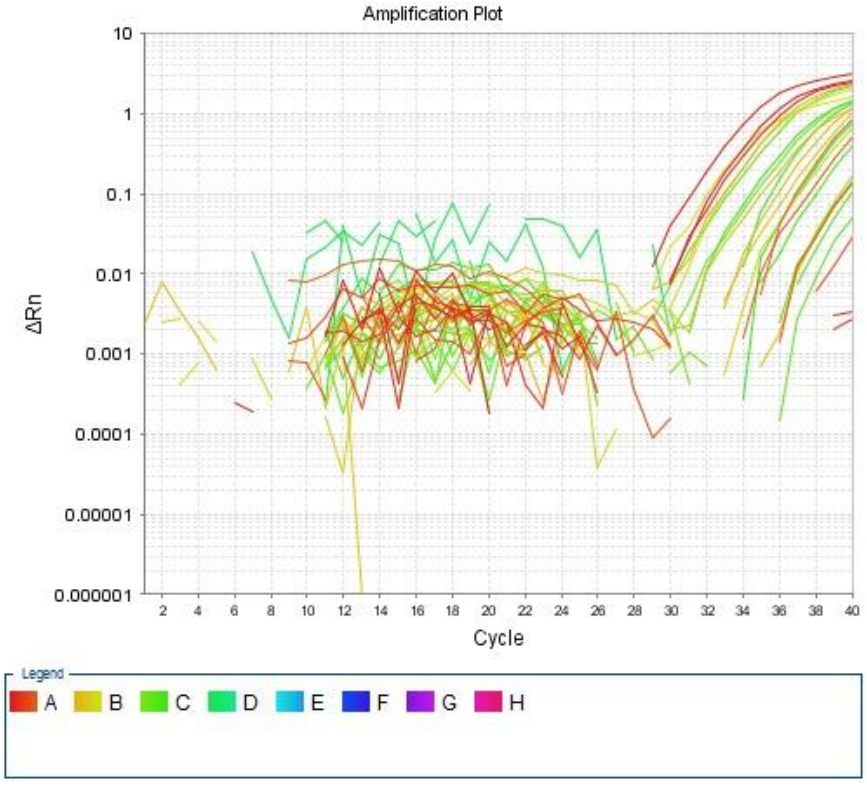


Figure 49: Amplification plot of plate 4

6.12 Appendix L: Melting curves

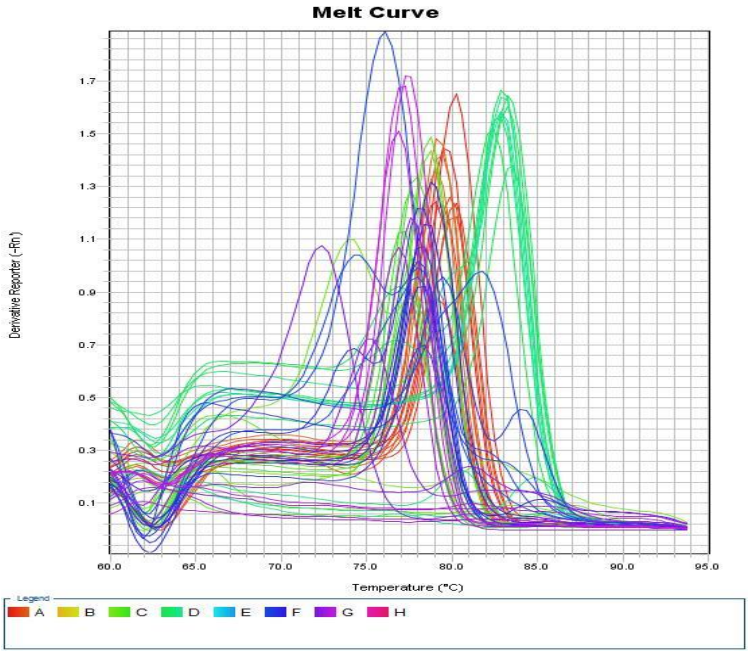


Figure 50: Melt Curve of plate 1

Melt curve depicts the specific amplification of RPLO, β-catenin, FoxA2, VEGFA and VEGFR1. Single specific peaks were seen corresponding to the temperature (°C). The sample under investigation were HT29 CD-, HT29 CD+, DLD1 CD- and DLD1 CD+.

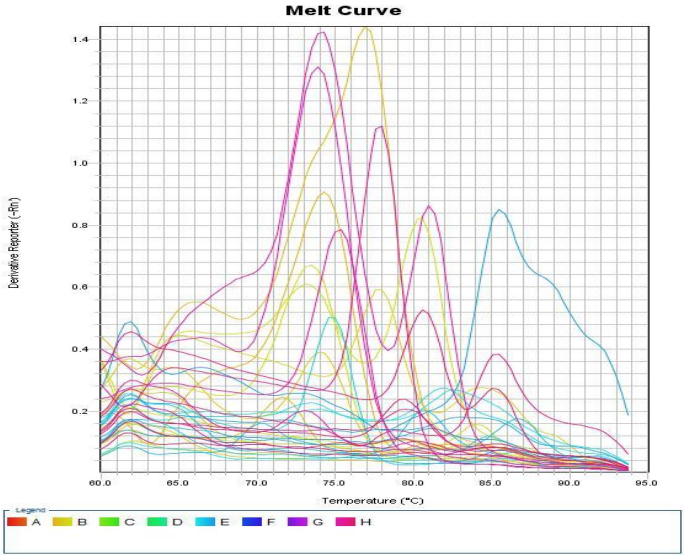


Figure 51: Melt Curve of plate 1, with non-specific amplification

The melt curve depicts non-specific amplification as you do not see clean single peaks corresponding to the temperature (°C). The genes that had non-specific amplification were Sox17, E-Cadherin and VEGFR2. Disclaimer VEGFR1 was had non-specific amplification in HT29 samples, this was observed when you look at singular melt curves of each gene. The samples under investigation where HT29 CD+, HT29 CD-, DLD CD- and HT29 CD+.

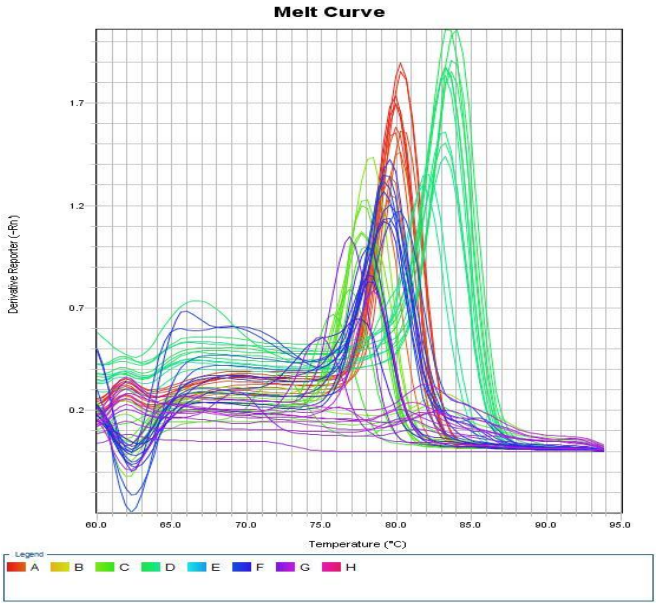


Figure 52: Melt Curve of plate 2

Melt curve depicts the specific amplification of RPLO, β-catenin, FoxA2, VEGFA and VEGFR1. Clean single specific peaks were seen corresponding to the temperature (°C). The sample under investigation were HT29 stem cells treated with active TDTC 1, TDTC 2, TDTC 4 and TDTC 5.

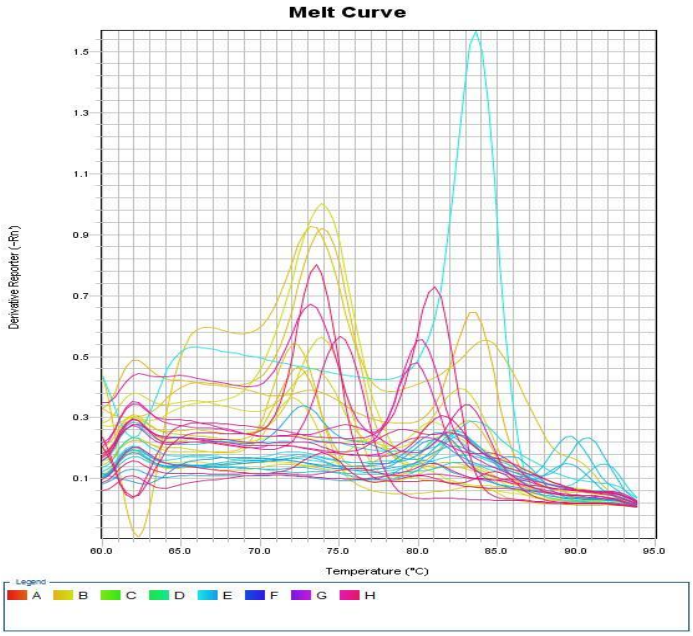


Figure 53: Melt Curve of plate 2, with non-specific amplification

The melt curve depicts non-specific amplification as you do not see clean single amplitudes corresponding to the temperature (°C). The genes that had non-specific amplification were Sox17, E-Cadherin and VEGFR2. Disclaimer VEGFR1 was had non-specific amplification in HT29 samples, this was observed when you look at singular melt

curves of each gene. The samples under investigation where HT29 stem cells treated with active TDTC 1, 2, 4 and 5 compounds.

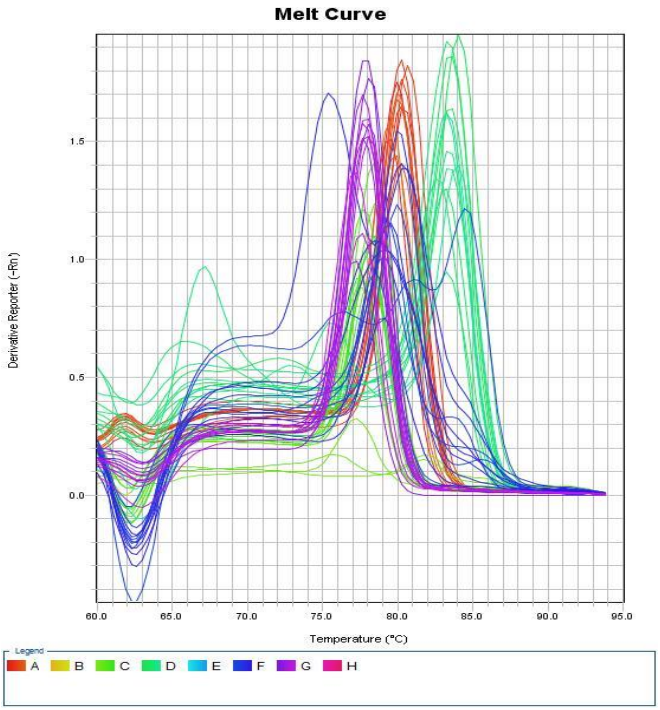


Figure 54: Melt Curve of plate 3

Melt curve depicts the specific amplification of RPLO, β-catenin, FoxA2, VEGFA and VEGFR1. Clean single specific peaks were seen corresponding to the temperature (°C). The sample under investigation were DLD1 stem cells treated with active TDTC 1, 2, 4 and 5 compounds.

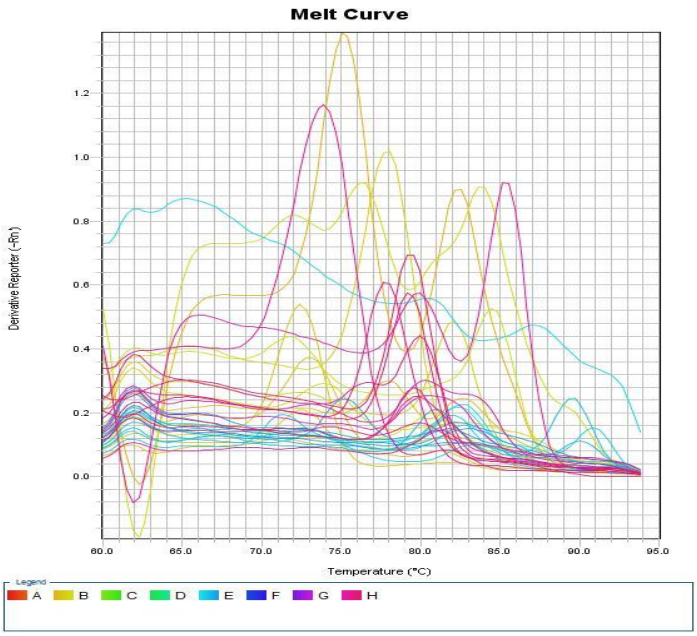


Figure 53: Melt Curve of plate 3, with non-specific amplification

The melt curve depicts non-specific amplification as you do not see clean single peaks corresponding to the temperature (°C). The genes that had non-specific amplification were Sox17, E-Cadherin and VEGFR2. The samples under investigation where DLD1 stem cell treated with active TDTC 1, 2, 4 and 5 compounds.

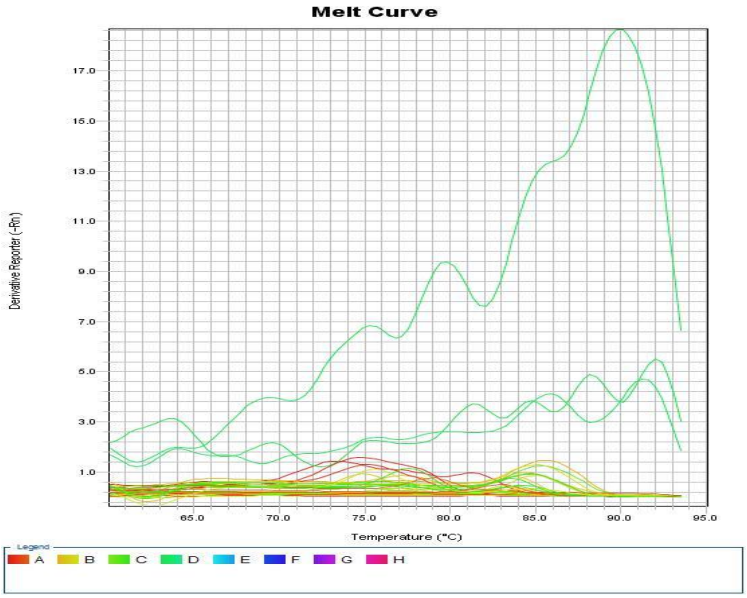


Figure 54: Melt Curve of VEGFR3

There was no single peak corresponding to temperature (°C), meaning the amplification was not specific. The samples under investigation where HT29 CD-, HT29 CD+ and HT29 stem treated with the active TDTC 1, 2, 4 and 5 compounds. DLD1 CD-, DLD1 CD+ and DLD1 stem cells treated with active TDTC 1, 2,4 and 5 compounds.

6.13 Appendix M: Troubleshooting unsuccessful Amplification

6.13.1 Gradient PCR after noticing primer dimer formation non-specificity of VEGFR1, VEGFR2, VEGFR3, E-Cadherin and Sox17.

Standard PCR was performed with different temperatures which were 55, 56, 57, 58,59 and 61°C. Taq DNA polymerase kit was used from New England BioLabs (M0273).

Table 17: Summary of components and reaction volume for performing standard gradient PCR.

Components of the Kit	Reaction Volume (µl)
10X Standard Taq Reaction Buffer	2.5
10 mM dNTPs	0.5
Template CDNA	3
Taq DNA Polymerase	0.125
Nuclease-free water	18.88

Total Volume	25
30 reactions were performed, and each reach had final volume of 25 µl	

The components were transferred into qPCR tubes on the ice-brick and then transferred to MiniAmp^{TM} thermocycler (Thermofisher).

Table 18: Cycling conditions for PCR.

Cycling conditions	Duration	Temperature °C	Step
Initial Denaturation	30 seconds	95	Denaturation
30 Cycles	15 seconds	95	Denaturation
	60 seconds	55,56,57,58,59,61	Annealing of Primers (Temperature gradient)
	60 seconds	68	Initial extension
Final Extension	5 minutes	68	
Hold	Infinity	4	
Two parts of the PCR were done first three and the second three annealing temperatures. Each PCR was 2 hours.			

6.13.2 PCR product visualization

Agarose gel electrophoresis l was used to visualize the PCR products. One percent (1 g) agarose (Lonza) was prepared in 100 ml of TAE buffer in the microwave. The agarose was dissolved and cooled down for 5 minutes; then 5 µl of ethidium bromide (EtBr) (Bio Basic Inc) was added into the solution. EtBr intercalates with the DNA, and when exposed to ultraviolet light, the EtBr fluoresces this allows for the DNA to be visualized. The gel was poured into a gel tray, a comb was inserted, and the agarose could set for 30 minutes. The comb establishes wells that the DNA sample will be pipetted into.

6.13.3 Sample Loading

The polymerised gel was placed in a gel tank and filled with 1X TAE buffer, until the wells were submerged. One microliter of 6X DNA loading buffer (Fermentas) was added to the DNA sample (PCR amplicon) of 5 microliters. GeneRuler 1 kb DNA Ladder (Thermo Scientific) of 3 µl, 2 µl of nuclease-free water and 1 µl of 6X DNA loading buffer (Fermentas) was mixed and added on the first lane. Followed by the samples. The gels were electrophoresed at 70V for 45 minutes. The DNA fragments were visualized, and images were captured using the Gel Doc™ Imager (Bio-Rad).

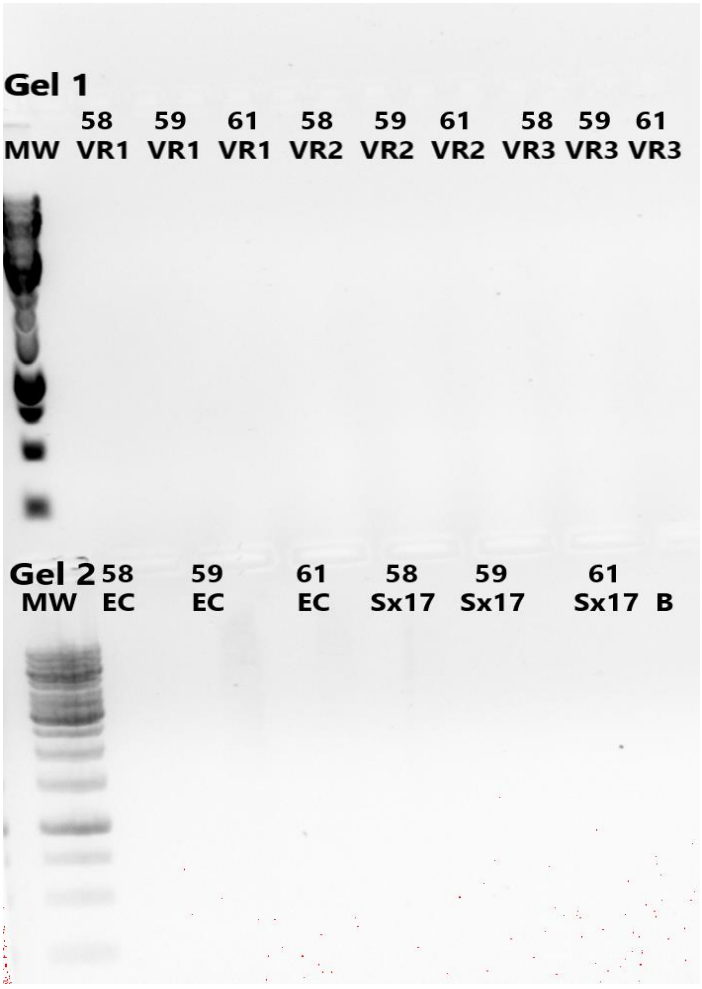


Figure 55: No product formed by 58, 59 and 61°C primer annealing temperatures.

Gel consisted of VR1=VEGFR1, VR2=VEGFR2 and VR3=VEGFR3 respectively. Gel 2 consisted of EC=E-Cadherin, Sx17= Sox17 and B=No amplicon control respectively. Each gene was amplified at 58, 59 and 61 °C. Molecular Weight Marker (1 kb DNA Ladder from Fementas) was at the first lane followed by the samples. No PCR product is seen on the gel. B=No amplicon control, there was no contamination.

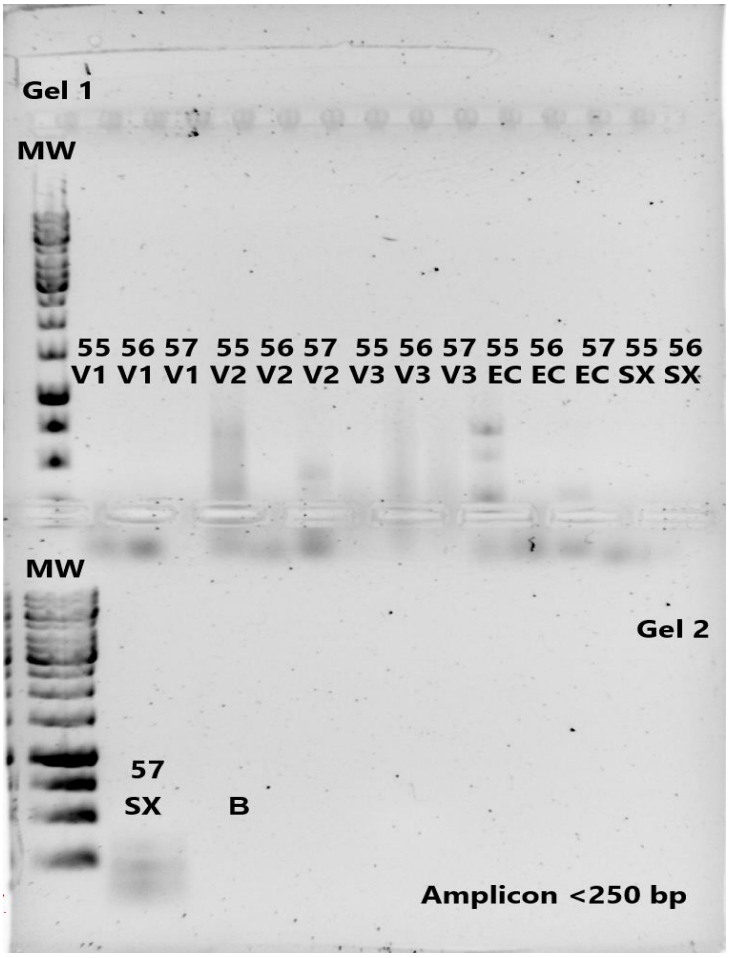


Figure 56: No so clear amplicons were seen at 55, 56 and 57°C.

Gel consisted of V1=VEGFR-1, V2=VEGFR-2, V3=VEGFR-3, EC= E-Cadherin, and two of SX= Sox17 respectively. Gel 2 consisted of one Sx17= Sox17 and B= No amplicon control respectively. Each gene was amplified at 55, 56 and 57 °C. Molecular Weight Marker (1 kb DNA Ladder from Fementas) was at first lane followed by the samples. Not so clear PCR product is seen on the gel. B=No amplicon control, no band observed thus there was no contamination.

6.13.4 The gene targets were subjected to troubleshooting using qPCR

The same procedure of qPCR was done to troubleshoot the genes that were not amplified, which are E-cadherin, Sox17, VEGFR2, VEGFR3, and VEGFR1 for HT29 cells. Untreated HT29 stem cells were used for the troubleshooting. The annealing temperature of the primers was set to 54°C instead of 60°C.

6.14 Appendix N: Cell count statistical analyses

Table 19: Summary of cell count statistical analyses of HEK293, HT29 and DLD1.

Vehicle Control vs. Treated HEK293, HT29 and DLD1 cells treated with active TDTCs (Trypan Blue Exclusion Assay)	Student T-test for Independent Samples Note: Variables were treated as independent samples P<0,05 significant (significant p value in red)					
	Mean Group 1	Mean Group 2	t-value	Degrees of freedom	p-value	Valid Number of samples
HEK293 vs. HT29	3.706923	30.39407	-4.25429	24	0.000277	13
HEK293 vs. DLD1	3.706923	41.47522	-5.80711	24	0.000005	13

Table 20: Summary of cell count statistical analyses of HT29 cells.

Vehicle control vs. Treated HT29 cells treated with active TDTCs (Trypan Blue Exclusion Assay)	Student T-test for Independent Samples Note: Variables were treated as independent samples P<0,05 significant (significant p value in red)					
	Mean Group 1	Mean Group 2	t-value	Degrees of freedom	p-value	Valid Number of samples
DMSO 0.1% vs. TDTC 1 0.3 mg/ml	1.085000	64.73934	-29.1568	2	0.001174	2
DMSO 0.1% vs. TDTC 1 0.2 mg/ml	1.085000	25.56356	-9.8677	2	0.010114	2
DMSO 0.1% vs. TDTC 1 0.1 mg/ml	1.085000	11.98500	-9.2819	2	0.011409	2
DMSO 0.1% vs. TDTC 2 0.3 mg/ml	1.085000	58.60000	-45.3504	2	0.000486	2
DMSO 0.1% vs. TDTC 2 0.2 mg/ml	1.085000	21.36500	-23.3606	2	0.001827	2
DMSO 0.1% vs. TDTC 2 0.1 mg/ml	1.085000	8.23500	-8.3396	2	0.014075	2
DMSO 0.1% vs. TDTC 4 0.22 mg/ml	1.085000	66.12500	-27.8191	2	0.001290	2
DMSO 0.1% vs. TDTC 4 0.2 mg/ml	1.085000	24.40000	-21.1909	2	0.002220	2
DMSO 0.1% vs. TDTC 4 0.1 mg/ml	1.085000	31.52500	-36.8530	2	0.000735	2
DMSO 0.1% vs. TDTC 5 0.3 mg/ml	1.085000	52.62000	-34.4669	2	0.000841	2
DMSO 0.1% vs. TDTC 5 0.2 mg/ml	1.085000	16.72000	-5.4565	2	0.031985	2
DMSO 0.1% vs. TDTC 5 0.1 mg/ml	1.085000	12.16000	-11.3596	2	0.007661	2

Table 21: Summary of cell count statistical analyses of DLD1 cells.

Vehicle Control vs. Treated DLD1 cells treated with active TDTCs (Trypan blue exclusion assay)	Student T-test for Independent Samples Note: Variables were treated as independent samples P<0,05 significant (significant p value in red)					
	Mean Group 1	Mean Group 2	t-value	Degrees of freedom	p-value	Valid Number of samples
DMSO 0.1% vs. T1 0.3 mg/ml	3.696217	37.02628	-6.3714	2	0.023760	2
DMSO 0.1% vs. T1 0.2 mg/ml	3.696217	51.73125	-3.2942	2	0.081099	2
DMSO 0.1% vs. T1 0.1 mg/ml	3.696217	67.81882	-14.2720	2	0.004874	2
DMSO 0.1% vs. T2 0.3 mg/ml	3.696217	56.36220	-6.6699	2	0.021748	2
DMSO 0.1% vs. T2 0.2 mg/ml	3.696217	63.41469	-21.5176	2	0.002153	2
DMSO 0.1% vs. T2 0.1 mg/ml	3.696217	68.94095	-17.3456	2	0.003307	2
DMSO 0.1% vs. T4 0.22 mg/ml	3.696217	53.74925	-24.3869	2	0.001677	2
DMSO 0.1% vs. T4 0.2 mg/ml	3.696217	9.17585	-3.5032	2	0.072710	2
DMSO 0.1% vs. T4 0.1 mg/ml	3.696217	8.28038	-3.0712	2	0.091673	2
DMSO 0.1% vs. T5 0.3 mg/ml	3.696217	21.70214	-11.0629	2	0.008072	2
DMSO 0.1% vs. T5 0.2 mg/ml	3.696217	43.01050	-25.1514	2	0.001577	2
DMSO 0.1% vs. T5 0.1 mg/ml	3.696217	54.26939	-11.5308	2	0.007437	2

Table 22: Summary of statistical analyses of HEK293 cells.

Vehicle Control vs. Treated HEK293 cells treated with active TDTCs (Trypan blue exclusion assay)	Students T-test for Independent Samples Note: Variables were treated as independent samples P<0,05 significant (significant p value in red)					
	Mean Group 1	Mean Group 2	t-value	Degrees of freedom	p-value	Valid Number of samples
0.1% DMSO vs. T1 0.3 mg/ml	2.490000	2.660000	-0.12032	2	0.915225	2
0.1% DMSO vs. T1 0.2 mg/ml	2.490000	2.740000	-0.14221	2	0.899950	2
0.1% DMSO vs. T1 0.1 mg/ml	2.490000	2.745000	-0.16130	2	0.886680	2
0.1% DMSO vs. T2 0.3 mg/ml	2.490000	4.485000	-1.29351	2	0.325084	2
0.1% DMSO vs. T2 0.2 mg/ml	2.490000	3.150000	-0.46611	2	0.686975	2
0.1% DMSO vs. T2 0.1 mg/ml	2.490000	3.900000	-0.67768	2	0.567861	2
0.1% DMSO vs. T4 0.22 mg/ml	2.490000	4.210000	-1.17355	2	0.361411	2
0.1% DMSO vs. T4 0.2 mg/ml	2.490000	3.260000	-0.53771	2	0.644602	2
0.1% DMSO vs. T4 0.1 mg/ml	2.490000	2.090000	0.11969	2	0.915669	2
0.1% DMSO vs. T5 0.3 mg/ml	2.490000	8.815000	-3.37444	2	0.077721	2
0.1% DMSO vs. T5 0.2 mg/ml	2.490000	5.795000	-1.48343	2	0.276208	2
0.1% DMSO vs. T5 0.1 mg/ml	2.490000	1.850000	0.35297	2	0.757843	2

6.15 Appendix O: Cell Cycle Statistics

Table 23: Summary of cell cycle statistical analyses of G0/G1 phase in HT29 cells.

Vehicle Control vs. Treated G0/G1 phase (Cell cycle assay)	Student T-test for Independent Samples Note: Variables were treated as independent samples P<0,05 significant (significant p value in red)					
	Mean Group 1	Mean Group 2	t-value	Degrees of freedom	p-value	Valid N
0.1% DMSO HT29 vs. TDTC 1 0.4 mg/ml	14.10000	17.85000	-1.49256	2	0.274099	2
0.1% DMSO HT29 vs. TDTC 2 0.4 mg/ml	14.10000	55.15000	-2.70821	2	0.113581	2
0.1% DMSO HT29 vs. TDTC 4 0.3 mg/ml	14.10000	24.50000	-3.56717	2	0.070390	2
0.1% DMSO HT29 vs. TDTC 5 0.35 mg/ml	14.10000	41.95000	-5.10408	2	0.036308	2

Table 24: Summary of cell cycle statistical analyses of S phase in HT29 cells

Vehicle Control vs. Treated S phase (Cell cycle assay)	Student T-test for Independent Samples Note: Variables were treated as independent samples P<0,05 significant (significant p value in red)					
	Mean Group 1	Mean Group 2	t-value	Degrees of freedom	p-value	Valid Number of Samples
0.1% DMSO HT29 vs. TDTC 1 0.4 mg/ml	31.20000	35.70000	-1.33396	2	0.313836	2
0.1% DMSO HT29 vs. TDTC 2 0.4 mg/ml	31.20000	32.95000	-0.10680	2	0.924695	2

0.1% DMSO HT29 vs. TDTC 4 0.3 mg/ml	31.20000	64.00000	-9.72305	2	0.010413	2
0.1% DMSO HT29 vs. TDTC 5 0.35 mg/ml	31.20000	47.70000	-4.49907	2	0.046020	2

Table 25: Summary of cell cycle statistical analyses of G2/M phase in HT29 cells.

Vehicle Control vs. Treated G2/M phase (Cell cycle assay)	Student T-test for Independent Samples Note: Variables were treated as independent samples P<0,05 significant (significant p value in red)					
	Mean Group 1	Mean Group 2	t-value	Degrees of freedom	p-value	Valid Number of Samples
0.9% DMSO vs. TDTC 1 0.4 mg/ml	42.45000	45.90000	-0.532584	2	0.647569	2
0.9% DMSO vs. TDTC 2 0.4 mg/ml	42.45000	11.30000	4.760721	2	0.041401	2
0.9% DMSO vs. TDTC 4 0.3 mg/ml	42.45000	11.45000	4.538016	2	0.045286	2
0.9% DMSO vs. TDTC 5 0.35 mg/ml	42.45000	10.10000	4.436818	2	0.047229	2

Table 26: Summary of cell cycle statistical analyses of G0/G1 phase in DLD1 cells.

Vehicle Control vs. Treated G0/G1 phase	Student T-test for Independent Samples Note: Variables were treated as independent samples P<0,05 significant (significant p value in red)					
	Mean Group 1	Mean Group 2	t-value	Degrees of freedom	p-value	Valid Number of Samples
0.1% DMSO DLD1 vs. TDTC 1 0.4 mg/ml	60.30000	39.90000	5.840503	2	0.028086	2
0.1% DMSO DLD1 vs. TDTC 2 0.4 mg/ml	60.30000	34.20000	7.303736	2	0.018235	2
0.1% DMSO DLD1 vs. TDTC 4 0.3 mg/ml	60.30000	37.70000	6.470361	2	0.023063	2
0.1% DMSO DLD1 vs. TDTC 5 0.35 mg/ml	60.30000	64.25000	-0.461736	2	0.689628	2

Table 27: Summary of cell cycle statistical analyses of S phase in DLD1 cells.

Vehicle Control vs. Treated S phase	Student T-test for Independent Samples Note: Variables were treated as independent samples P<0,05 significant (significant p value in red)					
	Mean Group 1	Mean Group 2	t-value	Degrees of freedom	p-value	Valid Number of Samples
0.1% DMSO DLD1 vs. TDTC 1 0.4 mg/ml	11.70000	30.15000	-2.4396	2	0.134849	2
0.1% DMSO DLD1 vs. TDTC 2 0.4 mg/ml	11.70000	34.05000	-15.3773	2	0.004202	2
0.1% DMSO DLD1 vs. TDTC 4 0.3 mg/ml	11.70000	24.15000	-5.3123	2	0.033656	2
0.1% DMSO DLD1 vs. TDTC 5 0.35 mg/ml	11.70000	22.80000	-2.1896	2	0.159982	2

Table 28: Summary of cell cycle statistical analyses of G2/M phase in DLD1 cells						
Vehicle Control vs. Treated G2/M phase	Student T-test for Independent Samples Note: Variables were treated as independent samples P<0,05 significant (significant p value in red)					
	Mean Group 1	Mean Group 2	t-value	Degrees of freedom	p-value	Valid Number of Samples
0.1% DMSO DLD vs. TDTC 1 0.4 mg/ml	27.90000	29.65000	-0.25201	2	0.824567	2
0.1% DMSO DLD vs. TDTC 2 0.4 mg/ml	27.90000	31.70000	-1.41226	2	0.293382	2
0.1% DMSO DLD vs. TDTC 4 0.3 mg/ml	27.90000	36.90000	-4.49439	2	0.046109	2
0.1% DMSO DLD vs. TDTC 5 0.35 mg/ml	27.90000	12.75000	4.25077	2	0.051135	2

6.16 Appendix P: Proteome Results statistics

Table 29: Summary of human stem cell biomarker proteome array statistical analyses of HT29 stem cells.						
Vehicle Control vs. Treated HT29 stem cells (Human stem cell biomarker Proteome Array)	Student T-test for Independent Samples Note: Variables were treated as independent samples P<0,05 significant (significant p value in red)					
	Mean Group 1	Mean Group 2	t-value	Degrees of freedom	p-value	Valid Number of Samples
0.1% DMSO (AFP) vs. TDTC 1 0.4 mg/ml	691.4300	517.0300	3.030139	2	0.093834	2
0.1% DMSO (AFP) vs. TDTC 2 0.4 mg/ml	691.4300	499.2400	4.288967	2	0.050296	2
0.1% DMSO (AFP) vs. TDTC 4 0.3 mg/ml	691.4300	538.0400	3.110730	2	0.089661	2
0.1% DMSO (E-Cadherin) vs. TDTC 1 0.4 mg/ml	12642.08	16781.13	-23.2076	2	0.001852	2
0.1% DMSO (E-Cadherin) vs. TDTC 2 0.4 mg/ml	12642.08	15362.18	-7.3220	2	0.018147	2
0.1% DMSO (E-Cadherin) vs. TDTC 4 0.3 mg/ml	12642.08	17486.17	-29.2204	2	0.001169	2
0.1% DMSO (FoxA2) vs. TDTC 1 0.4 mg/ml	4587.130	4898.715	-6.77747	2	0.021084	2
0.1% DMSO (FoxA2) vs. TDTC 2 0.4 mg/ml	4587.130	3315.115	32.97099	2	0.000919	2
0.1% DMSO (FoxA2) vs. TDTC 4 0.3 mg/ml	4587.130	1677.575	74.11207	2	0.000182	2
0.1% DMSO (GATA-4) vs. TDTC 1 0.4 mg/ml	1331.525	1122.330	2.65102	2	0.117694	2
0.1% DMSO CD- (GATA-4) vs. TDTC 2 0.4 mg/ml	1331.525	1520.930	-1.54491	2	0.262382	2
0.1% DMSO (GATA-4) vs. TDTC 4 0.3 mg/ml	1331.525	1758.250	-4.89057	2	0.039358	2
0.1% DMSO (GSC) vs. TDTC 1 0.4 mg/ml	1014.980	550.340	6.1545	2	0.025399	2
0.1% DMSO (GSC) vs. TDTC 2 0.4 mg/ml	1014.980	1270.490	-15.5262	2	0.004123	2
0.1% DMSO (GSC) vs. TDTC 4 0.3 mg/ml	1014.980	1299.795	-7.5226	2	0.017216	2
0.1% DMSO (HCG) vs. TDTC 1 0.4 mg/ml	1352.100	713.245	2.099403	2	0.170623	2
0.1% DMSO (HCG) vs. TDTC 2 0.4 mg/ml	1352.100	1264.655	0.303537	2	0.790146	2
0.1% DMSO (HCG) vs. TDTC 4 0.3 mg/ml	1352.100	1396.440	-0.153597	2	0.892025	2
0.1% DMSO (Oct3/4) vs. TDTC 1 0.4 mg/ml	1016.970	806.080	6.20533	2	0.025000	2
0.1% DMSO (Oct3/4) vs. TDTC 2 0.4 mg/ml	1016.970	1205.560	-1.40664	2	0.294794	2
0.1% DMSO (Oct3/4) vs. TDTC 4 0.3 mg/ml	1016.970	1221.995	-6.15809	2	0.025371	2
0.1% DMSO (Nanog) vs. TDTC 1 0.4 mg/ml	1272.315	1047.700	2.080884	2	0.172928	2
0.1% DMSO (Nanog) vs. TDTC 2 0.4 mg/ml	1272.315	1182.600	0.811824	2	0.502151	2
0.1% DMSO (Nanog) vs. TDTC 4 0.3 mg/ml	1272.315	1248.345	0.222114	2	0.844844	2
0.1% DMSO (Otx2) vs. TDTC 1 0.4 mg/ml	1091.555	1004.710	0.81771	2	0.499443	2
0.1% DMSO (Otx2) vs. TDTC 2 0.4 mg/ml	1091.555	1156.115	-1.42553	2	0.290080	2

0.1% DMSO (Otx2) vs. TDTC 4 0.3 mg/ml	1091.555	1476.235	-4.58845	2	0.044361	2
0.1% DMSO (PDX-1) vs. TDTC 1 0.4 mg/ml	1049.185	2266.125	-24.8617	2	0.001614	2
0.1% DMSO (PDX-1) vs. TDTC 2 0.4 mg/ml	1049.185	1934.665	-17.4678	2	0.003261	2
0.1% DMSO (PDX-1) vs. TDTC 4 0.3 mg/ml	1049.185	1644.320	-11.3978	2	0.007610	2
0.1% DMSO (Snail) vs. TDTC 1 0.4 mg/ml	927.8450	947.740	-0.29870	2	0.793344	2
0.1% DMSO (Snail) vs. TDTC 2 0.4 mg/ml	927.8450	1139.205	-3.15270	2	0.087591	2
0.1% DMSO (Snail) vs. TDTC 4 0.3 mg/ml	927.8450	1248.135	-7.51315	2	0.017258	2
0.1% DMSO (Sox2) vs. TDTC 1 0.4 mg/ml	1138.720	827.295	6.45963	2	0.023137	2
0.1% DMSO (Sox2) vs. TDTC 2 0.4 mg/ml	1138.720	1319.095	-3.28884	2	0.081332	2
0.1% DMSO (Sox2) vs. TDTC 4 0.3 mg/ml	1138.720	1398.105	-4.87457	2	0.039602	2
0.1% DMSO (TP63) vs. TDTC 1 0.4 mg/ml	1003.585	733.885	2.78698	2	0.108241	2
0.1% DMSO (TP63) vs. TDTC 2 0.4 mg/ml	1003.585	982.730	2.18264	2	0.160767	2
0.1% DMSO (TP63) vs. TDTC 4 0.3 mg/ml	1003.585	1277.380	-4.26097	2	0.050909	2
0.1% DMSO (VEGFR2) vs. TDTC 1 0.4 mg/ml	833.3600	598.040	8.0667	2	0.015022	2
0.1% DMSO (VEGFR2) vs. TDTC 2 0.4 mg/ml	833.3600	1163.105	-3.5409	2	0.071330	2
0.1% DMSO (VEGFR2) vs. TDTC 4 0.3 mg/ml	833.3600	1579.955	-27.6422	2	0.001306	2
0.1% DMSO (Sox17) vs. TDTC 1 0.4 mg/ml	931.2900	724.370	1.86655	2	0.202941	2
0.1% DMSO (Sox17) vs. TDTC 2 0.4 mg/ml	931.2900	1038.910	-1.66198	2	0.238408	2
0.1% DMSO (Sox17) vs. TTDTC 4 0.3 mg/ml	931.2900	1328.150	-5.82125	2	0.028265	2

Table 30: Summary of human stem cell biomarker proteome array statistical analyses of DLD1 stem cells.

Vehicle Control vs. Treated DLD1 stem cells (Human stem cell biomarker proteome array)	Student T-test for Independent Samples Note: Variables were treated as independent samples P<0,05 significant (significant p value in red)					
	Mean Group 1	Mean Group 2	t-value	Degrees of freedom	p-value	Valid Number of Samples
0.1% DMSO (AFP) vs. TDTC 1 0.4 mg/ml	576.5350	821.3550	-1.06938	2	0.396856	2
0.1% DMSO (AFP) vs. TDTC 2 0.4 mg/ml	576.5350	762.4000	-2.12127	2	0.167956	2
0.1% DMSO (AFP) vs. TTDTC 4 0.3 mg/ml	576.5350	780.0400	-2.40829	2	0.137687	2
0.1% DMSO (AFP) vs. TTDTC 5 0.35 mg/ml	576.5350	852.5400	-1.97606	2	0.186801	2
0.1% DMSO (E-Cadherin) vs. TTDTC 1 0.4 mg/ml	19041.28	21903.81	-8.63439	2	0.013149	2
0.1% DMSO (E-Cadherin) vs. TTDTC 2 0.4 mg/ml	19041.28	18246.95	2.76799	2	0.109495	2
0.1% DMSO (E-Cadherin) vs. TDTC 4 0.3 mg/ml	19041.28	17545.16	3.17129	2	0.086697	2
0.1% DMSO (E-Cadherin) vs. TDTC 5 0.35 mg/ml	19041.28	17348.94	7.86445	2	0.015786	2
0.1% DMSO (FoxA2) vs. TDTC 1 0.4 mg/ml	2496.415	1693.175	7.78499	2	0.016103	2
0.1% DMSO (FoxA2) vs. TTDC 2 0.4 mg/ml	2496.415	1478.615	12.09323	2	0.006768	2
0.1% DMSO (FoxA2) vs. TDTC 4 0.3 mg/ml	2496.415	1496.555	4.60487	2	0.044065	2
0.1% DMSO (FoxA2) vs. TDTC 5 0.35 mg/ml	2496.415	1622.595	9.39406	2	0.011143	2
0.1% DMSO (GATA-4) vs. TDTC 1 0.4 mg/ml	2512.015	2420.635	0.73851	2	0.537107	2
0.1% DMSO (GATA-4) vs. TDTC 2 0.4 mg/ml	2512.015	2833.285	-2.55306	2	0.125239	2
0.1% DMSO (GATA-4) vs. TDTC 4 0.3 mg/ml	2512.015	1754.635	6.12757	2	0.025614	2
0.1% DMSO (GATA-4) vs. TDTC 5 0.35 mg/ml	2512.015	2676.965	-1.26038	2	0.334662	2
0.1% DMSO (GSC) vs. TDTC 1 0.4 mg/ml	1088.955	1595.020	-4.96702	2	0.038224	2
0.1% DMSO (GSC) vs. TDTC 2 0.4 mg/ml	1088.955	1528.145	-4.35309	2	0.048931	2
0.1% DMSO (GSC) vs. TDTC 4 0.3 mg/ml	1088.955	884.740	1.99832	2	0.183732	2

0.1% DMSO (GSC) vs. TDTC 5 0.35 mg/ml	1088.955	1318.885	-1.96578	2	0.188241	2
0.1% DMSO (HCG) vs. TTDC 1 0.4 mg/ml	1393.105	1429.290	-0.67616	2	0.568649	2
0.1% DMSO (HCG) vs. TDTC 2 0.4 mg/ml	1393.105	1739.510	-2.55650	2	0.124963	2
0.1% DMSO (HCG) vs. TDTC 4 0.3 mg/ml	1393.105	1650.920	-2.13216	2	0.166649	2
0.1% DMSO (HCG) vs. TDTC 5 0.35 mg/ml	1393.105	1552.945	-1.70598	2	0.230130	2
0.1% DMSO (Oct3/4) vs. TDTC 1 0.4 mg/ml	1188.715	1409.645	-0.82303	2	0.497007	2
0.1% DMSO (Oct3/4) vs. TDTC 2 0.4 mg/ml	1188.715	1402.045	-2.19806	2	0.159026	2
0.1% DMSO (Oct3/4) vs. TDTC 4 0.3 mg/ml	1188.715	1061.355	3.60942	2	0.068918	2
0.1% DMSO (Oct3/4) vs. TDTC 5 0.35 mg/ml	1188.715	1206.800	-0.08700	2	0.938600	2
0.1% DMSO (Nanog) vs. TDTC 1 0.4 mg/ml	1278.365	1474.045	-0.64248	2	0.586381	2
0.1% DMSO (Nanog) vs. TDTC 2 0.4 mg/ml	1278.365	1739.470	-1.79915	2	0.213808	2
0.1% DMSO (Nanog) vs. TDTC 4 0.3 mg/ml	1278.365	925.140	1.39841	2	0.296877	2
0.1% DMSO (Nanog) vs. TDTC 5 0.35 mg/ml	1278.365	1395.555	-0.49341	2	0.670582	2
0.1% DMSO (Otx2) vs. TDTC 1 0.4 mg/ml	1555.575	1642.700	-1.58964	2	0.252871	2
0.1% DMSO (Otx2) vs. TDTC 2 0.4 mg/ml	1555.575	1495.505	1.05541	2	0.401904	2
0.1% DMSO (Otx2) vs. TDTC 4 0.3 mg/ml	1555.575	1458.155	1.32507	2	0.316265	2
0.1% DMSO (Otx2) vs. TDTC 5 0.35 mg/ml	1555.575	1385.850	1.87067	2	0.202301	2
0.1% DMSO (PDX-1) vs. TDTC 1 0.4 mg/ml	2555.230	2584.455	-0.50350	2	0.664592	2
0.1% DMSO (PDX-1) vs. TDTC 2 0.4 mg/ml	2555.230	1858.655	11.88435	2	0.007006	2
0.1% DMSO (PDX-1) vs. TDTC 4 0.3 mg/ml	2555.230	2384.320	1.00809	2	0.419550	2
0.1% DMSO (PDX-1) vs. TDTC 5 0.35 mg/ml	2555.230	1969.580	7.60842	2	0.016840	2
0.1% DMSO (Snail) vs. TDTC 1 0.4 mg/ml	1505.795	1368.580	1.603073	2	0.250101	2
0.1% DMSO (Snail) vs. TDTC 2 0.4 mg/ml	1505.795	1286.410	3.337553	2	0.079248	2
0.1% DMSO (Snail) vs. TDTC 4 0.3 mg/ml	1505.795	963.905	9.304191	2	0.011355	2
0.1% DMSO (Snail) vs. TDTC 5 0.35 mg/ml	1505.795	1195.285	3.633479	2	0.068099	2
0.1% DMSO (Sox2) vs. TDTC 1 0.4 mg/ml	1306.455	1504.545	-1.42138	2	0.291108	2
0.1% DMSO (Sox2) vs. TDTC 2 0.4 mg/ml	1306.455	1673.355	-2.43497	2	0.135266	2
0.1% DMSO (Sox2) vs. TDTC 4 0.3 mg/ml	1306.455	1114.275	2.50308	2	0.129352	2
0.1% DMSO (Sox2) vs. TDTC 5 0.35 mg/ml	1306.455	1703.685	-5.57847	2	0.030664	2
0.1% DMSO (TP63) vs. TDTC 1 0.4 mg/ml	1163.150	1149.630	0.065911	2	0.953444	2
0.1% DMSO (TP63) vs. TDTC 2 0.4 mg/ml	1163.150	1251.310	-0.747169	2	0.532861	2
0.1% DMSO (TP63) vs. TDTC 4 0.3 mg/ml	1163.150	1117.730	0.370759	2	0.746404	2
0.1% DMSO (TP63) vs. TDTC 5 0.35 mg/ml	1163.150	1082.905	0.616972	2	0.600132	2
0.1% DMSO (VEGFR2) vs. TDTC 1 0.4 mg/ml	1347.535	1399.355	-0.47998	2	0.678607	2
0.1% DMSO (VEGFR2) vs. TDTC 2 0.4 mg/ml	1347.535	1444.180	-1.20571	2	0.351219	2
0.1% DMSO (VEGFR2) vs. TDTC 4 0.3 mg/ml	1347.535	1019.865	4.74546	2	0.041652	2
0.1% DMSO (VEGFR2) vs. TDTC 5 0.35 mg/ml	1347.535	1120.355	1.68071	2	0.234837	2
0.1% DMSO (Sox17) vs. TDTC 1 0.4 mg/ml	1135.335	1533.210	-6.38975	2	0.023628	2
0.1% DMSO (Sox17) vs. TDTC 2 0.4 mg/ml	1135.335	1461.555	-9.63500	2	0.010601	2
0.1% DMSO (Sox17) vs. TDTC 4 0.3 mg/ml	1135.335	1027.290	2.85068	2	0.104179	2
0.1% DMSO (Sox17) vs. TDTC 5 0.35 mg/ml	1135.335	1311.965	-1.83234	2	0.208362	2

6.17 Appendix Q: Ethical Clearance

UNIVERSITY OF THE WITWATERSRAND, JOHANNESBURG

HUMAN RESEARCH ETHICS COMMITTEE (MEDICAL)

08/06/2018

Ref: W-CBP-180608-01

TO WHOM IT MAY CONCERN:

Waiver: This certifies that the following research does not require clearance from the Human Research Ethics Committee (Medical).

Investigator: Ms NT Mdluli
Student No. (if appropriate): 917036
Staff No. (if appropriate):

Supervisor: Professor CB Penny

School: Clinical Medicine
Department: Medicine
Internal Medicine Division
Oncology Division
Medical School

Project title: *Modulation of growth and stemness in colorectal cancer cells by anti-cancer agents*

Reason: In vitro study.
No human participants will be involved in the study.

Dr N Naran
For Chairperson: Human Research Ethics Committee (Medical)

Copy – HREC (Medical) Secretariat: Zanele Ndlovu and Rhulani Mkansi.

Research Office Secretariat:
Physical address: Phillip Tobias Building, 3rd Floor, Office 302, Corner York Road and Princess of Wales Terrace, Parktown, Johannesburg 2193.
Postal address: Private Bag 3, Wits 2050
Tel Nos. +27 (0)11-717-1234/2656/2700/1252
Office E-mail: HREC-Medical.ResearchOffice@wits.ac.za.
Website:http://www.wits.ac.za/research/about-our-research/ethics-and-research-integrity/

6.18 Appendix R: Turnit Report

917036:Thembeka_26MAY_2020_(1).pdf

ORIGINALITY REPORT

16%	9%	9%	11%
SIMILARITY INDEX	INTERNET SOURCES	PUBLICATIONS	STUDENT PAPERS

PRIMARY SOURCES

1	repozitorij.sumfak.unizg.hr Internet Source	1%
2	Kathleen Dillen, Jo Vandervoort, Guy Van den Mooter, Loes Verheyden, Annick Ludwig. "Factorial design, physicochemical characterisation and activity of ciprofloxacin-PLGA nanoparticles", International Journal of Pharmaceutics, 2004 Publication	<1%
3	wiredspace.wits.ac.za Internet Source	<1%
4	hdl.handle.net Internet Source	<1%
5	"Encyclopedia of Cancer", Springer Science and Business Media LLC, 2017 Publication	<1%
6	Amber Khan, Mohmmad Younus Wani, Abdullah Saad Al-Bogami, Kumar Subramanian, Jeyalakshmi Kandhavelu, Paul Ruff, Clement Penny. "Anticancer Activity of Novel Gabexate	<1%

	Mesilate Mimetics in Colorectal Cancer Cells", ChemistrySelect, 2018 Publication	
7	Submitted to University of Hong Kong Student Paper	<1%
8	www.mdpi.com Internet Source	<1%
9	B. D. Zeitlin, L. M. Ellis, J. E. Nor. "Inhibition of Vascular Endothelial Growth Factor Receptor-1/Wnt/ -catenin Crosstalk Leads to Tumor Cell Death", Clinical Cancer Research, 2009 Publication	<1%
10	worldwidescience.org Internet Source	<1%
11	epub.uni-regensburg.de Internet Source	<1%
12	"Encyclopedia of Signaling Molecules", Springer Nature, 2018 Publication	<1%
13	"Pharmaceutical Bioassays", Wiley, 2009 Publication	<1%
14	Submitted to University of Sheffield Student Paper	<1%
15	translational-medicine.biomedcentral.com Internet Source	<1%

16	Submitted to Grand Canyon University Student Paper	<1%
17	Submitted to University College London Student Paper	<1%
18	Submitted to University of Huddersfield Student Paper	<1%
19	www.rndsystems.com Internet Source	<1%
20	Submitted to National University of Singapore Student Paper	<1%
21	www.oncotarget.com Internet Source	<1%
22	Jamie R. Friedman, Stephen D. Richbart, Justin C. Merritt, Kathleen C. Brown et al. "Capsaicinoids: Multiple effects on angiogenesis, invasion and metastasis in human cancers", Biomedicine & Pharmacotherapy, 2019 Publication	<1%
23	Submitted to University of Witwatersrand Student Paper	<1%
24	www.spandidos-publications.com Internet Source	<1%
25	www.jove.com Internet Source	<1%

26	www.ncbi.nlm.nih.gov Internet Source	<1%
27	www.nature.com Internet Source	<1%
28	"Natural Products for Cancer Chemoprevention", Springer Science and Business Media LLC, 2020 Publication	<1%
29	Submitted to Cardiff University Student Paper	<1%
30	tessera.spandidos-publications.com Internet Source	<1%
31	www.um.edu.mt Internet Source	<1%
32	Submitted to University of Aberdeen Student Paper	<1%
33	Submitted to Staffordshire University Student Paper	<1%
34	journals.plos.org Internet Source	<1%
35	www.genes2cognition.org Internet Source	<1%
36	Submitted to Queen's University of Belfast Student Paper	<1%

37	Submitted to University of Keele Student Paper	<1%
38	link.springer.com Internet Source	<1%
39	Submitted to Napier University Student Paper	<1%
40	usir.salford.ac.uk Internet Source	<1%
41	Gaofeng Liang, Haojie Wang, Hao Shi, Mengxi Zhu, Junling An, Yijun Qi, Jingxia Du, Yan Li, Shegan Gao. " Promotes the Proliferation and Migration of Esophageal Squamous Cell Carcinoma through the miR-194/GRHL3/PTEN/Akt Axis ", ACS Infectious Diseases, 2020 Publication	<1%
42	cloneresources.com Internet Source	<1%
43	Submitted to University of Salford Student Paper	<1%
44	Submitted to Sabanci Universitesi Student Paper	<1%
45	Submitted to Universiti Putra Malaysia Student Paper	<1%

46	www.tandfonline.com Internet Source	<1%
47	discovery.ucl.ac.uk Internet Source	<1%
48	Submitted to Sydney Girls' High School Student Paper	<1%
49	Chi-Cheng Huang, Ming-Hung Shen, Shao-Kuan Chen, Shung-Haur Yang, Chih-Yi Liu, Jiun-Wen Guo, Kang-Wei Chang, Chi-Jung Huang. "Gut butyrate-producing organisms correlate to Placenta Specific 8 protein: Importance to colorectal cancer progression", Journal of Advanced Research, 2020 Publication	<1%
50	d-nb.info Internet Source	<1%
51	www.karger.com Internet Source	<1%
52	Submitted to St George's Hospital Medical School Student Paper	<1%
53	Submitted to University of Nottingham Student Paper	<1%
54	Submitted to University of Bradford Student Paper	<1%

55	Submitted to Vrije Universiteit Brussel Student Paper	<1%
56	qmro.qmul.ac.uk Internet Source	<1%
57	Submitted to University of Birmingham Student Paper	<1%
58	studentsrepo.um.edu.my Internet Source	<1%
59	www.frontiersin.org Internet Source	<1%
60	Submitted to Monash University Student Paper	<1%
61	Submitted to University of Wales, Bangor Student Paper	<1%
62	Submitted to Western Governors University Student Paper	<1%
63	patentscope.wipo.int Internet Source	<1%
64	Submitted to University of Wollongong Student Paper	<1%
65	Arthur Zimmermann. "Tumors and Tumor-Like Lesions of the Hepatobiliary Tract", Springer Science and Business Media LLC, 2017 Publication	<1%

66	Siti Aisyah Abdul Ahmad, Uma D. Palanisamy, Joon Joon Khoo, Amreeta Dhanoa, Sharifah Syed Hassan. "Efficacy of geraniin on dengue virus type-2 infected BALB/c mice", Virology Journal, 2019 Publication	<1%
67	journalotohns.biomedcentral.com Internet Source	<1%
68	digitalcommons.wustl.edu Internet Source	<1%
69	Submitted to University of Bath Student Paper	<1%
70	Submitted to Kyungpook National University Student Paper	<1%
71	Submitted to Cranfield University Student Paper	<1%
72	livrepository.liverpool.ac.uk Internet Source	<1%
73	Submitted to University of Newcastle upon Tyne Student Paper	<1%
74	www.jbc.org Internet Source	<1%
75	Intestinal Tumorigenesis, 2015. Publication	<1%

76	Submitted to University of Leicester Student Paper	<1%
77	Submitted to The University of Manchester Student Paper	<1%
78	epdf.pub Internet Source	<1%
79	Submitted to University of Westminster Student Paper	<1%
80	opensiuc.lib.siu.edu Internet Source	<1%
81	Mingyue Zhu, Wei Li, Yan Lu, Xu Dong, Bo Lin, Yi Chen, Xueer Zhang, Junli Guo, Mengsen Li. "HBx drives alpha fetoprotein expression to promote initiation of liver cancer stem cells through activating PI3K/AKT signal pathway", International Journal of Cancer, 2017 Publication	<1%
82	Submitted to Medizinischen Universität Wien Student Paper	<1%
83	Claudia Ceci, Maria Grazia Atzori, Pedro Miguel Lacal, Grazia Graziani. "Role of VEGFs/VEGFR-1 Signaling and Its Inhibition in Modulating Tumor Invasion: Experimental Evidence in Different Metastatic Cancer Models", International Journal of Molecular	<1%

	Sciences, 2020 Publication	
84	physiolgenomics.physiology.org Internet Source	<1%
85	www.hindawi.com Internet Source	<1%
86	Submitted to Sungkyunkwan University Student Paper	<1%
87	Abel Jacobus Bronkhorst, Johannes F. Wentzel, Janine Aucamp, Etresia van Dyk, Lissinda du Plessis, Piet J. Pretorius. "Characterization of the cell-free DNA released by cultured cancer cells", Biochimica et Biophysica Acta (BBA) - Molecular Cell Research, 2016 Publication	<1%
88	Submitted to University of Cape Town Student Paper	<1%
89	koreamed.org Internet Source	<1%
90	repositorio-aberto.up.pt Internet Source	<1%
91	Submitted to University of Sydney Student Paper	<1%
92	Lee, Y.Y.. "Transcriptional profiling of batch and fed-batch protein-free 293-HEK cultures",	<1%

	Metabolic Engineering, 200701 Publication	
93	E. Cikler-Dulger, I. Sogut. "Investigation of the protective effects of boric acid on ethanol induced kidney injury", Biotechnic & Histochemistry, 2020 Publication	<1%
94	Submitted to University of Edinburgh Student Paper	<1%
95	Submitted to Coventry University Student Paper	<1%
96	www.science.gov Internet Source	<1%
97	molecular-cancer.biomedcentral.com Internet Source	<1%
98	Submitted to University of Glamorgan Student Paper	<1%
99	Submitted to University of Strathclyde Student Paper	<1%
100	Submitted to Middlesex University Student Paper	<1%
101	Laura Keller, Klaus Pantel. "Unravelling tumour heterogeneity by single-cell profiling of circulating tumour cells", Nature Reviews Cancer, 2019	<1%

	Publication	
102	Submitted to Summit High School Student Paper	<1%
103	Ugo Testa, Elvira Pelosi, Germana Castelli. "Colorectal Cancer: Genetic Abnormalities, Tumor Progression, Tumor Heterogeneity, Clonal Evolution and Tumor-Initiating Cells", Medical Sciences, 2018 Publication	<1%
104	clinicalepigeneticsjournal.biomedcentral.com Internet Source	<1%
105	Zhang, Chong, Shuang-shuang Zhou, Lin-yi Feng, Da-yong Zhang, Neng-ming Lin, Li-huang Zhang, Jian-ping Pan, Jun-bo Wang, and Jie Li. "In vitro anti-cancer activity of chamaejasmenin B and neochamaejasmin C isolated from the root of Stellera chamaejasme L", Acta Pharmacologica Sinica, 2012. Publication	<1%
106	bmcgenomics.biomedcentral.com Internet Source	<1%
107	Stem Cells Handbook, 2013. Publication	<1%
108	Submitted to University of Brighton Student Paper	<1%

109	"Role of Transcription Factors in Gastrointestinal Malignancies", Springer Nature, 2017 Publication	<1 %
110	Kelly M. Elkins, Raelynn E. Kadunc. "An Undergraduate Laboratory Experiment for Upper-Level Forensic Science, Biochemistry, or Molecular Biology Courses: Human DNA Amplification Using STR Single Locus Primers by Real-Time PCR with SYBR Green Detection", Journal of Chemical Education, 2012 Publication	<1 %
111	Michael D. Paul, Kalina Hristova. "The RTK Interactome: Overview and Perspective on RTK Heterointeractions", Chemical Reviews, 2018 Publication	<1 %
112	Submitted to Yeungnam University Student Paper	<1 %
113	lib.dr.iastate.edu Internet Source	<1 %
114	Submitted to Drexel University Student Paper	<1 %
115	Methods in Molecular Biology, 2009. Publication	<1 %
116	Shun-Yao Ko, Shu-Chun Lin, Kuo-Wei Chang, Yong-Kie Wong, Chung-Ji Liu, Chin-Wen Chi,	<1 %

	Tsung-Yun Liu. "Increased expression of amyloid precursor protein in oral squamous cell carcinoma", International Journal of Cancer, 2004 Publication	
117	Submitted to University of Melbourne Student Paper	<1%
118	baadalsg.inflibnet.ac.in Internet Source	<1%
119	Marimuthu Saravanakumar, Halagowder Devaraj. "Notch signalling in cardiovasculogenesis: insight into their role in early cardiovascular development", Molecular Biology Reports, 2012 Publication	<1%
120	Submitted to Chulalongkorn University Student Paper	<1%
121	Submitted to Dokuz Eylul Universitesi Student Paper	<1%
122	John M. Pezzuto. "Resveratrol as an Inhibitor of Carcinogenesis", Pharmaceutical Biology, 2008 Publication	<1%
123	eprints.soton.ac.uk Internet Source	<1%
124	diposit.ub.edu Internet Source	<1%

125	Submitted to Universita' di Siena Student Paper	<1%
126	"Stem Cell Biology in Health and Disease", Springer Science and Business Media LLC, 2010 Publication	<1%
127	Submitted to Bilkent University Student Paper	<1%
128	Submitted to Far Eastern University – Nicanor Reyes Medical Foundation Student Paper	<1%
129	complete.bioone.org Internet Source	<1%
130	Erika S. Wittchen. "Isoform-specific differences between Rap1A and Rap1B GTPases in the formation of endothelial cell junctions", Small GTPases, 03/01/2011 Publication	<1%
131	www.recentmedicalfindings.com Internet Source	<1%
132	Submitted to Higher Education Commission Pakistan Student Paper	<1%
133	theses.gla.ac.uk Internet Source	<1%

134	Nan Gao, Peter White, Nicolai Doliba, Maria L. Golson, Franz M. Matschinsky, Klaus H. Kaestner. "Foxa2 Controls Vesicle Docking and Insulin Secretion in Mature β Cells", Cell Metabolism, 2007 Publication	<1%
135	citeseerx.ist.psu.edu Internet Source	<1%
136	Submitted to Mansoura University Student Paper	<1%
137	Wataru Kakuguchi, Takao Nomura, Tetsuya Kitamura, Satoko Otsuguro et al. "Suramin, screened from an approved drug library, inhibits HuR functions and attenuates malignant phenotype of oral cancer cells", Cancer Medicine, 2018 Publication	<1%
138	escholarship.org Internet Source	<1%
139	Submitted to Perdana University Student Paper	<1%
140	Submitted to J S S University Student Paper	<1%
141	cmbl.biomedcentral.com Internet Source	<1%

142	Submitted to Curtin University of Technology Student Paper	<1%
143	onlinelibrary.wiley.com Internet Source	<1%
144	T Shimada. "Characteristics of the peroxisome proliferator activated receptor gamma (PPARgamma) ligand induced apoptosis in colon cancer cells", Gut, 2002 Publication	<1%
145	Masyitah Hasan, Endang Kumolosasi, Malina Jasamai, Jamia Azdina Jamal, Norazrina Azmi, Nor Fadilah Rajab. "Evaluation of phytoestrogens in inducing cell death mediated by decreasing Annexin A1 in Annexin A1-knockdown leukemia cells", DARU Journal of Pharmaceutical Sciences, 2020 Publication	<1%
146	journals.physiology.org Internet Source	<1%
147	Submitted to Middle East Technical University Student Paper	<1%
148	elib.suub.uni-bremen.de Internet Source	<1%
149	www.embopress.org Internet Source	<1%

150	Submitted to Widener University Student Paper	<1%
151	www.astrazeneca-us.com Internet Source	<1%
152	www.mhsl.uab.edu Internet Source	<1%
153	www.elsevier.es Internet Source	<1%
154	Submitted to Brunel University Student Paper	<1%
155	Submitted to Dundalk Institute of Technology Student Paper	<1%
156	Swapna Asuthkar, Maheedhara R. Guda, Sarah E. Martin, Reuben Antony et al. "Hand1 overexpression inhibits medulloblastoma metastasis", Biochemical and Biophysical Research Communications, 2016 Publication	<1%
157	Submitted to Institute for Medical Research Student Paper	<1%
158	Yuling Li, Zhenbing Lv, Guoyang He, Jianmei Wang et al. "The SOX17/miR-371-5p/SOX2 axis inhibits EMT, stem cell properties and metastasis in colorectal cancer", Oncotarget, 2015	<1%

	Publication	
159	www.intechopen.com Internet Source	<1 %
160	Submitted to Bloomsbury Colleges Student Paper	<1 %
161	edoc.ub.uni-muenchen.de Internet Source	<1 %
162	portlandpress.com Internet Source	<1 %
163	mcb.asm.org Internet Source	<1 %
164	Submitted to University of Auckland Student Paper	<1 %
165	Suman Manandhar, Shama Prasada K, K. Sreedhara Ranganath Pai. "Aberrant Canonical Wnt signaling: Phytochemical based modulation", Phytomedicine, 2020 Publication	<1 %
166	www.cancer.org Internet Source	<1 %
167	pericles.pericles-prod.literatumonline.com Internet Source	<1 %
168	docplayer.org Internet Source	<1 %

169	"Cancer Stem Cells", Springer Science and Business Media LLC, 2018 Publication	<1%
170	Jackie R. Bickenbach, Katie L. Grinnell. "Epidermal stem cells: interactions in developmental environments", Differentiation, 2004 Publication	<1%
171	Submitted to University of South Australia Student Paper	<1%
172	Submitted to University of Durham Student Paper	<1%
173	Hong-Qiang Guo, Guo-Liang Huang, Ou-Fei Liu, Yan-Yan Liu et al. "p63 expression is a prognostic factor in colorectal cancer", The International Journal of Biological Markers, 2018 Publication	<1%
174	Margaret Stromecki, Nazanin Tatari, Ludivine Coudière Morrison, Ravinder Kaur et al. "Characterization of a novel OTX2-driven stem cell program in Group 3 and Group 4 medulloblastoma", Molecular Oncology, 2018 Publication	<1%
175	bmccancer.biomedcentral.com Internet Source	<1%
	Xian-hui Zhang, Wei Wang, Ya-qi Wang, Lei	

176	Zhu, Lan Ma. "The association of SOX2 with clinical features and prognosis in colorectal cancer: A meta-analysis", Pathology - Research and Practice, 2020 Publication	<1%
177	"Drug Resistance in Bacteria, Fungi, Malaria, and Cancer", Springer Science and Business Media LLC, 2017 Publication	<1%
178	Submitted to University of Glasgow Student Paper	<1%
179	www.biomedcentral.com Internet Source	<1%
180	www.researchsquare.com Internet Source	<1%
181	Submitted to University of Reading Student Paper	<1%
182	"Targeted Intracellular Drug Delivery by Receptor Mediated Endocytosis", Springer Science and Business Media LLC, 2019 Publication	<1%
183	E. A. Bray. "Genes commonly regulated by water-deficit stress in Arabidopsis thaliana", Journal of Experimental Botany, 09/10/2004 Publication	<1%
	Jieshu Wang, Bo Li, Kun Zhao, Xinyou Su. "2-	

184	Amino-4-(1-piperidine) pyridine exhibits inhibitory effect on colon cancer through suppression of FOXA2 expression", 3 Biotech, 2019 Publication	<1%
185	"Molecularly Targeted Therapy for Childhood Cancer", Springer Science and Business Media LLC, 2010 Publication	<1%
186	Submitted to University of Messina Student Paper	<1%
187	infoscience.epfl.ch Internet Source	<1%
188	Chathura D. Suraweera, Mohd Ishtiaq Anasir, Srishti Chugh, Airah Javorsky et al. "Structural insight into tanapoxvirus mediated inhibition of apoptosis", The FEBS Journal, 2020 Publication	<1%
189	Submitted to Queen Mary and Westfield College Student Paper	<1%
190	Submitted to University of Wolverhampton Student Paper	<1%
191	tel.archives-ouvertes.fr Internet Source	<1%
192	doras.dcu.ie Internet Source	<1%

193	Submitted to University of Oxford Student Paper	<1%
194	Nuria López-Pérez, Claudia Gil-Sanchis, Hortensia Ferrero, Amparo Faus et al. "Human Endometrial Reconstitution From Somatic Stem Cells: The Importance of Niche-Like Cells", Reproductive Sciences, 2018 Publication	<1%
195	P. Subramanian, M. Deshpande, S. Locatelli-Hoops, S. Moghaddam-Taaheri et al. "Identification of Pigment Epithelium-Derived Factor Protein Forms with Distinct Activities on Tumor Cell Lines", Journal of Biomedicine and Biotechnology, 2012 Publication	<1%
196	Zhong-Hua Li, Xue-Qi Liu, Peng-Fei Geng, Feng-Zhi Suo et al. " Discovery of [1,2,3]Triazolo[4,5-]pyrimidine Derivatives as Novel LSD1 Inhibitors ", ACS Medicinal Chemistry Letters, 2017 Publication	<1%
197	Wei, Cheng-Xi, Ming Bian, and Guo-Hua Gong. "Tetrazolium Compounds: Synthesis and Applications in Medicine", Molecules, 2015. Publication	<1%
198	ueaeprints.uea.ac.uk Internet Source	<1%

199	Submitted to Royal Holloway and Bedford New College Student Paper	<1%
200	Mingyue Zhu, Wei Li, Yan Lu, Xu Dong, Yi Chen, Bo Lin, Xieju Xie, Junli Guo, Mengsen Li. "Alpha fetoprotein antagonizes apoptosis induced by paclitaxel in hepatoma cells in vitro", Scientific Reports, 2016 Publication	<1%
201	Domenico Ribatti, Roberto Tamma, Tiziana Annese. "Epithelial-Mesenchymal Transition in Cancer: A Historical Overview", Translational Oncology, 2020 Publication	<1%
202	linknovate.com Internet Source	<1%
203	Submitted to Queen Margaret University College, Edinburgh Student Paper	<1%
204	Faustino Wahaia, Irmantas Kašalynas, Gintaras Valušis, Catia D. Carvalho Silva, Pedro L. Granja. "Chapter 13 Terahertz Spectroscopy for Gastrointestinal Cancer Diagnosis", IntechOpen, 2017 Publication	<1%
205	Submitted to Instituto Gulbenkian de Ciencia	

	Student Paper	<1%
206	Kulsum, Safeena, Sudheendra H V, Ramanan P, Ravindra D R, Gangotri Siddappa, Nisheena R, Priyanka Chevour, Balaji Ramachandran, Milind Sagar, Aravindakshan Jayaprakash, Alka Mehta, Vikram Kekatpure, Naveen Hedne, Moni A Kuriakose, and Amritha Suresh. "Cancer stem cell mediated acquired chemoresistance in head and neck cancer can be abrogated by Aldehyde dehydrogenase 1 A1 inhibition : Cancer stem cells in drug resistance", Molecular Carcinogenesis, 2016. Publication	<1%
207	Submitted to University Der Es Salaam Student Paper	<1%
208	Submitted to University of Pretoria Student Paper	<1%
209	gupea.ub.gu.se Internet Source	<1%
210	Ahmad Raza, Michael J. Franklin, Arkadiusz Z. Dudek. "Pericytes and vessel maturation during tumor angiogenesis and metastasis", American Journal of Hematology, 2010 Publication	<1%
211	www.readbag.com	

	Internet Source	<1%
212	Submitted to University of Lincoln Student Paper	<1%
213	aip.scitation.org Internet Source	<1%
214	Oza Zaheed, Julia Samson, Kellie Dean. "A bioinformatics approach to identify novel long, non-coding RNAs in breast cancer cell lines from an existing RNA-sequencing dataset", Non-coding RNA Research, 2020 Publication	<1%
215	Katharine M. Hardy, Brian W. Booth, Mary J. C. Hendrix, David S. Salomon, Luigi Strizzi. "ErbB/EGF Signaling and EMT in Mammary Development and Breast Cancer", Journal of Mammary Gland Biology and Neoplasia, 2010 Publication	<1%
216	Mohmmad Younus Wani, Aijaz Ahmad, Faisal Mohammed Aqlan, Abdullah Saad Al-Bogami. " Azole Based Acetohydrazide Derivatives of Cinnamaldehyde Target and Kill by Causing Cellular Apoptosis ", ACS Medicinal Chemistry Letters, 2020 Publication	<1%
217	Singh, R.P.. "A cancer chemopreventive agent	

	silibinin, targets mitogenic and survival signaling in prostate cancer", Mutation Research - Fundamental and Molecular Mechanisms of Mutagenesis, 20041102 Publication	<1%
218	openaccess.leidenuniv.nl Internet Source	<1%
219	Shan-Ju Yeh, Shuo-Wei Chen, Bor-Sen Chen. "Investigation of the Genome-Wide Genetic and Epigenetic Networks for Drug Discovery Based on Systems Biology Approaches in Colorectal Cancer", Frontiers in Genetics, 2020 Publication	<1%
220	Jiang, A.. "Inhibition of APE1/Ref-1 redox activity with APX3330 blocks retinal angiogenesis in vitro and in vivo", Vision Research, 201101 Publication	<1%
221	Submitted to Radboud Universiteit Nijmegen Student Paper	<1%
222	Abanoub A. Gad, Nariman Balenga. "The Emerging Role of Adhesion GPCRs in Cancer", ACS Pharmacology & Translational Science, 2020 Publication	<1%
223	Mehreen Ahmed, Nicholas Jinks, Roya Babaei-Jadidi, Hossein Kashfi et al. "Repurposing	<1%

Antibacterial AM404 As a Potential Anticancer Drug for Targeting Colorectal Cancer Stem-Like Cells", Cancers, 2019
Publication

---

224 Arun Thenappan, Ying Li, Kirti Shetty, Lynt Johnson, E. P. Reddy, Lopa Mishra. "New therapeutics targeting colon cancer stem cells", Current Colorectal Cancer Reports, 2009 <1%
Publication

---

225 www.wjgnet.com <1%
Internet Source

---

226 Andrš, Martin, Jan Korabecny, Daniel Jun, Zdenek Hodny, Jiri Bartek, and Kamil Kuca. "Phosphatidylinositol 3-kinase (PI3K) and phosphatidylinositol 3-kinase-related kinase (PIKK) inhibitors: the importance of the morpholine ring", Journal of Medicinal Chemistry <1%
Publication

---

227 Lan Thi Hanh Phi, Ita Novita Sari, Ying-Gui Yang, Sang-Hyun Lee, Nayoung Jun, Kwang Seock Kim, Yun Kyung Lee, Hyog Young Kwon. "Cancer Stem Cells (CSCs) in Drug Resistance and their Therapeutic Implications in Cancer Treatment", Stem Cells International, 2018 <1%
Publication

---

228 "Vaccine Design", Springer Science and Business Media LLC, 2016 <1%

	Publication	
229	jhoonline.biomedcentral.com Internet Source	<1%
230	Submitted to Sheffield Hallam University Student Paper	<1%
231	www.cuilab.cn Internet Source	<1%
232	MicroRNA Targeted Cancer Therapy, 2014. Publication	<1%
233	L H Klotz. "Novel antiproliferative flavonoids induce cell cycle arrest in human prostate cancer cell lines", Prostate Cancer and Prostatic Diseases, 03/2006 Publication	<1%
234	academic.oup.com Internet Source	<1%
235	Bohler, T.. "Tabebuia avellanedae extracts inhibit IL-2-independent T-lymphocyte activation and proliferation", Transplant Immunology, 200802 Publication	<1%
236	Submitted to University of Hull Student Paper	<1%
237	Submitted to Kwame Nkrumah University of Science and Technology	<1%

Student Paper

238	Submitted to The Robert Gordon University Student Paper	<1%
239	Submitted to Trinity College Dublin Student Paper	<1%
240	era.library.ualberta.ca Internet Source	<1%
241	Submitted to Universita degli Studi di Torino Student Paper	<1%
242	jeccr.biomedcentral.com Internet Source	<1%
243	Submitted to University of Wales Swansea Student Paper	<1%
244	cpb-ap-se2.wpmucdn.com Internet Source	<1%
245	www.dovepress.com Internet Source	<1%
246	Submitted to Jawaharlal Nehru Technological University Student Paper	<1%
247	Roberto Gomez-Casal, Chitralekha Bhattacharya, Michael Epperly, Per Basse et al. "The HSP90 Inhibitor Ganetespib Radiosensitizes Human Lung Adenocarcinoma	<1%

	Cells", Cancers, 2015 Publication	
248	emboj.embopress.org Internet Source	<1%
249	Marco Pfeifer. "L1CAM expression in endometrial carcinomas is regulated by usage of two different promoter regions", BMC Molecular Biology, 2010 Publication	<1%
250	Submitted to Presidency University, Kolkata Student Paper	<1%
251	Submitted to Nottingham Trent University Student Paper	<1%
252	"Stem Cells in Urology", Springer Science and Business Media LLC, 2020 Publication	<1%
253	cardinalscholar.bsu.edu Internet Source	<1%
254	Summya Rashid. "Cancer and Chemoprevention: An Overview", Springer Science and Business Media LLC, 2017 Publication	<1%
255	res.mdpi.com Internet Source	<1%
256	Natalie Patel, Monika Vyas, Romulo Celli,	

	Dhanpat Jain, Xuchen Zhang. "Adverse Histologic Features in Colorectal Nonpedunculated Malignant Polyps With Nodal Metastasis", The American Journal of Surgical Pathology, 2020 Publication	<1%
257	Submitted to University of California, Los Angeles Student Paper	<1%
258	Submitted to UT, Dallas Student Paper	<1%
259	Submitted to Chiang Mai University Student Paper	<1%
260	Submitted to King's College Student Paper	<1%
261	Dong-Qin Chen, Jia-Yuan Huang, Bing Feng, Ban-Zhou Pan, Wei De, Rui Wang, Long-Bang Chen. "Histone Deacetylase 1/Sp1/MicroRNA-200b Signaling Accounts for Maintenance of Cancer Stem-Like Cells in Human Lung Adenocarcinoma", PLoS ONE, 2014 Publication	<1%
262	Wang, K., N. Li, C. H. Yeung, J. Y. Li, H. Y. Wang, and T. G. Cooper. "Oncogenic Wnt/ -catenin signalling pathways in the cancer-resistant epididymis have implications for cancer	<1%

research", Molecular Human Reproduction, 2013.
Publication

263	Stem Cell Biology and Regenerative Medicine, 2014. Publication	<1%
264	Valverde, Araceli, Jon Peñarando, Amanda Cañas, Laura M. López-Sánchez, Francisco Conde, Vanessa Hernández, Esther Peralbo, Chary López-Pedrera, Juan de la Haba-Rodríguez, Enrique Aranda, and Antonio Rodríguez-Ariza. "Simultaneous Inhibition of EGFR/VEGFR and Cyclooxygenase-2 Targets Stemness-Related Pathways in Colorectal Cancer Cells", PLoS ONE, 2015. Publication	<1%
265	Céline Prunier, Barbara A. Hocevar, Philip H. Howe. "Wnt Signaling: Physiology and Pathology", Growth Factors, 2009 Publication	<1%
266	Peng Wang, Maria Voronkova, Sudjit Luanpitpong, Xiaoqing He, Heimo Riedel, Cerasela Z. Dinu, Liying Wang, Yon Rojanasakul. "Induction of Slug by Chronic Exposure to Single-Walled Carbon Nanotubes Promotes Tumor Formation and Metastasis", Chemical Research in Toxicology, 2017 Publication	<1%

267	Submitted to La Trobe University Student Paper	<1%
268	"Nuclear Signaling Pathways and Targeting Transcription in Cancer", Springer Science and Business Media LLC, 2014 Publication	<1%
269	M S Spitzer. "Antiproliferative and cytotoxic properties of bevacizumab on different ocular cells", British Journal of Ophthalmology, 7/26/2006 Publication	<1%
270	Submitted to University of East London Student Paper	<1%
271	Tomas Valenta. "The many faces and functions of β-catenin", The EMBO Journal, 05/22/2012 Publication	<1%
272	Submitted to University of Dundee Student Paper	<1%
273	Submitted to October University for Modern Sciences and Arts (MSA) Student Paper	<1%
274	Michelle McCabe, Yvonne Perner, Rindidzani Magobo, Sheefa Mirza, Clement Penny. "Descriptive epidemiological study of South African colorectal cancer patients at a Johannesburg Hospital Academic institution",	<1%

JGH Open, 2019
Publication

Exclude quotes	On	Exclude matches	Off
Exclude bibliography	On		